THE FORCED COMMUTATION OF THYRISTORS

CONNECTED IN SERIES

by

JOHN KEITH HALL, M.Sc.(Eng.), C.Eng., MIEE, MIMechE.

A Doctoral Thesis

submitted in partial fulfilment of the requirements

for the award of

Doctor of Philosophy of the Loughborough University of Technology

JULY 1972

SUMMARY

This work originated from the suggestion made by Mr. J.D. McColl, Engineering Director of GEC Rectifiers Limited, that insufficient knowledge existed about the problems of turning off series-connected thyristors, particularly under forced commutation. Widespread high voltage application of forced commutation was then, and still is, some years ahead. The thesis puts forward methods which have been devised for ensuring satisfactory thyristor turn-off in this context and suggests some possible future trends in application.

Individual thyristor turn-off characteristics are first studied together with the equivalent diode characteristics. The difficulties of using thyristors in series for high voltage working are described and the limitations of the conventional resistive-capacitive voltage sharing network discussed in relation to forced commutation.

Three forms of improved voltage sharing network are presented together with developments which use these in suitable combination. All have been tested with series-connected thyristors operating in a high voltage force-commutated chopper circuit. The advantages and disadvantages, and a design procedure, are given for each form of network. The two most appropriate voltage sharing arrangements are applied to the series thyristors and diodes in a high voltage, variable frequency d.c. chopper, and their overall influence on chopper performance is considered in detail.

Owing to the possibility of cascade failure when many semi-conductor devices are connected in series, extensive component

damage can result from circuit malfunction or incorrect component connection. Great care has therefore been necessary in the design, construction and checking of the high voltage experimental equipment.

It is concluded that the voltage sharing methods devised make possible forced commutation of thyristors at high voltages and do not, in themselves, provide the practical constraints on system performance. The methods are compared on a technical and economic basis.

Possible future applications are reviewed, with particular emphasis placed on the transformation of d.c. at high voltages using chopping techniques. Other problems which must be solved before such applications become realisable outside the laboratory are outlined and suggestions made for future work.

Acknowledgements are made to Professor J.W.R. Griffiths, Head of the Department of Electronic and Electrical Engineering, and to the Science Research Council for the provision of experimental facilities. I am grateful to colleagues for their support; in particular to Mr. E. Besag for assistance with specialised measurements, to Mr. D.W. Hoare for advice on micrologic circuitry and to Professor D.S. Campbell and Dr. S.A. Ferris for their criticisms of the thesis presentation. The interest shown by Mr. J.D. McColl, Engineering Director of GEC Rectifiers Limited, and his colleague Mr. J.J.L. Weaver, is greatly appreciated.

C O N T E N T S

Appendix

CHAPTER 1

INTRODUCTION TO THE THESIS

1.1 BACKGROUND

The upper limit of peak repetitive voltage rating for thyristors now commercially available is about 4kV; consequently series connection is usually adopted when the operating voltage exceeds one to two thousand volts. It seems unlikely that, in the near future, a single thyristor capable of withstanding upwards of a few tens of kilovolts will become available. The solution of problems associated with the operation of thyristors in series, of which turn-off is the most outstanding, is therefore likely to be of long term benefit for very high voltage working.

The main application at present is the high voltage d.c. converter, where the traditional mercury arc rectifier valve in each arm of a three-phase bridge connection is being superseded by a stack of series-connected thyristors[1]. The rectifiers are commutated (i.e. sequentially switched off) by the a.c. line voltage, this being termed natural commutation. Generally the rate of fall of forward current in the outgoing rectifier is limited to a low value by the appreciable inductance of the a.c. supply system and transformer.

The alternative method of commutation - termed forced or artificial - whereby auxiliary circuitry is used to quench the rectifier current rapidly to zero, has been little used with mercury

arc valves owing to the increased stress imposed and the consequential greater likelihood of arcback[2,3]. Thyristors, however, demonstrate no such phenomenon, and forced commutation is widely used at voltages below 1000V in choppers and inverters operating on a d.c. supply. A capacitor usually serves as the commutating energy source and additional passive circuit components control the thyristor stresses to an acceptable level.

Forced commutation of a few thyristors in series is being considered by various workers for chopper control of d.c. traction motors at line voltages up to 3kV[4,5,6,7]. There is, at the moment, no use made of forced commutation at very high voltages but, looking into the future, a number of possible applications can be envisaged which could radically extend the scope of high voltage d.c. working.

1.2 OBJECTS OF THE INVESTIGATION

The basic objective has been to devise satisfactory methods of ensuring a reliable turn-off, together with a safe distribution of voltage, across series connected thyristors under forced commutation. The principles involved are the same as with natural commutation, but the more arduous turn-off conditions imposed on the thyristors usually render inadequate the conventional voltage sharing networks[8,9].

Initially it was considered that each series thyristor might be turned off separately by its own commutating capacitor and auxiliary thyristor, instead of using a voltage sharing network and turning off the thyristor string as a complete unit. However, it became apparent that additional components would be required to

aid voltage sharing, and that no better performance would be gained to justify the added complexity. Additionally, the advantage of being able to uprate existing low voltage circuits for high voltage working, by the substitution of a series thyristor unit for a single thyristor, provided a powerful incentive for discarding the individual turn-off idea.

The detailed objectives therefore became:

(a) To establish voltage sharing networks which give satisfactory turn-off and safe voltage distribution for the series thyristors with forced commutation.

(b) To ascertain the relative merits of these voltage sharing networks in the context of possible applications.

(c) To fully prove and define the limitations of the best of these networks for a specific application by using them on all series thyristor strings and, suitably adapted, on all series diode strings.

(d) To consider the possible future application of force-commutated series thyristors and further problems which require solution.

1.3 ADOPTED PROCEDURE

An investigation into thyristor turn-off behaviour is a first requirement. This, together with comparable diode behaviour is covered in Chapter 2. The series operation of thyristors is considered in Chapter 3. Experimental results illustrating the turn-off

performance of the conventional resistive-capacitive voltage sharing network are quoted to justify the reasoning given and to provide a basis for later comparison. The chapter concludes with a discussion of the disadvantages of the network for forced commutation and a statement of the fundamental precepts by which improvement may be effected. The main circuits which are to be investigated for doing this are included.

The next three chapters each report an investigation into a particular form of improved voltage sharing network, these being distinguished by the components used. Chapter 4 describes the use of an additional series magnetic component, and Chapter 5 deals with added parallel magnetic components. The use of parallel voltage regulating diodes, both without and with resistive-capacitive components, is discussed in Chapter 6. Each chapter contains an analysis with experimental verification of the sharing network operation at turn-off, and states its advantages and disadvantages. The experimental results relate to operation of the sharing networks on a test string of twenty series thyristors in a constant frequency (50Hz), 5kV chopper circuit which provides suitable force-commutated turn-off. A design example for each form of network is given in Appendix III.

The two simplest and most suitable improved voltage sharing networks for the application are compared *in toto* in Chapter 7 by considering their performance in a 5kV d.c. chopper capable of controlling 60kW over a range of 50-2000Hz. The high upper frequency was chosen in order to subject the thyristors, diodes and sharing

networks to a severe duty. Additionally, the influence of voltage sharing components on main chopper operation, on output voltage and on efficiency are considered.

The conclusions to the thesis appear in Chapter 8, together with a discussion of the possible future applications of force-commutated thyristors at high voltages. Other associated technical problems are described and this leads to suggestions for future work.

CHAPTER 2

THYRISTOR TURN-OFF CHARACTERISTICS

2.1 INTRODUCTION

This discussion of thyristor turn-off characteristics serves as a preparation for the later chapters. It is written from the user's viewpoint and consequently only methods of measurement which can be applied to the complete thyristor, as manufactured, have been adopted. These measurements have been made in order to obtain first hand experience of thyristor turn-off behaviour and to provide data for the design of the voltage sharing networks which follow. Typical results are given.

It is appropriate also to consider diodes in this context, since they exhibit similar switching effects to thyristors. These effects are relevant to their sharing of reverse voltage when they are operated in series.

2.2 THYRISTOR TURN-OFF TIME

The thyristor is a three-electrode, four-layer *p–n–p–n* device (Figure 2.1) which operates as a latching switch. When anode-cathode voltage is applied, the thyristor will not conduct, apart from a very low leakage, providing its voltage rating is not exceeded. Forward conduction is initiated (turn-on), with positive anode-cathode voltage applied, by a triggering signal which takes the

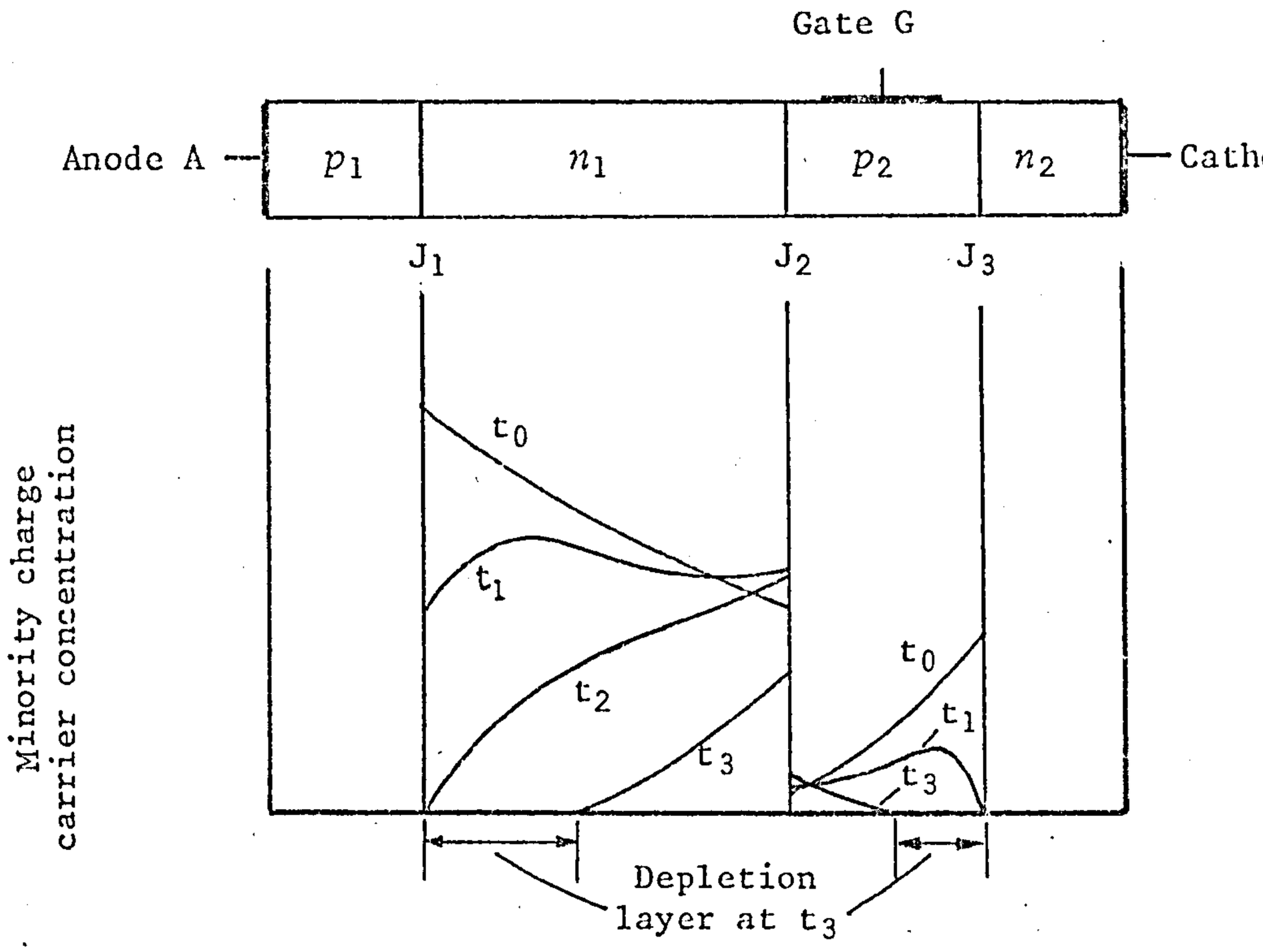

Figure 2.1: Thyristor base region minority-carrier charge distributions during turn-off.

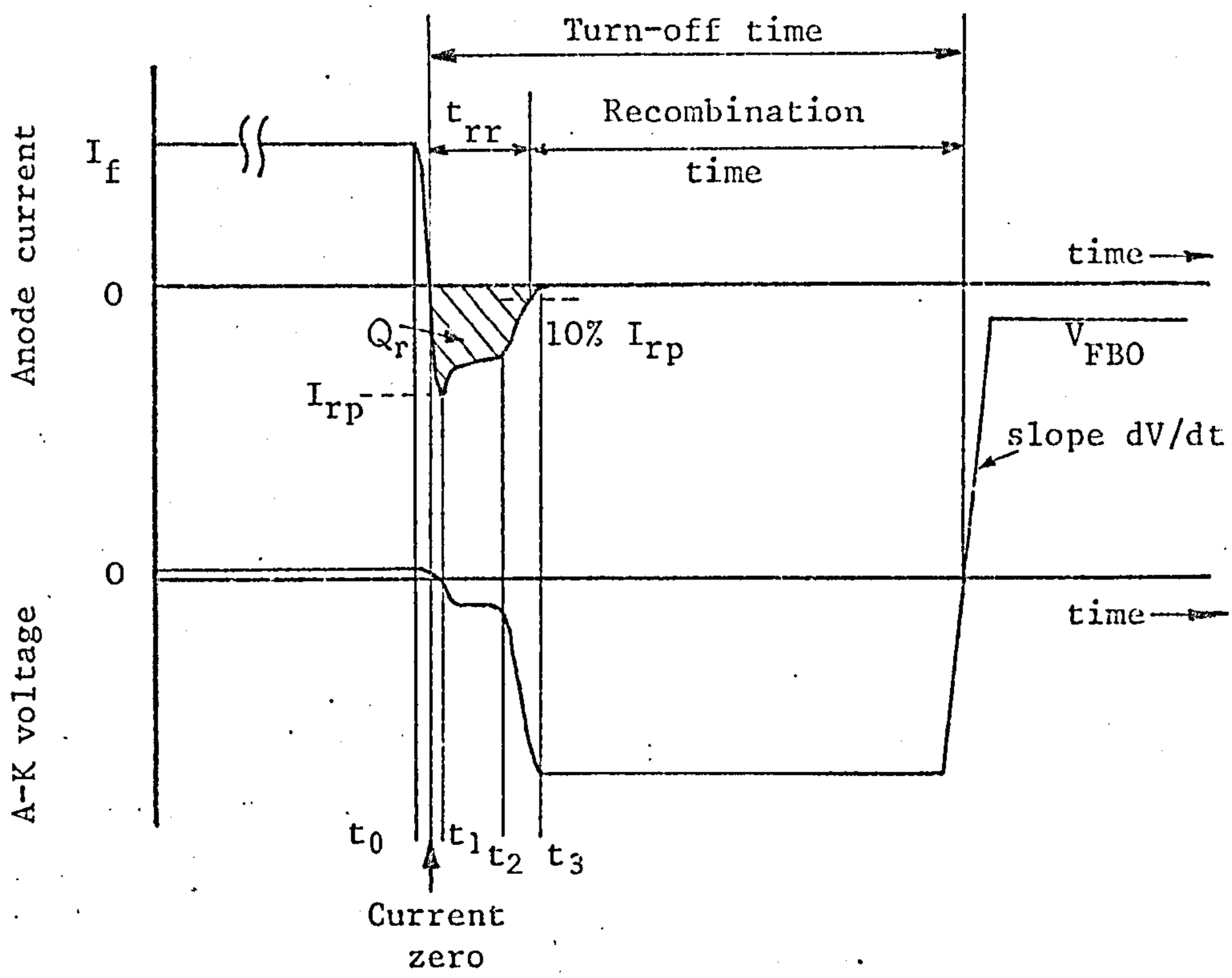

Figure 2.2: Waveforms for measurement of thyristor turn-off time.

gate electrodepositive relative to the cathode. Once main conduction is established (i.e. the current has risen to the latching, or holding, value[10]), the gate loses control and its signal may be removed. Cessation of forward current flow and a return to the forward blocking state (turn-off) must then be induced by using the main anode-cathode circuit.

Turn-off time is defined as the time required for the thyristor to achieve forward blocking capability after forward current has ceased to flow. It is measured from the current and voltage waveforms (Figure 2.2) obtained by operating the device in a turn-off time measuring circuit[11,12]. These waveforms may differ from those which apply in practice, but should be representative for applications where turn-off time is important. Turn-off time may be divided into two parts (Figure 2.2): the reverse recovery time t_{rr} and the recombination time[10]. These are considered in the following sections.

2.3 DEVICE CONSIDERATIONS

The two stable conditions of thyristor forward anode-cathode bias are:

(a) The forward conducting state, in which the forward biased emitter junctions (J_1 and J_3 in Figure 2.1) inject excess minority carriers into the base regions n_1 and p_2. These carriers maintain the central junction J_2 in a state of reverse breakdown, charge flow through the device then being relatively unimpeded and the forward voltage drop low.

(b) The forward blocking state, in which junction J_2 performs the blocking function; J_1 and J_3 are again forward biased.

Turn-off is the action of switching the thyristor from condition (a) to condition (b). There are two ways of doing this: by interrupting the forward current using external switching, or by the application of a reverse anode-cathode voltage.

The first method, termed starvation turn-off, is slow because the required decay of internal stored charge must take place purely by recombination. The speed of turn-off under reverse anode-cathode bias depends largely on the rate of fall of forward current. If the series inductance is large, as is usual with a.c. line commutated rectifiers, the internal recombination can 'follow' the slow rate of current fall, leaving little or no stored charge at current zero. Turn-off time is then short, but the overall commutation time is long. Where the series inductance is small, this being typical of forced commutation applications, little recombination occurs during the rapid fall of current. A substantial current reversal then occurs which removes a proportion of the total stored charge (Figure 2.2). This results in the fastest turn-off.

Only the main features of the turn-off mechanism under reverse anode-cathode bias will be given, the details can be found elsewhere [10,11,13,14]. Figure 2.1 shows a typical distribution of minority carriers in the thyristor base regions at various instants after turn-off has been initiated at t_o. The timings shown also relate to those of Figure 2.2. After current zero, with J_2 forward biased, minority carriers in bases n_1 and p_2 drift back across junctions

J_1 and J_3 respectively, and are replaced initially by carriers crossing J_2. This carrier flow constitutes the reverse storage current which is limited only by the external circuit resistance. Layer n_1 is lightly doped compared with p_2 so that the electron flow through J_2 into p_2 soon drops and the excess carrier concentration in p_2 falls. J_3 then commences to build up its depletion layer and block voltage at t_1, and reverse current decays from its peak value I_{rp}. J_3 is usually designed to avalanche at a low reverse potential of about 10V[11]. Thus, a reduced reverse current continues to flow, which facilitates removal of the heavy concentration of minority carriers in the n_1 layer, the thyristor reverse voltage remaining constant at the J_3 avalanche value. At t_2 the depletion layer of junction J_1 commences to build up, and at t_3 the thyristor withstands the full reverse voltage, most of which appears across J_1. The reverse current has now decayed to zero (neglecting leakage) and reverse recovery is complete. The substantial remaining hole concentration near J_2 must be allowed time to fall, by recombination, to a very low level which is insufficient to induce breakdown of J_2 when forward voltage is re-applied.

From the foregoing, it is clear that thyristor turn-off performance is controlled mainly by the minority positive carriers in the lightly-doped n_1 base layer. If the lifetime of these carriers is τ_p, the total excess hole charge Q_f with forward current I_f flowing is given approximately by

$$Q_f = \tau_p I_f \quad [10\ 14]. \tag{2.1}$$

When turn-off is initiated, if reverse current flow is neglected

the excess charge must decay purely by recombination. The excess charge q at any subsequent instant is then given by

$$q = Q_f e^{-t/\tau_p} ,$$

$$\text{then} \qquad q = \tau_p I_f e^{-t/\tau_p} . \qquad (2.2)$$

For the device to withstand a re-applied forward voltage, the excess charge in n_1 must have decayed to a value less than that corresponding to the holding current I_h. Letting this be Q_h ($= \tau_p I_h$) and the (turn-off) time required be T_{off}, then

$$Q_h = Q_f e^{-T_{off}/\tau_p} .$$

$$\text{Therefore} \qquad I_h = I_f e^{-T_{off}/\tau_p}$$

$$\text{and} \qquad T_{off} = \tau_p \ell_n \left(\frac{I_f}{I_h}\right) . \qquad (2.3)$$

The implied assumptions of forward current falling at an infinite rate, and zero reverse recovery current flow, result in equation (2.3) giving a high value of turn-off time.

For a fast turn-off, the minority-carrier lifetime τ_p should be small (equation 2.3). Unfortunately, the usual manufacturing technique for reducing the value of τ_p has practical limitations owing to other properties, notably voltage blocking capability and forward voltage drop, being adversely affected[15]. A compromise is therefore necessary.

2.4 CIRCUIT CONSIDERATIONS

The external circuit establishes the electrical environment in which the thyristor operates. It influences the turn-off time, the reverse recovery characteristic and the level of any parasitic transients generated by reverse recovery current flow.

Thyristor turn-off time increases with [10,11,12,15]:

(a) increase of forward current I_f, because this produces more excess charge;

(b) increasing rate of fall of forward current $\left(\left|\frac{di}{dt}\right|_{off} \right)$, owing to the reduced recombination during current fall;

(c) increasing junction temperature, which increases lifetime;

(d) increasing amplitude and slope dV/dt of the re-applied forward blocking voltage. Higher amplitude leads to increased field strength across J_2 junction, giving greater possibility of the available minority carriers inducing depletion layer breakdown. High dV/dt can produce sufficient injection from emitter junctions J_1 and J_3 to cause switch-on.

Turn-off time may increase if the period of forward current flow is insufficient for the thyristor to fully turn on across the complete silicon wafer area. This is due to the development of a local hot spot near the gate. Under these circumstances, the gate drive applied at turn-on can assume great importance at turn-off [16].

The quantity of removed charge Q_r likewise increases with the above factors (a), (b) and (c).

The effect of increasing the reverse voltage is to decrease the reverse recovery time and therefore the turn-off time; Q_r is increased. The peak reverse current I_{rp} is increased, leading to a more rapid decay of reverse current and a possibly serious increase in the short-duration transient e.m.f. induced across any inductance, stray or added, in series with the thyristor[17]. This 'hole-storage voltage spike' is felt across the thyristor in addition to the applied reverse voltage, whose value it can exceed by many times, and destruction of the device may result. Diodes behave in a similar way[18,19].

Appreciable values of inductance must frequently be included in series with the thyristors to limit di/dt at turn-on. The accepted practice for suppression of the resulting hole-storage voltage transient is to use a capacitor connected across the thyristor (or diode). A resistor is usually required in series with the capacitor to prevent excessive thyristor dissipation at turn-on, and to dampen the ringing between the inductance and capacitance.

2.5 TURN-OFF TIME MEASUREMENT

2.5.1 Measuring circuit

The variation of turn-off time to be expected with widely varying thyristor reverse voltage is of particular interest with series operation. For these measurements, very low reverse voltages are

obtained by connecting voltage-limiting diodes in parallel with the test thyristor.

The circuit used for measuring turn-off time (Figure 2.3) is based on that of Dyer and Houghton[12]. Full component details are given in Figure I.1. Appendix I also gives the thyristor gate pulse timing circuit and pulse amplifier circuit. The test thyristor is supplied from four separate sources, each fed from its own variable voltage a.c input and incorporating a rectifier with reservoir capacitor. The forward current amplitude source feeds constant current of the required magnitude through the air-cored inductor L_a. Thyristor Th_s and the test thyristor are gated together. When they turn on, the greater voltage of the forward current supply source results in its taking over the inductor current supply, the current magnitude remaining unchanged for the duration of the test thyristor current pulse. Test thyristor turn-off is produced by gating Th_r which applies the required reverse voltage. After a controlled delay, forward blocking voltage is applied by gating Th_f. Turn-off time is measured from the CRO waveforms (Figure 2.4) by advancing the forward blocking voltage wave to the limit where the thyristor just turns off.

This circuit provides independent variation of the forward current, reverse voltage and forward blocking voltage. Thyristor anode current pulses of 50μs at a 50Hz repetition rate are used to avoid heating the thyristor by conduction and switching loss. This pulse width allows complete turn-on for the small thyristors tested. As sufficient data is provided for later needs, the effect of temper-

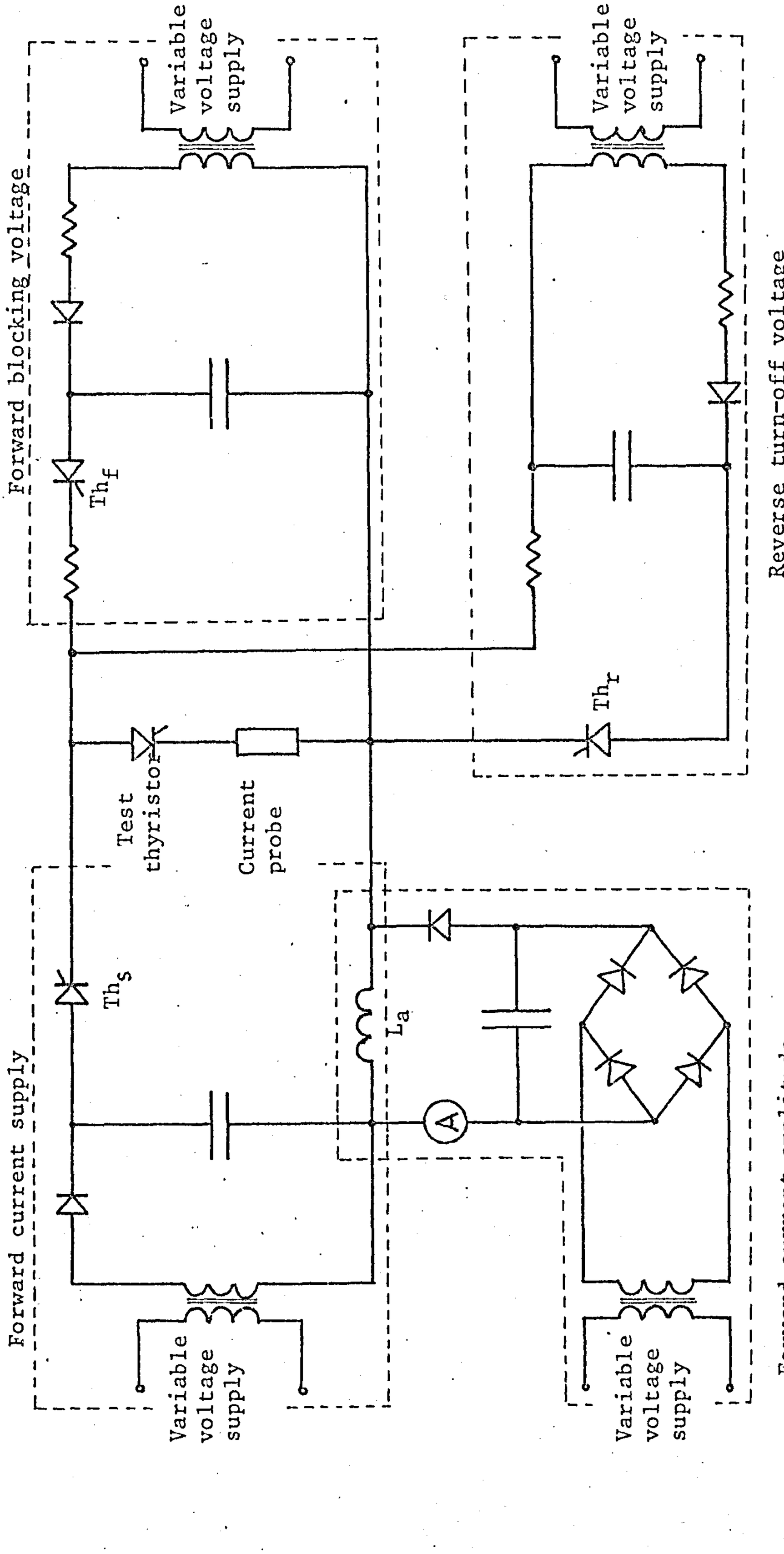

Figure 2.3: Turn-off time measuring circuit

Forward current amplitude

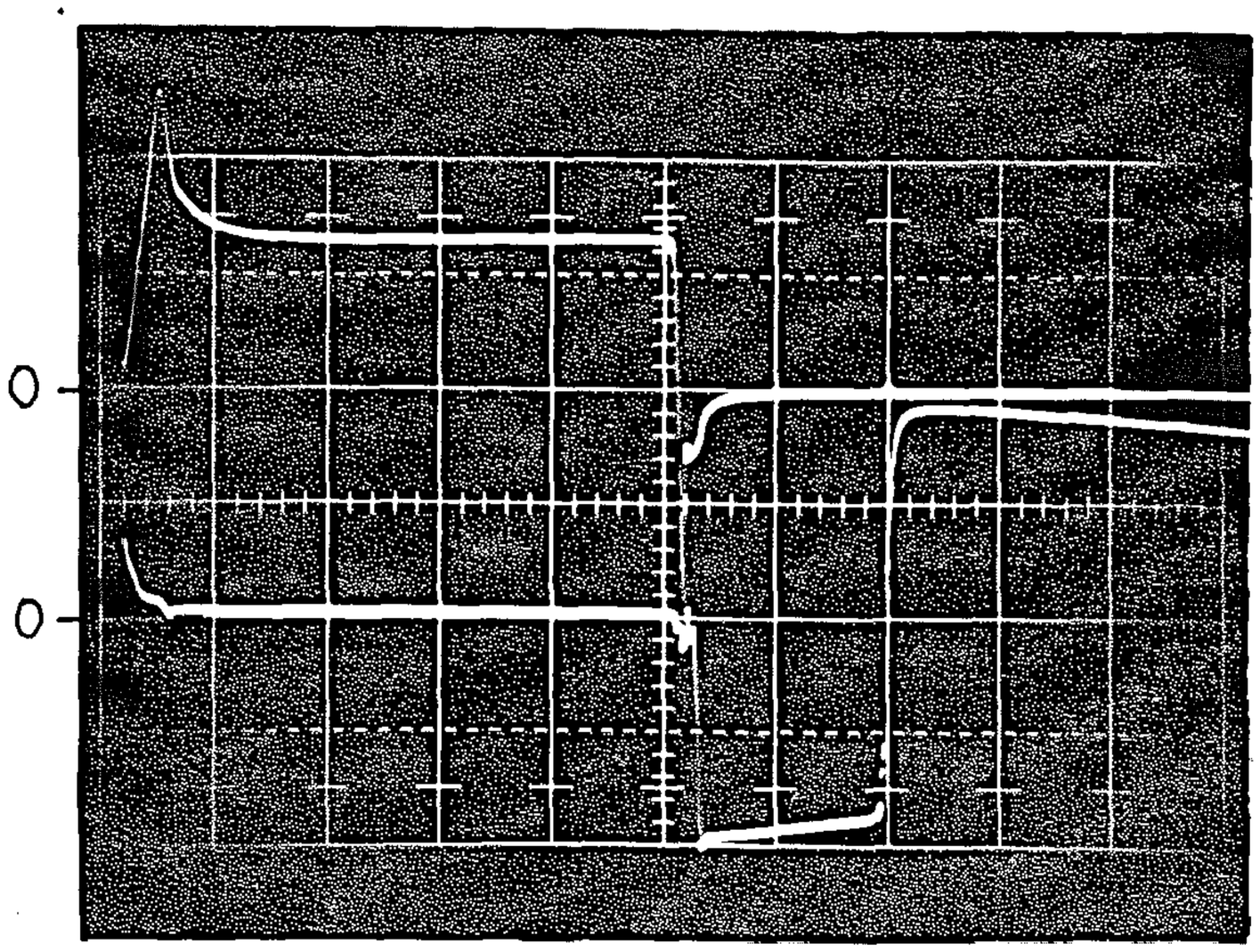

Figure 2.4: Oscillograms of turn-off time measuring circuit waveforms.

(a) Test thyristor current, (20A/cm, 10μs/cm).

(b) Test thyristor voltage, (50V/cm, 10μs/cm).

Measuring circuit - Figure 2.3

ature rise on turn-off time has not been measured.

2.5.2 Measured results

The variation of measured turn-off time with forward current for three thyristors of the same type, all selected for fast turn-off, is shown in Figure 2.5. As expected, turn-off time increases with forward current increase, but results show that it falls with increasing $\left|\frac{di}{dt}\right|_{off}$, which apparently contradicts point (b) in section 2.4. This occurs because $\left|\frac{di}{dt}\right|_{off}$ could not be controlled independently of the applied reverse voltage which therefore must be increased to provide a higher rate of current fall. The resulting decrease in reverse recovery time then becomes dominant.

It is evident that turn-off time is much more a property of the individual thyristor than a function of circuit conditions, provided dV/dt triggering is absent. By doubling the reverse turn-off voltage, turn-off time is decreased by about 10%; only a 13% increase . . . . results when the forward current is increased by a factor of three from the mean rated value.

The effect of severe reverse voltage limitation on turn-off time is shown in Figure 2.6 for the fastest and slowest thyristors (1) and (3) previously tested. The ultimate restriction is to block the reverse recovery current and apply zero reverse voltage. This can be accomplished by using a fast recovery diode in series with the test thyristor together with a small saturating reactor to block the low reverse current of the diode. It is expected that the longest turn-off times will then result (curves (d)). This does

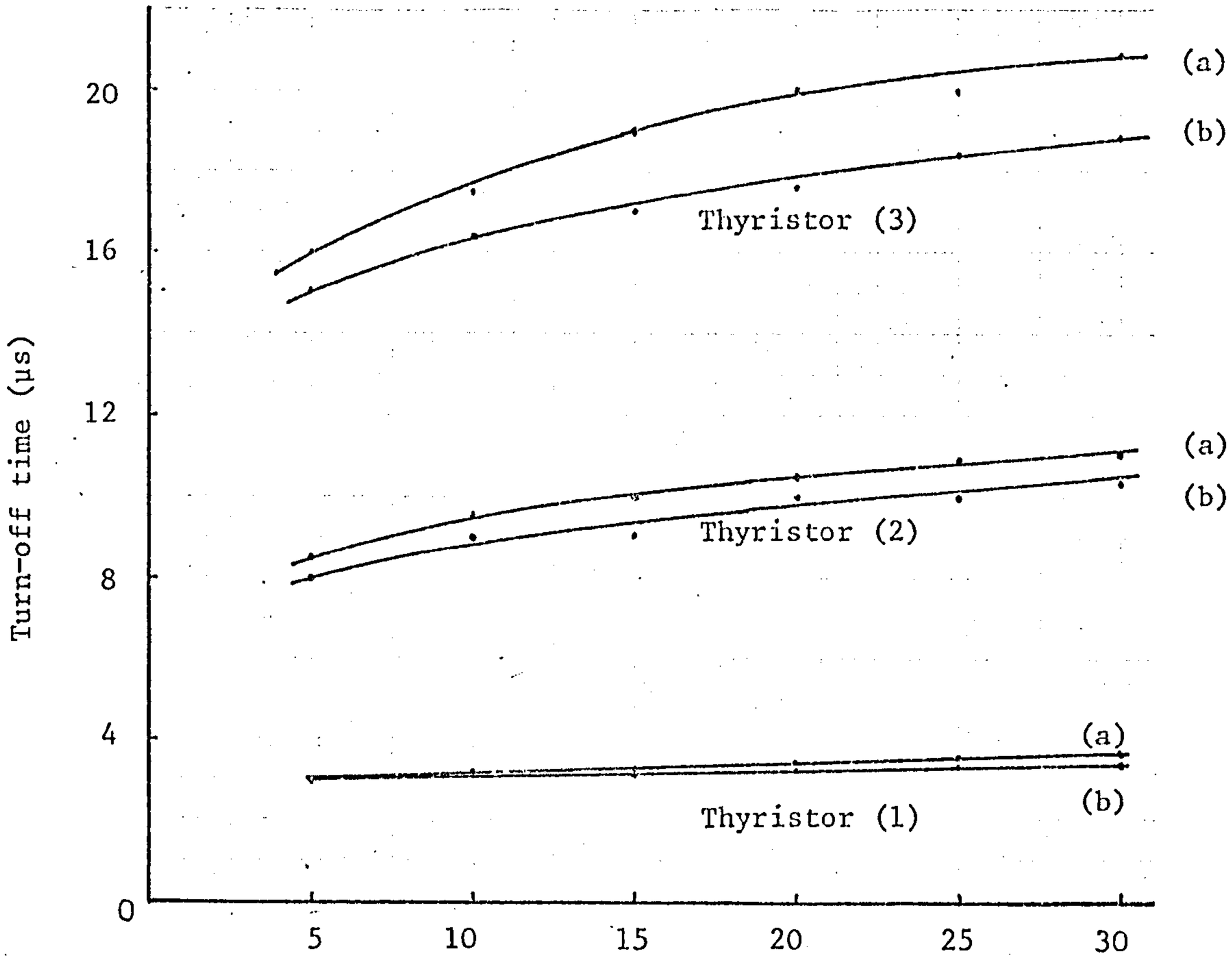

Figure 2.5: Variation of thyristor turn-off time with forward current.

Three thyristors - Westinghouse, type CS22E (10A, 100V).

(a) Reverse voltage = 45V, $\left|\frac{di}{dt}\right|_{off}$ = 30A/μs

(b) Reverse voltage = 90V, " = 60A/μs

V_{FBO} = 90V, dV/dt = 90V/μs, T_s = 21°C

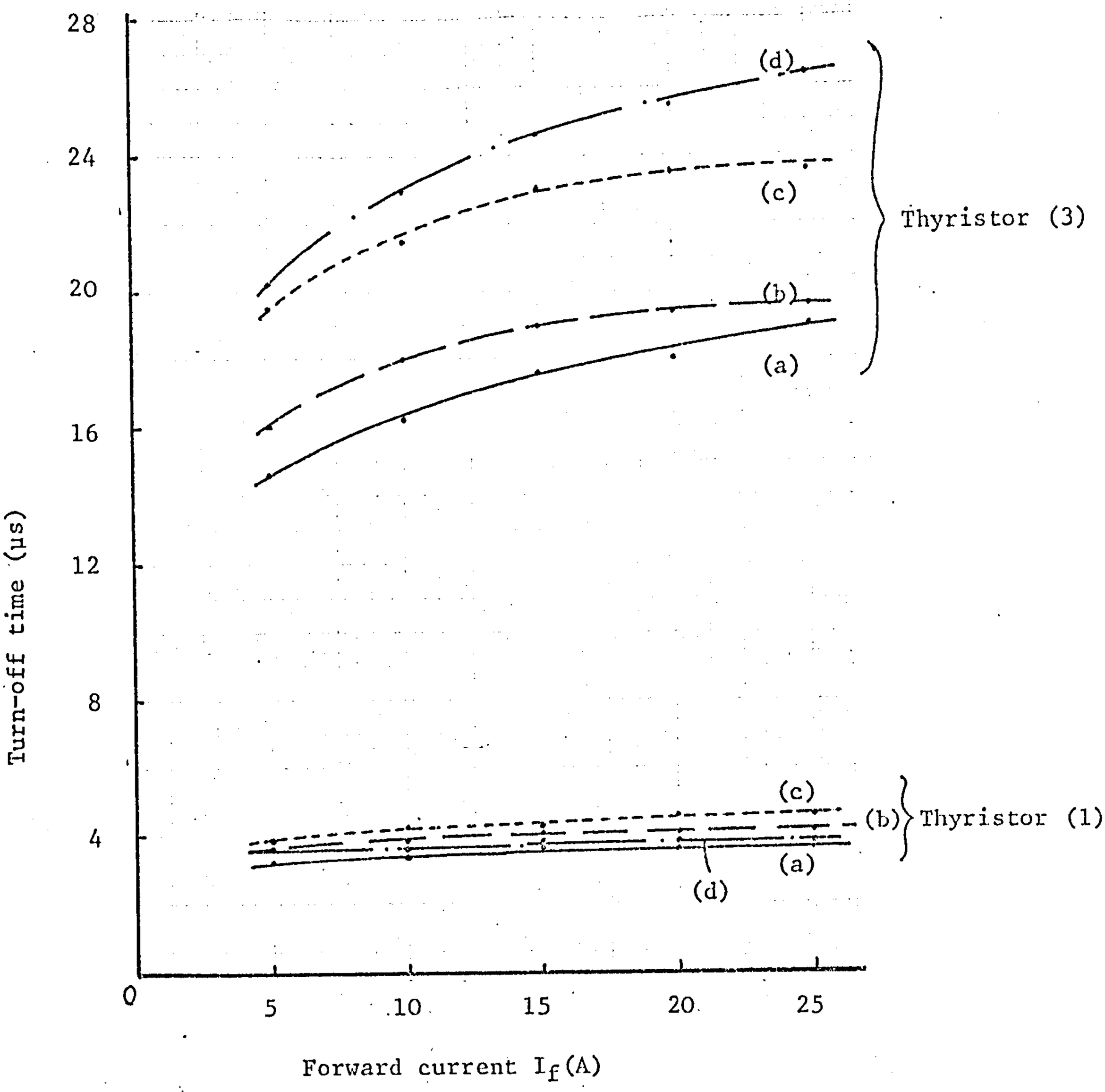

Figure 2.6: The effect on turn-off time of restricting the thyristor reverse voltage.

Thyristors - Westinghouse, type CS22E (10A, 100V)

(a) Reverse voltage = 90V

(b) Reverse voltage limited to 8V (by zener diode)

(c) " " " " 1V (by one diode)

(d) " " zero, reverse current blocked.

V_{FBO} = 90V, dV/dt = 90V/μs, $\left|\frac{di}{dt}\right|_{off}$ = 60A/μs, T_s = 21°C.

not apply to the fastest turn-off thyristor (1) however, the reason being that the small decrease in $\left|\frac{di}{dt}\right|_{off}$ produced by the saturating reactor allows appreciable recombination during the forward current fall.

It is significant that, providing $\left|\frac{di}{dt}\right|_{off}$ remains constant, turn-off time is increased very little by limiting the reverse voltage until this is reduced to a very few volts (c.f. curves (b) and (a)). Even with blocked reverse current, only a 40% increase is registered for the slowest turn-off thyristor (3). It can be concluded, therefore, that the turn-off time of very fast turn-off thyristors is little affected by a wide variation of reverse voltage.

2.6 MEASUREMENT OF REMOVED REVERSE RECOVERY CHARGE

2.6.1 Methods of measurement

It will be shown in Chapter 3 that when a number of thyristors are connected in series, the sharing of the reverse turn-off voltage is dependent on the amounts of charge Q_r removed from the thyristors during reverse recovery. Prior measurement of Q_r for each device under representative circuit conditions is therefore necessary. The same applies to diodes.

Measurement of Q_r can be made in a number of ways. A repetitively operating turn-off circuit allows measurement of the time-integral of the reverse recovery current to be made from the CRO waveform. A simpler method uses a single-shot circuit which can conveniently be operated manually. Direct measurement of Q_r is obtained by

connecting a fast recovery diode in series with the test thyristor, with a close tolerance, low leakage capacitor and high impedance voltmeter across the diode[20]. This measuring circuit, together with the modification required for diode measurements, is given in Figure I.4 and further described in section I.1(d).

2.6.2 Measured results

The measured variation of Q_r for the thyristors (1) and (3) is shown in Figure 2.7. Values of 0.5 and 4.1μs have been obtained for the minority-carrier lifetimes of these thyristors (see section 2.7), and the total stored charge Q_f ($= \tau_p I_f$) lines are drawn in. It is apparent that a reducing proportion of the total charge is extracted during reverse recovery as the forward current I_f is increased. The ratio Q_r/Q_f is approximately 50% for the slower recovery thyristor (3) at 25A with the highest rate of fall of current (plot (a)).

With constant reverse voltage applied and $\left|\frac{di}{dt}\right|_{off}$ halved by doubling the turn-off circuit inductance, Q_r is decreased by some 20-25% for thyristor (3) (plots (a) and (b), (c) and (d)); by halving the reverse voltage with $\left|\frac{di}{dt}\right|_{off}$ maintained constant, Q_r is decreased by approximately 7% (plots (b) and (c)). These results lead to the important inference that the reverse recovery charge is considerably dependent on the rate of fall of forward current; it is, however, little affected by reverse voltage level, provided this is sufficient to establish a depletion layer at both J_1 and J_3 junctions.

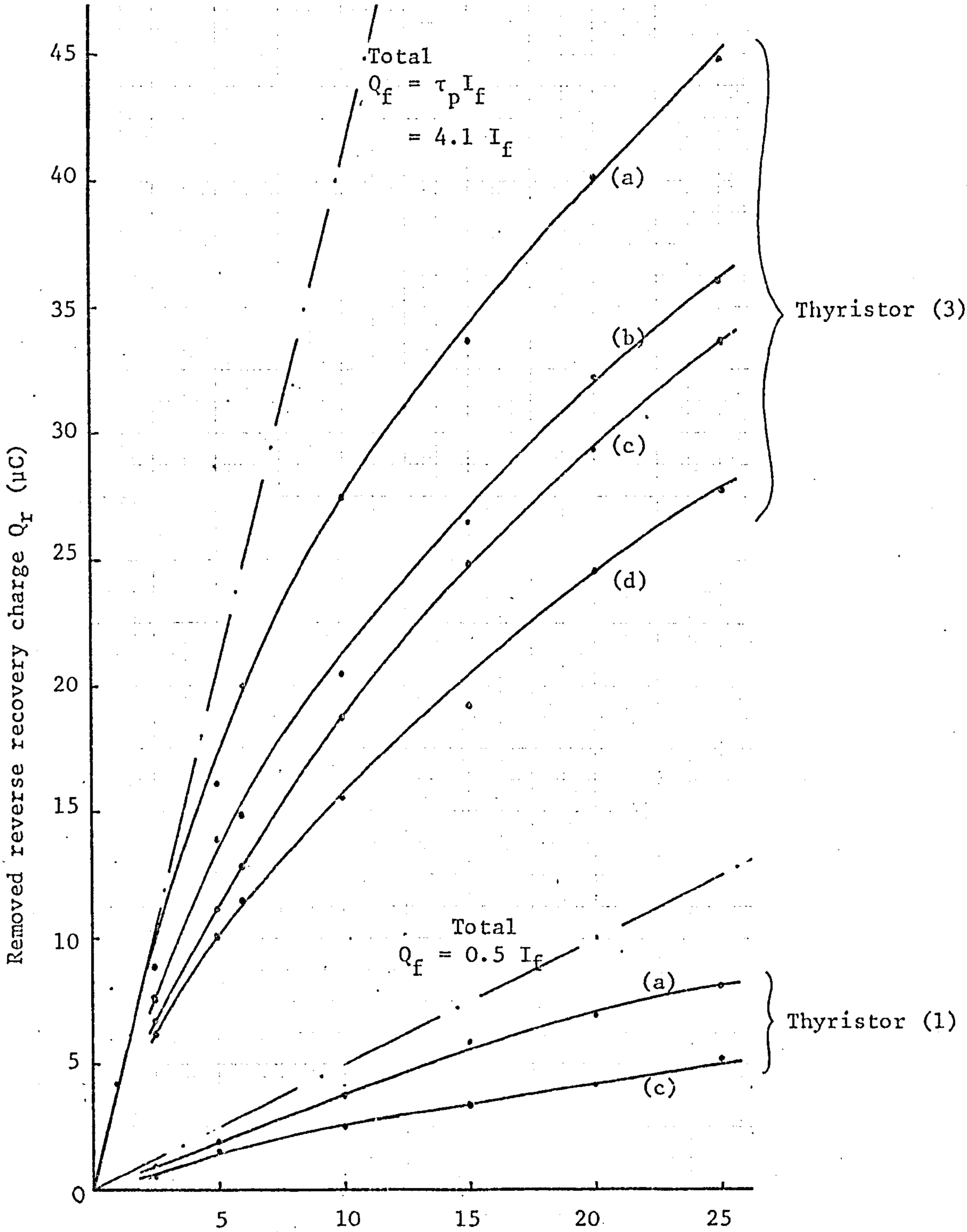

Figure 2.7: Thyristor reverse recovery charge measured on the manually-switched test circuit (Figure I.4).

(a) Reverse voltage = 100V, $\left|\frac{di}{dt}\right|_{off}$ = 40A/μs
(b) " " = 100V, " = 20A/μs
(c) " " = 50V, " = 20A/μs
(d) " " = 50V, " = 10A/μs

} $T_s = 21^{o}C$

If reverse voltage is restricted such that only J_3 depletion layer builds up, the step in the reverse recovery current waveform (Figure 2.2) is removed and I_{rp} is reduced. The resulting reduction of Q_r, measured from the CRO waveforms with reverse voltage restricted to 1V, is demonstrated in Figure 2.8. The presence of the voltage-limiting inverse-parallel connected diode prohibits the use of the manually-operated measuring circuit. The results of Figure 2.8 can only be taken as approximate.

The measured quantity of charge Q_r removed from diodes during reverse recovery varies in a generally similar manner to that from thyristors (Figure 2.9). This is to be expected because Q_r is influenced by the same circuit factors. The two diodes tested are standard general purpose components, and exhibit considerably higher values of Q_r than do the fast turn-off thyristors (Figure 2.7).

2.7 MEASUREMENT OF THYRISTOR *n*-BASE MINORITY-CARRIER LIFETIME

It has been shown that thyristor turn-off time and removed reverse recovery charge are both fundamentally controlled by the minority-carrier lifetime τ_p. This parameter can be estimated from two turn-off properties of the thyristor: the reverse recovery characteristic and the turn-off time itself.

Only the second current decay in the reverse recovery characteristic (Figure 2.2) is of significance for determining τ_p. If this decay is assumed exponential, it has been shown by Lebedev and Uvarov[13] that, when the density of acceptors in the *p*-base is appreciably greater than that of the donors in the *n*-base, the time

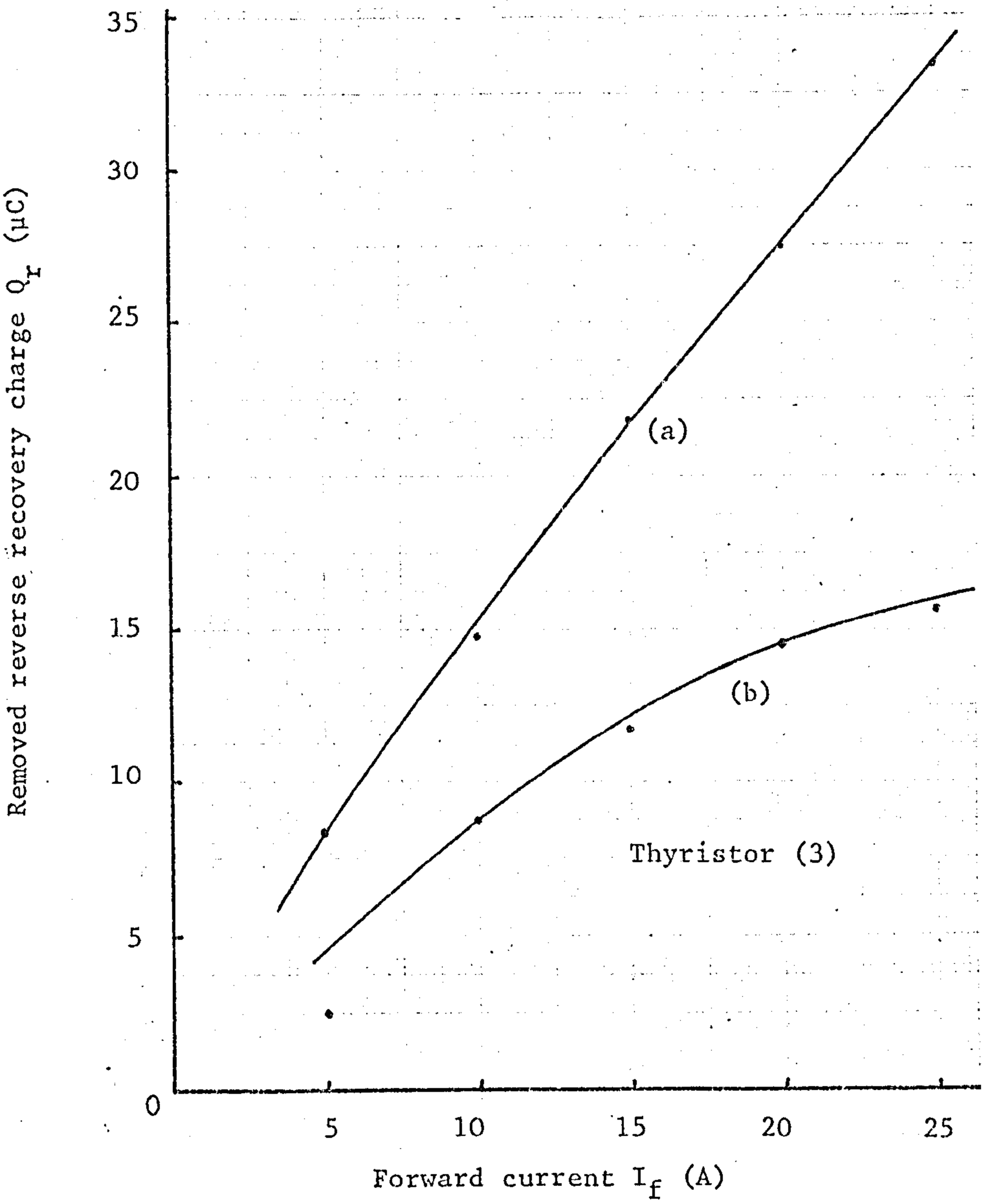

Figure 2.8: Thyristor reverse recovery charge with restricted reverse voltage measured from $\int i\,dt$ on the CRO.

(a) Reverse voltage unrestricted = 50V

(b) " " limited to 1V (by one diode)

$\left|\frac{di}{dt}\right|_{off}$ = 40A/μs, T_s = 21°C.

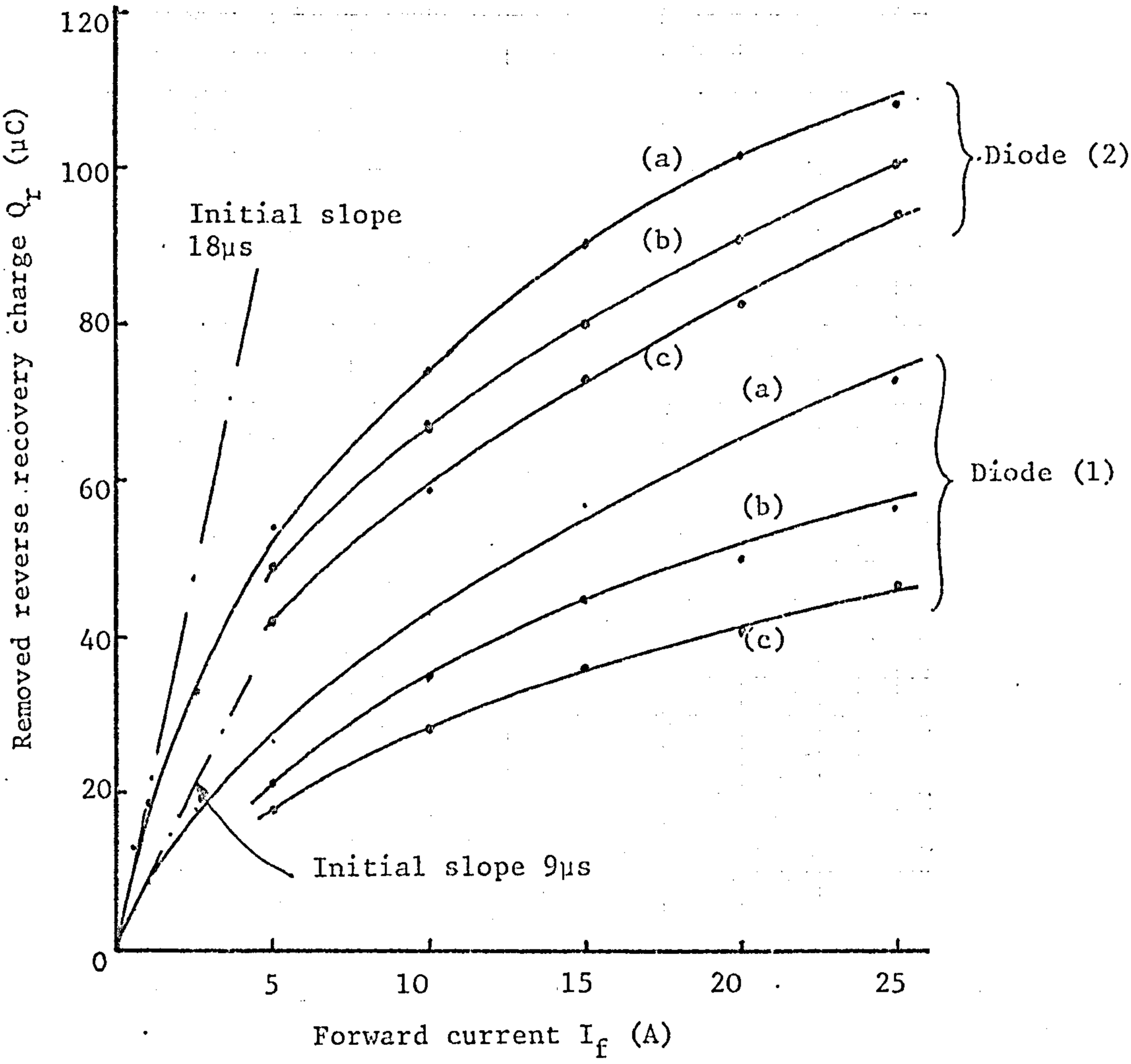

Figure 2.9: Diode reverse recovery charge measured on the manually-switched test circuit (Figure I.4).

Two diodes, (1) TAG type MP100 (40A, 1000V)
(2) IR type 25G100 (25A, 1000V)

(a) Reverse voltage = 200V, $\left|\frac{di}{dt}\right|_{off}$ = 80A/μs

(b) " " = 100V, " = 40A/μs

(c) " " = 50V, " = 20A/μs

T_s = 21°C.

constant of the decay is equal to the lifetime τ_p of the holes in the *n*-base. Owing to the stepped nature of the waveform, τ_p cannot be measured accurately from a CRO.

A better method[21], developed for the purpose of this thesis, uses measured turn-off times. It is arrived at by writing equation (2.3) in the form

$$T_{off} = \tau_p \ell_n(I_f) - \tau_p \ell_n(I_h). \qquad (2.4)$$

Assuming the holding current I_h to be constant, τ_p is obtained by plotting values of measured turn-off time at various forward currents I_f to a base of $\ell_n(I_f)$. The slope of the resulting straight line gives τ_p. Using this technique for the fastest and slowest turn-off thyristors ((1) and (3)) previously tested, the lifetime values are 0.5 and 4.1μs respectively (Figure 2.10).

Equation (2.4) allows only for recombination during turn-off, thus making it important that the turn-off time is measured with the reverse recovery current blocked. The measurement is performed with a fast recovery diode and a small saturating reactor connected in series with the thyristor (section 2.5.2).

2.8 MEASUREMENT OF DIODE *n*-BASE MINORITY-CARRIER LIFETIME

As there can be no question of turn-off time measurement with *p-n* junction diodes, the reverse recovery characteristic must be used for lifetime measurement. A number of methods are available and those which have been found useful are outlined below.

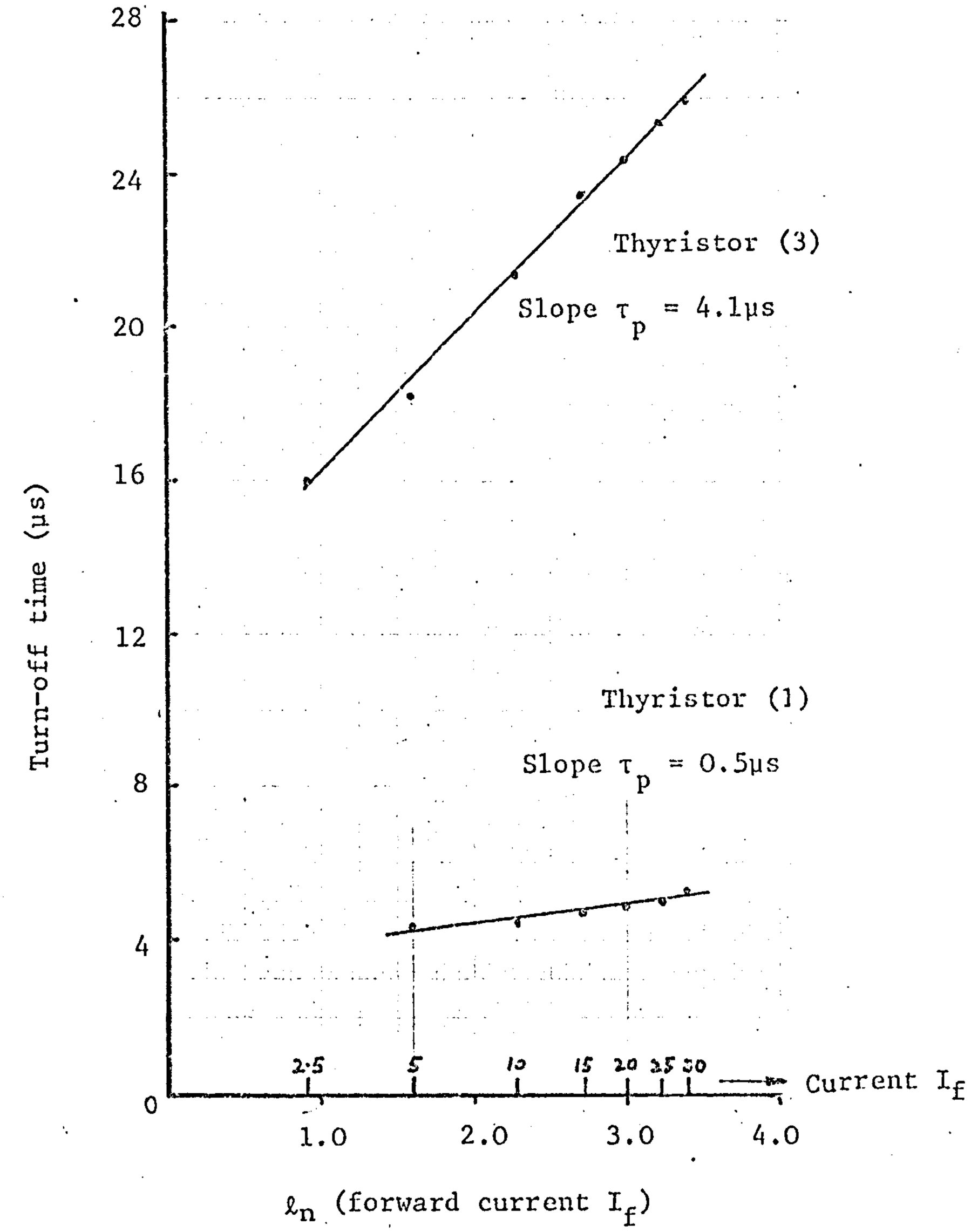

Figure 2.10: Determination of thyristor hole minority-carrier lifetime τ_p.

Zero reverse voltage, reverse current blocked.

$\left|\frac{di}{dt}\right|_{off}$ = 50A/μs, V_{FBO} = 90V, dV/dt = 90V/μs, T_s = 21°C

The chief problem in making measurements on the CRO is the interpretation of the reverse recovery current waveshape. The idealised waveform is given in Figure 2.11(a), while that relating to the two diodes tested is shown in Figure 2.11(b); the latter corresponds to an overdriven reverse bias condition. Kuno [22] derives the following expressions for the various time components given in the waveforms:

when not overdriven (Figure 2.11(a)),

$$t_s = \tau_f\left[\ell_n\left(1 + \frac{I_f}{I_{ro}}\right) - \ell_n\left(1 + \frac{\tau_r}{\tau_f}\right)\right], \qquad (2.5)$$

when overdriven (Figure 2.11(b)),

$$t_o = R_o C_J\left[\ell_n\left(1 + \frac{I_{rp}}{I_f}\right) - \ell_n\left(1 + \frac{\tau_f}{\tau_r}\right)\right], \qquad (2.6)$$

In both cases, the decay time is

$$t_d = 2{\cdot}3\left[\frac{\tau_r + R_o C_J}{1 + \tau_r/\tau_f}\right], \qquad (2.7)$$

where τ_f is the constant relating the total instantaneous excess forward charge and forward current, and τ_r similarly relates reverse charge and current. It will be assumed that these two constants are both equal to the minority-carrier lifetime τ_p. R_o and C_J are the turn-off circuit resistance and diode junction capacitance respectively.

The above equations may be used in two ways to determine τ_p. The various current and time components shown in Figure 2.11(b)

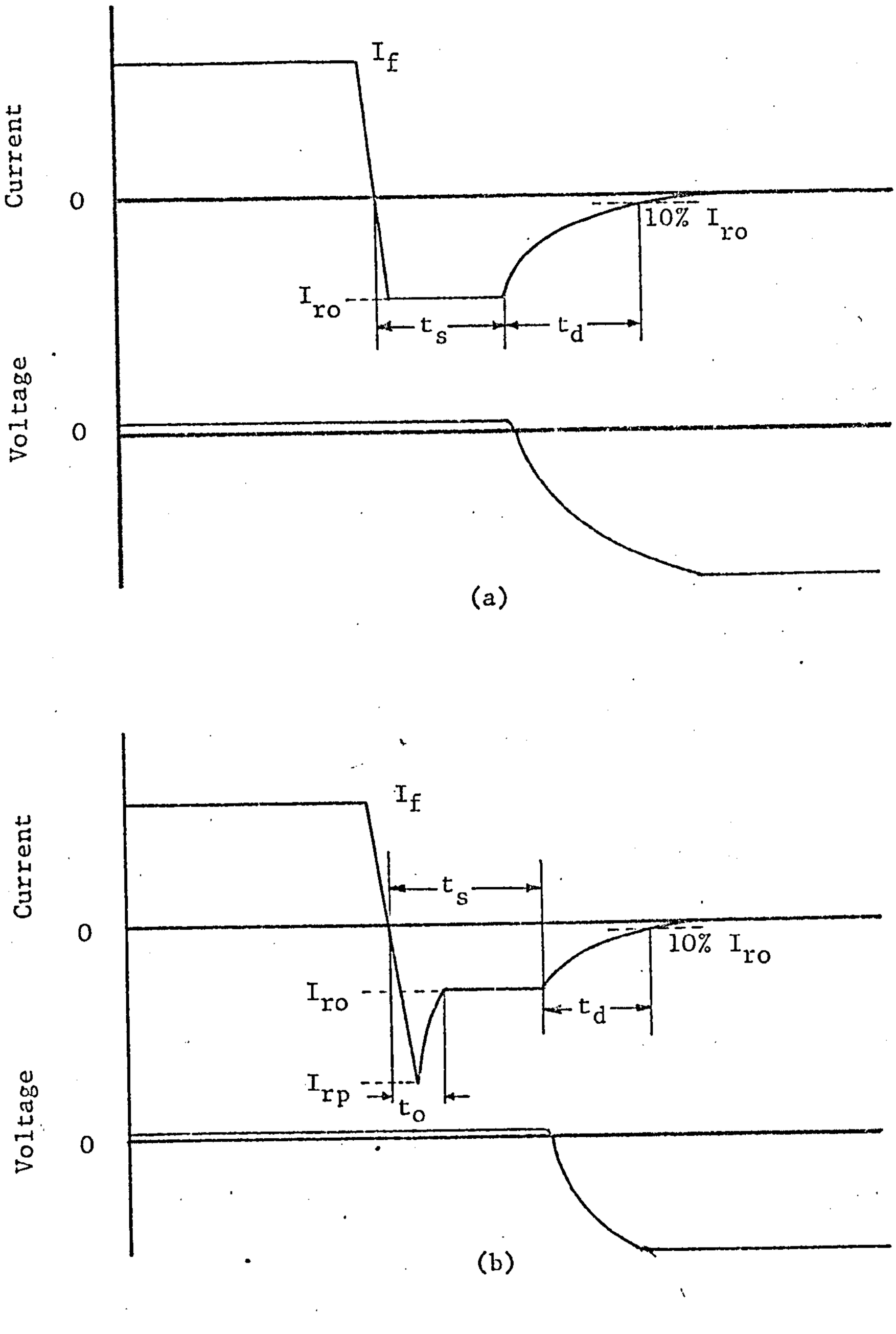

Figure 2.11: Diode reverse recovery waveforms

(a) When not overdriven

(b) When overdriven

are established by test under various drive conditions. Firstly, neglecting I_{rp}, t_s is plotted to a base of $\ell_n(1 + I_f/I_{ro})$ as shown in Figure 2.12. The resulting slope gives τ_p (equation 2.5). Secondly, t_o is plotted against $\ell_n(1 + I_{rp}/I_f)$, the slope giving R_oC_J (equation 2.6). R_oC_J is then used with t_d in equation (2.7) to obtain τ_p (= τ_r = τ_f). For the diodes tested, $R_oC_J << \tau_p$; therefore from equation (2.7),

$$\tau_p = 0{\cdot}87t_d, \text{ approximately.}$$

Kao and Davis[23] show that very simple relationships exist between τ_p and t_s, assuming the idealised waveform of Figure 2.11(a). These relationships depend on how hard the diode is driven by reverse voltage; in particular, if the maximum reverse current is equal to the forward current, then

$$\tau_p = 1{\cdot}25t_s. \qquad (2.8)$$

Applying this to the overdriven waveform (Figure 2.11(b)), with the reverse voltage adjusted to give $I_{rp} = I_f$ for each setting of I_f, gives measured values of t_s which are sensibly constant.

The average values of τ_p obtained by using the above three methods of measurement are quoted in Table 2.1, and are in acceptable agreement. Other methods have proved to be not so effective. For example, a number of authors[18,19,24] conclude that when $\left|\frac{di}{dt}\right|_{off}$ is very high, (i.e. $I_{rp} >> I_f$), recombination can be neglected, and hence all the stored charge is removed.

Then

$$Q_r = \tau_p I_f .$$

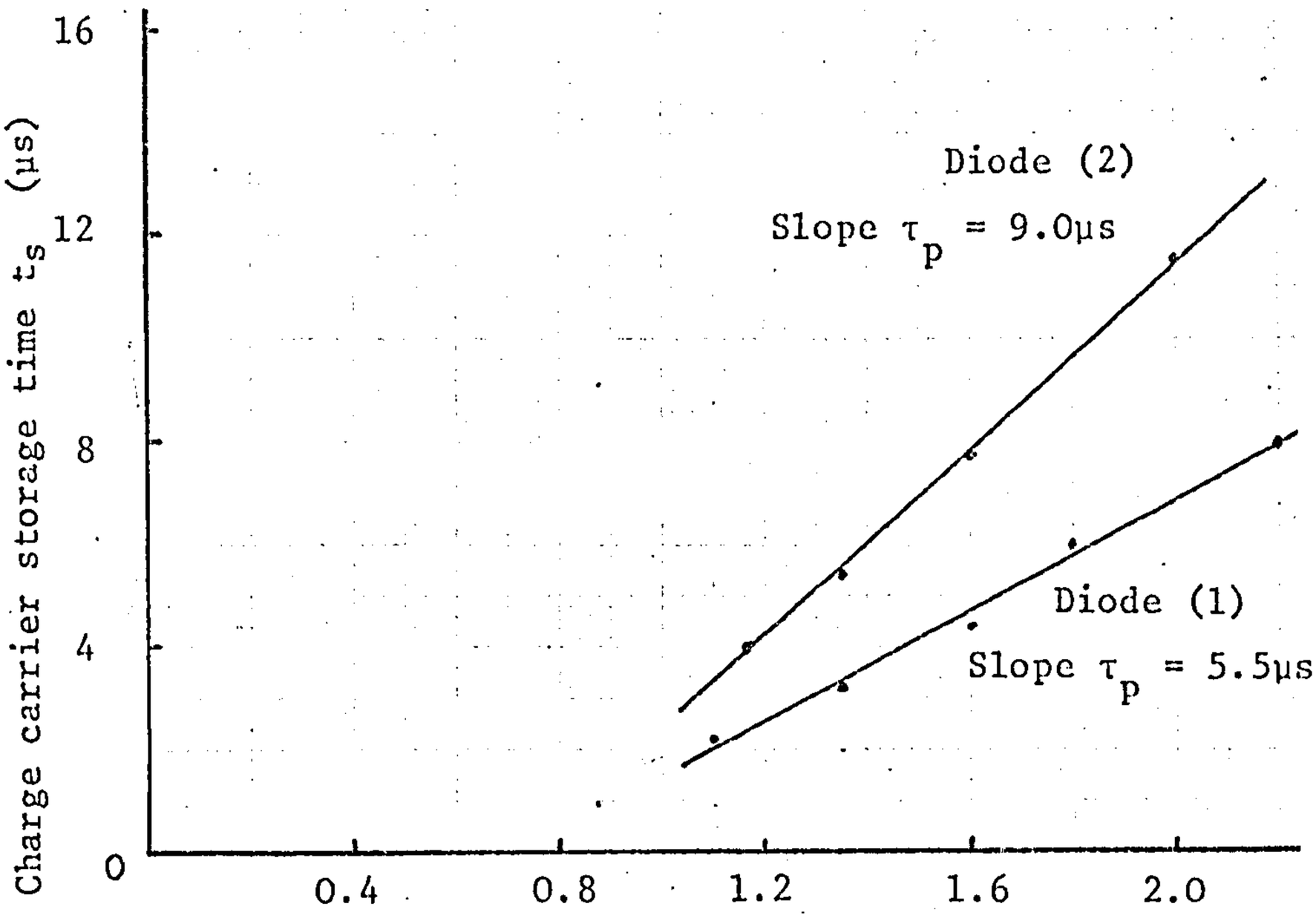

Figure 2.12: Determination of diode minority-carrier lifetime τ_p.

Diodes (1) TAG type MP100 (40A, 1000V)
(2) IR type 25G100 (25A, 1000V)

I_f = 20A, constant; reverse voltage, I_{ro} and $\left|\frac{di}{dt}\right|_{off}$ are variable;

T_s = 21°C.

Method of measurement	Measured lifetime (μs)	
	Diode (1)	Diode (2)
Kuno; Equation (2.5).	5.5	9.0
Kuno: Equations (2.6) and (2.7).	4.5	9.8
Kao and Davis: Equation (2.8).	5.3	9.8

Table 2.1: Measured values of diode minority carrier lifetime τ_p

Diode (1) - TAG type MP100, (40A, 1000V).

Diode (2) - IR type 25G100, (25A, 1000V).

Applying this result to the graphs of Figure 2.9, condition $I_{rp} >> I_f$ holds at very low forward currents, and the initial (maximum) slope should give τ_p. However, the values so obtained for the two diodes are approximately double those of Table 2.1.

2.9 GENERAL COMMENTS

The characteristics given in this chapter illustrate the thyristor and diode behaviour at turn-off. Some differences may be expected with other, perhaps larger, types of these devices, but the same basic principles are applicable. It is fortunate that reverse voltage does not have a great influence on turn-off time and on removed reverse recovery charge. Hence, previously measured values of these parameters can be used with confidence in the design of voltage sharing networks, in the knowledge that they are going to be little altered by the sharing network's performance.

CHAPTER 3

THE OPERATION OF THYRISTORS IN SERIES

3.1 INTRODUCTION

Thyristors of the same type exhibit wide differences in a number of characteristics which are particularly important to their sharing of the total applied voltage when connected in series. These are listed below:

(a) Differences of leakage impedance result in uneven steady-state and low-frequency blocking voltage distribution.

(b) Differences of anode-cathode capacitance produce uneven transient voltage distribution. The effective capacitance comprises the stray inter-electrode capacitance in parallel with the internal depletion layer capacitance of the thyristor. The latter is voltage-dependent[25].

(c) Differences of turn-on time produce an excessive forward voltage transient across those thyristors which are slower to develop forward conduction. These devices then trigger by forward breakover. This is not usually damaging to the thyristor, provided its increased internal switching dissipation is not excessive. Turn-on by this method is not recommended, however.

(d) Differences of reverse recovery time lead to excessive reverse voltage across the faster recovery thyristors.

If this exceeds the reverse voltage rating, failure of the device is likely unless it is of the controlled avalanche type, in which case it must be suitably derated.

(e) Differences of thyristor turn-off time may lead to some devices failing to accept re-applied forward blocking voltage.

3.2 STANDARD TECHNIQUES

3.2.1 The basic voltage sharing network

The basic network usually adopted for improving thyristor voltage sharing is shown in Figure 3.1. Its operation is well covered in the literature[8,9,10,17] and it has been widely used, sometimes with modification, for a.c. line commutated applications at very high voltages[26,27,28,29]. The resistive-capacitive (R-C) components are used across series connected diodes to counteract voltage mis-sharing produced by the effects of (a), (b) and (d) listed in section 3.1, which are applicable to the reverse biased condition.

3.2.2 The functions of series inductor L

In practice, L may be stray or a component added to aid voltage sharing. Its purpose can be fourfold. Firstly, it controls the di/dt of fast-rising anode currents at turn-on[31]. Secondly, the L-R-C combination controls, if necessary, the rate of rise of forward blocking voltage to avoid dV/dt triggering of the thyristors (section 2.4,

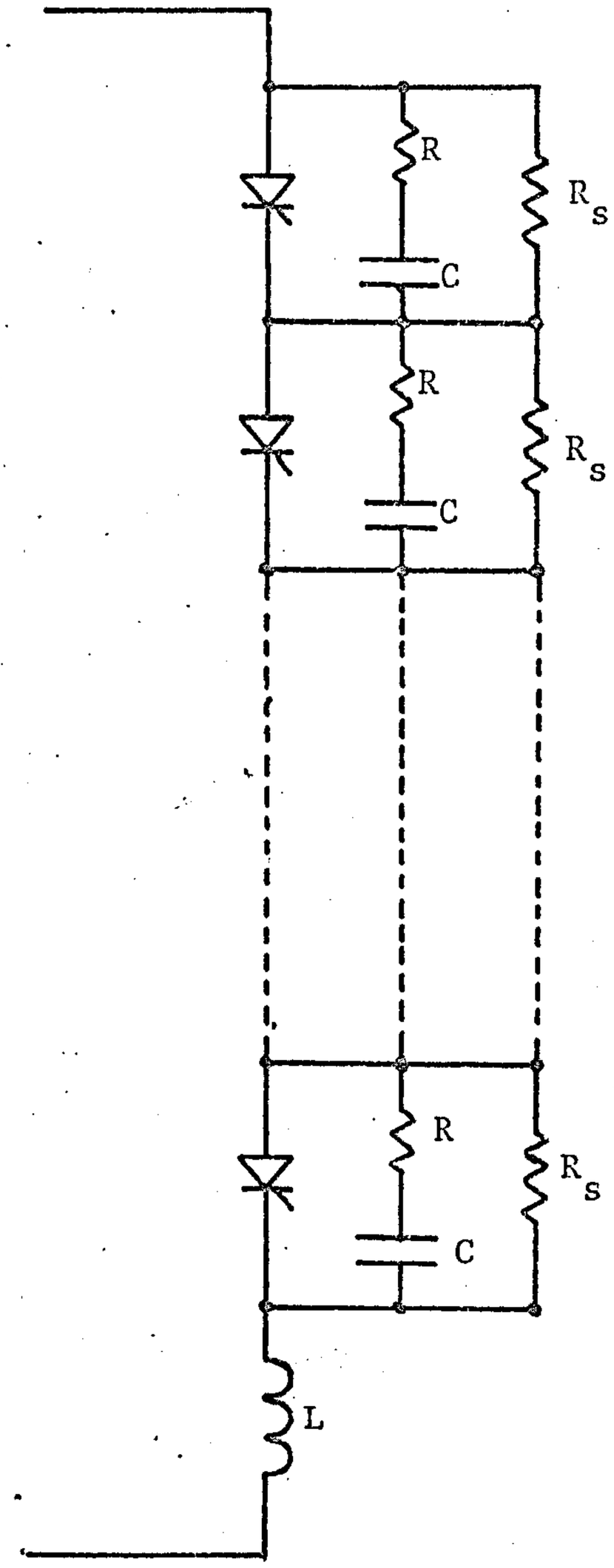

Figure 3.1: Basic R-C voltage sharing network

para (d)). Since C is usually large, it has no effect on the initial (maximum) dV/dt at zero voltage. Then,

$$\text{maximum thyristor } dV/dt = \frac{V_F R}{L} \quad [17]. \tag{3.1}$$

Again in conjunction with the R-C components, L limits the transient forward overvoltage across the slow turn-on thyristors. It is advantageous with series thyristors to use heavy gate drive to minimise any turn-on time difference Δt_{on}, which will then be only a very few microseconds. As C is large, the current flow round a slow turn-on thyristor during Δt_{on} is controlled largely by L and R. Assuming the worst case of just one slow turn-on thyristor, the voltage applied across its R-C components and L in series is $V_F(1 - 1/n)$, where V_F is the forward line voltage.

Then,

$$\text{maximum } \frac{di}{dt} = \frac{V_F}{L}\left(1 - \frac{1}{n}\right).$$

Assuming this di/dt to be constant over short interval Δt_{on}, the peak of the voltage transient across the slowest turn-on thyristor ΔV_F is given by

$$\Delta V_F = \frac{di}{dt} \Delta t_{on} R$$

$$\Delta V_F = \frac{V_F}{L} R \Delta t_{on}\left(1 - \frac{1}{n}\right). \tag{3.2}$$

The above is based on the simplifying assumption of instantaneous collapse of forward blocking voltage, and is often sufficient in practice. For greater accuracy, the summed differences of previously measured thyristor anode-cathode volt-second areas should be used for

$\left(V_F \Delta t_{on}(1 - 1/n)\right)$ in equation (3.2)[17].

Finally, L reduces the rate of fall of forward current at turn-off, leading to a reduction of removed reverse recovery charge.

The series inductance must be sufficient to satisfy any or all of the first three requirements if necessary; the effects of reverse recovery charge can be largely controlled by the parallel components (see section 3.2.4). Added inductance values are typically between twenty and a few hundred microhenries. The use of non-linear inductors is considered later.

3.2.3 The function of shunt resistors R_s

Resistors R_s improve the steady-state and low frequency voltage distribution. R_s usually has a value of about one tenth of the minimum thyristor leakage impedance [3,10,30], and hence swamps any inequalities.

3.2.4 The functions of shunt capacitors C

Capacitors C perform a number of duties. They improve transient voltage distribution, and dV/dt distribution, by swamping the device anode-cathode capacitance and stray capacitance to earth. The presence of R is, however, detrimental to this function.

It is at turn-off that the capacitors fulfil their most onerous role. The high, hole-storage voltage spike induced across L by the abrupt cessation of reverse recovery current flow (section 2.4) is both reduced and distributed evenly along the string by the

capacitors. The R-C branches across the faster reverse recovery thyristors provide a current path for the reverse recovery current of the slower thyristors and, ideally, prevent excessive voltages appearing across the former. The final voltage unbalance with the capacitor chain charged to the full reverse voltage is dependent on the differences of removed thyristor reverse recovery charge and the capacitance of C. Obviously, by making C very large, the voltage unbalance can be minimised, but this has its disadvantages. Device selection can only economically be used to provide thyristors having parameters of reverse recovery time and charge Q_r within a restricted range, so that the choice of capacitors C is still governed by this consideration[8,9,10,17,30] (see section 3.3.1). Typically, C lies between 0.1 and 1.0μF in practice, though if reverse recovery current effects were absent, 0.01-0.05μF would usually be adequate.

3.2.5 The functions of shunt resistors R

Resistors R basically perform two functions. They damp any oscillation between inductor L and capacitors C when the thyristor blocking voltage is applied. R is essential for limiting thyristor dissipation at turn-on when the capacitors, charged by the forward blocking voltage, discharge round the local loop formed by the switching thyristor. It also serves to damp any oscillation caused by local loop inductance at turn-on.

The value of R should be as low as possible due to its adverse effects on voltage sharing performance. Equations (3.1) and (3.2) show that R greatly controls the forward blocking dV/dt and turn-on overvoltage. Its effect at turn-off is discussed in the next section. Values of 20-100 ohms are usual.

3.3 VOLTAGE SHARING CONSIDERATIONS AT TURN-OFF

3.3.1 Reverse voltage distribution

The time constant $C(R_s + R)$ of charge equalisation for capacitors C in the resistive-capacitive chain is usually very much longer than the commutation interval with forced commutation. Hence, the effect of R_s on the voltage distribution during turn-off is very small, and its presence will be neglected. When reverse voltage is applied to the thyristor string to initiate turn-off, the thyristors block in the order of their reverse recovery times. Capacitors C should be large enough to satisfy three conditions:

(a) The impedance presented by the operative sections of the R-C chain to the reverse current flow of the slower recovery thyristors, must not impair their reverse recovery.

(b) The final reverse voltage across the fastest reverse recovery thyristor, with the capacitors of the R-C chain fully charged, must not be excessive.

(c) Sufficient reverse voltage must be impressed across the slowest reverse recovery thyristor to at least turn it off.

The prediction of individual thyristor voltage, using reverse recovery charge concepts, is made as follows. Let Q_{r1} be the minimum removed charge from the fastest reverse recovery thyristor (No. 1) in the string, and Q_{r2}, Q_{r3}, etc. be successively increasing values from thyristors 2 and 3 respectively to a maximum of Q_{rn} from the slowest n^{th} thyristor. When the latter has just blocked, the

reverse voltage across the fastest recovery thyristor is $(Q_{rn}-Q_{r1})/C$. If the R-C chain is further charged to the full reverse line voltage V_R, each capacitor gaining additional voltage V_{rn} equal to that finally across the slowest recovery thyristor, the final reverse voltage V_r across any thyristor having a removed charge Q_r is given by

$$V_r = \frac{Q_{rn} - Q_r}{C} + V_{rn}. \tag{3.3}$$

For the fastest recovery thyristor,

$$V_{r1} = \frac{Q_{rn} - Q_{r1}}{C} + V_{rn}$$

$$V_{r1} = \frac{\Delta Q_{r_{max}}}{C} + V_{rn}. \tag{3.4}$$

The total reverse voltage V_R across the string is the sum of the individual thyristor reverse voltages, that is

$$V_R = \frac{1}{C}\left[\Delta Q_{rn-1} + \Delta Q_{rn-2} + \ldots \Delta Q_{rn-(n-1)}\right] + nV_{rn}$$

$$V_R = \frac{1}{C} \sum \Delta Q_r + nV_{rn}. \tag{3.5}$$

Basing the choice of C on a given allowable maximum value of V_{r1}, and assuming the worst possible condition of one fast recovery thyristor and all the others equally slow ($\Delta Q_{rn-2} = \Delta Q_{rn-3}$ etc. = 0), then equations (3.4) and (3.5) give

$$C = \frac{(n-1)\,\Delta Q_{r_{max}}}{nV_{r1} - V_R}. \tag{3.6}$$

For a given value of C, the extreme thyristor voltages V_{r1} and

V_{rn}, which are of chief interest, can be obtained by using the average thyristor voltage V_R/n and the average of the removed charge values Q_{rav}. Equation (3.5) can be expressed

$$V_R = \frac{1}{C}\left[n\, Q_{rn} - \sum Q_r\right] + nV_{rn} .$$

Substituting nQ_{rav} for $\sum Q_r$ gives

$$V_{rn} = \frac{V_R}{n} - \frac{1}{C}\left[Q_{rn} - Q_{rav}\right] . \qquad (3.7)$$

Using this equation with equation (3.4) gives

$$V_{r1} = \frac{V_R}{n} + \frac{1}{C}\left[Q_{rav} - Q_{r1}\right] . \qquad (3.8)$$

In addition to the unbalance of final steady reverse voltage across the thyristors, the faster reverse recovery thyristors experience a reverse voltage spike produced by the flow of slow thyristor reverse recovery current through the parallel R component. The magnitude and duration of this spike depends on the spread of the thyristor reverse recovery characteristics and the value of R.

3.3.2 Forward blocking voltage distribution

When the forward blocking voltage V_F is applied to the string after turn-off, a charging current flows through the series capacitors, each receiving the same charge q, where

$$q = \frac{C}{n}\left(V_F + V_R\right) .$$

Hence, the final forward voltage V_f following reverse voltage V_r

across any one thyristor is

$$V_f = \frac{1}{n}\left(V_F + V_R\right) - V_r. \qquad (3.9)$$

The maximum forward voltage therefore occurs across the slowest reverse recovery thyristor which has experienced minimum reverse voltage (i.e. $V_r = V_{rn}$). This is a disadvantage from turn-off considerations because this thyristor has the longest turn-off time.

3.3.3 The effect of applied voltage waveform

The ideal voltage sharing network would produce, across each thyristor, a replica of the applied string voltage waveform having $(1/n)^{th}$ of its magnitude. For all waveforms except that having a step applied forward blocking voltage, any uneven reverse voltage distribution results in the reverse bias time of the faster recovery thyristors being increased and that of the slower thyristors reduced, in comparison with the reverse bias time of the string. As the latter thyristors have the longest turn-off time, the disadvantage of this is obvious. Figure 3.2 demonstrates the effect with four waveshapes met in practice, the thyristor peak reverse voltages being spread between maximum and minimum values V_{r1} and V_{rn} respectively.

This effect is of particular importance in applications where the reverse voltage is variable. Satisfactory turn-off must be taken as that where all thyristors in the string turn-off under reverse bias. Therefore the allowable minimum value of V_{rn} is governed by the turn-off time of the slowest recovery

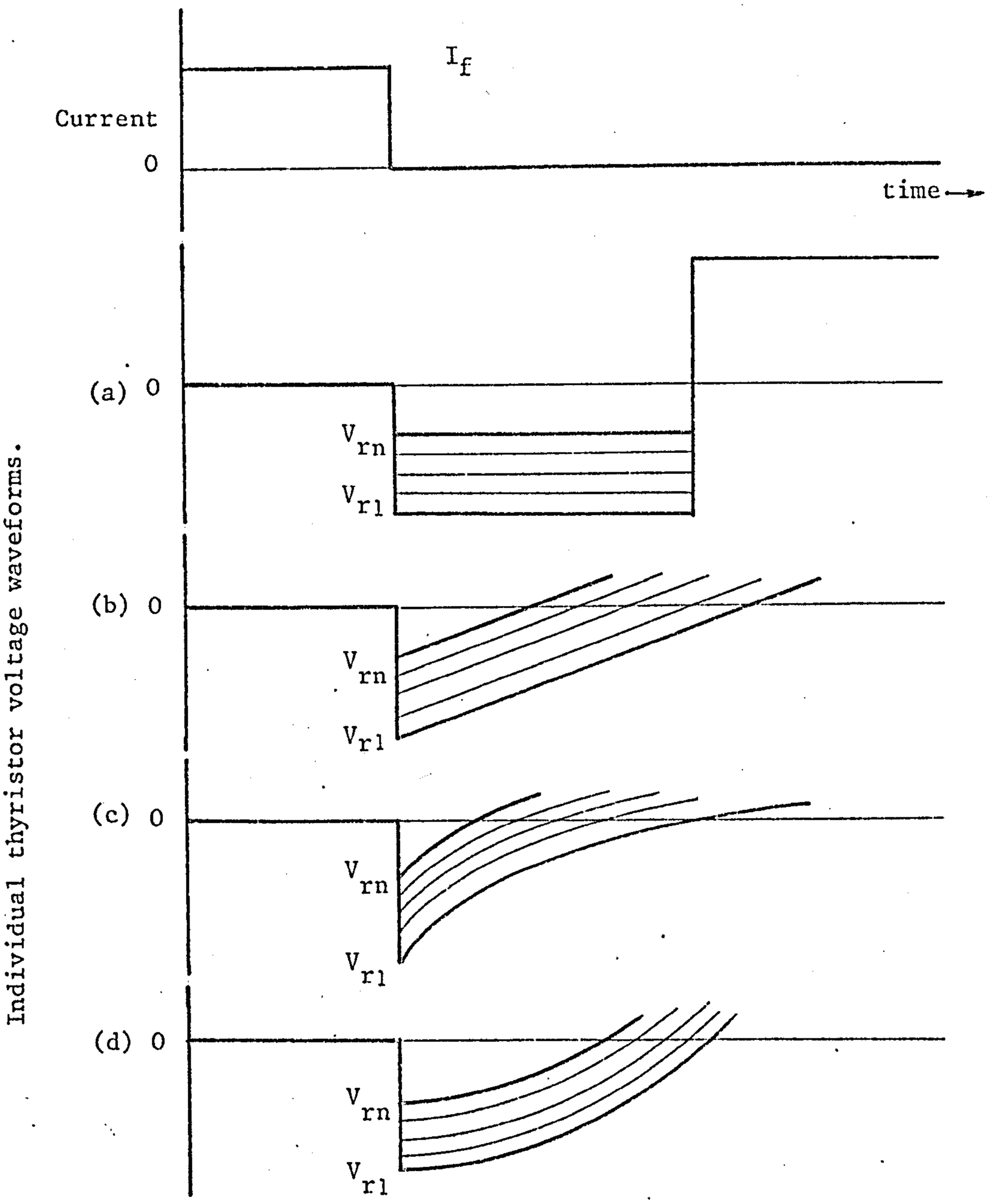

Figure 3.2: Idealised waveforms showing the effect of uneven reverse voltage distribution on thyristor reverse bias time.

(a) Constant reverse voltage
(b) Linearly changing reverse voltage
(c) Exponentially " " "
(d) Cosine form " " "

thyristor. Considering the linear voltage waveform (Figure 3.2(b)) of slope α, then,

$$\text{allowable minimum } V_{rn} = \alpha T_{off}. \tag{3.10}$$

Equation (3.5) can be used to define the corresponding allowable minimum string voltage V_R.

3.3.4 Thyristor string derating factor

It is the usual practice to include more thyristors in series than would be indicated by a simple division of the repetitive peak string voltage by the repetitive peak voltage rating of the thyristors. This is to allow for a degree of uneven voltage distribution , for reverse voltage spikes (sections 3.2.4 and 3.3.1), and for any line-borne transients. In h.v.d.c. practice it is also usual to provide some built-in redundancy - that is, to allow for failure of a small proportion of the thyristors - so that the thyristor 'valve' may remain in service until it can conveniently be withdrawn for replacements to be made. To facilitate quotation of the over-voltage allowance made in this way, a string voltage derating factor is frequently used, this being defined as

$$f_s = \frac{\text{Maximum repetitive voltage across the string}}{n \times \text{thyristor repetitive voltage rating}}. \tag{3.11}$$

Typical values of f_s are between 0.25 and 0.5. Alternatively, the inverse of f_s may be quoted as a safety, or design, factor[29,32].

In order to provide a basis for demonstrating the voltage sharing performance produced experimentally by the different arrangements

considered in this thesis, an experimental voltage derating factor will be defined in terms of the measured peak string voltage $\hat{V}_{sm}$ and the measured maximum peak thyristor voltage (including any spike) $\hat{V}_{tm}$. As both forward and reverse voltage distributions must be quoted separately, two experimental voltage factors, f_{fm} and f_{rm} respectively, are required; $\hat{V}_{sm}$ and $\hat{V}_{tm}$ are measured in the appropriate direction. Then,

$$f_{fm} \text{ (or } f_{rm}) = \frac{\hat{V}_{sm}}{n\ \hat{V}_{tm}} .$$

A value of unity for f_{fm} or f_{rm} indicates perfect voltage equalisation. Letting the thyristor voltage for this condition be $\bar{V}_{tm}$ $(= V_{sm}/n)$ gives

$$f_{fm} \text{ (or } f_{rm}) = \frac{\bar{V}_{tm}}{\hat{V}_{tm}} . \qquad (3.12)$$

$\bar{V}_{tm}$ will be the average thyristor voltage with uneven distribution provided the individual thyristor voltages sum to the total value across the string. This holds for final steady voltages but not for spikes.

3.4 EXPERIMENTAL RESULTS

3.4.1 Test circuit

The circuit used for investigating voltage sharing network turn-off performance (Figure 3.3) is a modified version of a well-known d.c. chopper circuit. It has its operating sequence timed to coincide with the peak of each positive half-cycle of the a.c.

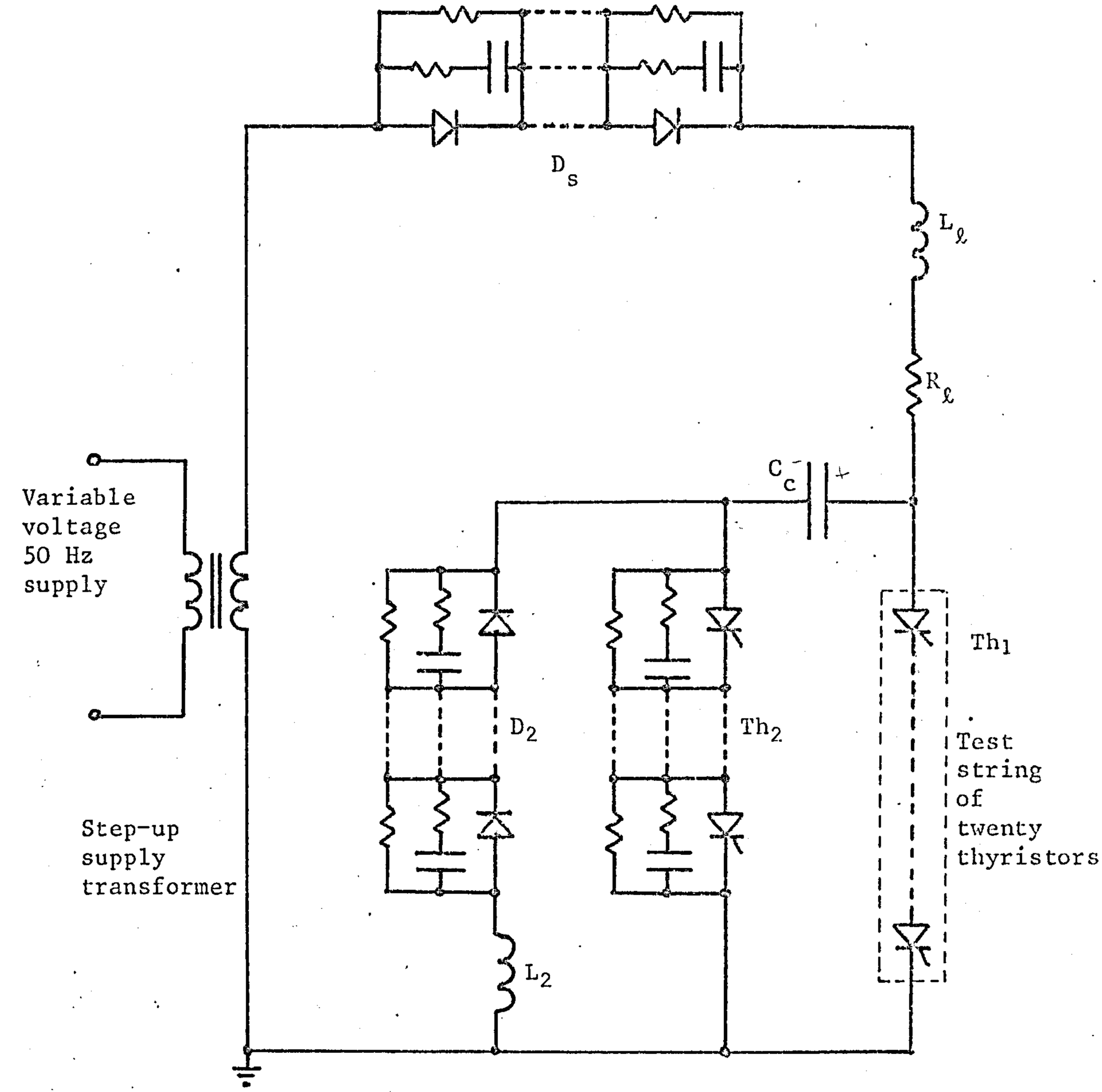

Figure 3.3: Voltage sharing network test circuit.

supply voltage. Series diodes D_S block the negative half-cycle and also allow the energy stored in L_ℓ, when thyristors Th_1 are turned off, to boost the commutating capacitor C_c voltage from the 1500V supply peak to 5kV. The latter appears as the forward blocking voltage across Th_1. Only the main circuit components are shown together with the R-C voltage sharing networks across diodes D_S, D_2 and turn-off thyristors Th_2. The voltage sharing networks for the test thyristor string Th_1 are omitted since they are described, where appropriate, in this and the following chapters.

The operating sequence is as follows. Th_2 is first gated to charge C_c. Th_1 is then gated and it conducts two current components: an approximately exponentially rising load current supplied from the source, and a commutating capacitor charge reversal current flowing through L_2 and D_2, the latter blocking the current after one oscillatory half-cycle. Th_2 is gated to turn off Th_1 after 550μs conduction and C_c discharges and recharges positively through R_ℓ, L_ℓ, Th_2 and the supply, thereby receiving its voltage boost. Component details appear in Appendix I and the circuit is fully analysed in Appendix II. Oscillograms of Th_1 current and voltage for the test conditions employed are shown in Figure 3.4.

3.4.2 Results obtained

The basic resistive-capacitive voltage sharing network of Figure 3.1 gives the voltage sharing performance depicted in Table 3.1. Thyristor leakage is small enough to allow R_s to be dispensed with, and no series inductor L is necessary due to the thyristor di/dt, and

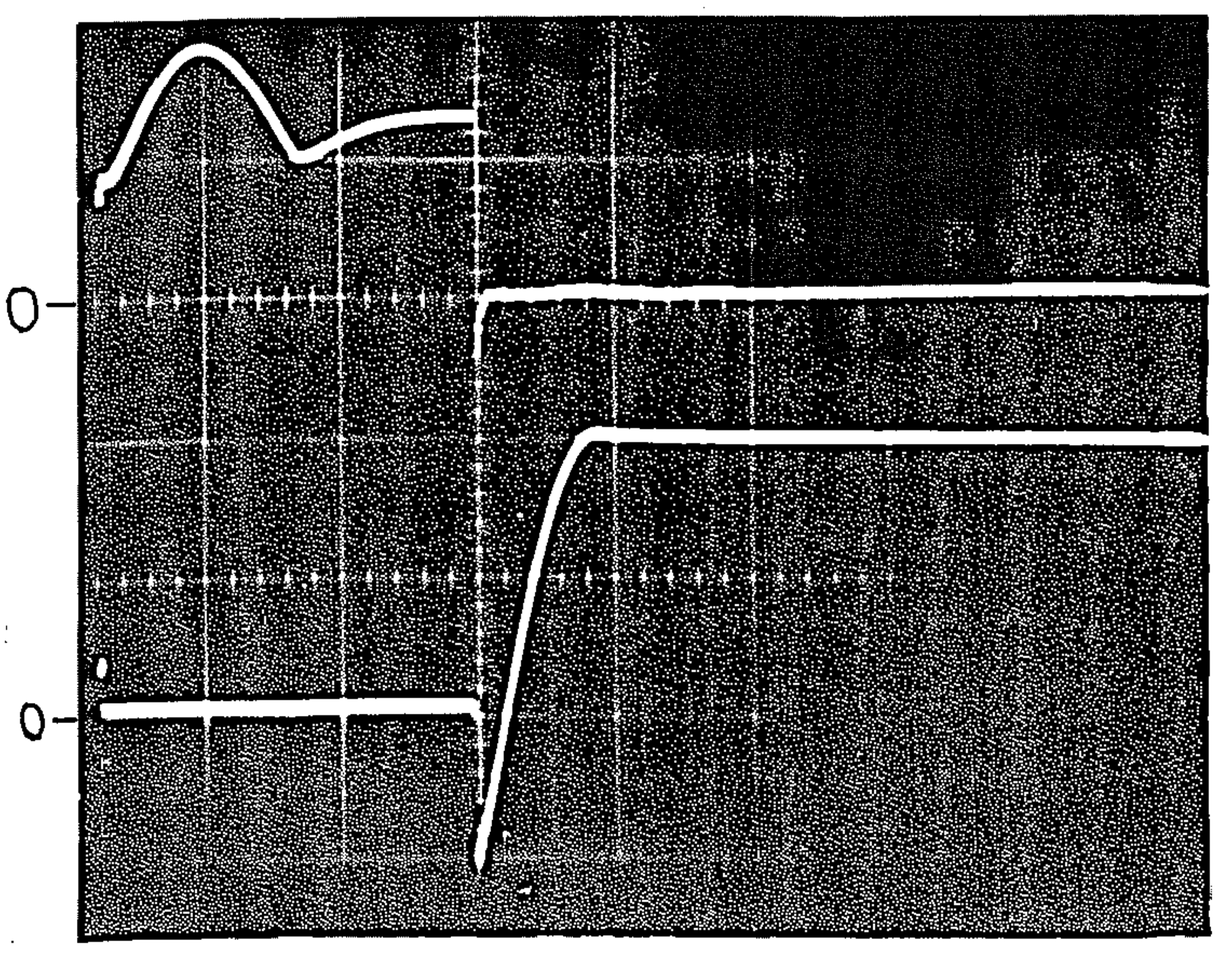

Figure 3.4: Test thyristor string Th_1 current and voltage waveforms

(a) Current, (20A/cm, 200μs/cm).

(b) Voltage, (2.5kV/cm, ").

Test circuit - Figure 3.3.

	Voltage sharing components			Measured thyristor voltages with predicted values shown ( )				String voltage factors	
Row	C (μF) 20% tolerance	R (Ω) 5% tolerance	R_s (Ω)	Maximum reverse spike (across fastest recovery thyristor) (V)	Maximum reverse steady peak (across fastest recovery thyristor) (V)	Minimum reverse steady peak (across slowest recovery thyristor) (V)	Maximum forward peak (across slowest recovery thyristor) (V)	f_{rm}	f_{fm}
(a)	0.5	100	-	615	155 (153)	100 (113)	280 (272)	0.47	0.89
(b)	0.5	22	-	260	145 (152)	115 (112)	280 (272)	0.77	0.89
(c)	0.1	22	-	270	225 (229)	35 (27)	375 (377)	0.74	0.72

Table 3.1: Voltage sharing performance of the basic R-C network (Figure 3.1)
Test circuit - Figure 3.3

overvoltage, at turn-on being controlled by L_ℓ and L_2. Figure 3.5 shows plotted values of measured individual thyristor voltages.

Throughout the investigation, thyristor voltage measurements have been made from the CRO waveforms by using two Tektronics type P6013 high voltage probes supplying a type Z differential amplifier unit plugged into a type 555A Tektronics oscilloscope. Since probe tolerance seriously reduces the amplifier common mode rejection ratio, the readings quoted are always the average of the two obtained by connecting the probes alternate ways into the amplifier. An accuracy of ±5V is the best that can be expected for the individual thyristor steady peak voltage measurements; the accuracy for spikes is lower. Current waveforms are obtained by using a clip-over probe (Hewlett Packard type 1110A), with the associated amplifier (type 1111A).

3.5 DISCUSSION OF EXPERIMENTAL RESULTS

The results of Table 3.1 show that, with the high values of C used, the magnitude of the reverse voltage spike across the fastest recovery thyristor (section 3.3.1) depends solely on the value of R (c.f. row (a) with rows (b) and (c)). This is reflected in the values of f_{rm}. Comparison of rows (a) and (b) with row (c) illustrates the more uniform steady peak voltage distribution produced by the larger capacitors C. The reverse voltage extremes are much less diverse and the maximum forward voltage is lower, giving a higher value for f_{fm}. The predicted steady peak voltages (using equations 3.3, 3.4 and 3.5) agree well with those measured. The required values of removed reverse recovery charge Q_r, previously measured under similar circuit

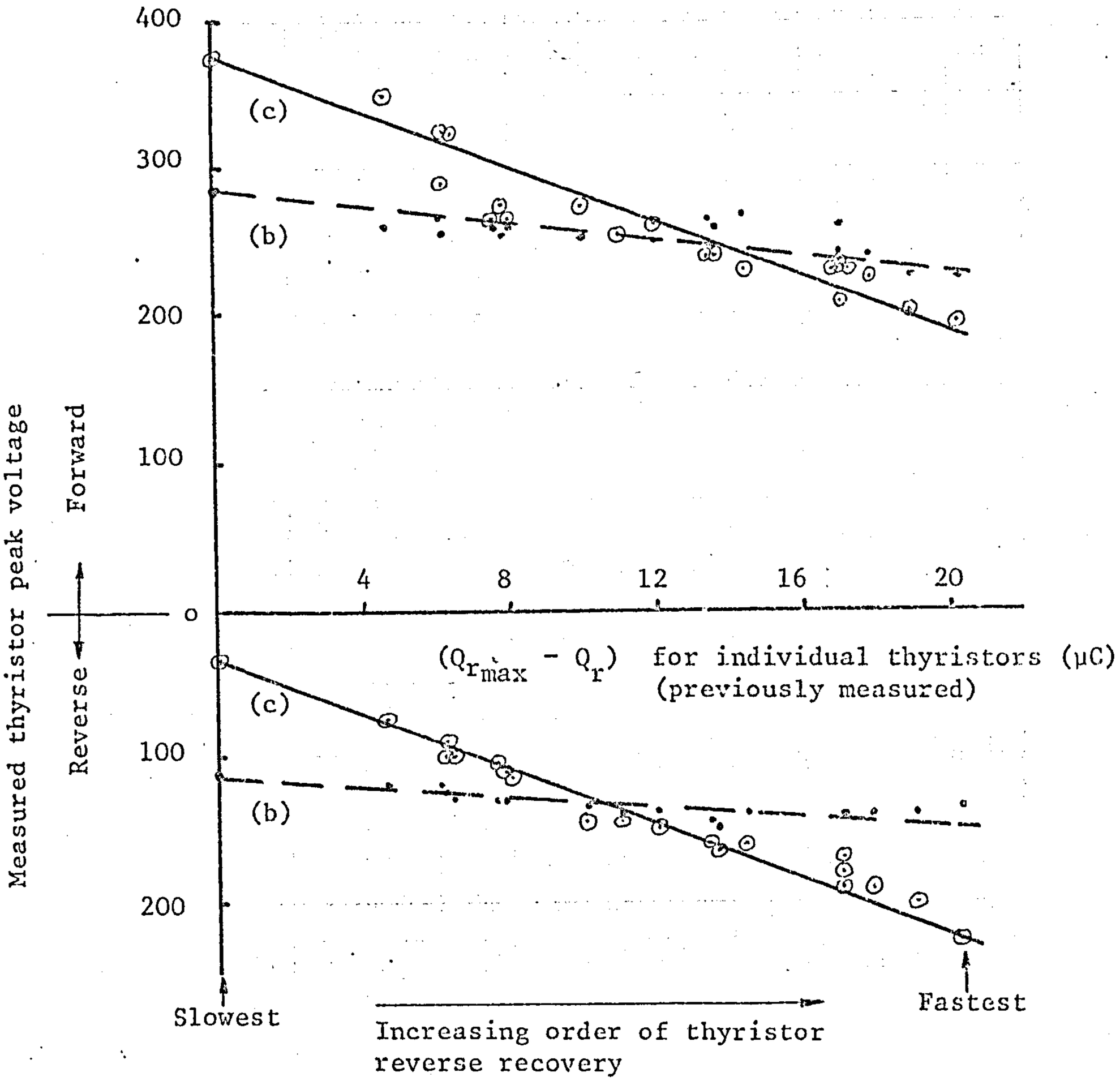

Figure 3.5: Measured peak voltages, neglecting any reverse spike, across each thyristor in the test string of twenty in series with the basic R-C sharing network.

(b) Components as Table 3.1, row (b)

(c) " " " , row (c)

Test circuit - Figure 3.3.

conditions by the manual circuit (section 2.6.1), are given in Table I.1.

The dependence of the steady peak reverse and forward voltage distributions on the value of C is further demonstrated by Figure 3.5 which shows measured voltage plotted against ΔQ_r (= $Q_{r_{max}} - Q_r$) for each thyristor. The graphs realistically express equations (3.3) and (3.9), the slopes of both forward and reverse voltage plots being approximately 1/C in each case.

3.6 DISADVANTAGES OF THE BASIC R-C SHARING NETWORK

3.6.1 Voltage sharing performance at turn-off

The two inadequacies of the R-C network in fulfilling its voltage sharing function with forced commutation have been discussed in the previous section. Summarised, these are:

(a) A possibly large, uncontrolled reverse voltage spike is generated across the faster reverse recovery thyristors. This defines the required thyristor reverse voltage rating.

(b) Approximately uniform steady reverse and forward voltage distribution can only be achieved by using a relatively large value of C. Apart from space and cost considerations this has disadvantages which are described in the following sections.

3.6.2 Voltage sharing network losses

The sharing network losses occur principally in components R_s and R. The total loss P_s in resistors R_s is given by

$$P_s = \frac{(\text{r.m.s. string voltage})^2}{n\ R_s} \text{ watts.} \qquad (3.13)$$

In order to determine the total energy loss W_R per cycle in resistors R, let ΔV be any variation of final thyristor reverse voltage from the mean value V_R/n after reverse recovery. The subsequent forward voltage will also differ from the average value by the same amount ΔV, but in the opposite sense. Assuming a normal distribution, where the mean voltage is equal to the median value between the extremes, then the total energy loss becomes

$$W_R = C \sum \left(\frac{V_R}{n} \pm \Delta V\right)^2 + C \sum \left(\frac{V_F}{n} \mp \Delta V\right)^2$$

$$= \frac{C}{n}\left(V_R^2 + V_F^2\right) + 2C \sum \Delta V^2$$

$$W_R = \frac{C}{n}\left(V_R^2 + V_F^2\right) + \frac{2}{C} \sum \left(Q_{rav} - Q_r\right)^2. \qquad (3.14)$$

The two separate components of energy loss in equation (3.14) are firstly, that which represents loss under equalised voltage conditions and secondly, the additional loss caused by uneven voltage distribution. Neglecting voltage unbalance, the energy loss is proportional to capacitance C. The added loss due to unbalance is inversely proportional to C. Reducing C therefore reduces the total loss but increases the loss component caused by

uneven distribution, which may then amount to about 10% of the total. The energy loss is independent of the value of R. The power loss ($W_R \times f$) is proportional to frequency; typical values of C therefore prohibit the use of high operating frequencies if excessive voltage sharing network loss is to be avoided.

3.6.3 Drain of commutating energy

With force-commutated applications, the R-C networks across the thyristor and diode strings can produce a serious drain of energy from the commutating capacitor. The result is a lowering of the reverse biasing voltage across the thyristors and a reduction of circuit output voltage. The drain occurs in two parts:

(a) By exponential discharge through resistors R_s during thyristor and diode blocking periods. The effect is worst at low operating frequencies.

(b) Due to the charging requirement of capacitors C during build-up of blocking voltage. Each time a chain of voltage sharing capacitors is charged by the commutating capacitor C_c, the voltage of the latter falls to a fraction $\left(\frac{C_c}{C/n + C_c}\right)$ of its previous value. The product of all such factors, as required by the operating cycle, allows for the overall voltage drop from this cause. The drop may be partially offset by some capacitor chains discharging into the commutating capacitor.

Only consideration of the particular circuit will allow detailed calculation of these voltage drops. This is done for the application

studied in Chapter 7.

It is appropriate to consider here the charge drawn from the commutating capacitor when it is switched across a thyristor string to reverse bias it for turn-off. The charge flow has three components:

(i) that which cancels the forward current;

(ii) that which supplies the thyristor reverse recovery requirements;

(iii) that which charges the sharing capacitor C chain.

Neglecting the stray capacitance to earth and the minute flow through resistor R_s during the few microseconds interval, the charge flow through any one thyristor and its parallel voltage sharing components is constant. If the commutating capacitor voltage falls from an initial V_{RO} to a final value V_R when reverse voltage has built up across the string, and assuming $\left|\frac{di}{dt}\right|_{off}$ to be constant, then for the fastest (No. 1) reverse recovery thyristor,

$$C_c(V_{RO} - V_R) = \frac{1}{2} I_f^2 \Big/ \left|\frac{di}{dt}\right|_{off} + Q_{r1} + CV_{r1}. \qquad (3.15)$$

For the slowest (n^{th}) recovery thyristor,

$$C_c(V_{RO} - V_R) = \frac{1}{2} I_f^2 \Big/ \left|\frac{di}{dt}\right|_{off} + Q_{rn} + CV_{rn} \qquad (3.16)$$

Subtracting these equations gives the relationship between maximum and minimum thyristor voltages expressed in equation (3.4).

3.6.4 Refinements of the basic R-C network

The basic R-C sharing network (Figure 3.1) has been developed considerably in order to reduce some of its disadvantages, particularly for application to the h.v.d.c. thyristor 'valve'[26,27,28]. The refinements have usually taken the form of dividing the L, C and R components into a number of smaller units, each fulfilling its own particular duty in the overall voltage sharing scheme, thereby obtaining increased effectiveness and, perhaps, efficiency.

The introduction of many more components is likely to reduce the reliability of the equipment, which makes these networks unattractive. In addition, they are unlikely to be satisfactory at high commutating frequencies on account of their losses.

3.7 METHODS OF IMPROVING TURN-OFF PERFORMANCE

The prime reason for uneven thyristor reverse voltage distribution at turn-off is that the series devices produce differing amounts of reverse recovery charge. There are, in principle, two methods of approach for improving turn-off performance:

(a) By use of an added series switching component to block reverse recovery current flow by holding off reverse voltage from the thyristors until their internal excess charge has recombined.

(b) By use of additional shunt components which will allow full charge removal but control the level of reverse (and if necessary, forward) voltage build up across the thyristors.

Any method of achieving better voltage distribution should not significantly increase thyristor turn-off time and should produce little additional drain on the commutating capacitor.

The main voltage sharing networks which have been produced by this investigation are shown in Figure 3.6. Minor variations to these will be described where appropriate in the later chapters. All the networks are suitable, sometimes with modification, for use with series diodes. Those networks which utilise magnetic components in addition to R-C components (Figures 3.6(a), (b) and (c)) have already been reported by the author[9,21].

The novelty of the series saturating reactor SR (Figures 3.6(a) and (g)) lies in basing its design on the reverse recovery process (para (a) above). It is primarily intended for use with R-C components (Figure 3.6(a)). However, although unnecessary from voltage sharing considerations, it introduces advantages when used with parallel voltage regulating diodes (Figure 3.6(g)), and has been used in this way in the final experimental assessment (Chapter 7).

The circuits of Figures 3.6(b) to (g) utilise additional parallel components in the manner of para (b) above; these comprise parallel transformers and voltage regulating diodes. The latter may allow the R-C components to be dispensed with. Parallel-connected voltage regulating diodes have been mentioned as a suitable means of equalising series thyristor voltage distribution[10], though there is only a little evidence of them being employed in high power equipment[33]. An important and difficult problem is to establish the required regulating diode power rating. This is discussed in Chapter 6.

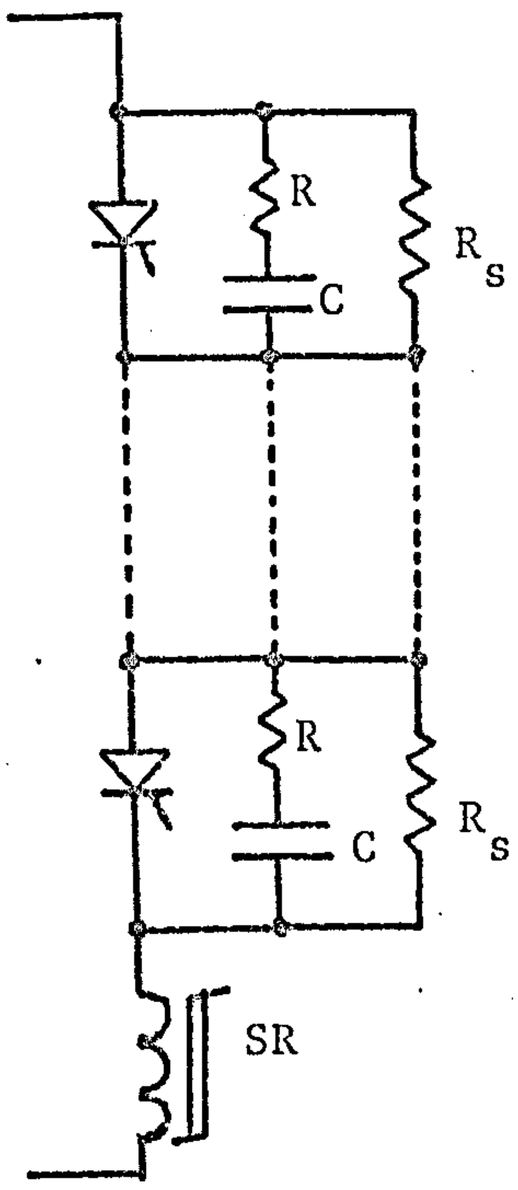

(a)

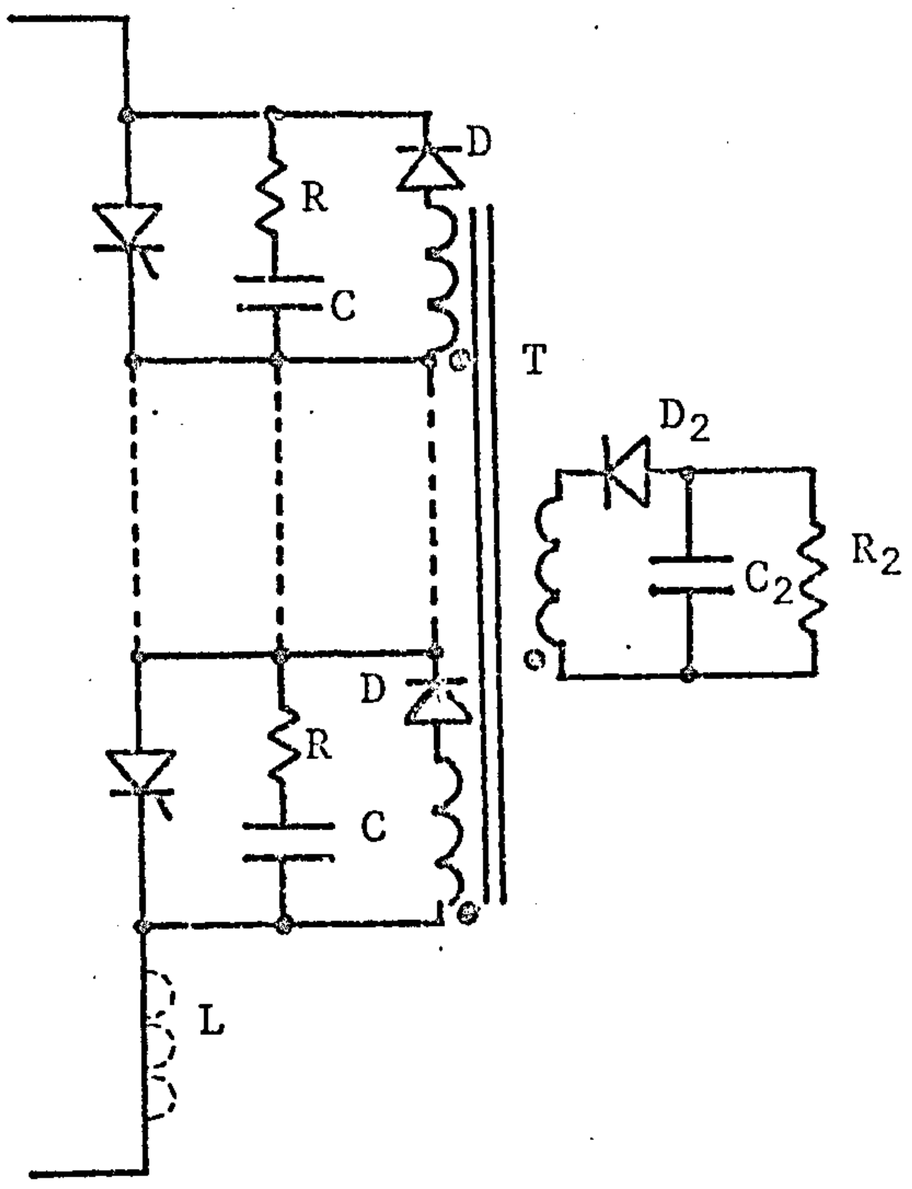

(b)

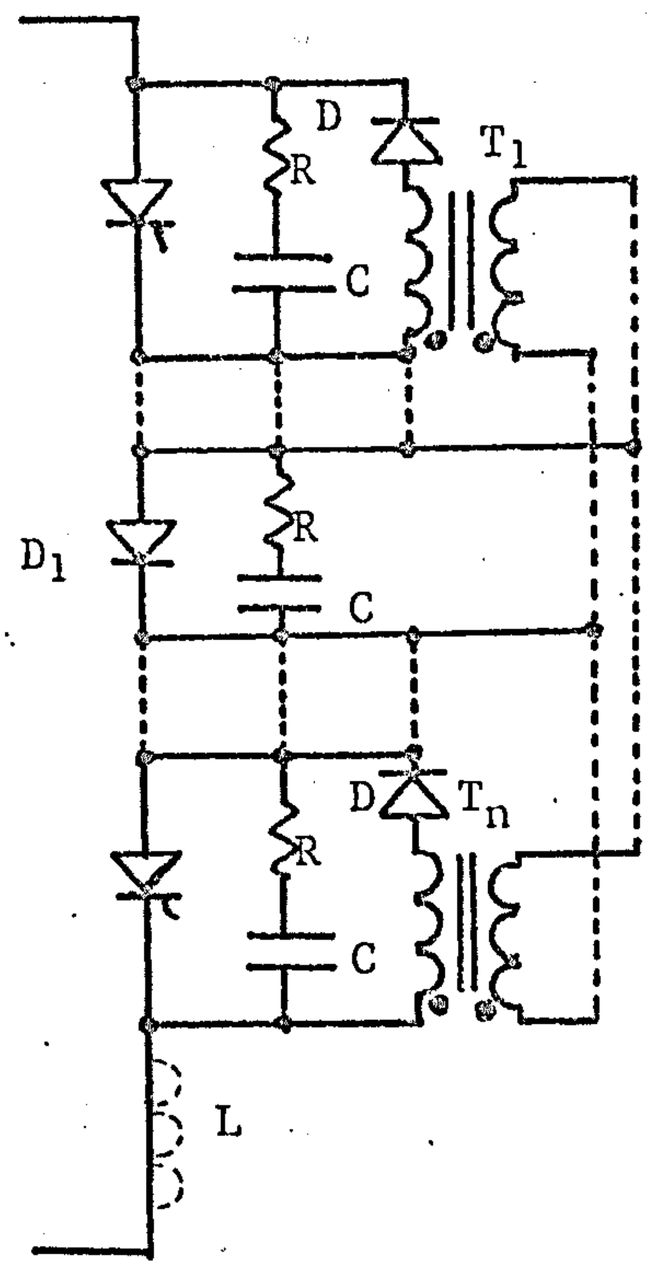

(c)

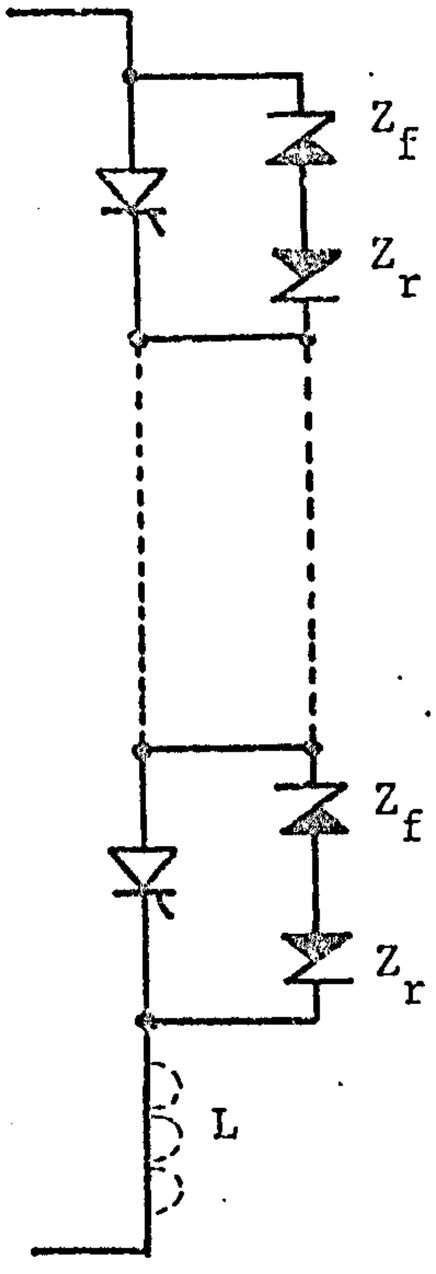

(d)

Figure 3.6: Principal voltage sharing networks investigated.

(continued over)

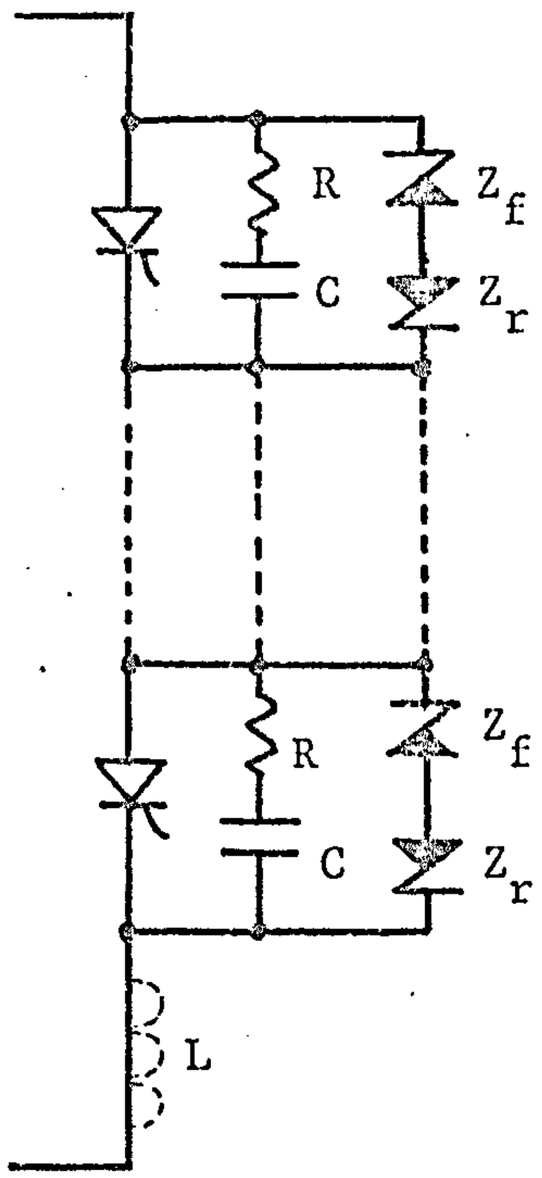

(e)

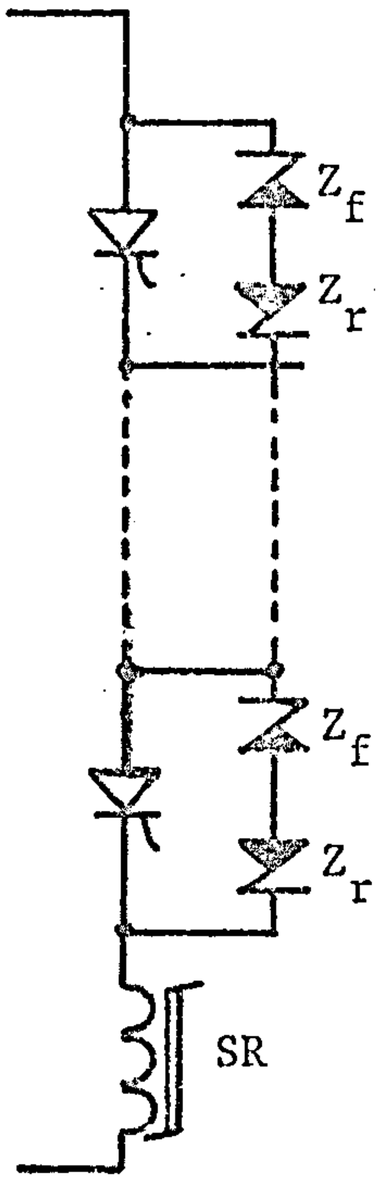

(g)

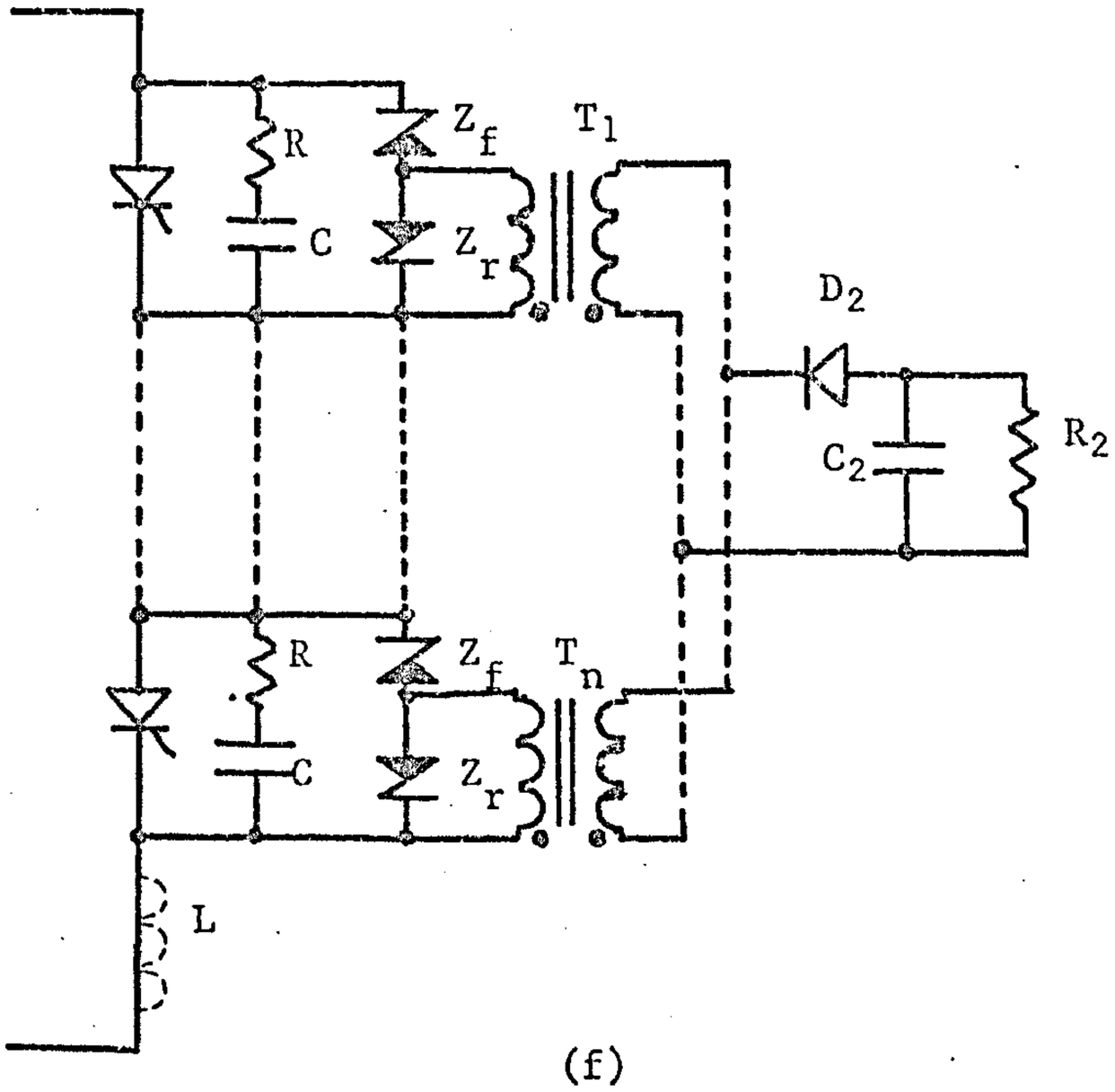

(f)

Figure 3.6: Principal voltage sharing networks investigated.

CHAPTER 4

VOLTAGE SHARING BY SERIES SATURATING REACTOR AND SHUNT R-C COMPONENTS

4.1 INTRODUCTION

Parallel components are necessary to operate in conjunction with the series saturating reactor at thyristor turn-off and to perform the other required voltage sharing functions. Shunt resistive-capacitive components are retained here (Figure 3.6(a)).

The saturating reactor SR functions as a switch (section 3.7, para (a)). If switching could be perfect, SR would prevent any removal of reverse recovery charge. Then, on application of the reverse voltage to the thyristor string, uniform voltage distribution would result.

4.2 SWITCHING ACTION OF THE SATURATING REACTOR

The operation of the saturating reactor is most easily illustrated by reference to its magnetisation (B-H) characteristic shown as core flux Φ plotted against magnetising current i_m. The idealised shape (Figure 4.1(a)) has horizontal saturated regions at flux levels $\pm\Phi_s$. SR, when operating in these regions, offers zero impedance to current flow; this represents the closed position of the switch. The open switch situation is provided by operation in the vertical unsaturated region, which gives infinite impedance.

The idealised operation of SR is as follows. With the forward

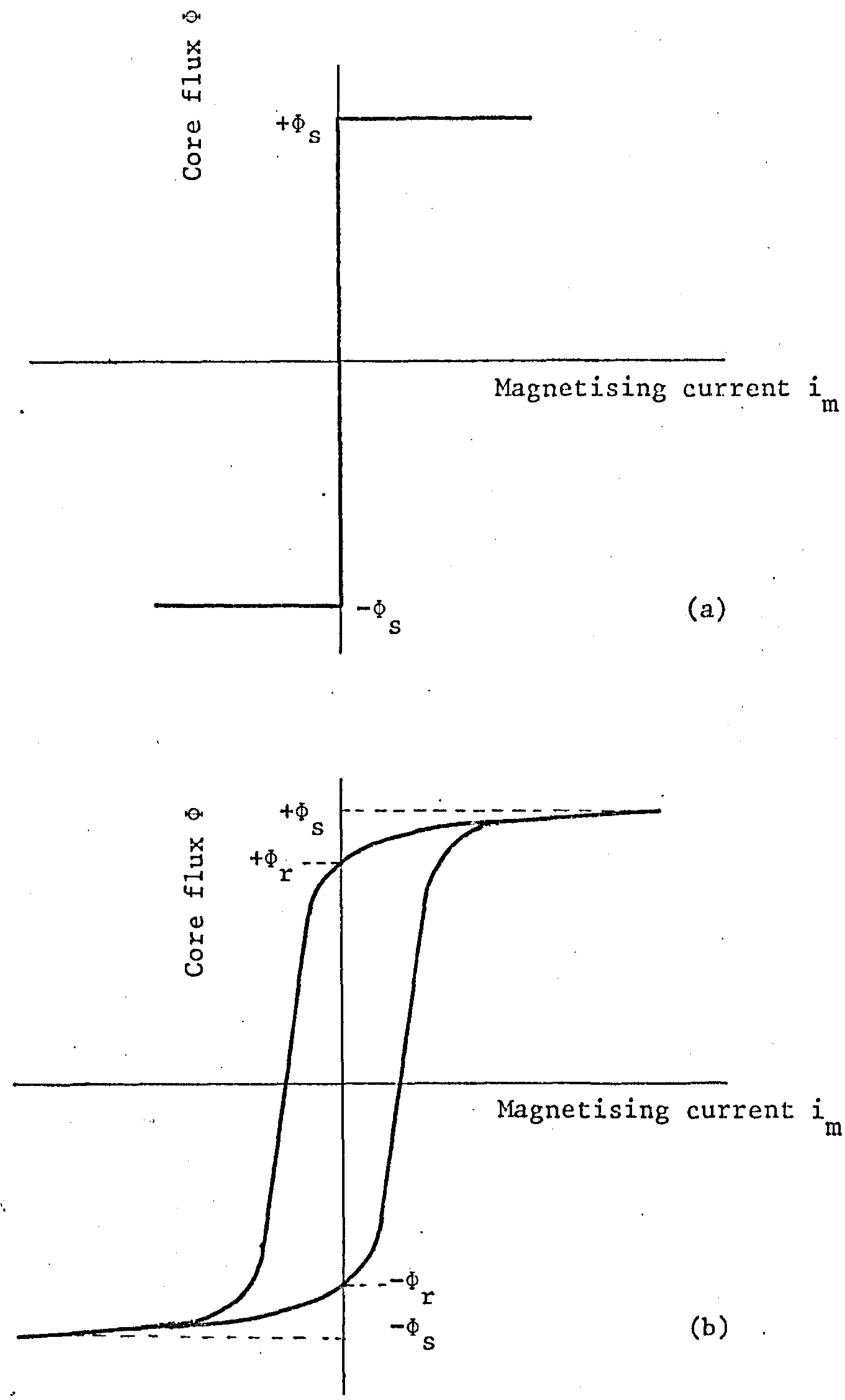

Figure 4.1: Saturating reactor magnetisation characteristics

(a) Ideal

(b) Practical

thyristor current flowing, the core is saturated at $+\Phi_s$. When reverse line voltage is applied to effect turn-off, the forward current drops to zero and SR, blocking the voltage, is magnetised negatively from $+\Phi_s$ to $-\Phi_s$. The time required is dependent on the volt-second rating of the reactor and the applied reverse voltage waveshape, where

$$\text{SR volt-second rating} = \int e\,dt \text{ of the applied voltage}$$

and

$$\text{SR volt-second (V-s) rating} = 2N\,\Phi_s \quad [34]. \tag{4.1}$$

N is the number of turns on SR. The time taken for SR to magnetise from $+\Phi_s$ to $-\Phi_s$ should be sufficient to allow complete recombination of the thyristor internal excess charge. On negative saturation the reverse voltage is applied to the thyristor string. A time delay in the application of forward voltage to the thyristors when they are next gated may similarly occur, but this depends very much on the shunt voltage sharing components and on the applied forward voltage waveform (see section 4.3).

A more practical form of magnetisation characteristic is shown in Figure 4.1(b). The slightly rounded characteristic gives a retentivity flux $\Phi_r < \Phi_s$, and the switching from the unsaturated to the saturated state is not instantaneous. A small current is required to magnetise the core. This imperfect characteristic has some advantages and disadvantages. The low magnetising current flow during SR reverse blocking produces a small removal of thyristor internal stored charge which leads to some degree of uneven voltage

sharing. However, this charge removal assists thyristor turn-off which is only slightly prolonged for fast turn-off types when reverse recovery current is blocked (section 2.5.2).

The required properties of the saturating reactor core are that it should require a low magnetising force and have a high saturation flux density. This gives a low product of turns and core area, hence least core volume. The core should respond to high frequencies. It is usual to use square B-H loop cores for switching duty, but this is not essential here. In fact, the characteristics of soft iron alloys may vary widely with differing applied voltage waveforms[35,36].

The operation of the saturating reactor will next be analysed for two widely-met waveshapes, assuming an idealised core characteristic.

4.3 ANALYSIS WITH IDEALISED OPERATION

4.3.1 Step voltage waveform (Figure 4.2(a)).

Consider the commutation sequence to begin with a reverse line voltage V_R applied to turn off the conducting thyristors. The appropriate instants of time corresponding to the following operating sequence are similarly designated ((i), (ii), etc.) in Figure 4.2.

(i) Reverse line voltage V_R applied, SR blocking.

SR is magnetised in the reverse direction from $+\Phi_s$ to $-\Phi_s$ for a period given by

$$t_{rs} = \frac{\text{V-S rating}}{V_R} \qquad (4.2)$$

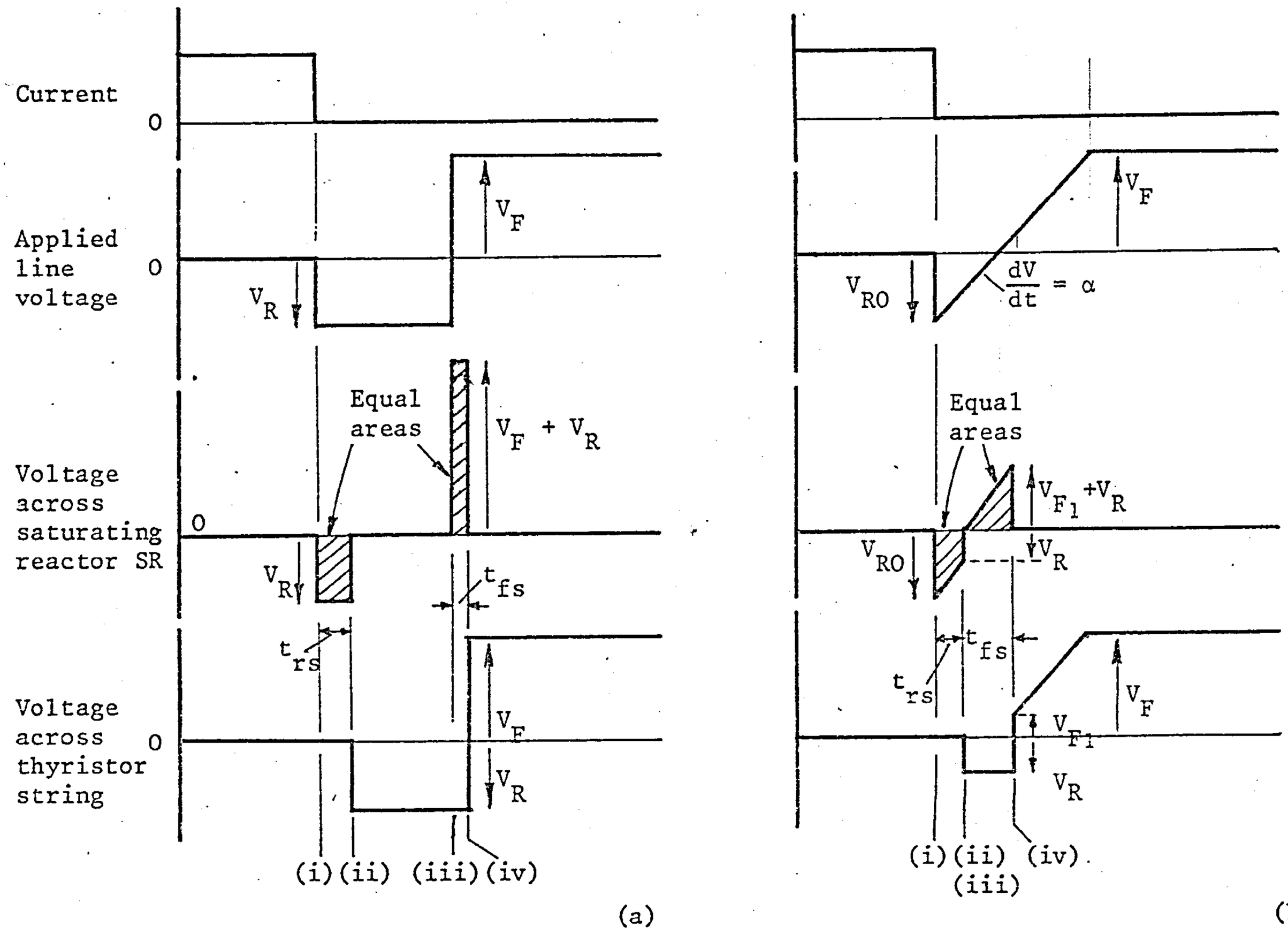

Figure 4.2: Idealised current and voltage waveforms for the R-C plus series SR network (Figure 3.6(a))

(a) Stepped voltage waveform.
(b) Ramp voltage waveform.

(ii) Reverse line voltage applied, SR saturated negatively.

When SR saturates, the previously uncharged capacitors C charge exponentially, time constant CR being no greater than a few microseconds. A voltage V_R/n is applied across each thyristor.

(iii) Forward line voltage V_F applied, SR blocking.

SR now resets positively from $-\Phi_s$ to $+\Phi_s$. The capacitors retain their negative voltage, giving a voltage $(V_F + V_R)$ across SR which saturates in a time t_{fs}, where

$$t_{fs} = \frac{\text{V-S rating}}{V_R + V_F} \qquad (4.3)$$

(iv) Forward line voltage applied, SR saturated positively.

The capacitors charge exponentially from their initial reverse voltage V_R/n to a forward voltage V_F/n.

The main points which emerge are that the time taken by SR to reset positively represents a delay t_{fs} in applying forward blocking voltage to the thyristors, and that the core is suitably magnetised to allow forward thyristor conduction immediately they are next gated.

4.3.2 Ramp voltage waveform (Figure 4.2(b))

If the initial reverse line voltage applied is V_{RO} and the slope of the linear voltage rise is α, at any subsequent instant t, the line voltage is $(-V_{RO} + \alpha t)$.

(i) Reverse line voltage applied, SR blocking.

SR saturates negatively in time t_{rs} at which instant the reverse line voltage is V_R, where

$$V_R = - V_{RO} + \alpha t_{rs}$$

and

$$t_{rs} = \frac{2(\text{V-S rating})}{V_{RO} + V_R} .$$

These two expressions give a quadratic equation in t_{rs}, the solution of which is

$$t_{rs} = \frac{V_{RO}}{\alpha} - \sqrt{\frac{V_{RO}^2}{\alpha^2} - \frac{2}{\alpha}(\text{V-S rating})} \qquad (4.4)$$

The higher alternative solution is inadmissible because, if SR is to saturate negatively, $t_{rs} < V_{RO}/\alpha$.

(ii) Reverse line voltage applied, SR saturated negatively.

Assuming zero time delay while the R-C chain charges when SR saturates (time constant CR being very low), the individual reverse capacitor voltage is V_R/n. As reverse line voltage further reduces linearly, the tendency is for the capacitors to discharge with a current of approximate value $C\alpha/n$ (R being small). This current flow, being positive, is prevented by SR which commences to reset positively immediately the capacitor chain is charged to voltage V_R.

(iii) Voltage linearly changing positively, SR blocking.

Since capacitor discharge is prevented, the thyristor string voltage remains constant at V_R. Negative line voltage is

given by $(V_R - \alpha t)$ and therefore the linearly rising voltage αt is applied across SR until it saturates in the forward direction after time t_{fs}, where

$$t_{fs} = \sqrt{\frac{2}{\alpha}(\text{V-S rating})}. \qquad (4.7)$$

(iv) Voltage linearly changing positively, SR saturated positively.

At the instant when SR saturates positively, assuming that $(t_{rs} + t_{fs}) > V_{RO}/\alpha$, line voltage will be positive and is given by

$$V_{F1} = \alpha t_{fs} - V_R$$
$$= \alpha(t_{rs} + t_{fs}) - V_{RO} .$$

Again, with time constant CR being small, the individual capacitor and thyristor voltages rapidly change from $-V_R/n$ to $+V_F/n$.

Subsequently the thyristor voltage increases linearly with the line voltage to a final value V_F/n across each.

The main points demonstrated by the analysis are the rapid positive voltage rise introduced across the thyristors when SR saturates, which increases the risk of dV/dt triggering, and the delay of forward blocking voltage application across the thyristors. Here this delay is $(t_{rs} + t_{fs} - V_{RO}/\alpha)$. Again the core is suitably magnetised to allow forward thyristor conduction immediately they are next gated.

Operation with any other voltage waveshape which can be expressed mathematically may be treated in a similar manner.

4.4 THE CHOICE OF SATURATING REACTOR TURNS

The practical core magnetisation characteristic allows circuit operation to be very close to the ideal discussed in the previous section. The small magnetising current flow during thyristor reverse recovery has little influence on the main circuit operation but determines the degree of thyristor voltage mis-sharing.

An appropriate reverse blocking time t_{rs} based on thyristor internal excess charge recombination must be first assumed. Since internal charge decay is exponential (equation 2.2), a value of three to four times the minority-carrier lifetime τ_p of the slowest turn-off thyristor is suitable for t_{rs}. Then, when SR saturates negatively, only approximately 2% of the total excess charge (Q_f) can be removed. This compares with up to about 50% charge removal with SR absent (Figure 2.7). The above reasoning is justified by the experimental results of section 4.7.

With t_{rs} established, the applied reverse volt-second integral ($\int e\,dt$) is obtained from the waveform and, for a suitable core of known saturation flux Φ_s, the required number of turns N is given by equation 4.1.

4.5 PREDICTION OF VOLTAGE SHARING PERFORMANCE

Before the maximum and minimum thyristor reverse voltages can be determined, the reverse recovery charge flow allowed by the saturating reactor must be estimated. It is assumed that the charge removal and recombination processes are independent, which is reasonable so

long as the reverse current is small. The excess minority-carrier charge q remaining in a thyristor at any instant after reverse line voltage has been applied to the series thyristor and SR combination, will be that left uncombined less that already removed, that is,

$$q = Q_f\, e^{-t/\tau_p} - \int_0^t i_m dt . \qquad (4.8)$$

This equation can only be solved graphically to give the time at which q = 0.

The charge flow through SR during magnetisation $(\int i_m dt)$ is determined from its core B-H magnetisation characteristic, plotted as change of flux density ΔB against H for the reverse voltage waveform applied. If the reverse voltage V_R is constant, dB/dt (= V_R/N × core area) is constant. Neglecting coil resistance and losses, the ΔB axis can be re-scaled in terms of time change Δt. With the H axis re-scaled to magnetising current i_m, the area enclosed by the curve to any chosen value of Δt gives the required $\int i_m dt$. Hence a graph of charge flow against time can be deduced and plotted together with the exponential minority-carrier decay $(Q_f\, e^{-t/\tau_p})$ to give, at the intersection, the time taken for the stored charge to fall to zero. Also given is the amount of charge removed before this happens.

For other than constant reverse voltage, [e.g. as Figure 4.2(b)], the procedure is more involved because the time intervals for assumed equal increments of flux density change will not be constant. The individual time for each ΔB increment must then be based upon the mean voltage level during the increment, and hence the incremental charge flow ascertained.

Figure 4.3 shows the magnetisation characteristic for one of the saturating reactors used experimentally. Figure 4.4(a) and (b) shows the derived charge 'let-through' characteristic and the graphical solution of equation (4.8) for the fastest and slowest reverse recovery thyristors whose minority-carrier lifetimes have been measured by the method of section 2.7. The difference of the two removed charge values so obtained (δQ_{max}) can then be used to give the estimated reverse voltage difference ($\delta Q_{max}/C$) for these two thyristors. For the example given, the difference voltage is (1.8 - 0.2)μC/0.1μF, giving 16V.

To perform this exercise for each thyristor and then use equations (3.4) and (3.5) to calculate the extreme thyristor voltages would be excessively laborious. Since the voltage difference is small, it is usually sufficiently accurate to assume the extreme voltages equally above and below the average voltage V_R/n. Forward thyristor voltages are again given by equation (3.9).

This method of predicting the extremes of reverse voltage distribution is directly applicable to use of the same sharing network for series diodes. The diode minority-carrier lifetime is then measured as described in section 2.8.

4.6 EXPERIMENTAL RESULTS

The results obtained with this voltage sharing network, applied to the test string of twenty thyristors (Figure 3.3) are given in Table 4.1. The performance of various saturating reactors using two core materials, a soft alloy HCR tape and a ferrite, is illustrated.

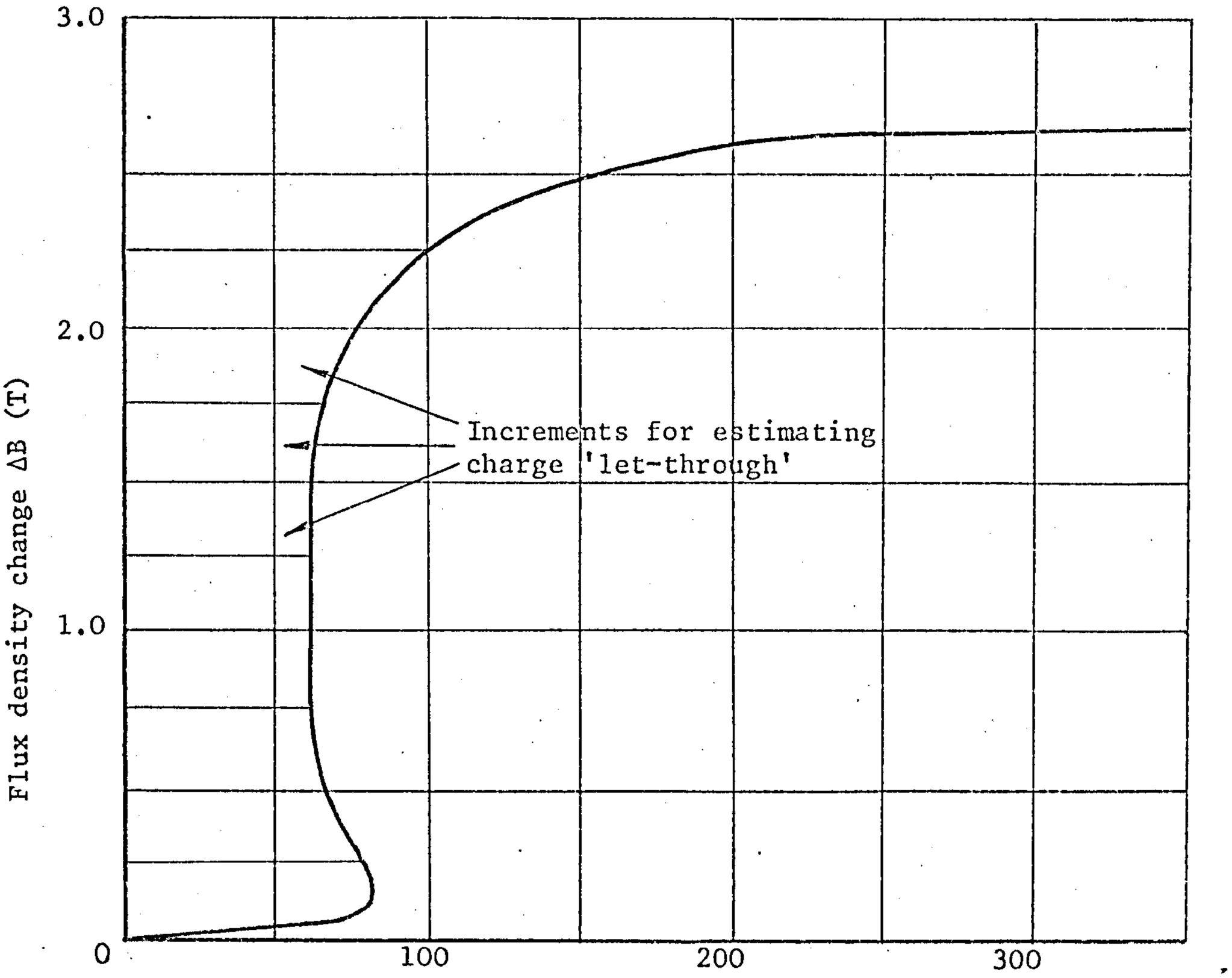

Figure 4.3: Magnetisation characteristic for HCR alloy, 0.005in. tape, used for one saturating reactor SR core (Table 4.1, row (a)).

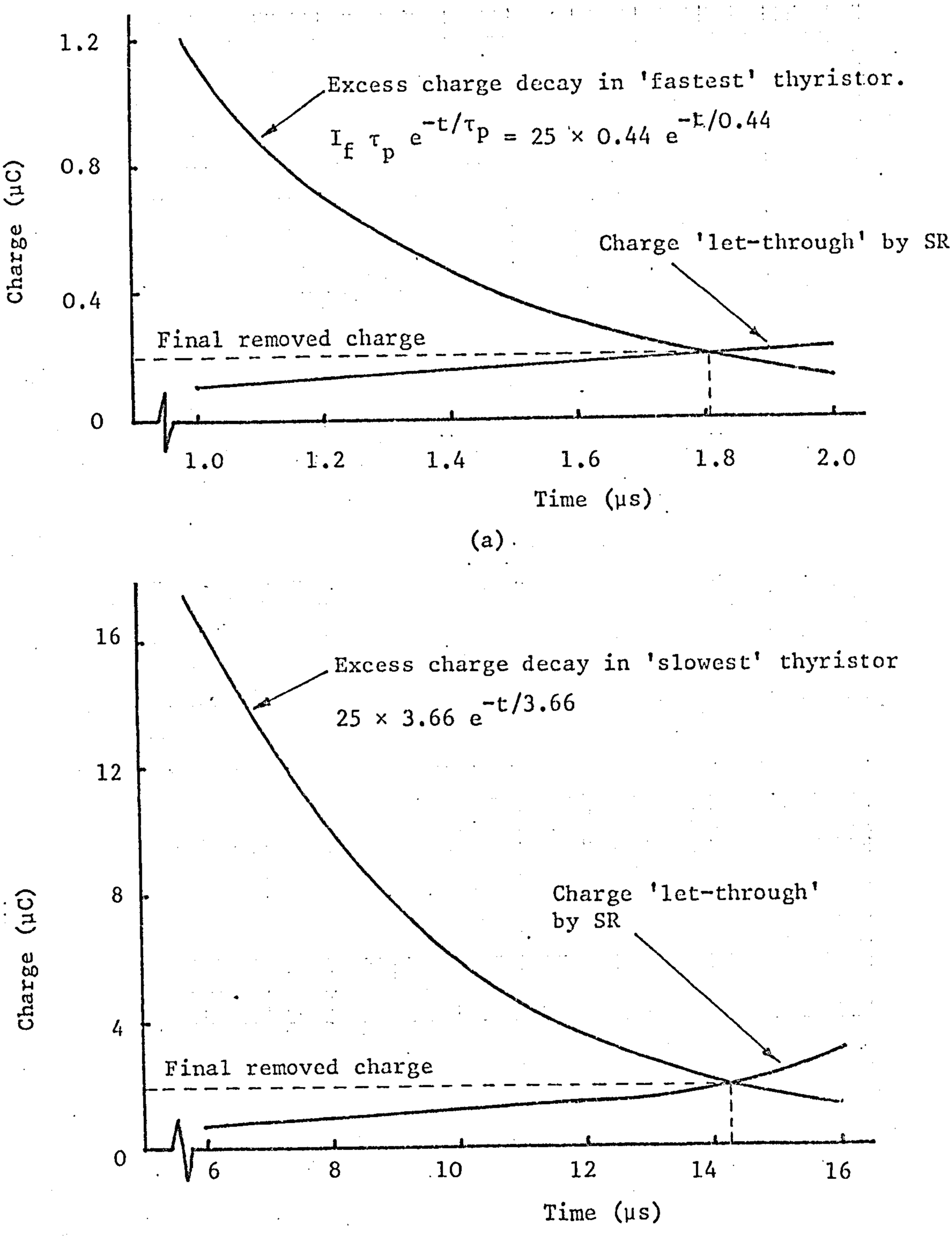

Figure 4,4: Prediction of the charge removed from the fastest and slowest reverse recovery thyristors in the test string of twenty devices (Table I.1).

Voltage sharing components as Table 4.1, row (a).

	Saturating reactor details				Measured thyristor voltages with predicted values shown ()			String voltage factors	
Row	Core	Turns	V-s rating	Time to saturate under reverse voltage t_{rs} (μs)	Max reverse steady peak (across fastest recovery thyristor) (V)	Min reverse steady peak (across slowest recovery thyristor) (V)	Max forward peak (V)	f_{rm}	f_{fm}
(a)	Telcon HCR 0.0005" strip size 9b	130	33.7×10^{-3}	15	110 (98)	85 (82)	275 (263)	0.82	0.93
(b)	ditto	110	28.6×10^{-3}	12	135 (126)	95 (94)	285 (270)	0.82	0.89
(c)	Mullard Ferrite FX1076	280	33.7×10^{-3}	15	110 (94)	85 (86)	280 (259)	0.82	0.91
(d)	ditto	210	28.6×10^{-3}	12	140 (121)	95 (99)	285 (266)	0.79	0.89
(e)	Telcon HCR 0.002" strip size 9a	154	52.5×10^{-3}	23	95 (89)	60 (63)	280 (277)	0.84	0.94
(f)	Telcon 0.002" strip size 7b	30	6.5×10^{-3}	2	210	60	340	0.64	0.75

Table 4.1: Voltage sharing performance of various saturating reactors with shunt R-C components (Figure 3.6(a))
C = 0.1μF, 20% tolerance; R = 22Ω, 5% tolerance; R_s = absent. Test circuit - Fig 3.3

Figure 4.5 shows measured individual thyristor voltages plotted to a base of reverse recovery charge difference (previously measured without SR) in the same way as Figure 3.5. For ease of comparison, plots (c) of Figure 3.5 are repeated as lines (z) in Figure 4.5 to represent the results with the same R-C components but with SR absent (Table 3.1, row (c)).

Figure 4.6 shows oscillograms of the test thyristor current and line, thyristor string and SR voltage waveforms with the components given in Table 4.1, row (a). These components are used also in the illustrative design example of section III.1. The oscillograms well verify the idealised waveforms of Figure 4.2(b). The individual thyristor waveforms are almost identical to that of Figure 4.6(c), making due allowance for magnitude.

4.7 DISCUSSION OF EXPERIMENTAL RESULTS

The marked improvement in thyristor voltage sharing produced by the inclusion of SR is extremely well demonstrated by comparison of plots (a) and (c) with lines (z) in Figure 4.5. It is not so apparent from a comparison of voltage factors f_{rm} quoted in Table 4.1 with that of Table 3.1, row (c), because the linearly falling reverse voltage gives a reduced value of V_R across the thyristors when SR saturates. The predicted extreme thyristor voltages compare quite well with the measured values given in Table 4.1. The greater discrepancy with the forward voltages is due to slight overshoot.

Comparison of the results obtained with saturating reactors of the same volt-second rating but different core types (rows (a)

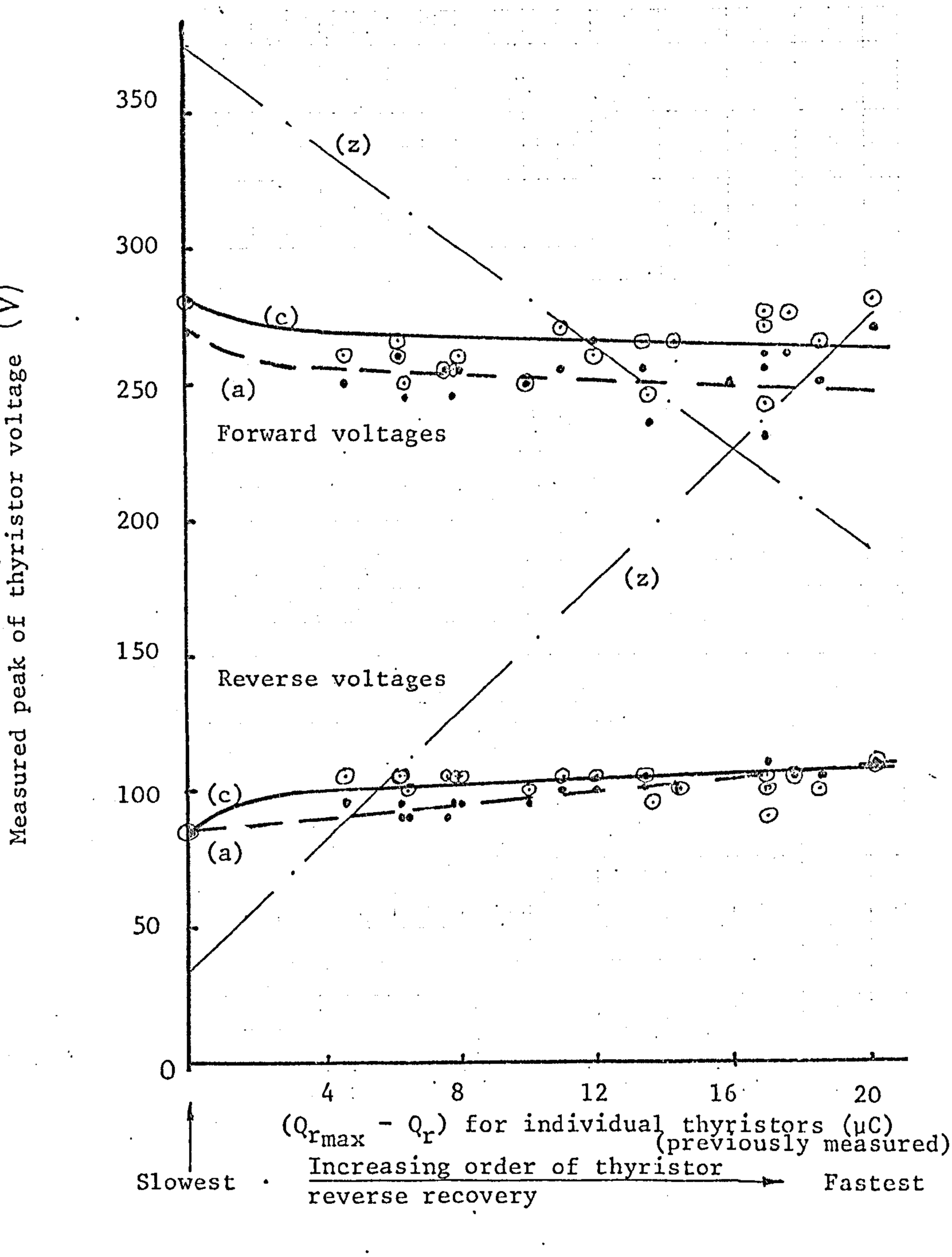

Figure 4.5: Measured peak voltages across each thyristor in the test string of twenty, with the R-C plus series SR network.

(a) Network details as Table 4.1, row (a)

(c) " " " " , row (c)

(z) " " " Table 3.1, row (c), SR absent.

Test circuit - Figure 3.3.

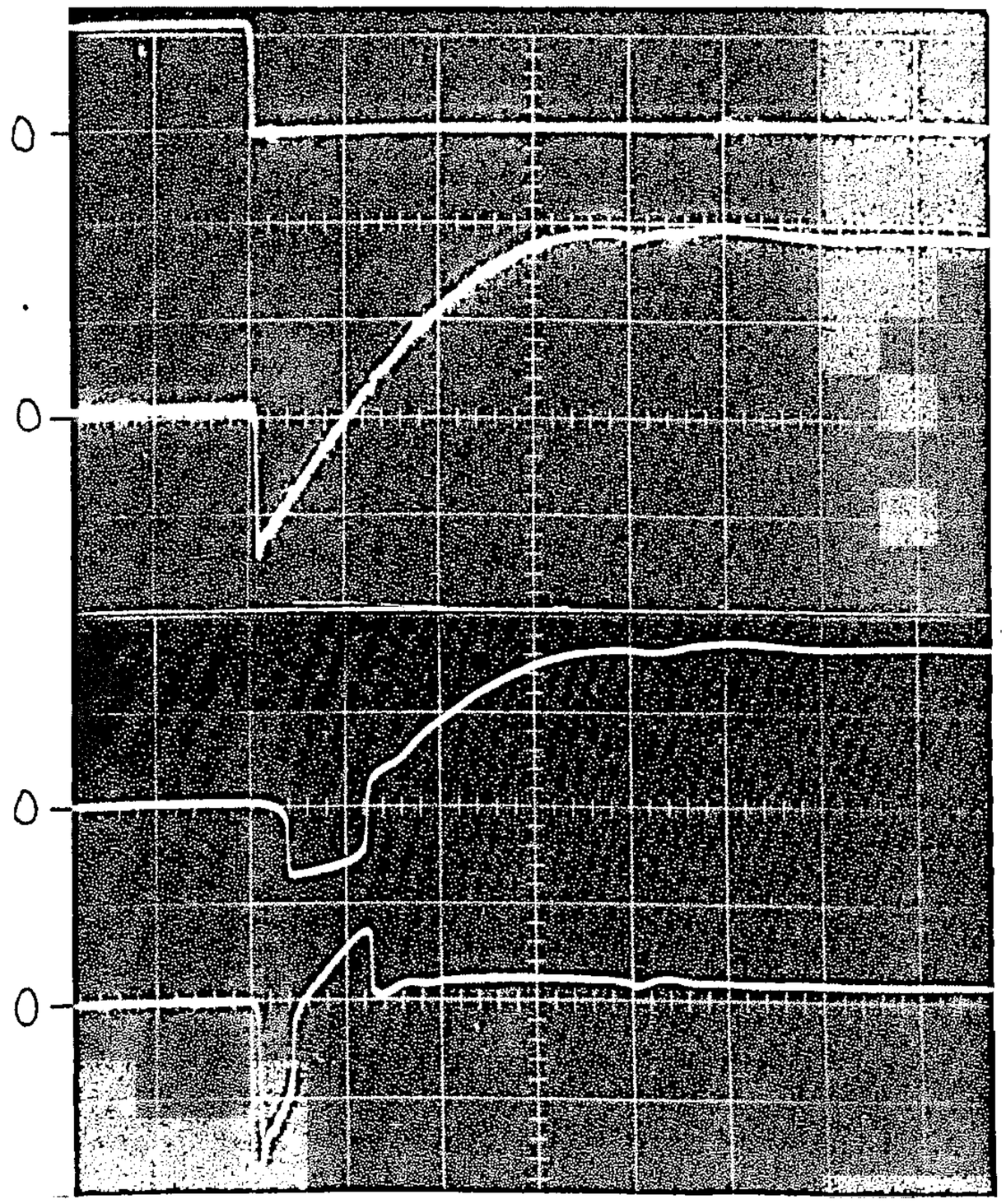

Figure 4.6: Oscillograms of current and voltages with the R-C plus series SR sharing network.

(a) Test thyristor Th_1 current, (20A/cm, 50μs/cm).

(b) Voltage across thyristors and SR, (2.5kV/cm, 50μs/cm).

(c) Voltage across thyristor Th_1 string, " "

(d) Voltage across SR, (2.5kV/cm, 50μs/cm).

Network details as Table 4.1, row (a). Test circuit - Figure 3.3.

and (c), (b) and (d) of Table 4.1 and plots (a) and (c) of Figure 4.5) show very little difference in their performance. The HCR soft alloy cores possess a squarer magnetisation characteristic than the ferrite core, but this is not shown by the results to be of any great advantage. The HCR core, having a higher loss, does provide better damping of spurious oscillation.

It is apparent from Figure 4.4(b) that, owing to the exponential nature of the thyristor excess charge decay, there is little to be gained by increasing the saturating reactor volt-second rating above the value which gives $t_{rs} = 4\tau_p$. This is illustrated by the results (e) of Table 4.1 which show only marginal voltage sharing improvement compared with rows (a) to (d) inclusive, despite the use of a considerably larger saturating reactor.

Some improvement of voltage sharing is produced whatever the volt-second rating of the saturating reactor. If it is reduced so that saturation occurs before the thyristor excess charge has fallen to zero, the resulting increased charge flow becomes thyristor controlled as the depletion layers build up. Some stored charge will then be retained to recombine internally (section 2.3). The method discussed (section 4.5) for predicting voltage distribution then becomes invalid. Results (f) in Table 4.1 illustrate such a case, where a very small saturating reactor is used to control the initial reverse voltage spike (Table 3.1, row (c)).

Apart from capacitor tolerance, the differences between the measured and predicted voltage sharing performance are due to the following possible reasons:

(a) The initial assumption of the independence of thyristor charge recombination and removal processes may not be justified when the internal charge drops to a low value.

(b) Possible inaccuracy of the core magnetisation characteristic and the previously measured minority-carrier lifetime τ_p.

(c) The neglect of any charging current for the stray capacitance across the saturating reactor.

(d) Possible inaccuracy inherent in adopting the average thyristor reverse voltage V_R/n as the base on which to superimpose the calculated maximum voltage spread.

4.8 CONSIDERATIONS OTHER THAN TURN-OFF

The design of the saturating reactor for turn-off performance must not result in mal-operation of the thyristors in other respects. The practical core magnetisation characteristic (Figure 4.1(b)) produces a slow enough switching speed to adequately restrict the forward dV/dt across the thyristors when SR saturates positively after turn-off. However, the rounded loop, giving $\Phi_r < \Phi_s$, can be troublesome at turn-on. After being saturated positively by the applied forward blocking voltage, the core flux remains at $+\Phi_r$ with the thyristors blocking until they are next gated. Before the thyristors can be fully conducting, the flux must rise to $+\Phi_s$. SR therefore exerts a volt-second withstand of $N(\Phi_s - \Phi_r)$. If single, short-duration gate pulses are used, difficulty will be experienced if the SR prevents the thyristor anode current rising to

the latching value before the gate pulse ends.

This property of the core can be usefully employed with series thyristors to protect the slow turn-on thyristors against over-voltage (section 3.2.2). The di/dt control provided is also useful in reducing thyristor turn-on dissipation. The ideal characteristic for this purpose is defined by Paice and Wood[37]. Here this ideal may not be approached because SR is designed for turn-off performance, but useful thyristor protection at turn-on is provided.

4.9 ADVANTAGES AND DISADVANTAGES OF THE METHOD

The advantages of using a series saturating reactor SR in the manner described in this chapter are as follows:

(a) SR controls the short-duration transients as well as the final steady thyristor reverse voltage distribution.

(b) Transient oscillations due to stray capacitance which occur when reverse voltage is first applied are felt across SR, not the thyristors.

(c) SR can also provide thyristor protection at turn-on.

(d) Depending on the volt-second rating of SR, the re-application of forward blocking voltage across the thyristors may be delayed (Figure 4.2). This automatically allows for the small increase of thyristor turn-off time resulting from the reduced charge removal (section 2.5.2).

(e) Thyristor voltage distribution can be predicted with reasonable accuracy.

(f) The available improvement in voltage distribution can be traded for a reduction in the value of sharing capacitor C, though the capacitor's other functions must be observed.

(g) The more uniform thyristor voltage distribution results in satisfactory thyristor turn-off at much lower reverse applied voltages.

The disadvantages are:

(a) Voltage distribution at turn-off cannot be made quite uniform and is still inherently dependent on the value of capacitors C.

(b) The possibility exists of the thyristors failing to turn-on with short-duration gate pulses.

(c) Optimum operation of SR occurs only at the reverse voltage for which it is designed. If the reverse voltage is lowered, slightly improved voltage distribution results though excessive delay in turn-off may be introduced. Increased reverse voltage worsens the voltage distribution.

(d) For high power applications, the physical size of SR will be large. A number of smaller, nominally identical, units may be used in series to give the same total volt-second rating.

CHAPTER 5

VOLTAGE SHARING BY SHUNT TRANSFORMER AND R-C COMPONENTS

5.1 INTRODUCTION

An alternative to preventing removal of the minority-carrier charge is to provide a low (ideally zero) impedance path across each thyristor until all have completed their reverse recovery; then switch the paths simultaneously to a high impedance state, thereby allowing reverse voltage to build up evenly across the thyristors. This can be effected by using a single transformer, or multiple transformers, with the high voltage primary windings connected across the thyristors, voltage control being exercised from the common, low-voltage secondary side.

Two basic transformer arrangements are considered together with two methods of secondary side control which approximate to the above ideal. These are arranged in Figure 5.1 to show the natural progression of ideas. The shunt R-C components are retained to cater for all other aspects of voltage sharing except turn-off; additional active components are avoided as their use is undesirable from complexity and reliability standpoints.

5.2 SINGLE MULTIWINDING TRANSFORMER NETWORK: CONTROL BY CAPACITOR AND DIODE

The multiwinding transformer T (Figure 5.1(a)) has a high voltage primary winding with an equal-turn section for each thyristor. The

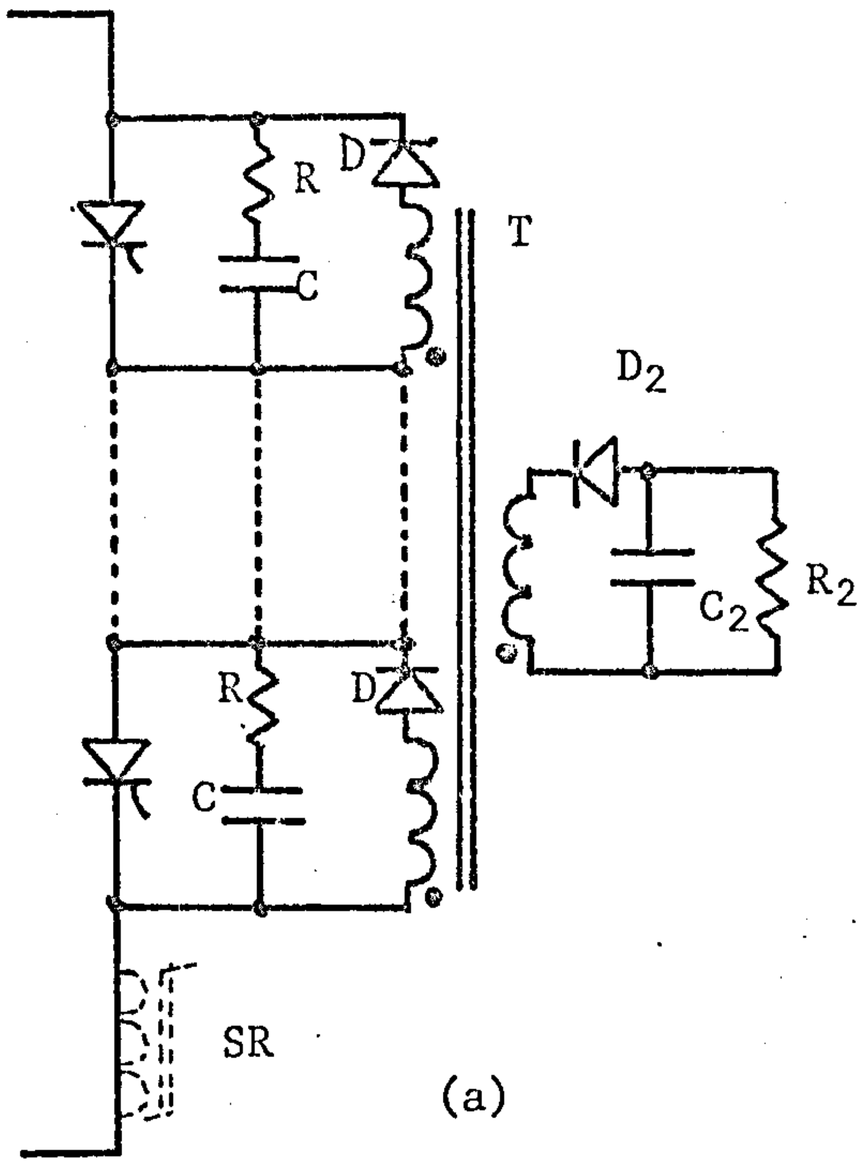

(a)

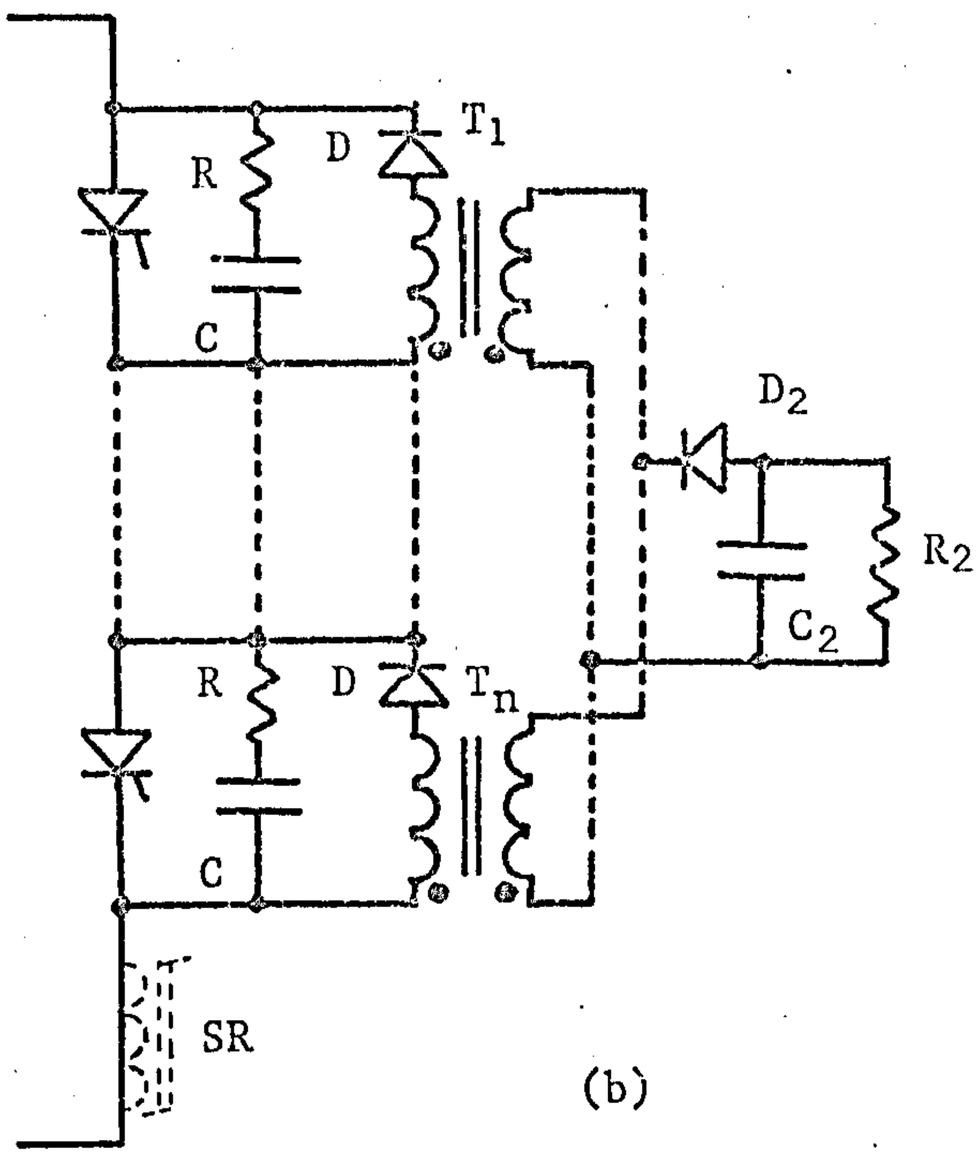

(b)

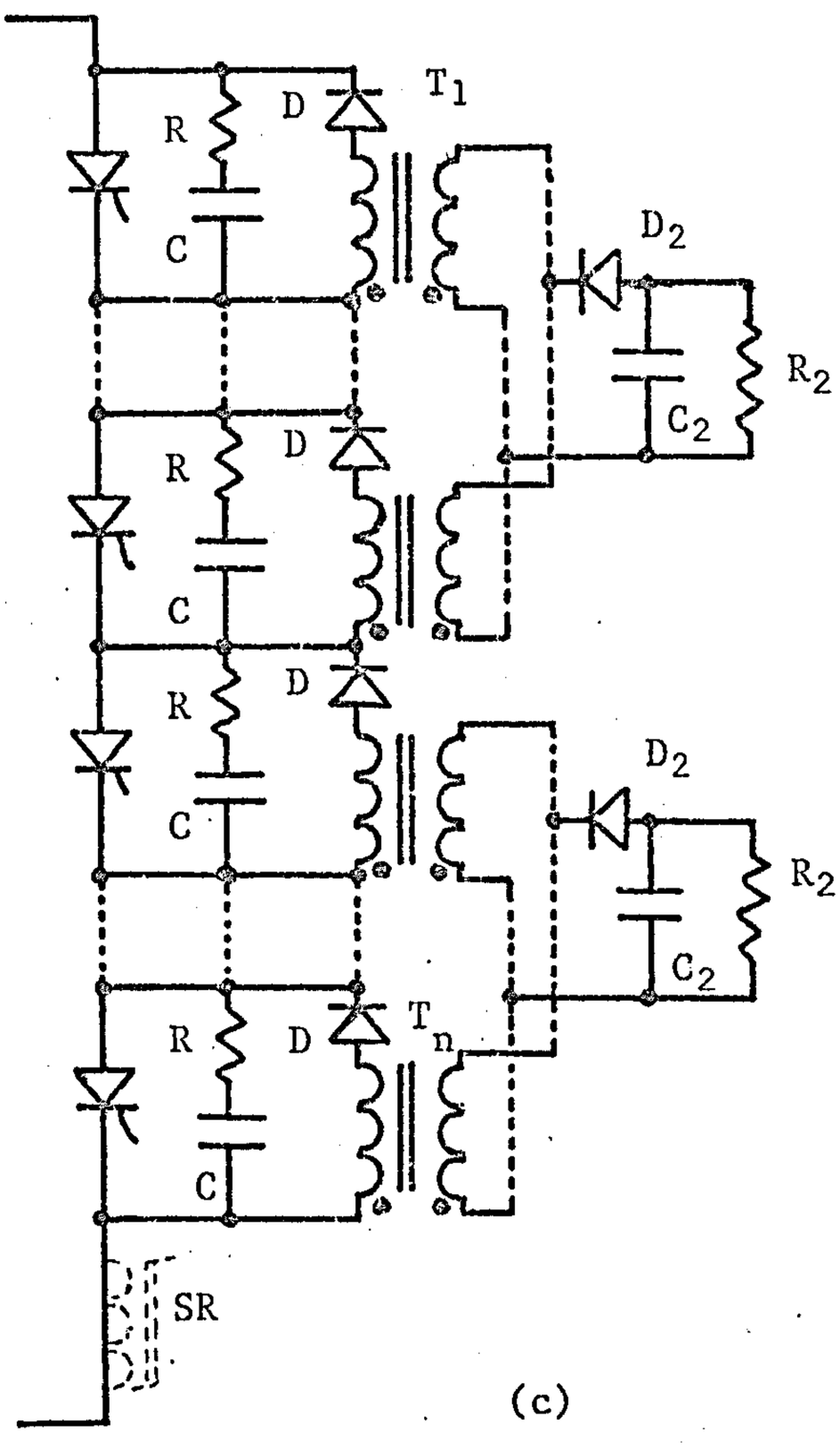

(c)

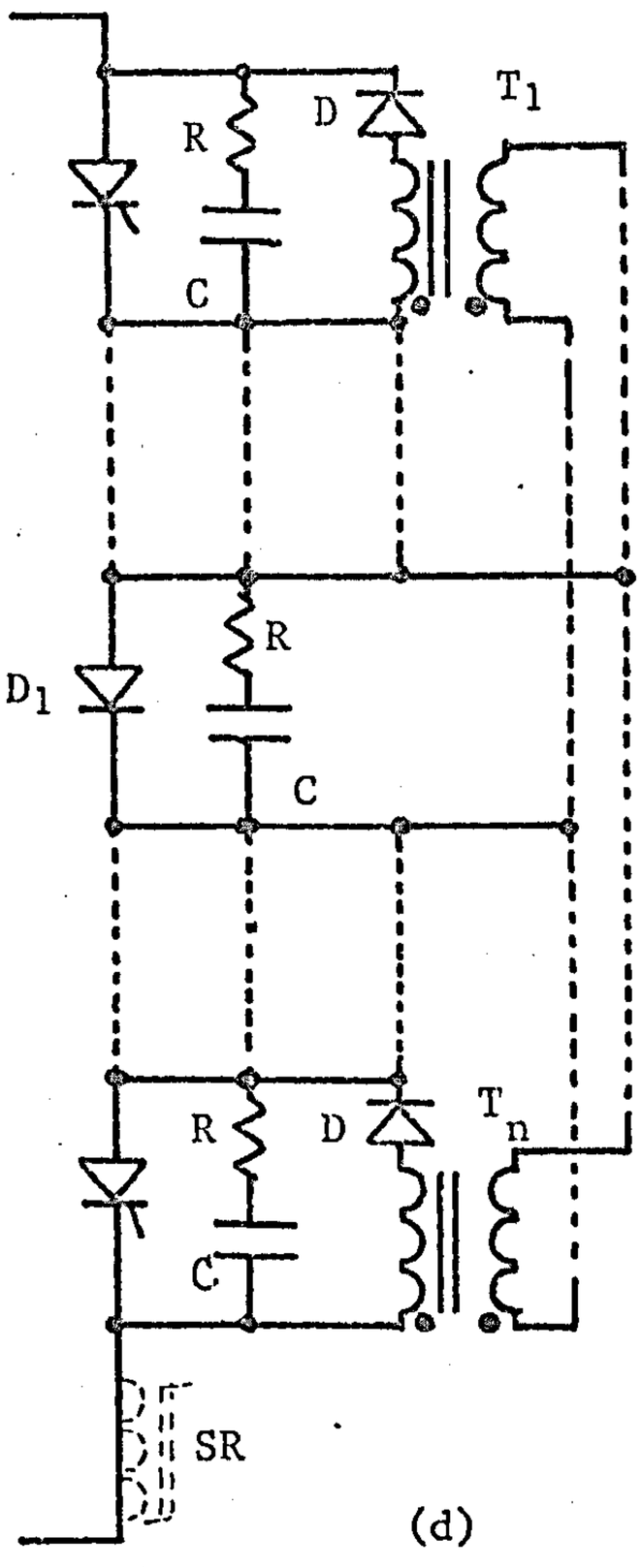

(d)

Figure 5.1: Voltage sharing networks with shunt transformers

transformer core must not saturate, and for waveforms having a much lower negative than positive volt-second integral, which is usual with forced commutation, the transformer size is greatly reduced by using diodes D to block the forward voltage. The transformer insulation poses a severe problem due to the proximity of windings which are subjected to the full line voltage. Developments which reduce this problem are considered later. The detailed operation, which is basic to all the shunt transformer arrangements, will be described here in the context of the multiwinding transformer.

When the reverse turn-off voltage is first felt across the thyristor string, the short circuit of the initially uncharged capacitor C_2 is reflected to the high voltage side, allowing reverse recovery current flow through the appropriate primary sections as the thyristors block in turn. If the differing reverse recovery times of the thyristors are neglected, application of the reverse voltage to the full primary winding effectively acts as a step input to the simplified equivalent circuit (Figure 5.2). The transformer magnetising reactance and the high resistance R_2 are considered infinite and stray capacitances are neglected. If the total transformer winding resistance referred to the secondary side (R_{t2}) is ignored, C_2 charges with an oscillatory current half-cycle, the duration of which (Appendix IV) is

$$T_{C2} = \pi \sqrt{L_{t2}\, C_2} \quad . \tag{5.1}$$

The peak value of this current is

$$I_{2pk} = V_R \left(\frac{N_2}{n \cdot N_1}\right) \sqrt{\frac{C_2}{L_{t2}}} \quad , \tag{5.2}$$

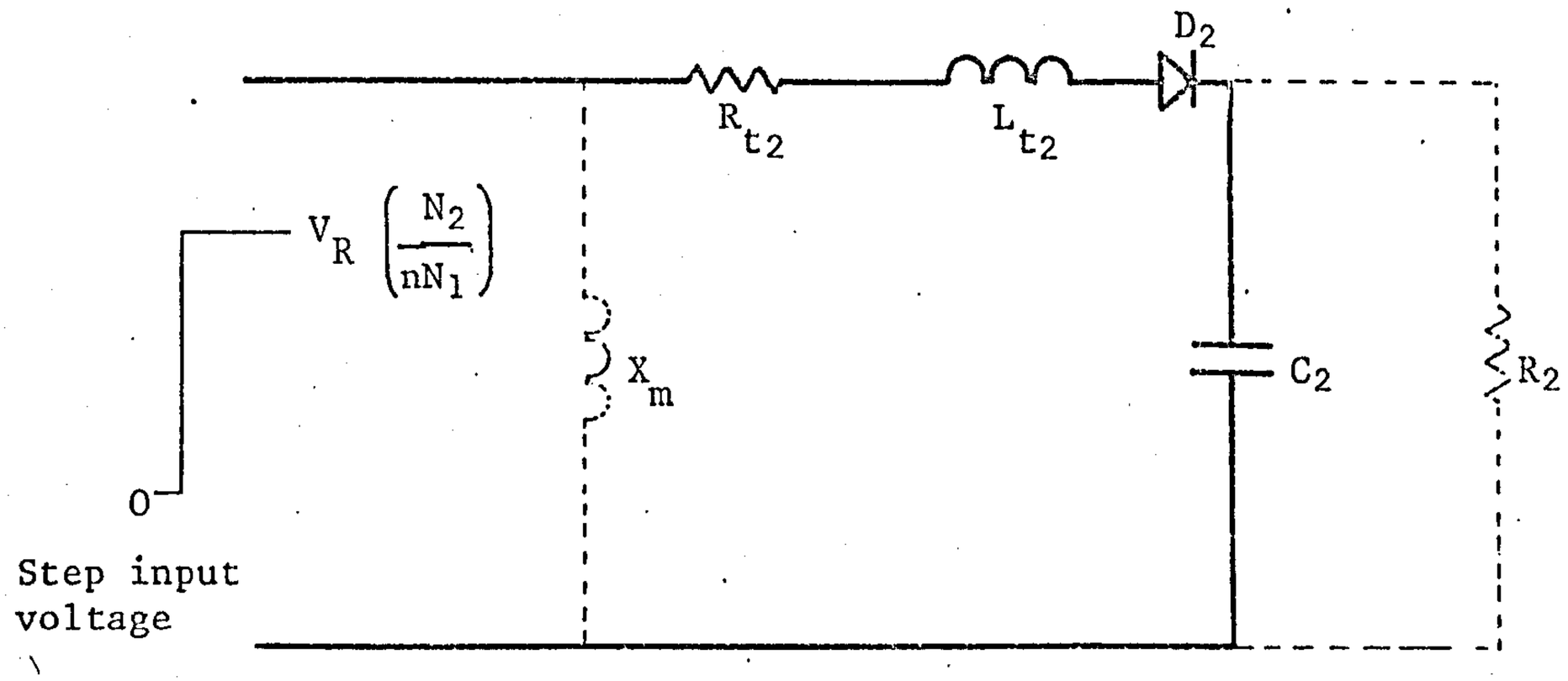

Figure 5.2: Simplified equivalent circuit for the shunt transformers (referred to the secondary side) with capacitor and diode control.

where N_1 is the primary winding turns per section and N_2 is the secondary winding turns. Diode D_2 prevents an oscillatory discharge of C_2, and the reverse blocking voltage on the primary is sustained, distribution being theoretically uniform. When the forward thyristor blocking voltage is applied, diodes D block and C_2 discharges through the high resistance R_2 ready for the next commutation.

Owing to the differing thyristor reverse recovery times, the individual transformer primary sections are sequentially brought in, giving a turns ratio which increases progressively from N_1/N_2 with only the fastest thyristor blocking, to nN_1/N_2 with all the thyristors blocking. Commencement of the secondary current oscillation is delayed until the fastest thyristor reverse recovery commences; then the initial rate of secondary current rise is increased by the high voltage reflected from the primary when only the faster recovery thyristors have developed reverse blocking capability. A small increase in the oscillation current peak can result. Additionally, the effective transformer leakage inductance L_{t_2} changes during this period. This is difficult to analyse, however, because a transformer with more than three windings cannot be represented by a simple equivalent circuit[38]. As the total thyristor reverse recovery time is only a low proportion of T_{C2} in practice, the simplified analysis given in Appendix IV, which ignores reverse recovery, is adequate.

The low line impedance in series with the thyristors is relied upon to limit the reverse voltage across those which recover first. For the line impedance to be effective, the transformer leakage inductance should be as low as possible to give optimum reflection

of the secondary conditions to the primary side. C_2 must present a low impedance across the thyristors for a period sufficient for their reverse recovery and yet prevent unnecessary drain on the commutating capacitor, if used. This drain, however, is likely to be very low owing to the secondary current oscillation being reflected to the primary side in the ratio N_2/nN_1, once thyristor reverse recovery is complete. A further factor limiting the capacitance of C_2 - of particular importance at high operating frequencies - is the loss in the discharge resistor R_2.

With only the fastest recovery thyristor blocking, and its associated primary winding section carrying the reverse recovery current of all the others, the charge reflected into C_2 before the next thyristor blocks (assuming instantaneous reverse switching) is $(\Delta Q_{r2-1} \times N_1/N_2)$. With just two sections operative, the reflected charge is $(\Delta Q_{r3-2} \times 2N_1/N_2)$, and so on. To ensure that the secondary current continues to increase as the thyristors successively block reverse voltage, the voltage across C_2 must always be less than that applied via the primary. Finally, when the slowest (n^{th}) thyristor blocks, the instantaneous voltage across C_2 must not be greater than $V_R N_2/nN_1$,

that is,

$$\frac{V_R\ N_2}{n\ N_1} \geq \frac{1}{C_2}\ \frac{N_1}{N_2}\left[\Delta Q_{r2-1} + 2\Delta Q_{r3-2} + 3\Delta Q_{r4-3} + \ldots\ (n-1)\Delta Q_{rn-(n-1)}\right] \qquad (5.3)$$

In other words, the secondary oscillatory current must have just (or not quite) reached its peak. This is the criterion for the lowest

acceptable value for C_2. It is difficult to use equation (5.3) in practice and instead of summing the individual Q_r differences as shown, it is easier to replace them by an assumed average value $\Delta Q_{rmax}/n$ multiplied by the sum of the above coefficients $\left(1 + 2 + 3 + \ldots (n-1)\right)$, which is $(n-1)n/2$. In the limit, the minimum capacitance of C_2 is then given by

$$C_2 = \frac{n}{2}(n - 1)\left(\frac{N_1}{N_2}\right)^2 \frac{\Delta Q_{rmax}}{V_R} \qquad (5.4)$$

The accuracy of this equation depends on the statistical distribution of the thyristor Q_r values, but it provides a realistic provisional value for C_2. It must then be checked that C_2 provides, in conjunction with L_{t2}, a duration T_{C_2} of secondary current flow such that thyristor reverse recovery is completed in the first quarter of T_{C_2}. This ensures a relatively low reflected voltage from C_2, thereby giving the required low impedance path across the thyristors. The upper value of C_2 is not critical.

While the oscillatory secondary current is falling from its peak, C_2 charges to a voltage in excess of $V_R N_2/nN_1$ though, owing to the resistance R_{t2}, the peak voltage does not approach double this value. This excess voltage is reflected across to the thyristors, though their individual reverse voltage waveforms vary slightly owing their differing reverse recovery characteristics and variations in transformer winding coupling.

The leakage inductance of the winding sections of transformer T prevent the initial high, short duration, reverse transient voltage across the fast recovery thyristors (section 3.3.1) from being

suppressed. It is necessary, therefore, with these shunt transformer networks, to include a small series saturating reactor to provide additional line impedance for the first few microseconds after the reverse voltage is applied. Typical waveforms are given in the oscillograms of Figure 5.3 with such a saturating reactor included.

5.3 MULTIPLE TRANSFORMER NETWORKS: CONTROL BY CAPACITOR AND DIODE

The basic operation of the network is unaltered by replacing the multiwinding transformer with separate, two-winding transformers, one for each thyristor. The primary windings, each connected across a thyristor, are in series and the secondary windings are in parallel (Figure 5.1(b)).

The separate transformers, unlike the multiwinding transformer, can be represented by a simple equivalent circuit for the effective switching sequence provided by the thyristors' reverse recovery. The individual transformer resistances and leakage inductances are paralleled by the successively blocking thyristors; the total resistance and leakage inductance (referred to the common secondary side) can therefore be calculated with any number of thyristors blocking. But again, for practical purposes, only the fully paralleled value with all the thyristors blocking need be considered. Operation is the same as before and equations (5.1) and (5.2) apply, ratio N_1/N_2 now being the individual transformer turns ratio.

The use of multiple transformers reduces the transformer inter-winding insulation problem since, with the secondary circuit floating, the windings which experience maximum voltage stress (i.e. those of

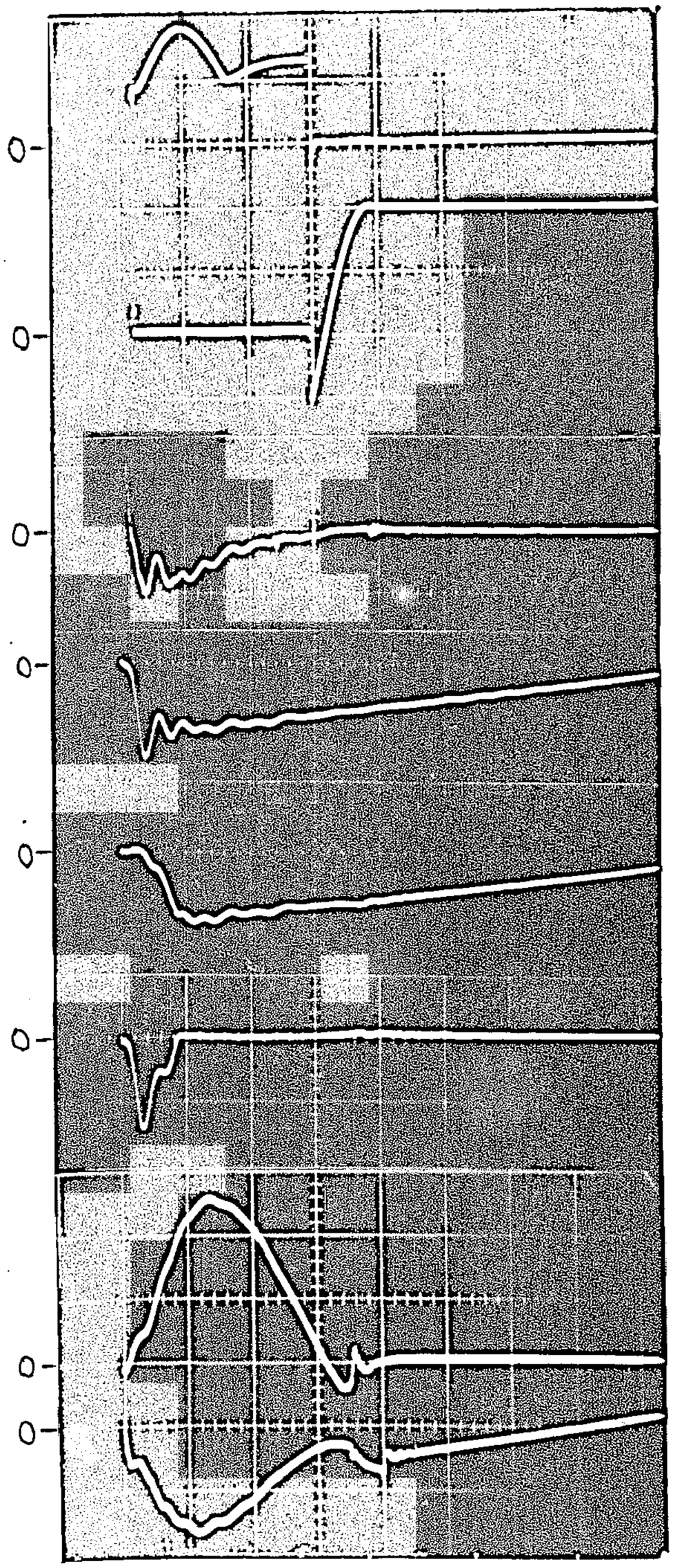

(a) Thyristor string Th_1 current, (20A/cm, 200μs/cm).

(b) Voltage across the thyristor string and series SR, (2.5kV/cm, 200μs/cm).

(c) Thyristor supply line current during reverse recovery, (10A/cm, 5μs/cm).

(d) Corresponding voltage across the thyristor string and SR, (2.5kV/cm, 5μs/cm).

(e) Corresponding voltage across the thyristor string, (2.5kV/cm, 5μs/cm).

(f) Corresponding voltage across the series SR, (2.5kV/cm, 5μs/cm).

(g) Shunt transformer secondary current, (20A/cm, 5μs/cm).

(h) Voltage across the fastest reverse recovery thyristor, (100V/cm, 5μs/cm).

Figure 5.3: Oscillograms of currents and voltages with the shunt transformer and secondary capacitor and diode network.

Network details as Table 5.1, row (b).

Test circuit - Figure 3.3.

the two transformers at the ends of the thyristor string) are subjected to approximately half the line voltage. A further reduction of the interwinding voltage can be produced by dividing the paralleled secondary windings into two or more separate equal groups, each with its own voltage controlling capacitor circuitry. The division between the groups should be one half, one third etc. of the way along the thyristor string, as appropriate for the number of groups. An arrangement of this form, with two secondary groups, is shown in Figure 5.1(c).

The individual transformer groups should operate in a nominally identical manner and equations (5.1) and (5.2) can be applied to each group. Considering each of two groups, for example, both V_R and the effective turns ratio (nN_1/N_2) are half their total values; L_{t2} is doubled. For the same duration of secondary current half-cycle T_{C_2}, C_2 in each group must be half that for the single group arrangement. This results in a reduction of the peak secondary current by a factor of two.

Irrespective of the number of secondary groupings, the transformer primary volt-second rating must not allow core saturation. That of each transformer is simply $(1/n)^{th}$ of the total.

5.4 MULTIPLE TRANSFORMER NETWORKS: CONTROL BY SERIES DIODE

As an alternative to using a capacitor C_2 with diode D_2 for thyristor reverse voltage control, the transformer secondary windings can be connected across a slow recovery diode D_1 in series with the thyristors (Figure 5.1(d)). The reverse recovery characteristic of

the diode is thereby used to control the reverse voltage build up across the thyristors, provided its reverse recovery time is longer than that of any thyristor. D_1 contributes to the reverse voltage rating of the thyristor string, though not to the forward voltage rating, and should be situated in the middle of the string to give the lowest value of maximum transformer interwinding voltage.

The slowest reverse recovery thyristor in the string may be used instead of a diode D_1, but its forward blocking property is rendered ineffective if the transformer cores saturate positively through the secondary windings. A consequential advantage is that the core reset reduces the number of transformer turns required, but the severe local oscillation which occurs round the C-R-transformer secondary loop across the controlling thyristor, makes the method unattractive. The use of much larger transformers would prevent such saturation and allow the diodes D to be dispensed with.

A single, multiwinding transformer can, of course, be used instead of the multiple transformers. When used without the diodes D in the manner latterly described, it functions as a tapped auto-transformer, and has previously been used with a few thyristors in series at a moderate voltage level[39].

The total transformer reverse volt-second withstand, and hence the required number of primary turns per transformer, can be calculated on the basis of one transformer for each of the n devices (thyristors and diode(s)) in the string, provided:

.(a) the transformers each have a 1/1 ratio;

(b) the primary and secondary windings are close coupled;

(c) it can be assumed that the primary magnetising current divides evenly between the secondary windings.

Considering a single secondary grouping (Figure 5.1(d)), the individual transformer secondary current is a fraction $1/(n-1)$ of the primary magnetising current, which increases the transformer magnetising ampere-turns to $\left(1 + 1/(n-1) = n/(n-1)\right)$ of the value with just the primary energised. Since there are (n-1) transformers, the total magnetising ampere-turns, and total volt-second rating, are the same as that for n transformers with only the primary windings carrying magnetising current.

Again, the multiple transformer arrangement lends itself to operation with more than one parallel secondary grouping, in which case the series controlling diode for each group should be strategically situated in the thyristor string for minimum inter-winding voltage. These diodes must have matched reverse recovery characteristics.

5.5 EXPERIMENTAL RESULTS

The measured voltage sharing performance of the shunt transformer networks of Figure 5.1 is given in Table 5.1. Rows (a) and (b) give the results from a single multiwinding transformer arrangement used without, and with, a small series saturating reactor to control the initial reverse voltage spikes. The effect of reducing the size of capacitor C is shown in row (c). The results obtained with

Row	Voltage sharing components								Measured thyristor voltages			String voltage factors	
	Connection as Figure:	C (μF) 20% tol.	R (Ω) 5% tol.	Small SR	Shunt transformer details	No. of trans. sec. groups	C_2 (μF) 20% tol.	R_2 (Ω) 5% tol.	Max. re-verse (V)	Min. re-verse (V)	Max. for-ward (V)	f_{rm}	f_{fm}
(a)	5.1(a)	0.1	22	-	Single, ferrite FX1076 core, 20 × 80 primary turns, 80 sec. turns	-	2.0	2000	290	120	270	0.73	0.91
(b)	5.1(a)	0.1	22	✓	ditto	-	2.0	2000	170	145	270	0.82	0.91
(c)	5.1(a)	0.025	22	✓	ditto	-	2.0	2000	210	135	270	0.81	0.91
(d)	5.1(b)	0.1	22	-	Multiple, ferrite FX1239 cores, 210 turns pri. and sec.	One	2.0	2000	305	160	320	0.69	0.85
(e)	5.1(b)	0.1	22	✓	ditto	One	2.0	2000	195	145	320	0.72	0.83
(f)	5.1(c)	0.1	22	✓	ditto	Two	2 × 1.0	2 × 1000	185	140	320	0.76	0.81

Table 5.1: Voltage sharing performance of the shunt transformer networks (continued over)

Voltage sharing components								Measured thyristor voltages				String voltage factors	
Row	Connection as Figure:	C (μF) 20% tol.	R (Ω) 5% tol.	Small SR	Shunt transformer details	No. of Transf. sec. groups	Slow rec. diode(s) D_1	Max. reverse (V)	Min. reverse (V)	Max. forward (V)	Measured D_1 voltage spike (V)	f_{rm}	f_{fm}
(g)	5.1(d)	0.1	22	✓	Multiple, ferrite FX1239 cores, 210 turns pri. and sec.	One	One	175	80	330	310	0.82	0.80
(h)	5.1(d) modified	0.1	22	✓	ditto	Two	Two	190	90	330	295	0.72	0.80
(j)	5.1(d) modified	0.1	22	✓	ditto	One	None. Control by slowest recovery thyristor.	220	120	320	-	0.68	0.83

NOTES: 1. Small SR - Telcon HCR, 0.002" strip, size 7b, 30 turns, 6.5×10^{-3}Vs, giving 2.2μs reverse voltage withstand.
2. Diode D_1 - STC type RS 660 AF (30A, 600V), previously measured Q_r = 30μC at 25A.

Table 5.1: Voltage sharing performance of the shunt transformer networks. Test circuit - Figure 3.3

multiple transformers follow, with both single and double secondary groupings; secondary side capacitor and diode control (rows (d), (e) and (f)) and series diode control (rows (g) and (h)) are both included. Finally, row (j) illustrates the use of the slowest recovery thyristor in the string for control of voltage sharing in place of a slow recovery diode D_1 (Figure 5.1(d)).

The components given in row (b) produce the waveforms shown in Figure 5.3, to which the design example of section III.2.1 also relates. A graphical plot of measured thyristor voltages is not given (as Figure 3.5) since the distribution is random and bears no definite relationship to the previously measured thyristor reverse recovery charge. The thyristor voltages are influenced mainly by the slight differences of transformer leakage inductance.

5.6 DISCUSSION OF EXPERIMENTAL RESULTS

Considering the results quoted in Table 5.1, it is apparent that, allowing for experimental inaccuracy, none of the shunt transformer networks give an outstandingly good performance. By comparison with the results of Table 3.1, row (c), the maximum reverse voltages are little reduced, though minimum reverse voltages are appreciably increased, giving a more reliable turn-off. Maximum reverse voltage, including any spike, is considerably reduced by introducing a series saturating reactor (c.f. rows (a) and (b), (d) and (e)). Forward voltage distribution is improved considerably on that with R-C's alone, though this is less evident with the separate transformers, which produced more forward voltage overshoot.

Control by a series diode D_1 gives less uniform thyristor voltage distribution than does the capacitor plus diode control though, owing to the presence of the small SR, maximum reverse voltages are little different. The reverse recovery characteristic of D_1 does not provide as effective a low impedance secondary winding path as does capacitor C_2. This applies also to the slowest thyristor reverse recovery characteristic (row (j)). The controlling diode D_1 (or the slowest recovery thyristor) experiences a considerable voltage spike induced by the interruption of current flow through the transformer leakage inductances as reverse recovery is completed.

The turn-off performance of the networks with multiple transformer secondary groupings is virtually the same as that with a single grouping (c.f. rows (e) and (f), (g) and (h)). More difference is apparent with slow recovery diode control than with secondary capacitor plus diode control; ostensibly because the two slow recovery diodes used were not very well matched.

Comparison of the string voltage factors f_{fm} and f_{rm} of rows (b) and (c) demonstrates that the shunt transformer networks make voltage sharing at turn-off substantially independent of the value of capacitance C.

5.7 ADVANTAGES AND DISADVANTAGES OF THE METHOD

The advantages of using shunt transformer(s) to assist the R-C sharing network at thyristor turn-off are as follows:

(a) Improved voltage sharing is provided, particularly if a small series saturating reactor is also used.

(b) Voltage sharing at turn-off is made largely independent of the shunt capacitance C. C must, however, be large enough to handle other voltage sharing duties.

(c) Reverse voltage is induced across all the thyristors, and turn-off is satisfactory with very low applied reverse voltages.

(d) There is low drain on the commutating energy source.

The disadvantages are:

(a) The transformer leakage inductance makes a small series saturating reactor necessary for the suppression of the initial reverse voltage spikes.

(b) The individual thyristor voltage waveshapes differ due to slight differences between the transformer sections.

(c) Secondary capacitor and diode control gives thyristor reverse voltages which are in excess of $(1/n)^{th}$ of the total applied voltage, owing to oscillatory overshoot.

(d) The voltage sharing performance cannot be predicted.

(e) Insulation problems arise with the single multiwinding transformer.

(f) Cumbersome magnetic components are required, though these are not particularly expensive.

The further advantages of the multiple, two-winding transformer arrangement are:

(i) Reduced transformer insulation level is required.

(ii) In the event of a transformer fault, only the individual faulty unit needs to be replaced.

CHAPTER 6

VOLTAGE SHARING BY SHUNT VOLTAGE REGULATING DIODES

6.1 INTRODUCTION

Voltage regulating diodes connected back to back across each thyristor, with or without other components, will limit the forward and reverse voltages applied. They can be used to control all over-voltages met in normal steady operation, but additional protection will be necessary if high energy line transients are anticipated. The regulating diodes do not afford protection against excessive di/dt at turn-on or against excessive forward blocking dV/dt; these conditions necessitate the use of additional components.

Regulating (zener) diodes are not, at present, manufactured with nominal voltages greater than about 200V. A number must therefore be connected in series, as required, to provide the desired clipping voltage. Unfortunately, the higher voltage 'avalanche diodes' now available are unsuitable for this application because their avalanching voltage can only be guaranteed within limits which are far in excess of the tolerances required.

The voltage- current characteristic of the voltage regulating diode is well known[40,41], the variations of voltage from the nominal breakover (zener) value being due to the following reasons:

(a) Manufacturing tolerance.

(b) Increasing operating temperature results in slight increase

of breakdown voltage for the higher voltage devices, which have a positive temperature coefficient.

(c) The dynamic resistance R_Z, being the incremental slope of the voltage-current characteristic after breakdown, gives increasing voltage drop as reverse current is increased. R_Z is not constant, but decreases with increasing current. Typically quoted values, corresponding to one or two low specified currents, are not applicable to high current pulse loading. It is assumed then that the regulating diode voltage will not rise more than 15% above the nominal value for a 5% tolerance device.

(d) Many regulating diodes exhibit a voltage overshoot at switching [42]. However, since recovery normally occurs within a few hundred nanoseconds, this overshoot is unlikely to be damaging to a thyristor.

In this chapter, control of voltage sharing solely by regulating diodes, under conditions of moderate turn-on di/dt and forward blocking dV/dt, is first considered. This is followed by a brief discussion of their use in association with R-C components and then with R-C components combined with a shunt transformer arrangement.

6.2 OPERATION OF THE REGULATING DIODES

The regulating diodes Z_f and Z_r, connected in parallel with the thyristors as in Figure 3.6(d), clip the forward and reverse voltages respectively; each diode shown may, in practice, consist

of a number of such devices in series. There are two distinct operating conditions at turn-off:

(a) If the applied reverse voltage is slightly greater than the summed breakover voltages of regulating diodes Z_r (i.e. $V_R > nV_{zr}$), the thyristor reverse voltage distribution will be equalised, but unwanted diode Z_r power dissipation occurs while the commutating capacitor discharges to voltage nV_{zr}. With a stiff voltage source, operation in this way is usually impossible.

(b) When $V_R \leq nV_{zr}$, not all the regulating diodes operate and voltage distribution may be very uneven. No excess dissipation occurs in the regulating diodes Z_r.

The conditions described in (b) form the more practical case. To avoid excessive dissipation in diodes Z_f, $V_F \leq nV_{zf}$ always. The regulating diode nominal voltages V_{zf} or V_{zr} should be about 85% of the thyristor peak repetitive voltage rating to allow for the possible variations of clipping voltage. This gives a string voltage derating factor f_s of 0.85 assuming the applied voltage is equal to the summed regulating diode voltages, forward or reverse as appropriate.

The regulating diodes have to counteract all the effects which can lead to uneven thyristor voltage sharing (section 3.1). Hence, the diodes' functions are to control the steady-state and transient voltage distribution, and to limit thyristor overvoltages at turn-on and turn-off. Each of these duties must be taken into account when estimating the regulating diode power rating.

Preparatory to this, the question of thyristor voltage waveforms and turn-off must be considered.

6.3 VOLTAGE WAVEFORM CONSIDERATIONS

The individual thyristor voltage waveforms vary widely and in many cases bear only superficial resemblence to that of the voltage across the complete string. The factors which influence the waveform are as follows.

A low thyristor leakage impedance leads to that device accepting a low voltage compared with the others in series, under steady-state or low frequency conditions.

At turn-off, the faster reverse recovery thyristors are the first to accept reverse voltage. Slow recovery devices may not be reverse biased.

Capacitive effects are difficult to assess accurately. If the regulating diodes are absent, analysis shows[33] that, for the idealised situation of constant equal thyristor capacitance C_d and equal electrode capacitance to earth C_g (Figure 6.1), uneven transient voltage distribution occurs. Voltages progressively increase from a minimum across the thyristor at the earthy end to a maximum across that at the high voltage end of the string. The thyristor blocking dV/dt also increases in a similar manner. The addition of voltage regulating diodes controls the level of the voltage but not dV/dt, although the diode capacitances have influence and must be included in C_d.

In order to establish the maximum thyristor dV/dt relative to

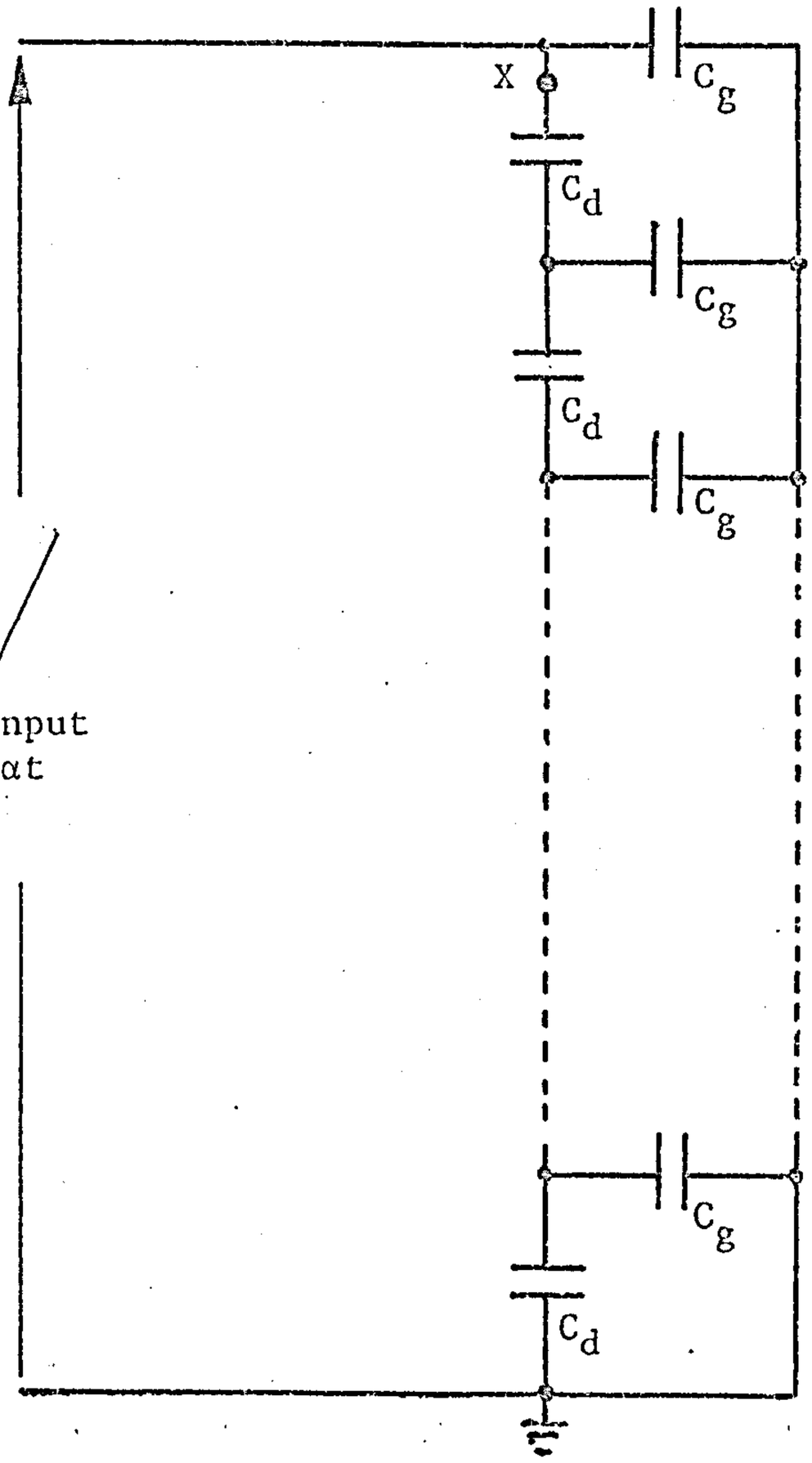

Figure 6.1: Idealised equivalent circuit of the device and stray capacitances to earth.

that applied to the string, consider a ramp voltage of slope α applied to the equivalent capacitor network of Figure 6.1. If C_x is the capacitance between point X and earth (neglecting the uppermost C_g), the charging current at X is given by αC_x. Hence, the maximum thyristor dV/dt is $\alpha C_x/C_d$, which is a proportion C_x/C_d of the total dV/dt applied. Now as the number of thyristors (n) used in series is increased, or as the number of thyristors effectively increases as more progressively accept forward blocking voltage under the influence of the regulating diodes, C_x reduces from a value of C_d for a single thyristor to an almost constant value when n approaches ten or more, depending on the C_g/C_d ratio. Thus, the ratio of the maximum thyristor dV/dt to the total applied dV/dt decreases correspondingly from unity to a value which is independent of the number of thyristors in series (Figure 6.2). This is a disadvantage with 'long' strings since the ratio of the maximum dV/dt to the average dV/dt, (α/n), for the thyristors then increases in proportion to n.

In practice C_d consists of the internal depletion layer capacitances of the thyristor and parallel regulating diodes, plus stray interelectrode capacitance. The fact that the former capacitances vary with blocking voltage according to an inverse cubic relationship[25] adds complication. The above simplified approach is, however, adequate for qualitative explanation of the thyristor waveforms.

6.4 TURN-OFF CONSIDERATIONS

No thyristor will turn-on if the current through it is prevented from rising to the latching value. This fact is of fundamental

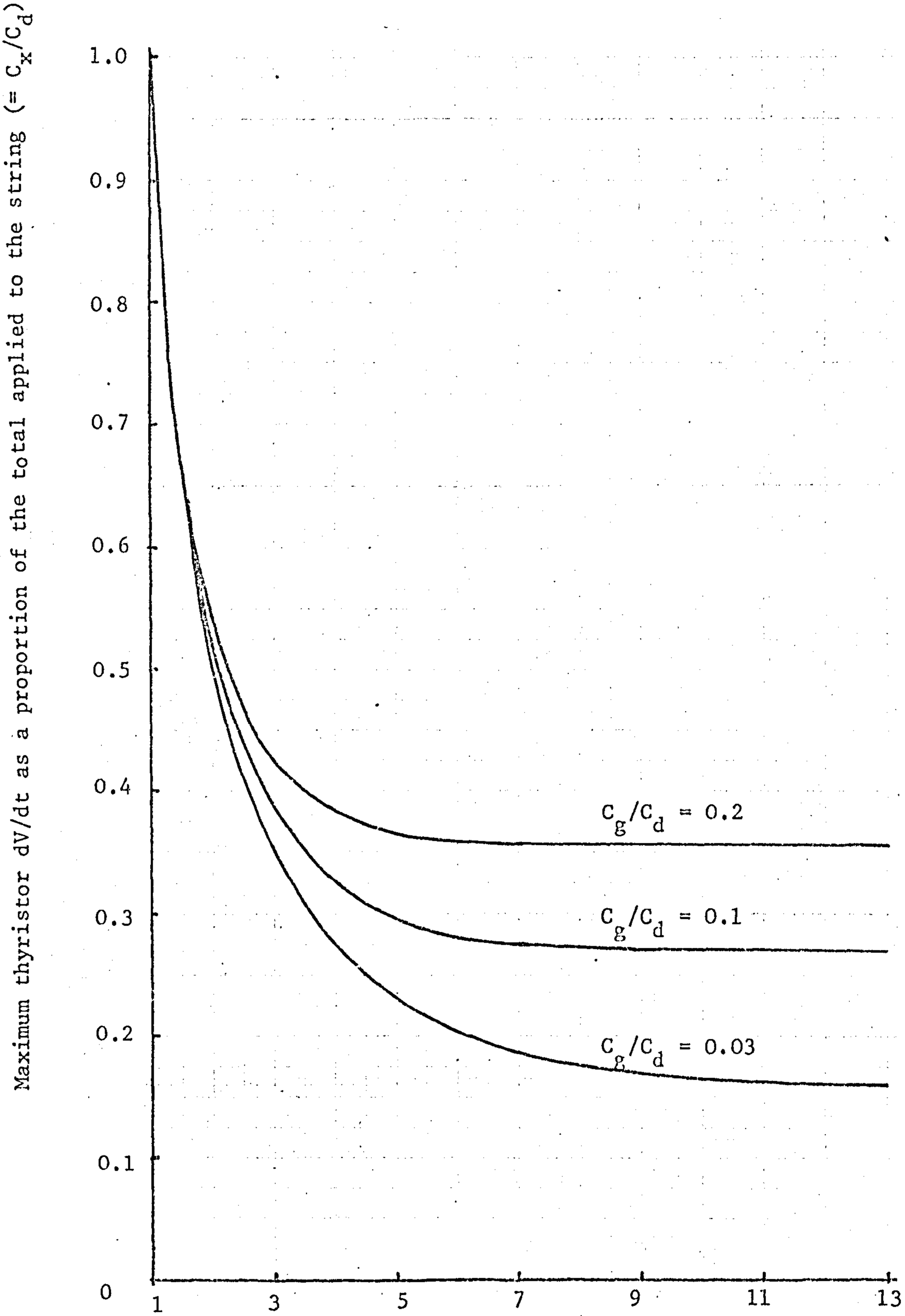

Figure 6.2: Variation of the dV/dt across the thyristor at the high voltage end of the string as the effective number of thyristors is increased (capacitance distribution as Figure 6.1).

importance when considering the turn-off of series thyristors which experience widely differing voltage waveforms (e.g. Figure 6.3). It follows that, after the faster recovery thyristors have turned off under reverse bias, the slower recovery thyristors will turn-off by starvation providing the faster thyristors and their parallel regulating diodes restrict forward current to a leakage level. The critical condition for turn-off of all the thyristors is that a sufficient number (n) must have turned off in order to withstand the forward blocking voltage as it rises to its full value V_F. For the full voltage, this can be expressed as $n \geq V_F/V_{fz}$. If this condition is not met, the regulating diodes across the faster recovery thyristors will be destroyed.

The problem of dV/dt triggering is exacerbated by the increased dV/dt experienced by the thyristors at the high voltage end of the string. If, during the applied forward blocking rise, these thyristors turn on, there is the risk of a cascade turn-on of all the thyristors from this cause.

6.5 REGULATING DIODE POWER RATING

6.5.1 Estimation of the rating from the duty cycle

Precise representation of the regulating diode duty cycle is difficult, and accurate calculation of the power dissipation is not possible. Given here is a working method of calculating a safe power rating. Since individual diode power dissipation depends on its position in the string, the worst condition must always be

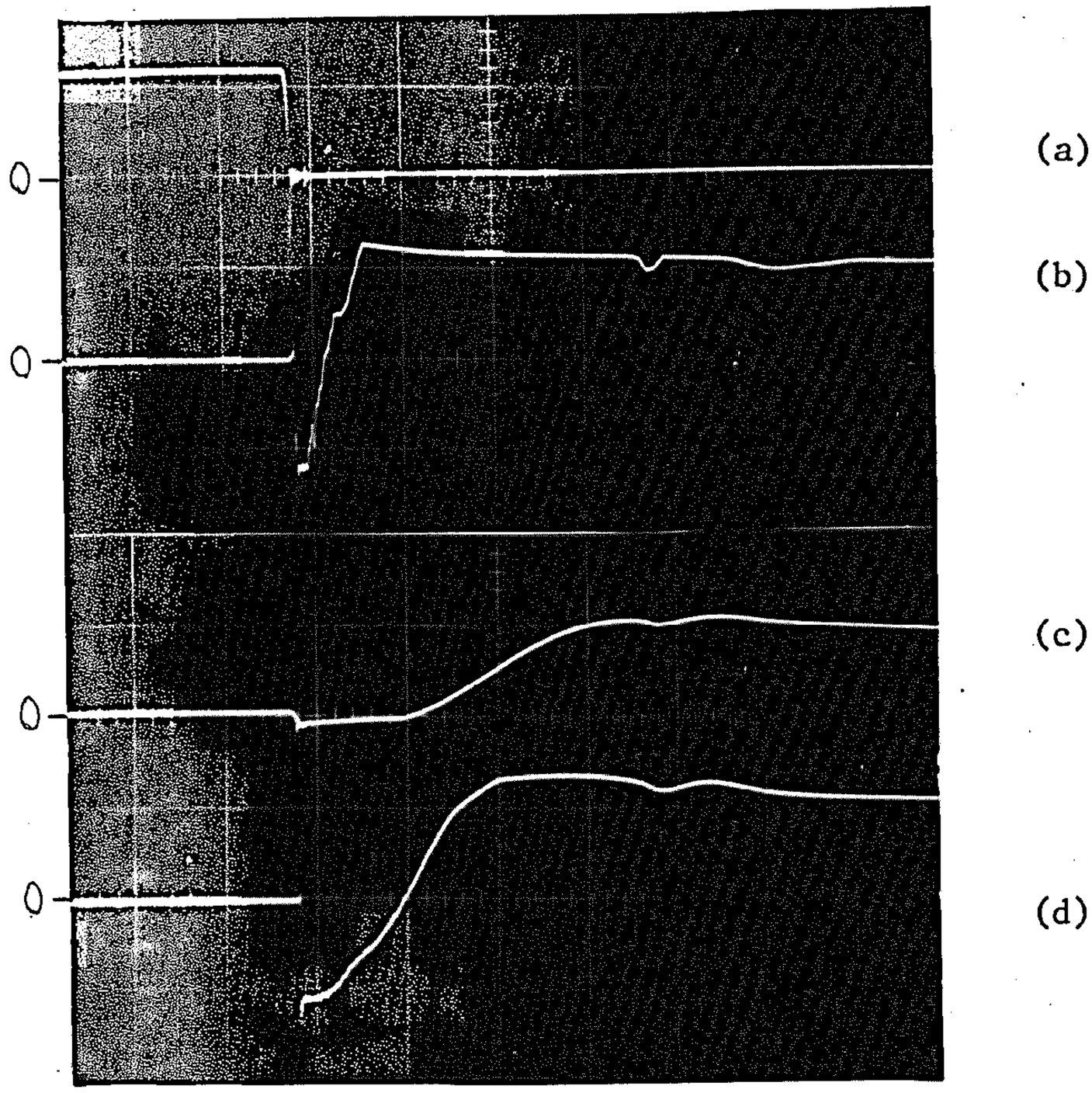

Figure 6.3: Individual test thyristor waveforms with the shunt regulating diode sharing network.

(a) Thyristor string Th_1 current (20A/cm).

(b) Voltage across the fastest recovery thyristor at the high voltage end of the string (250V/cm).

(c) Voltage across the slowest recovery thyristor at the earthy end of the string (250V/cm).

(d) Voltage across the second fastest recovery thyristor situated next to the slowest at the earthy end (250V/cm).

(All 50μs/cm)

Network details as Table 6.1, row (b).

Test circuit - Figure 3.3.

assumed. For simplification it is reasonable to neglect the dissipation due to diode forward conduction and leakage.

Estimation of the mean power dissipation is most easily made by assuming a constant breakover voltage of 1.15Vz to account for variations of regulating diode breakover voltage (section 6.1, para (c)). Then,

$$\text{mean power dissipation} = \frac{1.15}{T} Vz \int_0^{t_p} i \, dt \, , \qquad (6.1)$$

where t_p is the pulse width and T is the period of the duty cycle. Equation (6.1) can be used for each individual function which the diode performs and the separate values summed to give the total mean dissipation. Use of the time integral of current allows the simple substitution of ΔQ_r values for $\int i \, dt$ when considering turn-off dissipation. The factor 1.15 is unnecessary when the peak power is low.

However, when semiconductors are subjected to a repetitive pulse duty, the junction temperature T_J fluctuates during the cycle. Since the maximum allowable junction temperature is the criterion on which device power rating is based, the calculated mean power dissipation is likely to prove inadequate.

A technique for handling non-rectangular pulses is to first calculate the highest peak power (P) in the duty cycle and the total pulse energy (or average power)[10,43]. The duration of an equivalent rectangular pulse (t_p), having the same peak power and average power is then determined, and standard expressions are used

to calculate the junction temperature rise $(T_J - T_A)$ above ambient temperature T_A. For such a rectangular pulse,

$$T_J - T_A = P \cdot \theta_1 , \tag{6.2}$$

where θ_1 is the effective transient thermal impedance, given by

$$\theta_1 = \theta \cdot \frac{t_p}{T} + \left(1 - \frac{t_p}{T}\right) \theta_{(T+t_p)} - \theta_{(T)} + \theta_{(t_p)}.^{10} \tag{6.3}$$

Here θ is the steady-state thermal resistance, $\theta_{(T+t_p)}$ and $\theta_{(T)}$ are transient thermal impedances for pulse durations $(T+t_p)$ and (t_p) respectively. The very high power pulses at turn-on and turn-off have a typical duration of a few microseconds; this creates difficulty in applying equation (6.3) because manufacturers only quote transient thermal impedance characteristics for pulse durations down to 100μs. For lower durations extrapolation can be made using the relationship $\theta_{(t_p)} \propto \sqrt{t_p}$ [44], but this only applies for $t_p \geq 10\mu s$. This relationship has been used as a guide in the design example of section III.3, even for lower pulse widths.

Since t_p is usually small, $t_p/T << 1$ and $\theta_{(T+t_p)} = \theta_{(T)}$ approximately. Therefore equation (6.3) simplifies to

$$\theta_1 = \theta \frac{t_p}{T} + \theta_{(t_p)} . \tag{6.4}$$

The term $\theta_{(t_p)}$ allows for the additional temperature rise due to pulsation since, if it is neglected, equation (6.2) gives

$$T_J - T_A = P \frac{t_p}{T} \theta .$$

This is equivalent to using the average power equation (6.1). If charge concepts are used, as for turn-off, an appropriate current pulse waveform and duration must be assumed in order to estimate the peak pulse power.

Firstly, then, the mean and peak power dissipations produced by the separate functions of each diode Z_f and Z_r must be determined; the method is given in the following sections. The total mean dissipation for each diode is then estimated and a suitable device, having a power rating above the total mean dissipation, chosen. Using its published transient thermal impedance characteristic, the peak junction temperature is then checked by equations (6.4) and (6.2) for the equivalent rectangular pulse per cycle.

6.5.2 Steady-state and low frequency voltage sharing duty

Consider the extreme case where one thyristor has zero leakage and all the others have maximum leakage; only the regulating diode across the zero leakage thyristor operates. Regulating diode leakage will be neglected since it is usually about one thousandth of that of a thyristor. The analysis applies equally to forward and reverse voltage sharing, therefore only the former will be considered. The equivalent circuit (Figure 6.4(a)) shows the leakage current (i) path, where

$$i = \frac{V_F - V_{zf}}{(n-1)R_{th} + R_z} .$$

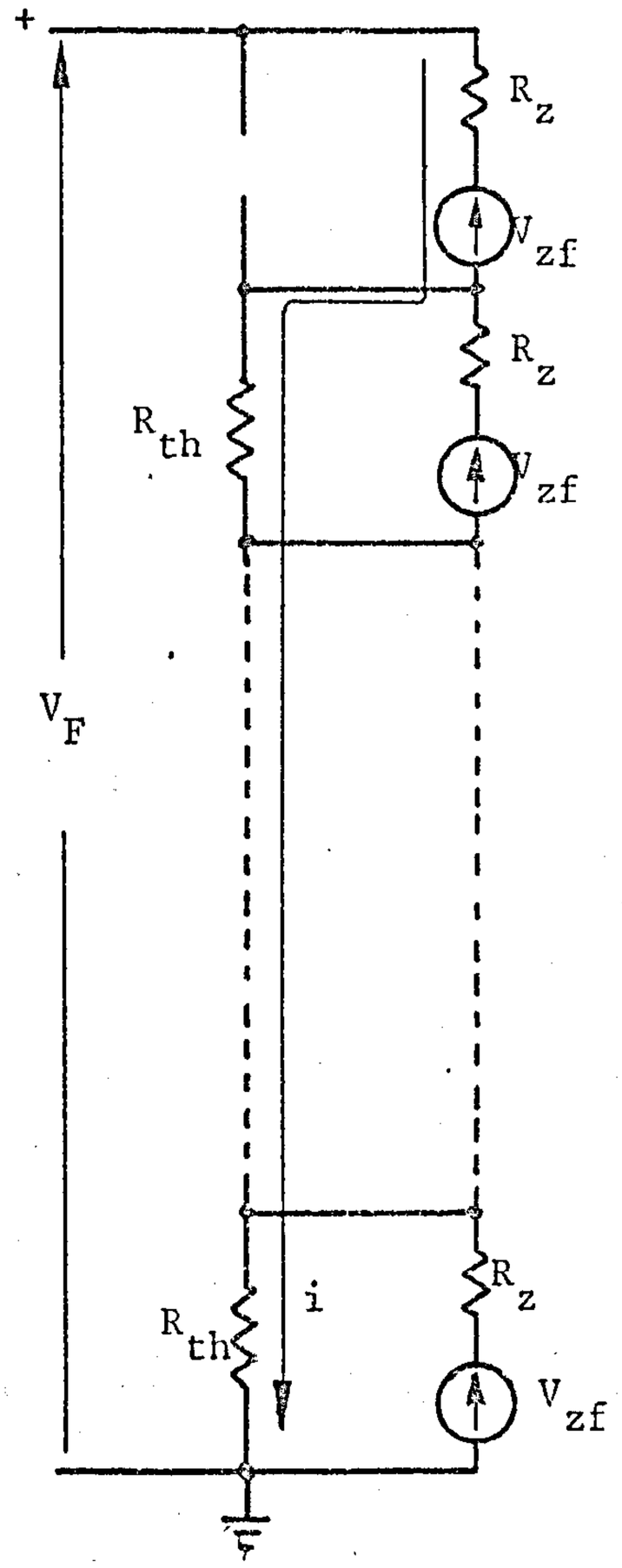

(a)

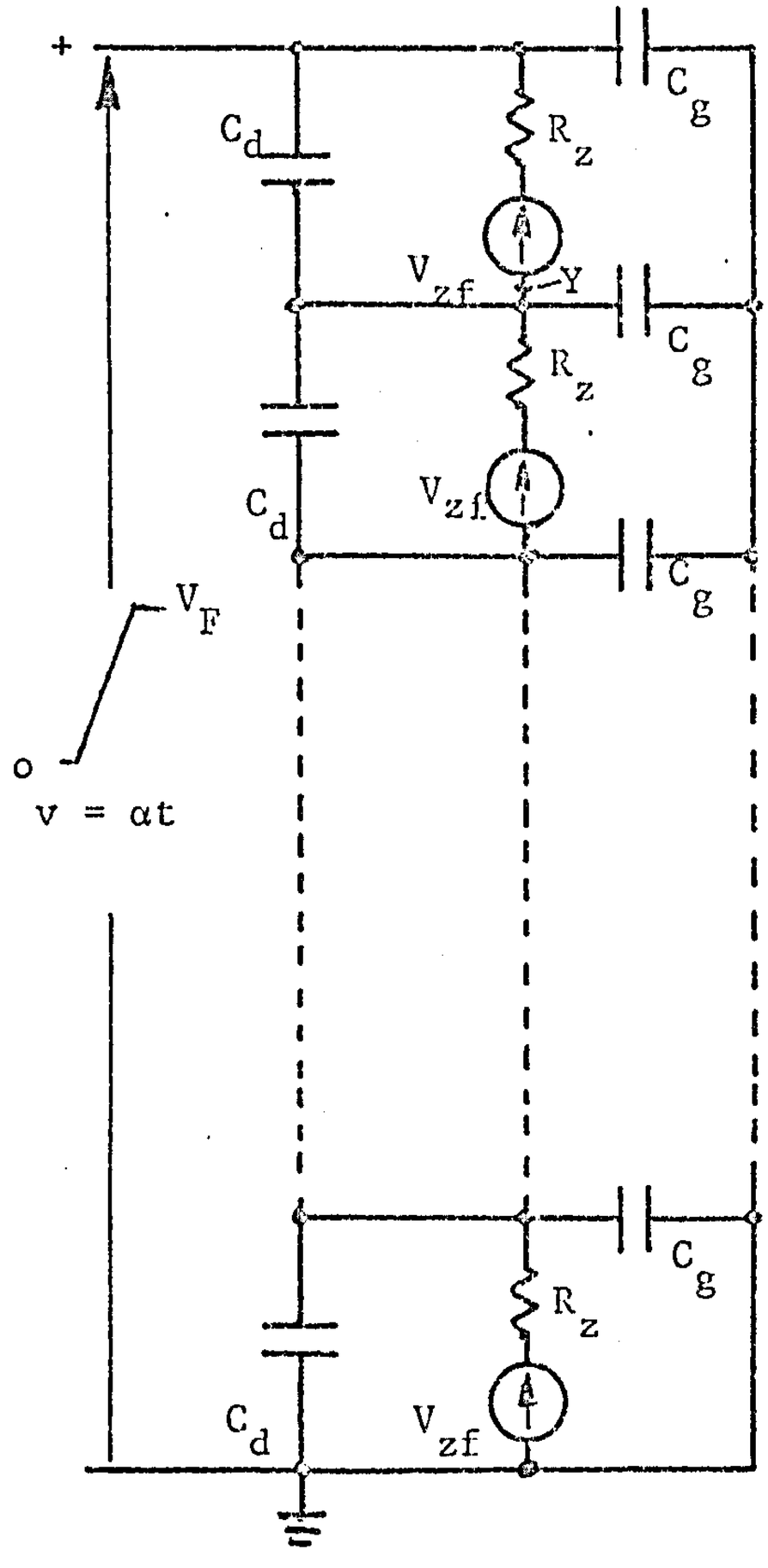

(b)

Figure 6.4: Equivalent circuits for the estimation of regulating diode power dissipation.

(a) For steady-state voltage sharing.

(b) For transient voltage sharing.

For the operative regulating diode,

$$\text{power dissipation} = V_{zf}i + i^2R_z \ .$$

Now $R_z << (n-1)R_{th}$; approximately therefore,

$$\text{power dissipation} = V_{zf}\left(\frac{V_F - V_{zf}}{(n-1)R_{th}}\right) + \left(\frac{V_F - V_{zf}}{(n-1)R_{th}}\right)^2 R_z. \quad (6.5)$$

The mean dissipation during the cycle is calculated by multiplying equation (6.5) by the forward blocking time expressed as a fraction of the total period.

6.5.3 Transient voltage sharing duty

Maximum dissipation on transient voltage sharing duty takes place in that regulating diode (forward or reverse as appropriate) across the thyristor at the high voltage end of the string. This dissipation will be greatest if the thyristor voltages are perfectly equalised by the diodes.

Consider a ramp forward voltage applied to the equivalent network of Figure 6.4(b). Comparing the incoming charge flow with that which returns in the earthy line during the applied forward voltage rise from zero to V_F, the charge flow through the capacitances C_d and C_g, and the regulating diode ($= Q_{zfh}$) at the high voltage end must equal that through C_d and the regulating diode ($= Q_{zf\ell}$) at the earthy end plus that through all the capacitances C_g to earth. Assuming that the final voltage sharing is uniform ($V_F = nV_{zf}$) and that $Q_{zf\ell} = 0$, then

$$V_F C_g + C_d V_{zf} + Q_{zfh} = C_d V_{zf} + Q_{zf\ell} + \left(V_{zf} C_g + 2V_{zf} C_g + \ldots nV_{zf} C_g\right)$$

$$= C_d V_{zf} + V_{zf} C_g \left(1 + 2 + 3 + \ldots + n\right)$$

$$nV_{zf} C_g + Q_{zfh} = V_{zf} C_g \frac{n(n+1)}{2}$$

$$Q_{zfh} = V_{zf} C_g \frac{n(n-1)}{2} .$$

Therefore, for the regulating diode at the high voltage end,

$$\text{mean power dissipation} = 1.15\, V_{zf}^2 C_g \frac{n(n-1)}{2} f . \qquad (6.6)$$

As the derivation of equation (6.6) is based on charge flow, it is applicable to any applied voltage waveform.

The current through the diode must be estimated in order to calculate the peak power. This diode clips voltage first, since the high voltage end thyristor experiences the greatest dV/dt. Thereafter it carries the charging current of the complete network below point Y in Figure 6.4(b) which experiences the full applied dV/dt (= α). The product of the effective capacitance and α gives the regulating diode current (I_{zf}). Then,

$$\text{peak power dissipation} = (V_{zf} I_{zf} + I_{zf}^2 R_z). \qquad (6.7)$$

As an alternative to equation (6.6), the mean dissipation can be calculated by multiplying equation (6.7) by the diode operating period as a fraction of the total period.

6.5.4 Forward voltage sharing duty at turn-on

Again consider the extreme case of one slow turn-on thyristor and all the others equally fast. The regulating diode Z_f across the former must, in conjunction with a series inductance L, suppress the overvoltage at turn-on. Assuming L is constant and using a similar approach to that of section 3.2.2, the peak regulating diode current I_{zfpk} is given by

$$I_{zfpk} = \frac{\Delta t_{on}}{L} \left[V_F - 1.15\ V_{zf} \right] . \qquad (6.8)$$

Then,

$$\text{peak pulse power} = 1.15\ V_{zf} I_{zfpk} . \qquad (6.9)$$

The linear current rise allowed by constant inductance L gives an idealised current waveform of triangular shape which falls abruptly from I_{zfpk} when the thyristor turns on. Therefore

$$\text{pulse energy} = \frac{1}{2}\ I_{zfpk}\ \Delta t_{on}\ 1.15 V_{zf} .$$

For the complete cycle,

$$\text{mean power dissipation} = 0.58\ V_{zf} I_{zfpk}\ \Delta t_{on} f . \qquad (6.10).$$

6.5.5 Reverse voltage sharing duty at turn-off

The power dissipation in the regulating diodes Z_r during thyristor reverse recovery arises from two features. These will be considered separately.

(a) Difference of thyristor reverse recovery charge.

When the reverse turn-off voltage V_R is applied to

the string, the faster recovery thyristors become biased to the regulating diode voltage V_{zr}; their number x is given approximately by $x = V_R/V_{zr}$. The remaining thyristors experience low or zero reverse voltage and it will be assumed that the charge removed from these will equal that removed from the x^{th} fastest thyristor ($=Q_{rx}$).

The charge flow through the regulating diode Z_r shunting the fastest thyristor (No. 1) is therefore given by

$$\Delta Q_{rx-1} = Q_{rx} - Q_{r1} .$$

Using this relationship in equation (6.1) gives

$$\text{mean power dissipation} = 1.15\ V_{zr} \Delta Q_{rx-1} f.$$

(b) Suppression of the hole storage voltage spike

When the peak reverse recovery current I_{rpx} in the x^{th} thyristor abruptly falls, the energy stored in the series inductance L prolongs the current flow through the diodes Z_r across the x fastest thyristors. Assuming the current fall to be instantaneous and neglecting the lead resistance and any additional reverse recovery loss in the (n - x) slower thyristors, the energy stored in L is dissipated in the x regulating diodes which are operative. For each of these,

$$\text{energy dissipated per cycle} = \frac{1}{2} \frac{L}{x} I_{rpx}^2 .$$

Therefore,

$$\text{mean power dissipation} = \frac{1}{2}\frac{L}{x} I_{rpx}{}^2 f.$$

The practical difficulty in using this expression lies in estimating I_{rpx} which depends on the reverse voltage applied and the turn-off circuit resistance. The latter usually comprises lead and inductor winding resistance, and its value is difficult to assess before construction. Thus there is no accurate information by which current I_{rpx} can be calculated. Experience shows, however, that a value equal to the forward current before turn-off is not unreasonable. Since the fall of thyristor reverse recovery current is not instantaneous, the above approach is generous.

The maximum total mean power dissipation in any regulating diode Z_r at thyristor turn-off is given by the sum of the components established in (a) and (b); namely,

$$\text{total mean dissipation at turn-off} = \left(1.15V_{zr}\, Q_{rx-1} + \frac{1}{2}\frac{L\, I_{rpx}{}^2}{2}\right) f \cdot \qquad (6.11)$$

In order to estimate the peak pulse power, a regulating diode current waveshape and duration must be assumed. In practice the current is approximately sinusoidal with a duration similar to the difference of the reverse recovery times of the fastest and x^{th} fastest thyristors, Δt_{rx-1}.

Using these approximations gives

$$\text{peak pulse power} = \frac{\pi}{2\Delta t_{rx-1}}\left(1.15V_{zr}\Delta Q_{rz-1} + \frac{1}{2}\frac{L\, I_{rpx}{}^2}{x}\right) \qquad (6.12)$$

6.6 THE USE OF SHUNT R-C COMPONENTS WITH REGULATING DIODES

6.6.1 The reason for adding resistors and capacitors

The conditions of high turn-on di/dt and high dV/dt, which the regulating diodes cannot control, necessitate the use of additional L-R-C components (section 3.2). The shunt R-C components can be connected across the complete string, across groups or tiers of thyristors[33] or across the individual thyristors. The disadvantage of using a single resistance and capacitance across the string is that the lead inductance might limit the effectiveness of these components.

Equal thyristor dV/dt is provided by including additional R-C components across each thyristor (Figure 3.6(e)). The separate use of R-C components and regulating diodes has already been considered in detail. When used together, the only new facet of operation concerns thyristor turn-off which will be discussed next.

6.6.2 Turn-off considerations

Assume that C (Figure 3.6(e)) is large enough to swamp the device and stray capacitances, yet insufficient for voltage equalisation. If, under low reverse voltage conditions, the voltage distribution is so uneven as to produce zero voltage across the slowest recovery thyristors, it is possible that these will fail to turn-off. Those which do turn off may be insufficient in number to withstand re-applied forward voltage; their parallel regulating

diodes will then be overloaded and destroyed.

Under these conditions, the constant reverse voltage waveform (Figure 3.2(a)) is least likely to give rise to turn-off failure provided the zero reverse biased thyristors are allowed time to turn-off before forward voltage is re-applied. When the applied voltage is linearly changing (Figure 3.2(b)), although reverse voltage distribution will be improved by those regulating diodes which operate, turn-off conditions are basically the same as for R-C's used alone (section 3.3.3).

The mechanism by which those thyristors with low or zero reverse bias fail to turn off is important. As the voltage rises positively from the V_R value (Figure 3.2(b)), the discharge current from the reverse charged capacitors flows in a forward direction through those thyristors without reverse bias, which are therefore not turned off. If this current is equal to or above the latching value, these thyristors will turn on. If it is below the latching current, they will turn off and commence to accept forward voltage after an interval governed by their own recombination characteristics. The criterion for the satisfactory turn-off of any thyristor is therefore

$$C \frac{dV}{dt} < I_h ,$$

where the holding current I_h is assumed to be equal to the latching current. For a constant linear voltage slope α across the string,

$$C \frac{\alpha}{n} < I_h . \qquad (6.13)$$

This reasoning leads to the conclusion that, for any given minimum applied reverse voltage and dV/dt across the thyristor string, there is a prohibited range of values for capacitors C. When C is above this range, turn-off is satisfactory because adequate reverse bias is provided across all the thyristors; when C is below the range, the non-reverse biased thyristors turn off by starvation.

6.7 THE USE OF SHUNT R--C COMPONENTS AND TRANSFORMERS WITH REGULATING DIODES

The problem of turn-off when the required value of C is within the prohibited range can be overcome by utilising the technique of section 5.2 or 5.3. A parallel transformer arrangement, with control by a secondary side capacitor and diode, induces a reverse voltage across all the thyristors during the secondary current oscillation (Figure 5.3(g)), the duration of which is controllable by the choice of capacitance C_2. Figure 3.6(f) shows the complete voltage sharing network with R-C components, regulating diodes and multiple two-winding transformers.

6.8 EXPERIMENTAL RESULTS

The performance of the regulating diode networks used with the test string of twenty thyristors (Figure 3.3) is given in Table 6.1. Row (a) refers to regulating diodes used alone, with their nominal voltages chosen to equalise the reverse voltage distribution. Voltage mis-sharing is introduced by using regulating diodes Z_r having a higher nominal voltage (row (b)). The oscillograms of Figure 6.3 refer to this arrangement.

Voltage sharing components										Measured thyristor voltages with predicted values shown ( )				String voltage factors	
Row	Fig. 3.6	C (μF) 20% tol.	R (Ω) 5% tol.	Reg. diode nom. voltage 5% tol		Shunt transformers T_1 to T_n		C_2 (μF)	R_2 (Ω)	Maximum reverse spike (V)	Maximum reverse steady peak (V)	Minimum reverse steady peak (V)	Maximum forward peak (V)	f_{rm}	f_{fm}
				Z_f	Z_r	Core	Turns								
(a)	(d)	-	-	300	139	-	-	-	-	240 (139)	170 (139)	0	330 (300)	0.75	0.68
(b)	(d)	-	-	300	300	-	-	-	-	340 (300)	300 (300)	0 (0)	340 (300)	0.68	0.72
(c)	(e)	0.1	22	300	139	-	-	-	-	165 (139)	150 (139)	120 (139)	290 (265)	0.97	0.91
(d)	(e)	0.1	22	300	139	-	-	-	-	140 (139)	140 (139)	20 (20)	240 (250)	0.89	0.65
(e)	(e)	0.01	22	300	300	-	-	-	-	320 (300)	280 (300)	0 (0)	320 (300)	0.70	0.75
(f)	(f)	0.01	22	300	300	Mullard FX1239	Pri-200 Sec-200	2.0	2000	335 (300)	200 (160)	100 (160)	310 (300)	0.75	0.68

Table 6.1: Experimental voltage sharing performance of the regulating diode networks.
Connections as Figure 3.6(d), (e) or (f) Test circuit - Figure 3.3

The use of resistors and capacitors with the regulating diodes is demonstrated by the results of rows (c), (d) and (e). Firstly, the regulating diodes have been chosen to provide equalised voltage distribution, the R-C components being identical with those of Table 3.1, row (c) to allow direct comparison. The effect of then reducing the operating voltage to the minimum which will provide safe thyristor turn-off is illustrated by row (d). A critical turn-off condition is introduced by using diodes with a higher nominal voltage V_{zr} and a reduced value of C (row (e)), to which the oscillograms of Figure 6.5 relate. The improvement in turn-off performance then produced by adding a shunt transformer network is demonstrated in row (f).

In general, the random nature of the voltage distribution makes a graphical representation (as Figure 3.5) not worthwhile.

6.9 DISCUSSION OF EXPERIMENTAL RESULTS

The oscillograms of the thyristor voltage waveforms (Figure 6.3) illustrate the very poor voltage sharing with regulating diodes used alone. Reverse and forward voltage clipping by the regulating diodes is apparent, particularly for the fastest recovery thyristor situated at the high voltage end of the string. Only the faster recovery thyristors are reverse biased (numbering V_R/V_{zr}) and the effect of stray capacitance to earth, explained in section 6.3 is well demonstrated. The dV/dt across the thyristor at the high voltage end is much higher than that across the second fastest recovery thyristor situated near the earthy end. Also, this maximum

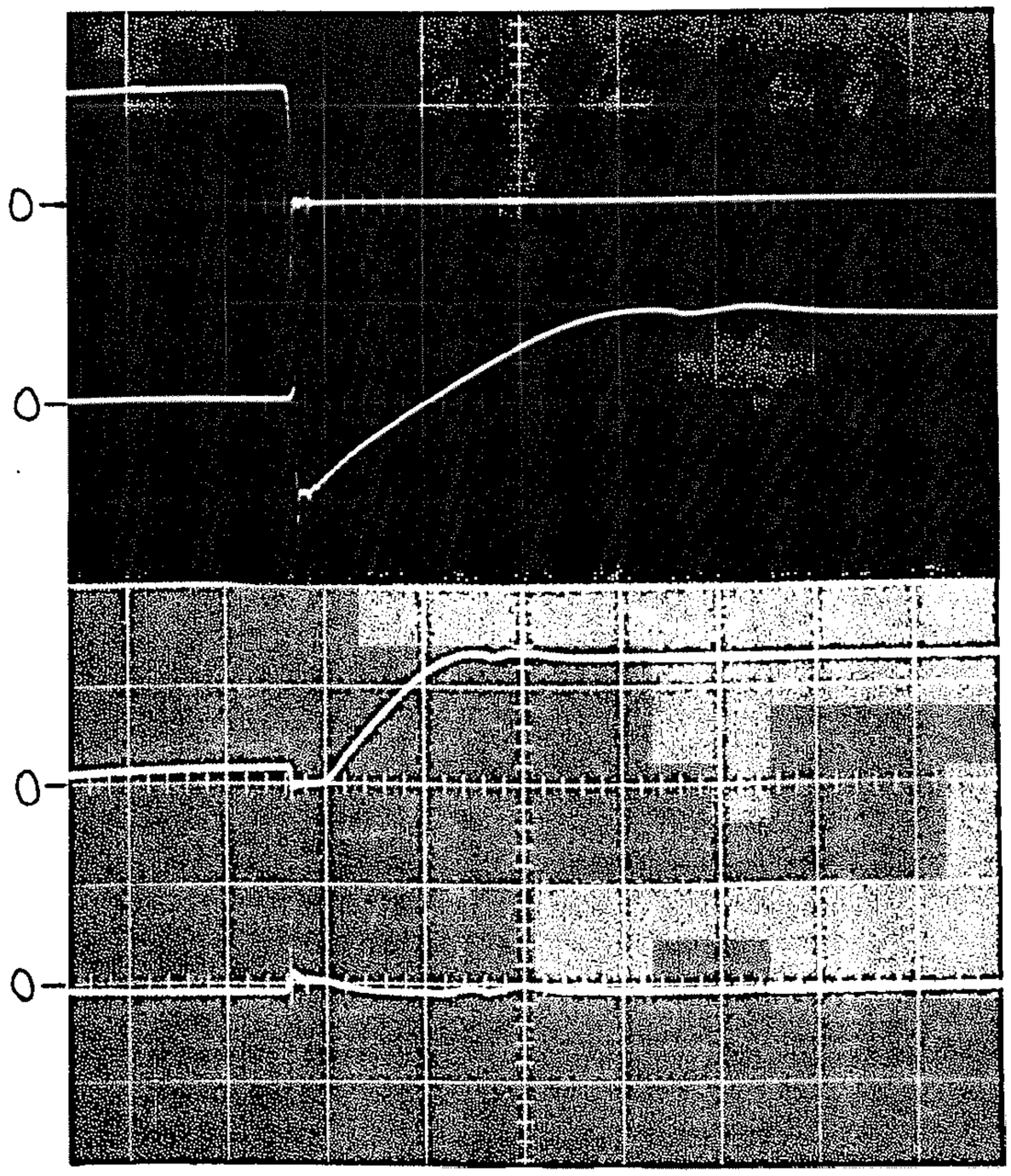

Figure 6.5: Individual test thyristor waveforms with the shunt regulating diode plus R-C sharing network

(a) Thyristor string Th_1 current, (20A/cm).

(b) Voltage across the fastest recovery thyristor at the high voltage end of the string, (250V/cm).

(c) Voltage across the slowest recovery thyristor at the earthy end of the string, (250V/cm).

(d) Voltage across the single intermediate thyristor which fails to turn off. (250V/cm).

(All 50μs/cm)

Network details as Table 6.1, row (c).

Test circuit - Figure 3.3.

dV/dt is apparently reduced as other thyristors successively block and commence their voltage rise. Despite the lack of reverse voltage across some thyristors, turn-off is satisfactory in all cases. The poor voltage sharing is reflected in the low string voltage factors f_{rm} and f_{fm} in rows (a) and (b) of Table 6.1. The maximum reverse voltages in rows (a) and (c) exceed the value of $1.15V_{zr}$ previously assumed (section 6.1, para (c)), the reason being that for the 139V (V_{zr}) diodes, the commutating capacitor voltage is greater than nV_{zr} (section 6.2, para (a)).

The best voltage sharing performance is provided by the inclusion of R-C's with regulating diodes chosen to equalise reverse voltage. Values of f_{rm} and f_{fm} in row (c) show a great improvement on the equivalent values without regulating diodes (Table 3.1, row (c)). The calculated minimum allowable thyristor reverse voltage (equation 3.10) agrees well with that measured (row (d)), as does the calculated maximum forward voltage (equation 3.9) which occurs across the same thyristor. Voltage sharing is grossly uneven with 300V regulating diodes (Z_r) and C reduced in value to 0.01μF (Table 6.1, row (e) and Figure 6.5). Considering thyristor turn-off, criterion (6.13) gives a current of 30mA (n = 20, α = 60V/μs), which is greater than the quoted typical thyristor holding current of 20mA. Turn-off is therefore at risk for the thyristors which are not reverse biased, since the capacitors C used lie within the prohibited range. This is borne out by one thyristor failing to turn off (Figure 6.5 (d)).

Satisfactory turn-off is regained by the introduction of an

additional shunt transformer network. All the thyristors are reverse biased by at least 100V (Table 6.1, row (f)). The added network is identical to that which gave the waveforms of Figure 5.3.

It is evident from the results that, despite the extremely poor voltage sharing when voltage regulating diodes are used alone, thyristor turn-off is perfectly satisfactory and, for the applied test voltage waveform, there is little point in using a more complex voltage sharing network. If, for other waveforms, added R-C components are required to reduce dV/dt, turn-off may be in doubt. This can be overcome by the further addition of a parallel transformer arrangement.

The use of a series saturating reactor in association with the above networks has not been discussed as, in general, it constitutes an alternative solution to the problem. For example, if R-C components are necessary under high dV/dt conditions, an additional series saturating reactor would be first considered in preference to regulating diodes and shunt transformers. However, a series saturating reactor does reduce regulating diode power dissipation at thyristor turn-on and turn-off, and can therefore be of great advantage at high operating frequencies. This is considered in the next chapter.

6.10 ADVANTAGES AND DISADVANTAGES OF THE METHOD

The advantages of using regulating diodes for control of voltage sharing are:

(a) Accurate control of the maximum thyristor voltage is provided.

(b) When R-C components are also used, the thyristor voltage waveforms are good and some reduction in the size of capacitors C may be allowable.

(c) With regulating diodes used alone, the R-C component losses are replaced by the much lower dissipation in the regulating diodes.

(d) In the event of failure, the regulating diode becomes short-circuited and thereby protects the associated thyristor.

(e) Regulating diodes can be used to control series diode reverse voltage sharing. Regulating diodes Z_f can be replaced by a low voltage plain diode to block any forward load current flow through the parallel diode path.

The disadvantages are:

(a) The unpredictability of thyristor voltage waveforms with regulating diodes used alone.

(b) The turn-off limitations with the regulating diode plus R-C network.

(c) The necessity of using a number of regulating diodes in series to achieve nominal voltages commensurate with present day thyristor voltage ratings. This may improve in the future.

(d) The higher sensitivity of regulating diodes to overload could lead to a higher failure rate than would occur with

R-C components.

(e) The difficulty of accurately calculating the required regulating diode power rating.

CHAPTER 7

D.C. CHOPPING AT HIGH VOLTAGES

7.1 INTRODUCTION

The d.c. chopper provides a way of directly changing mean d.c. voltage level, whereas the alternative static system[34] requires an intermediate a.c. stage between an inverter and rectifier in order to utilise the conventional a.c. transformer. Chopper circuits for step-up or step-down of voltage have been devised[34,45], although only step-down will be considered here.

Output voltage may be constant or variable, the latter being very common owing to the ease by which it can be attained using time ratio control[34]. This provides variation of the ratio 'on time'/'off time' (or mark (m)/space (p)) for which the d.c. supply is rapidly switched to the load. The idealised theory of step-down chopping is given in Appendix V. It shows that if all the internal voltage drops are neglected, the ratio of mean output voltage V_ℓ to the mean input voltage V_d is equal to the mark/period ratio k of the cycle. That is,

$$k = \frac{m}{m + p} = \frac{m}{T} = \frac{V_\ell}{V_d}, \qquad (7.1)$$

where T (= 1/f) is the period of the cycle.

The mean output voltage therefore depends on the mark/space ratio m/p, and is independent of frequency, providing the mark/space ratio is constant. Hence, the output voltage can be varied by using:

(a) Fixed frequency and variable mark/space ratio.

(b) Fixed mark or space duration, with variation of frequency to provide the adjustment of mark/space ratio.

(c) Variation of both frequency and mark/space ratio according to some prescribed relationship.

Each of these methods has applications. The last is the most versatile, since control can be adapted to provide some specific requirement such as minimum, or constant, output current ripple[5,6,46]. Such control is considered further in Appendix V.

In practice, there are limitations to the minimum allowable durations of the mark and space. The reasons for this depend, to some extent, on the individual chopper circuit. In general, the minimum allowable mark is determined by the time required for the commutation circuit to fully reset in preparation for turning off the main thyristor; the minimum allowable space is governed by the main thyristor turn-off time. Refinements have been made in chopper circuitry which overcome these limitations[47], but at the expense of added complexity and cost.

In principle, chopper circuits which function satisfactorily at low voltages should be adaptable to high voltage working, but the practical and economic considerations of using many devices in series eliminate some of the alternatives. Experimental choppers for traction application, operating with a few thyristors in series at up to 3000V and 400Hz, have utilised voltage sharing networks based on the conventional R-C arrangement[4,6,7].

The chief aim here is to use the variable frequency d.c. chopper as a vehicle for fully proving the voltage sharing networks discussed in the earlier chapters. At the same time, it is useful to consider the level of performance which can be attained practically from such a chopper, as this is relevant to the possible future application of choppers at high voltages.

7.2 THE TEST CHOPPER CIRCUIT

The variable frequency chopper circuit (Figure 7.1) utilises three strings of fifteen devices in series and one (D_f) having twenty-nine in series. The voltage sharing components shown for illustration are regulating diodes, which are used in association with a series saturating reactor except for diodes D_f. Component details are given in Figure 7.10 and Appendix I; those of the sharing networks are in Table 7.1. The chopper is basically the same as that used previously (Figure 3.3), but it is here fed by a smoothed d.c. supply and operates without voltage boost. The following reasons governed the choice of this circuit:

(a) Having few basic components, the circuit has low losses, allowing the voltage sharing network losses to appear as an appreciable proportion of the total.

(b) Operation over a wide range of frequency and mark/space ratio is possible.

(c) The cost is comparatively low.

The operation is identical to that described in section 3.4.1

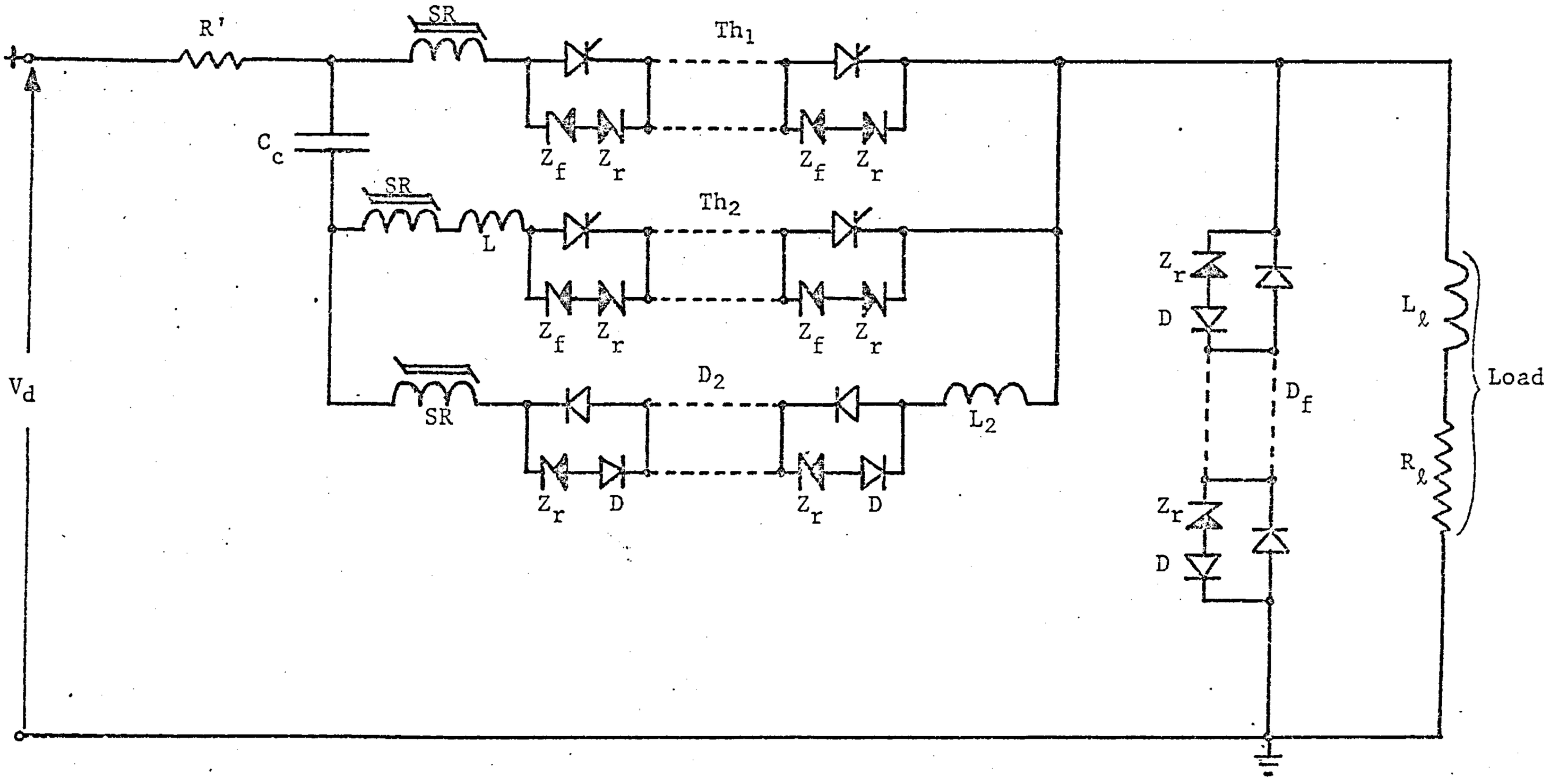

Figure 7.1: Experimental variable frequency chopper circuit.
(Regulating diode plus SR voltage sharing networks shown).

Arrangement	Device string	Number of devices per string	Nominal string derating factor f_s	Voltage sharing components (Figures 3.6(a) and 7.1)						Z_r 5% tol.	Z_f 5% tol.	D (10V, 1A)
				C (μF) 20% tol	R(Ω) 5% tol	R_s(Ω) 5% tol	SR Core	SR Turns	SR V-S rating			
(a)	Th_1	n_{t_1} = 15	0.37	0.083 (C_{t_1})	56 (200W)	10k (60W)	Telcon HCR 0.002" strip size 11b	65	47.2 $\times 10^{-3}$			
	Th_2	n_{t_2} = 15	0.37	0.083 (C_{t_2})	56 (200W)	10k (60W)	Mullard Ferrite FX1076	50	9.1 $\times 10^{-3}$			
	D_2	n_{d_2} = 15	0.34	0.05 (C_{d_2})	500 (40W)	34k (26W)	Telcon HCR 0.002" strip size 11b	100	72.6 $\times 10^{-3}$			
	D_f	n_{d_f} = 29	0.35	0.1 (C_{d_f})	157 (48W)	34k (32W)	Telcon Mumetal 0.002" strip size 11b	2 × 100	48.4 $\times 10^{-3}$			
(b)	Th_1	n_{t_1} = 15	0.37				Telcon HCR 0.002" strip size 11b	65	47.2 $\times 10^{-3}$	3×200V (1W) in series	3×200V (1W) in series	
	Th_2	n_{t_2} = 15	0.37				Mullard Ferrite FX1076	50	9.1 $\times 10^{-3}$	ditto	ditto	
	D_2	n_{d_2} = 15	0.34				Telcon HCR 0.002" strip size 11b	100	72.6 $\times 10^{-3}$	ditto		✓
	D_f	n_{d_f} = 29	0.35							3×200V (1W) or 3×200V (10W)		✓

Table 7.1: Voltage sharing network details

until, after a controlled interval (t_{m1}) of Th_1 conduction, Th_2 is gated. C_c then discharges and recharges positively through the source, Th_2 and load L_ℓ and R_ℓ at an almost constant rate which is dependent on the load current. When the voltage across C_c reaches that of the supply (V_d), the freewheeling diode D_f becomes forward biased and takes over load current conduction from Th_2, which turns off by starvation. The load current then decays exponentially until Th_1 is next gated to repeat the cycle. If Th_2 conducts for a time t_{m2}, the mark/period ratio k(equation 7.1) is:

$$k = \frac{t_{m1} + t_{m2}}{T}$$

For a given L_ℓ/R_ℓ ratio, the load current is discontinuous or continuous, depending upon the values of k and chopping frequency. This is well illustrated by the oscillograms of Figures 7.2 and 7.3 which show current and voltage waveforms at the extreme operating frequencies of 50 and 2000Hz. A full circuit analysis is given in Appendix II.

The provision of semiconductor overcurrent protection has presented difficulties owing to the non-availability of suitably rated fuses for high voltage d.c. working. The use of many low voltage fuses in series is not recommended by the manufacturers owing to the slight inherent differences of fuse melting characteristic. Considering the complete chopper supply system of a single-phase bridge rectifier with L-C filter (Figure I.9), there are two sources from which energy can be fed into a chopper fault:

(i) The a.c. generator feeding the supply rectifier.

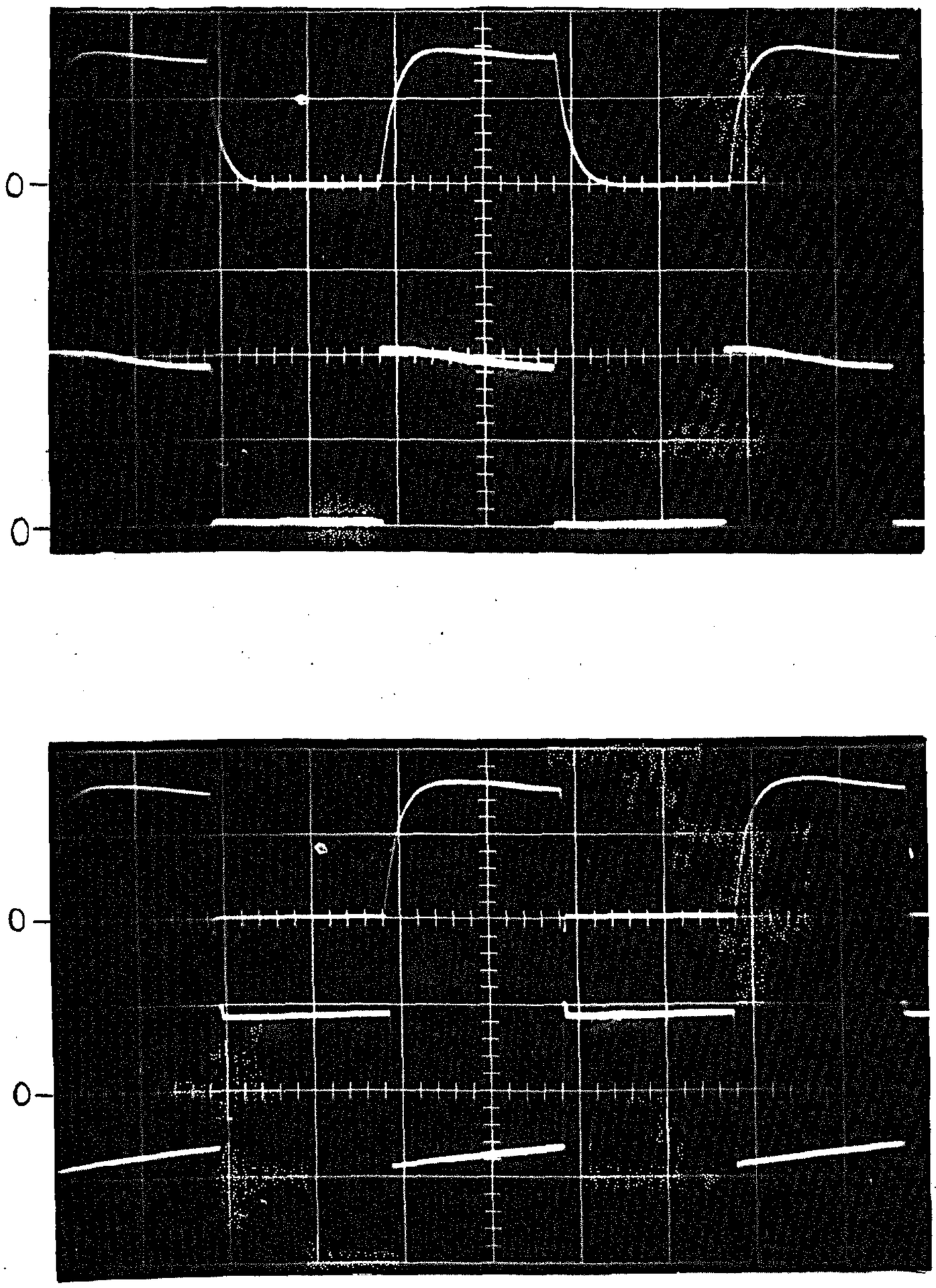

(a)

(b)

(c)

(d)

Figure 7.2: Oscillograms of chopper-waveforms at 50Hz, (k = 0.5) with the R-C plus series SR sharing network.

(a) Load current, (10A/cm,)
(b) Load voltage; (2.5kV/cm,)
(c) Input line current, (10A/cm,)
(d) Commutating capacitor C_c voltage, (5kV/cm,)

} (5ms/cm)

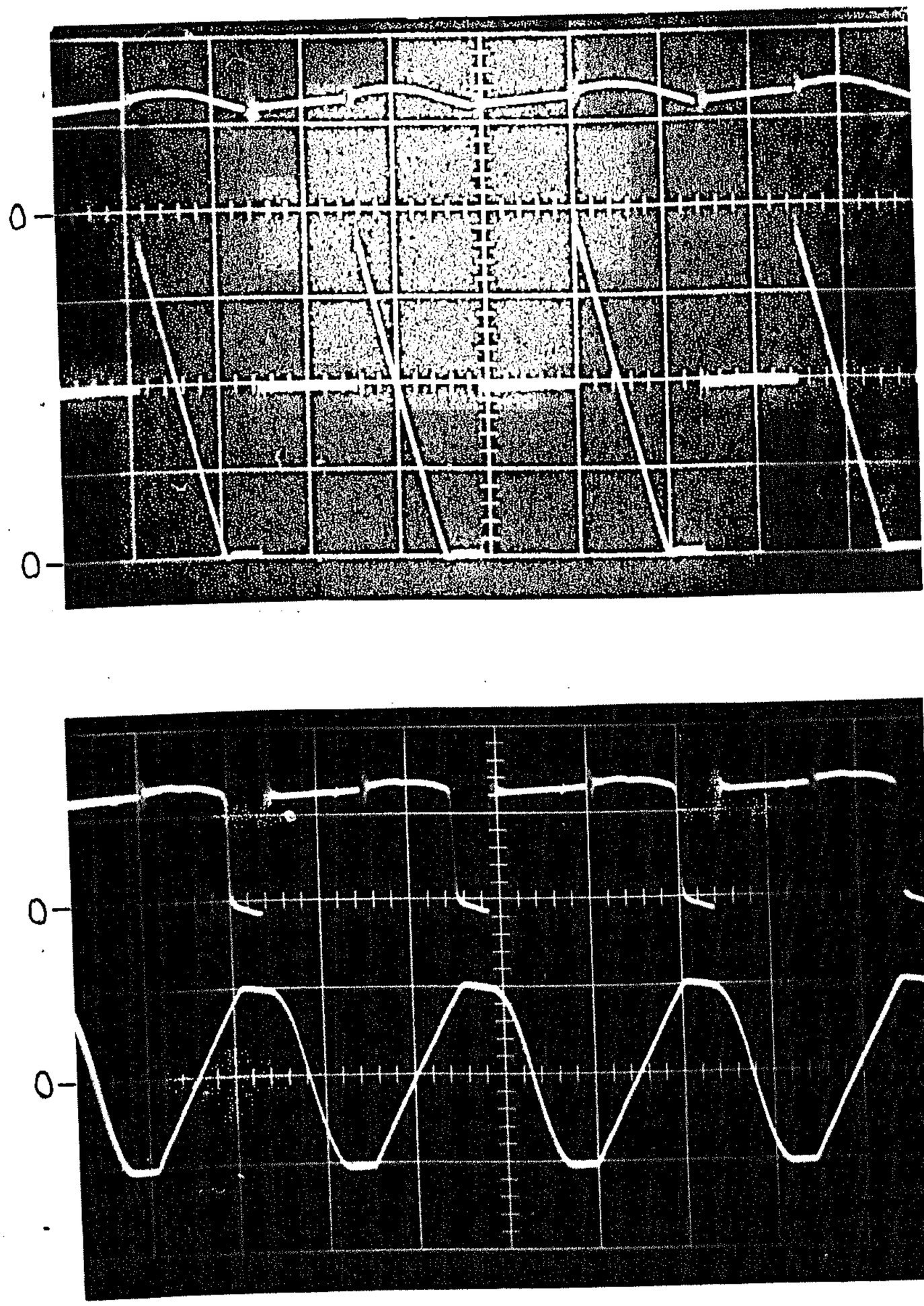

(a)

(b)

(c)

(d)

Figure 7.3: Oscillograms of chopper waveforms at 2010 Hz (k = 0.83) with the R-C plus series SR sharing network.

(a) Load current, (10A/cm,)
(b) Load voltage, (2.5kV/cm,) } (200μs/cm).
(c) Input line current, (10A/cm,)
(d) Commutating capacitor C_c voltage, (5kV/cm,)

(ii) The filter capacitor at the rectifier output.

An 11kV, 20A industrial fuse is included in each arm of the rectifier bridge to interrupt fault energy from the supply. Its I^2t and cut-off characteristics are such as to give protection for the thyristors and diode strings in the supply rectifier and chopper. A low ohmic resistor R' is used in the d.c. supply line to absorb the energy of the filter capacitor under chopper fault. In addition, ten 1000V, 20A semiconductor fuses in series are situated in the d.c. supply line to serve as the primary protection, in order to avoid blowing the 11kV fuses where possible (Figure 7.10).

7.3 HIGH FREQUENCY OPERATION OF THYRISTORS

7.3.1 Device ratings

The thyristor internal power loss is made up of separate components produced by the gate drive, turn-on, forward conduction, reverse recovery, and the leakage current when blocking. The first two losses are inappropriate for diodes. Since the maximum junction temperature rise governs the device current rating, if the other losses become significant compared with the forward conduction loss, the device must be appropriately derated.

At frequencies above about 400Hz, switching losses assume importance. These occur because turn-on and turn-off (more specifically, reverse recovery) take a finite time, during which rising or falling device current and voltage may simultaneously have large magnitudes. These losses depend greatly on the circuit-controlled variables and,

therefore, are impossible to predict accurately. A number of methods of measurement have been used under conditions which are representative of those in service[48]. If di/dt at turn-on is severe, it may be necessary to allow for the resulting loss at low frequencies[49].

Manufacturers have only recently commenced publication of thyristor rating data for high frequency operation on more than a minimal scale. The earliest characteristics accounted for half sine-wave current pulses only[50]; now the data is being extended to cover operation under rectangular current pulse loading[51,52]. Such information is only published for thyristors intended for high frequency working and none is available for those used in the test chopper.

7.3.2 The influence of voltage sharing components

The inductance in series with the thyristors has a large influence on the switching losses. Lowering the rate of change of rising and falling anode current reduces the internal loss at turn-on and turn-off respectively, though a high induced hole storage voltage spike at turn-off increases the loss. A series saturating reactor, of adequate size, is very effective, since it almost completely eliminates the switching losses by delaying the application of voltage until the devices have switched on, or completed reverse recovery.

In all cases except one, saturating reactors are connected in series with the thyristor and diode strings in the test chopper.

The reason for the exception is discussed later.

7.4 VOLTAGE SHARING NETWORK CONSIDERATIONS

7.4.1 Factors of importance

For practical simplicity and best performance, the voltage sharing networks utilising shunt R-C's with a series saturating reactor, and shunt voltage regulating diodes, merit consideration for this application. The shunt transformer alternatives offer no additional advantages and introduce further complication and loss. A comparison is made, in the following sections, of the chopper performance with each of the two networks used on all the thyristor strings and, when suitably adapted, on all the diode strings.

The voltage sharing components should have the minimum detrimental effect on main chopper operation. The following factors, some of which have already been explained in section 3.6, assume special significance for high voltage, variable frequency working:

(a) Voltage sharing network losses.

(b) The reduction of commutating capacitor voltage caused by its discharge through the voltage sharing components.

(c) The effects of (a) and (b) on chopper output voltage and efficiency.

(d) The effects of time delays introduced by the series saturating reactors.

7.4.2 Shunt R-C and series SR components

Full details of the voltage sharing components are given in

arrangement (a) of Table 7.1. The low values of nominal string derating factor f_s quoted, and the high wattage ratings of the thyristor voltage sharing resistors, are a result of the original intention to operate the chopper up to 10kV. However, owing to the power supply limitation of 60kW for only a few minutes, a maximum voltage of 5kV has been used to allow an unrestricted variation of mark/period ratio within the chopper minimum mark and space limits.

The volt-second ratings of the saturating reactors are based on the experience gained during the earlier work reported in Chapter 4. That in series with the diodes D_2 (Figure 7.1) is of particular importance, since it is imperative that the reverse recovery current is blocked; otherwise, there is a risk of premature interruption of Th_1 forward conduction as the commutating capacitor recharge oscillation through D_2 is completed. Additionally, the presence of inductor L_2 leads to a high hole storage voltage spike across D_2 if SR is omitted. Mumetal cores are used for the series SR with diodes D_f, owing to the rounder B-H loop compared with HCR alloy. The volt-second withstand between the retentivity and saturation flux levels dampens oscillation across the diodes at the second jump in the output voltage waveform (Figure 7.3(b)) when Th_2 turns on, the reactor having already switched at the first jump when Th_1 turns on.

7.4.3 Shunt regulating diode and series SR components

The series saturating reactors are retained to operate with the regulating diodes in order to reduce their rating and to reduce

the switching losses in the series thyristors and diodes. Although the reactors are not necessary from voltage sharing considerations, that in series with diodes D_2 is essential for the reasons already given. Owing to overshoot of the commutating capacitor voltage - a problem which is discussed in the next section - no SR has been included in series with diodes D_f for the chopper performance tests.

Table 7.1, arrangement (b), gives the voltage sharing component details. The regulating diodes are connected back-to-back for the thyristors, whereas for the diode strings, Z_f is replaced by a low voltage diode D (Figure 7.1) to block any forward current path round the main diode. 10 watt regulating diodes are required across the faster recovery diodes in string D_f owing to the inadequacy of 1 watt devices at the higher operating frequencies. This is a direct result of omitting the series saturating reactor.

The only new operating feature concerns the saturating reactors. Any SR is saturated positively during the forward conduction of its associated thyristor or diode string. It is then magnetised negatively as it holds reverse voltage when this is applied. If its volt-second rating is low, SR can saturate negatively before the thyristor, or diode, reverse recovery is complete. With higher volt-second ratings, negative magnetisation ceases (if device leakage is neglected) when V_R/V_{zr} (= x) devices have completed their reverse recovery; the shunt regulating diodes do not thereafter provide a good magnetising path as does the R-C chain. The core therefore operates on some minor loop of its B-H characteristic, with the negative displacement of flux from the positive saturation level providing a volt-second hold-off of forward conduction when this

is next due.

7.4.4 The saturating reactor in series with the freewheeling diode string

Consider a series saturating reactor SR used in conjunction with regulating diodes across the freewheeling diode string D_f (not shown in Figure 7.1). When load current flow is continuous, the forward current through D_f is interrupted when Th_1 is gated to switch the d.c. supply to the load at the commencement of the mark period of the output voltage. The SR core is magnetised during the diode reverse recovery, as described in the previous section. If the SR volt-second rating is low, the core flux may revert to $-\Phi_r$ (Figure 4.1 (b)). At the end of output voltage mark, the linearly falling output voltage reaches zero (Figure 7.4(b)) as the commutating capacitor C_c voltage rises to the level V_d. SR will not allow diodes D_f to take over load current conduction at this point, since it must saturate positively (perhaps from $-\Phi_r$) first. C_c therefore continues to charge to a voltage greater than V_d, the output voltage then going negative to the level required to provide the necessary volt-second integral to saturate SR positively. As SR saturates, the output voltage abruptly reverts to zero (neglecting D_f forward voltage drop). If the d.c. source can accept reverse current (as here), C_c then discharges back through D_f, L_2 and D_2 with an oscillatory half-cycle; the voltage reduction is approximately equal to the initial overshoot above V_d. The oscillograms of Figure 7.4 well demonstrate this effect, which necessitates the use of a

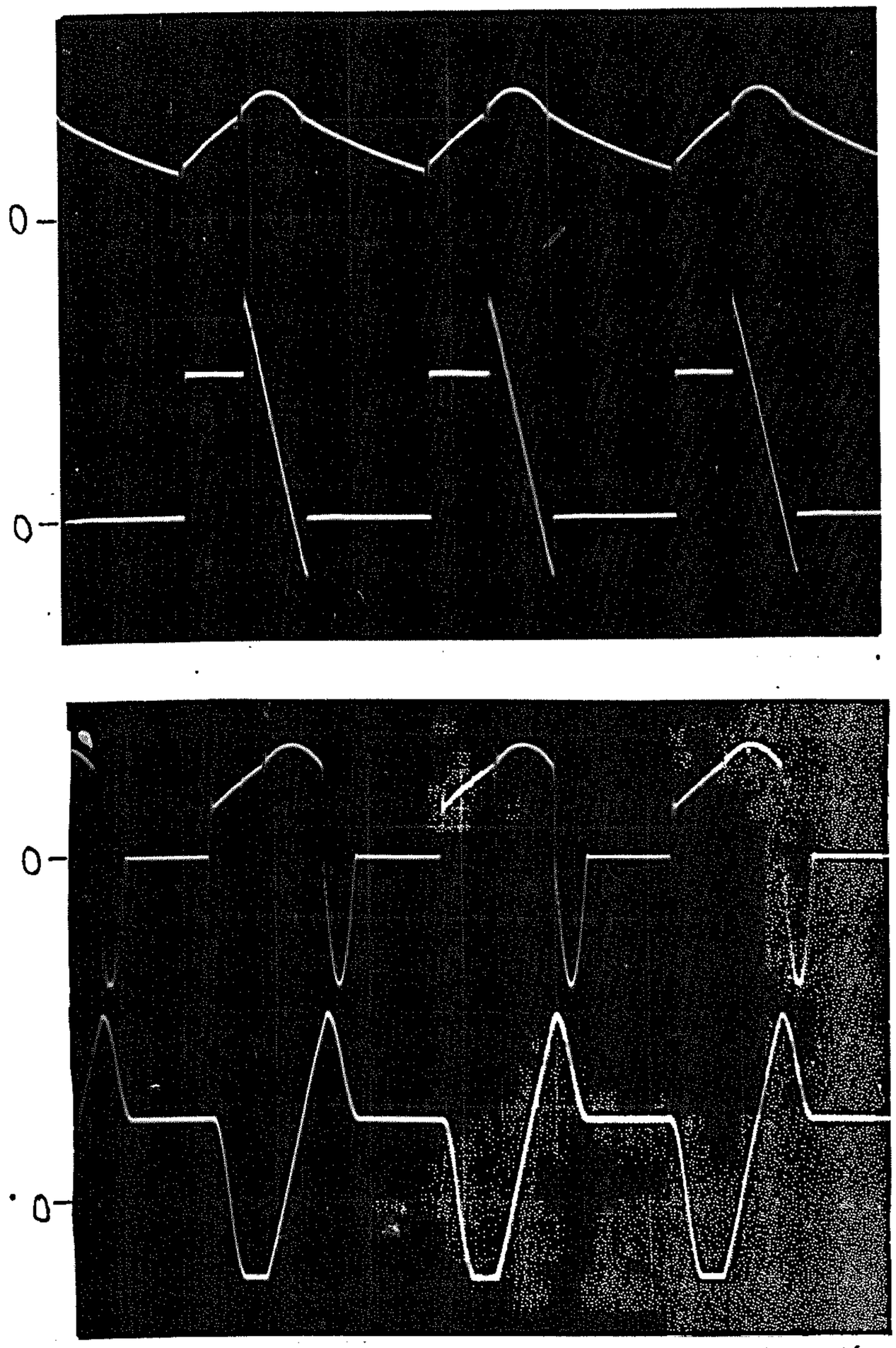

Figure 7.4: Oscillograms of chopper waveforms illustrating the effect of using a series SR with shunt regulating diode components for the freewheeling diode string.

(a) Load current, (5A/cm,)
(b) Load voltage, (2.5kV/cm,)
(c) Supply line current, (5A/cm,)
(d) Commutating capacitor C_c voltage, (2.5kV/cm,)
} (500μs/cm).

Frequency = 805 Hz, supply voltage = 3450V.

reduced operating voltage.

This overshoot problem is not so severe when a saturating reactor is used in conjunction with shunt R-C components. Unlike the regulating diodes, the R-C components allow SR to reset positively during the linear fall of output voltage, in the same way as described in section 4.3.2. The reset may be completed before the output voltage reaches zero, the time to saturate being again given by equation (4.7), in which case the presence of SR introduces no appreciable overshoot. A small degree of overcharging of C_c is produced by the supply inductance and that in series with thyristors Th_2, although this is not felt across the load. The oscillograms of Figure 7.5 illustrate this behaviour and allow comparison with those of Figure 7.4. The calculated time for SR to saturate during the linear fall of voltage (from equation 4.7) is 58μs.

The adverse effects of the commutating capacitor voltage overshoot are as follows:

(a) The mean output voltage and current, and the mean input current, are reduced.

(b) The forward blocking voltage which Th_1 must withstand is increased.

(c) The turn-off conditions of Th_2 are more severe.

(d) The energy available for commutation is lowered, giving a consequent reduction of Th_1 reverse bias time.

It is evident, therefore, that the size of any saturating reactor connected in series with the freewheeling diode string must be

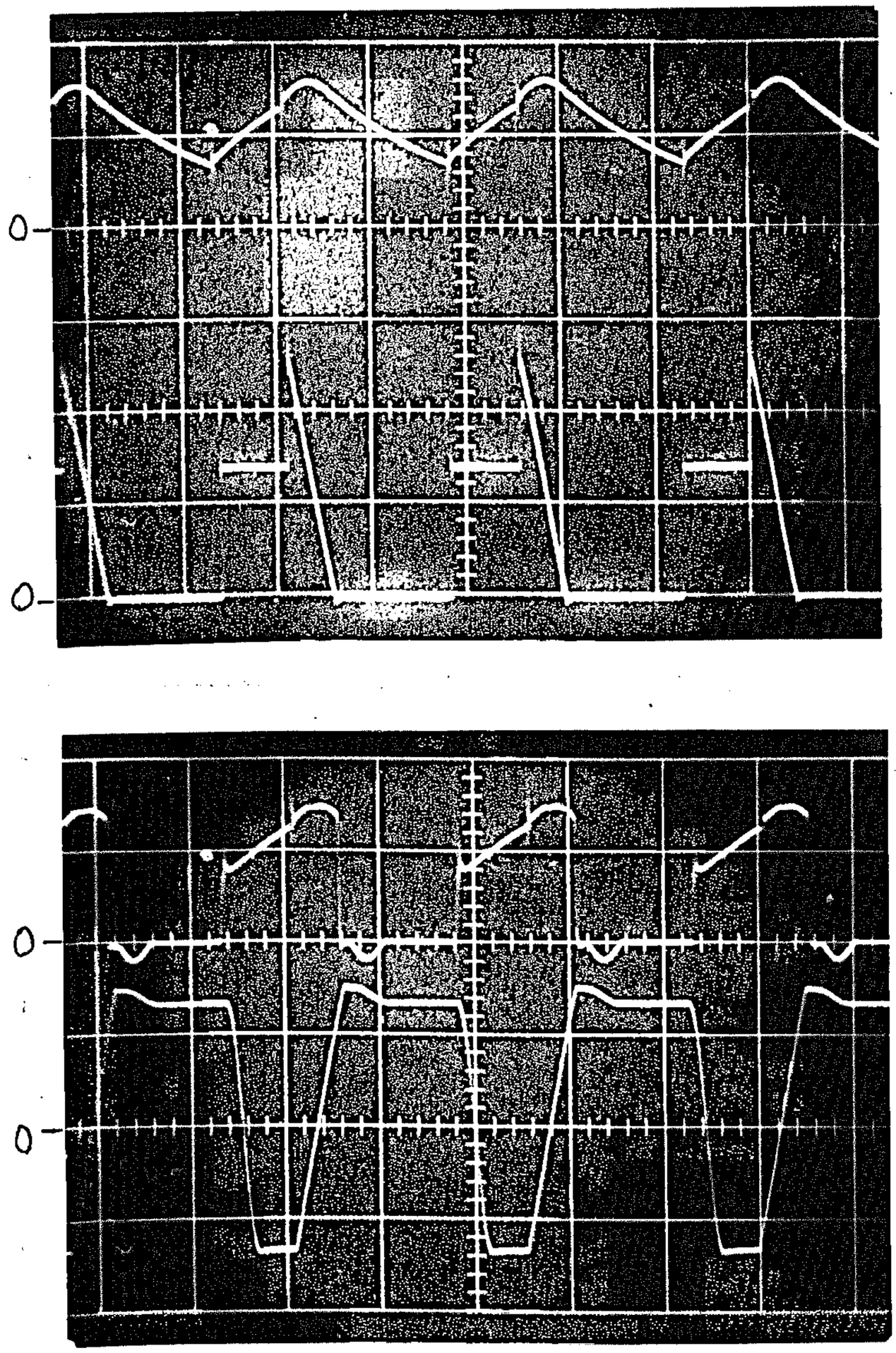

(a)

(b)

(c)

(d)

Figure 7.5: Oscillograms of chopper waveforms illustrating the effects of using a series SR with shunt R-C components for the freewheeling diode string.

(a) Load current, (5A/cm,)
(b) Load voltage, (2.5kV/cm,)
(c) Input line current, (5A/cm,)
(d) Commutating capacitor C_c voltage, (2.5kV/cm,)

} (500μs/cm).

Frequency = 805 Hz, supply voltage = 345OV.

limited in order to produce zero or a very small overshoot. If shunt regulating diodes are used, SR may have to be dispensed with, thereby increasing the regulating diode dissipation and the main power diode switching loss.

7.5 CHOPPER MEAN D.C. OUTPUT VOLTAGE

7.5.1 Variation of output voltage with mark/period ratio k

The mean d.c. output voltage V_ℓ ideally varies in direct proportion to k and is therefore given for the test chopper circuit by

$$V_\ell = \left(\frac{t_{m1} + t_{m2}}{T}\right) V_d .$$

Making allowance for the forward voltage drop V_{t1} of Th_1, for the reduction of the output voltage peak from the ideal $2V_d$ to $(V_d - V_{t1} + V_R)$, and for the voltage drop across the series line resistance R', the mean output voltage is given by

$$V_\ell = \frac{1}{T}\left[(V_d - V_{t1})t_{m1} + \frac{1}{2}\, t_{m2}(V_d - V_{t1} + V_R)\right] - R'(\text{mean } I_d). \qquad (7.2)$$

It is apparent that the fall in output voltage below the ideal is very much dependent on V_R and the proportion of the mark m taken by t_{m2}. The calculation of V_R, making allowance for the voltage drops, is discussed in the next sections for each of the two voltage sharing networks considered.

7.5.2 Voltage drops with the R-C network

Neglecting the delay introduced by the saturating reactor in series with Th_1, the drop in capacitor C_c voltage from the initial (ideal) V_d to the final V_R must be determined by considering the separate drops which occur during successive stages of the operating sequence (section 3.6.3). The individual components are:

(a) The assumed constant forward voltage drops V_{t1}, V_{t2} and V_{d2} of Th_1, Th_2 and D_2 respectively.

(b) The Q factor of L_2 gives a voltage reduction by a factor of $e^{-\pi/2Q}$ during the commutating capacitor charge reversal oscillation (the duration is $\pi\sqrt{L_2C_c}$ approximately, from Appendix II).

(c) The requirement to charge the capacitors C across the blocking thyristors and diodes gives a voltage reduction by a factor of $\left(\frac{C_c}{C_c + C/n}\right)$ in each case.

(d) The discharge of C_c through the R_s chains across D_2 and Th_2 in parallel, for an interval equal to $(t_{m1} - \pi\sqrt{L_2C_c})$.

(e) The charge required to cancel Th_1 forward current produces a voltage drop $I_f^2/2C_c\left|\frac{di}{dt}\right|_{off}$. Where series saturating reactors are present, the discharge due to device reverse recovery charge flow can be safely neglected.

Assume that C_c is initially charged to the supply voltage V_d. On completion of the charge reversal oscillation through Th_1, D_2 and L_2, the voltage across C_c is given by

$$\left(V_d e^{-\pi/2Q} - V_{t1} - V_{d2}\right)\left(\frac{C_c}{C_c + C_{t2}/n_{t2}}\right)\left(\frac{C_c}{C_c + C_{d_2}/n_{d_2}}\right).$$

The symbols previously undefined are given in Table 7.1. Devices Th_2 and D_2 next block for a time $(t_{m1} - \pi\sqrt{L_2C_c})$; the time constant of C_c discharge during this time is 0.03 seconds, calculated from the appropriate values of C_c and R_s (Table 7.1). Then, when Th_2 is gated, Th_1 forward current is first cancelled and the capacitor chains across Th_1 and D_f are charged, giving a final value for V_R equal to

$$\left[\left(V_d e^{-\pi/2Q} - V_{t1} - V_{d2}\right)\left(\frac{C_c}{C_c + C_{t2}/n_{t2}}\right)\left(\frac{C_c}{C_c + C_{d2}/n_{d2}}\right)e^{-(t_{m1}-173)/(0.03\times10^6)}\right.$$

$$\left. - \frac{1}{2C_c}\frac{I_f^2}{\left|\frac{di}{dt}\right|_{off}} - V_{t2}\right] \times \left(\frac{C_c}{C_c + C_{t1}/n_{t1}}\right)\left(\frac{C_c}{C_c + C_{df}/n_{df}}\right). \qquad (7.3)$$

7.5.3 Voltage drops with the regulating diode network

The voltage drops introduced by capacitors C and resistors R_s are now absent. Equation (7.3) can therefore be directly modified to give

$$V_R = V_d e^{-\pi/2Q} - V_{t1} - V_{d2} - \frac{1}{2C_c}\frac{I_f^2}{\left|\frac{di}{dt}\right|_{off}} - V_{t2}. \qquad (7.4)$$

7.5.4 Chopper voltage regulation

In a.c. power transformer practice, the output voltage drop from the nominal (ideal) value is usually quoted as a voltage

regulation. It is convenient to similarly define a voltage regulation for the d.c. chopper in terms of the mean d.c. voltages. Then

$$\text{voltage regulation} = \frac{kV_d - V_\ell}{kV_d} \times 100\%. \qquad (7.5)$$

7.6 CHOPPER LOSSES AND EFFICIENCY

7.6.1 Prediction of losses

The main chopper losses can be estimated relatively easily from the measured (or calculated) currents, voltages and durations of conduction t_{m1}, t_{m2} and the period T of the operating cycle. Some approximation is necessary in order to restrict the labour involved. The losses, grouped in two categories are listed below:

(a) Main Chopper component losses.

Thyristor and diode forward conduction losses.

Thyristor and diode switching losses.

Resistance losses in inductor L_2 and the line resistor R'.

(b) Voltage sharing network losses.

Steady-state sharing resistance R_s loss, or the equivalent regulating diode steady-state loss.

Transient sharing component R loss, or the equivalent regulating diode loss.

Core loss in the series saturating reactors.

Appendix VI gives the idealised waveforms and the derived expressions

from which the above losses have been calculated for the test chopper. The results are shown in Figures 7.6 and 7.7 for a fixed chopper mark/period ratio k and variable frequency, and in Figures 7.8 and 7.9 for a fixed frequency and variable k.

The specific loss behaviour patterns depend on the detailed operation of the chopper, but the principal effects can readily be discerned from the characteristics. The sharing network transient loss increases in proportion to frequency, whilst the steady-state loss decreases slightly with frequency because more of each cycle is taken up with the commutation process. The saturating reactor core losses increase with frequency. The transient voltage sharing losses are unaffected by a changing mark/period ratio k (Figure 7.8) except with regulating diode voltage sharing. Then the absence of a saturating reactor to control the reverse recovery current of diodes D_f leads to increased regulating diode dissipation as the interrupted free-wheeling current increases with increasing k. The steady-state losses similarly increase slightly with k due to Th_2, D_2 and D_f blocking for an increasing period.

The most important result is the reduction of the voltage sharing network losses obtainable at high frequencies by using regulating diodes instead of R-C's (Figures 7.6 and 7.7). This is offset to a small extent by the increased reverse recovery loss of the freewheeling diodes D_f, which shows in the higher thyristor and diode losses (Figures 7.7 and 7.9). The thyristor and diode conduction losses increase slightly with both frequency (due to the commutating capacitor recharge oscillation) and with k (due to the increased durations of device conduction).

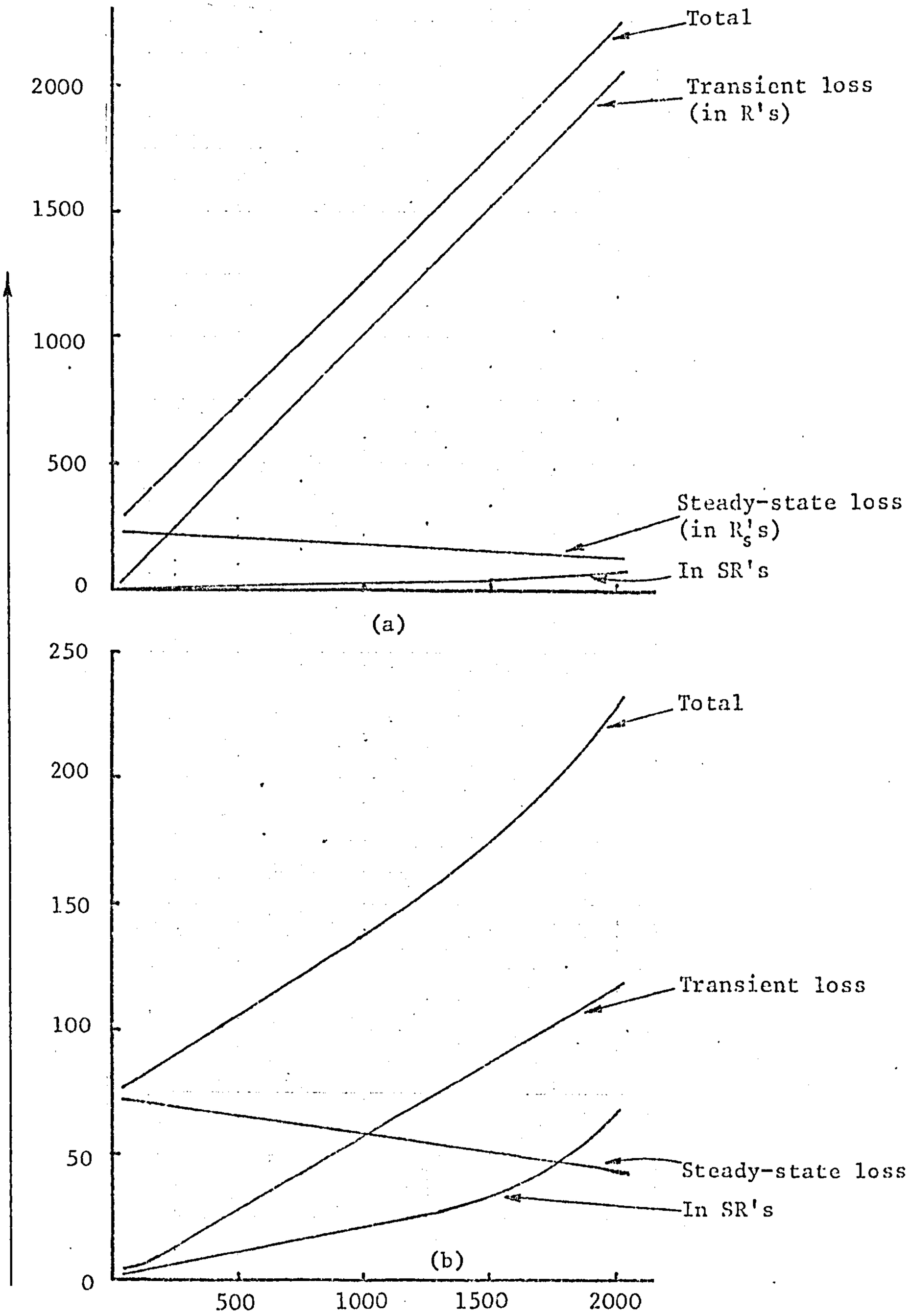

Figure 7.6: Variation of calculated voltage sharing network losses with frequency, mark/period ratio being maintained constant (= 0.887).

(a) R-C plus SR components
(b) Regulating diode components
} (Table 7.1)

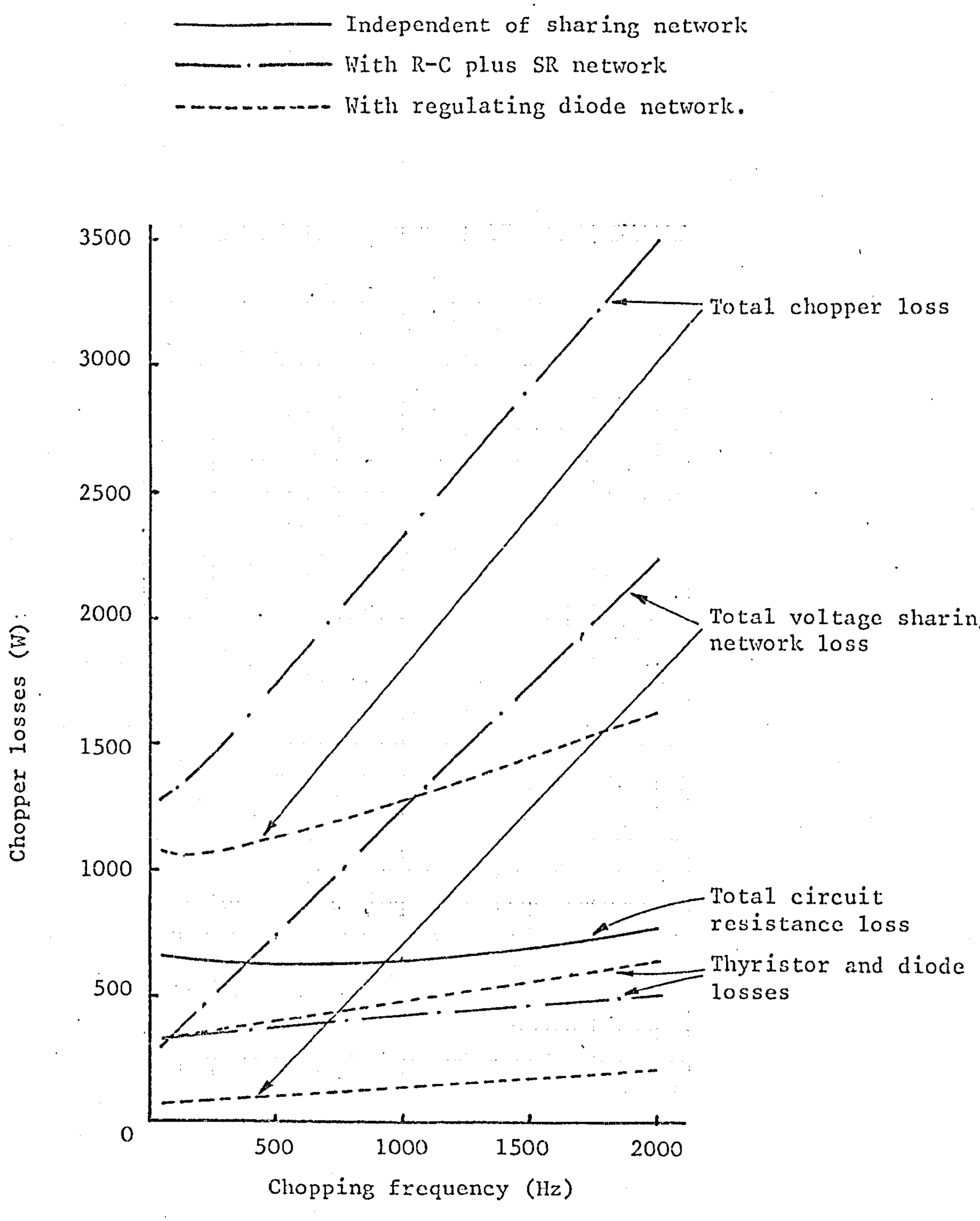

Figure 7.7: Comparison of calculated chopper losses using both voltage sharing networks, with frequency variable and mark/period ratio constant (= 0.887).

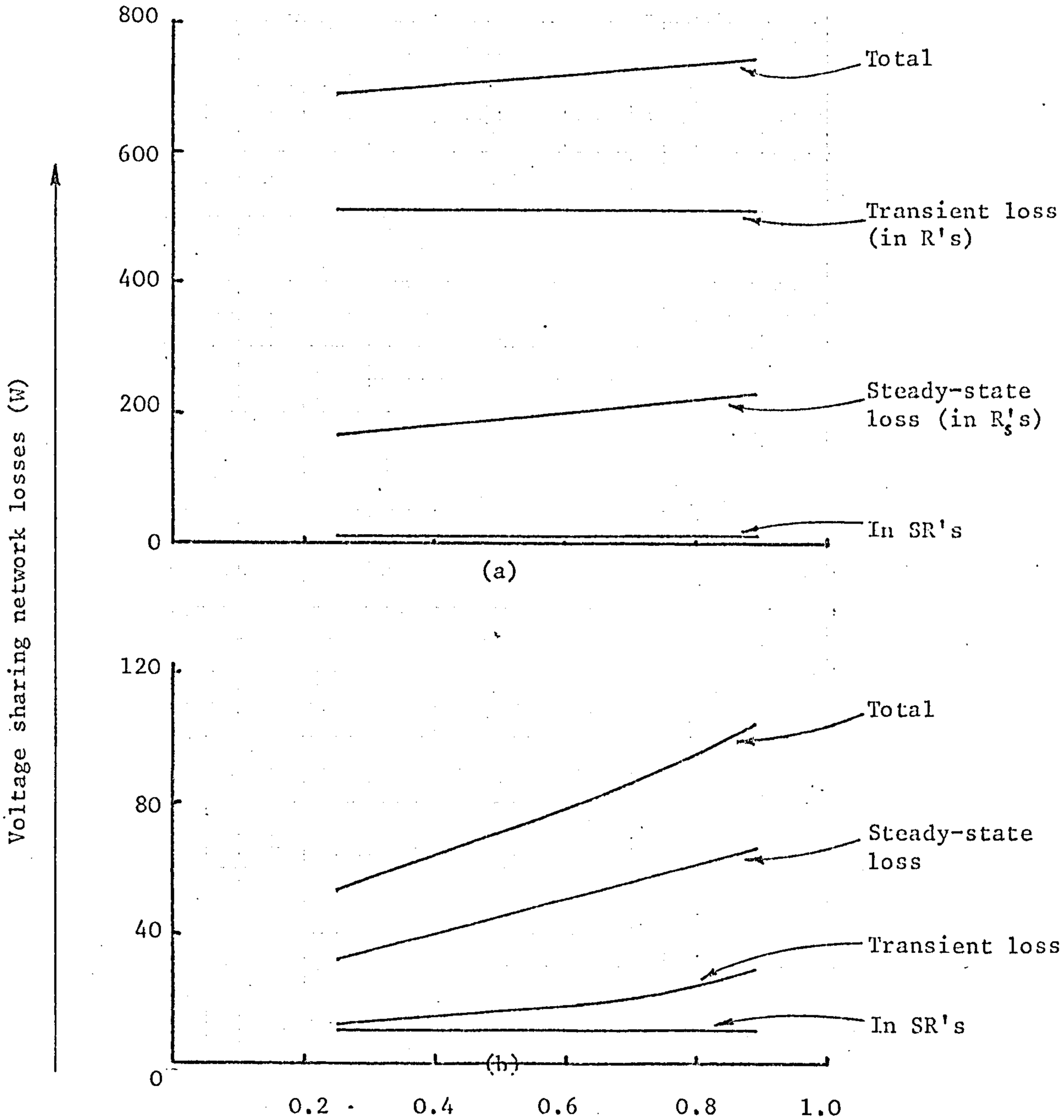

Figure 7.8: Variation of voltage sharing network losses with mark/period ratio, frequency being maintained constant (500 Hz).

(a) R-C plus SR components
(b) Regulating diode components
} (Table 7.1)

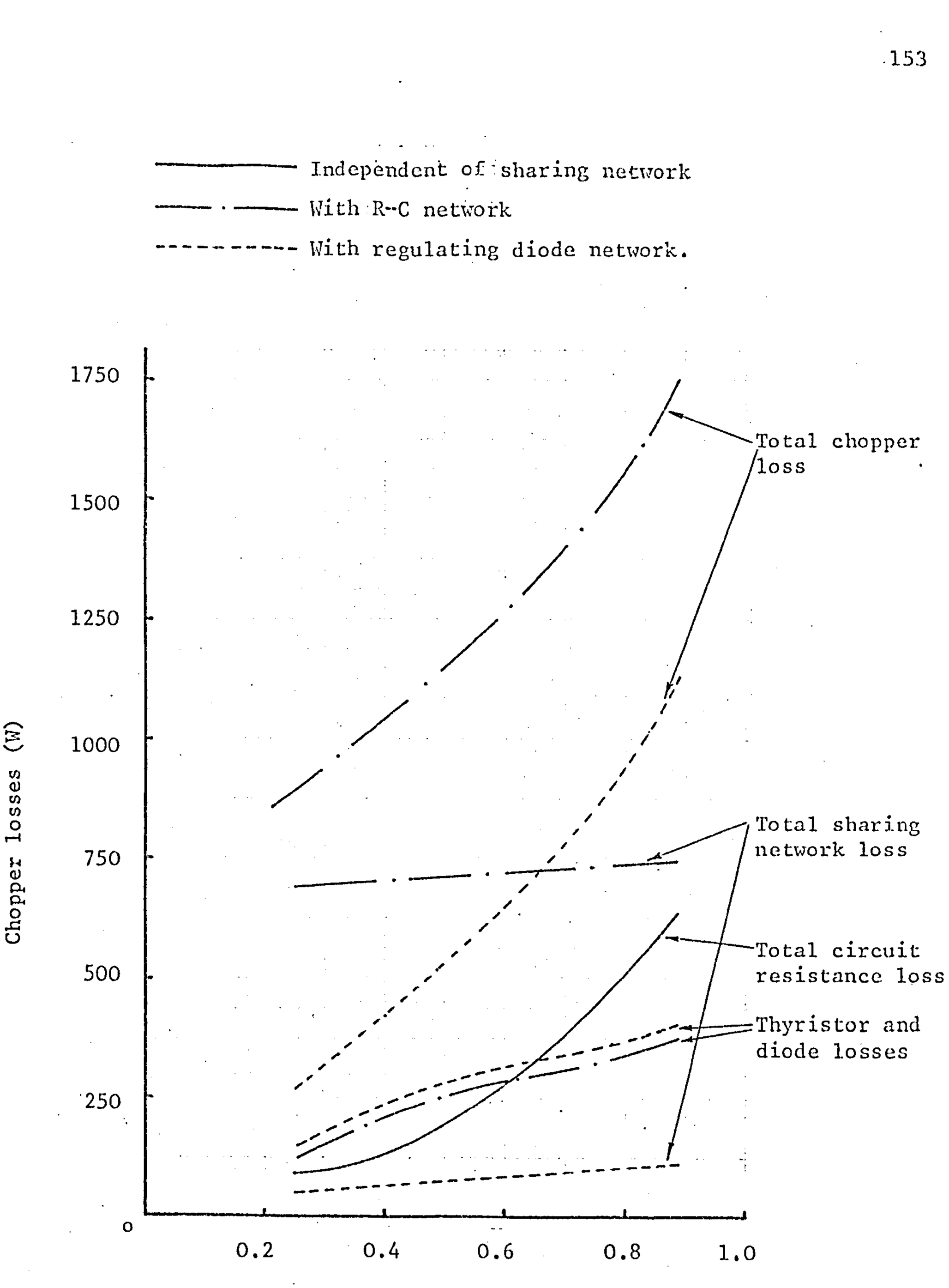

Figure 7.9: Comparison of calculated chopper losses using both voltage sharing networks, with mark/period ratio variable and frequency constant (500 Hz).

It is apparent that a very serious loss is introduced by the inclusion of the line resistor R'. Although not strictly a chopper component, it is a necessary part of the protective system and its detrimental effect on chopper operation must be acknowledged.

7.6.2 Chopper efficiency

Chopper efficiency will be quoted in three ways which are related to the methods used for power measurement (see section 7.8.1). Considering the primary chopper function of d.c. transformation, the ratio of d.c. output power to d.c. input power will be termed the d.c. efficiency. Then, if subscript 'ℓ' denotes load and 'd' denotes d.c. supply, and all values are mean unless otherwise stated,

$$\text{d.c. efficiency} = \frac{V_\ell \; I_\ell}{V_d \; I_d} \cdot \qquad (7.6)$$

The supply voltage V_d will be assumed constant.

If the load current ripple is high, the above definition will not represent the 'overall' efficiency of the chopper. The total output power must be then used to give a realistic efficiency value. The output power is obtained in two ways: by subtracting the total calculated loss (Figures 7.7 and 7.9) from the measured chopper input, and by using the measured r.m.s. load current and the load resistance. Hence,

$$\text{efficiency} = \frac{V_d I_d - \text{total loss}}{V_d I_d} , \qquad (7.7)$$

and

$$\text{efficiency} = \frac{(\text{r.m.s. } I_\ell)^2 \times R_\ell}{V_d I_d} \cdot \qquad (7.8)$$

7.7 LOAD CURRENT RIPPLE

The basic chopper theory given in Appendix V shows that for the idealised chopper with a load of resistance R_ℓ and inductance L_ℓ, with d.c. supply voltage V_d, the peak-peak load current ripple ΔI_ℓ is given by

$$\Delta I_\ell = \frac{V_d}{R_\ell}\left[\frac{e^{-TR_\ell/L_\ell} - e^{(T-m)R_\ell/L_\ell} - e^{mR_\ell/L_\ell} + 1}{e^{TR_\ell/L_\ell} - 1}\right] \qquad (V.11)$$

This expression is based on an exponential current rise. The test chopper load current includes an additional oscillatory current peak during t_{m2} (Appendix II and Figure 7.3(a)). Therefore the peak-peak ripple will be a little higher than is given above.

7.8 EXPERIMENTAL RESULTS

7.8.1 Instrumentation

The requirement for measuring voltage, current and power with pulsed waveforms over a frequency range of 50-2000Hz at voltages which reach 10kV peak are unusual. Accurate power measurement is particularly difficult.

The instrumentation is chosen from that immediately available and is shown in Figure 7.10. The voltage sharing networks are omitted but the main chopper component values are given since these, in certain

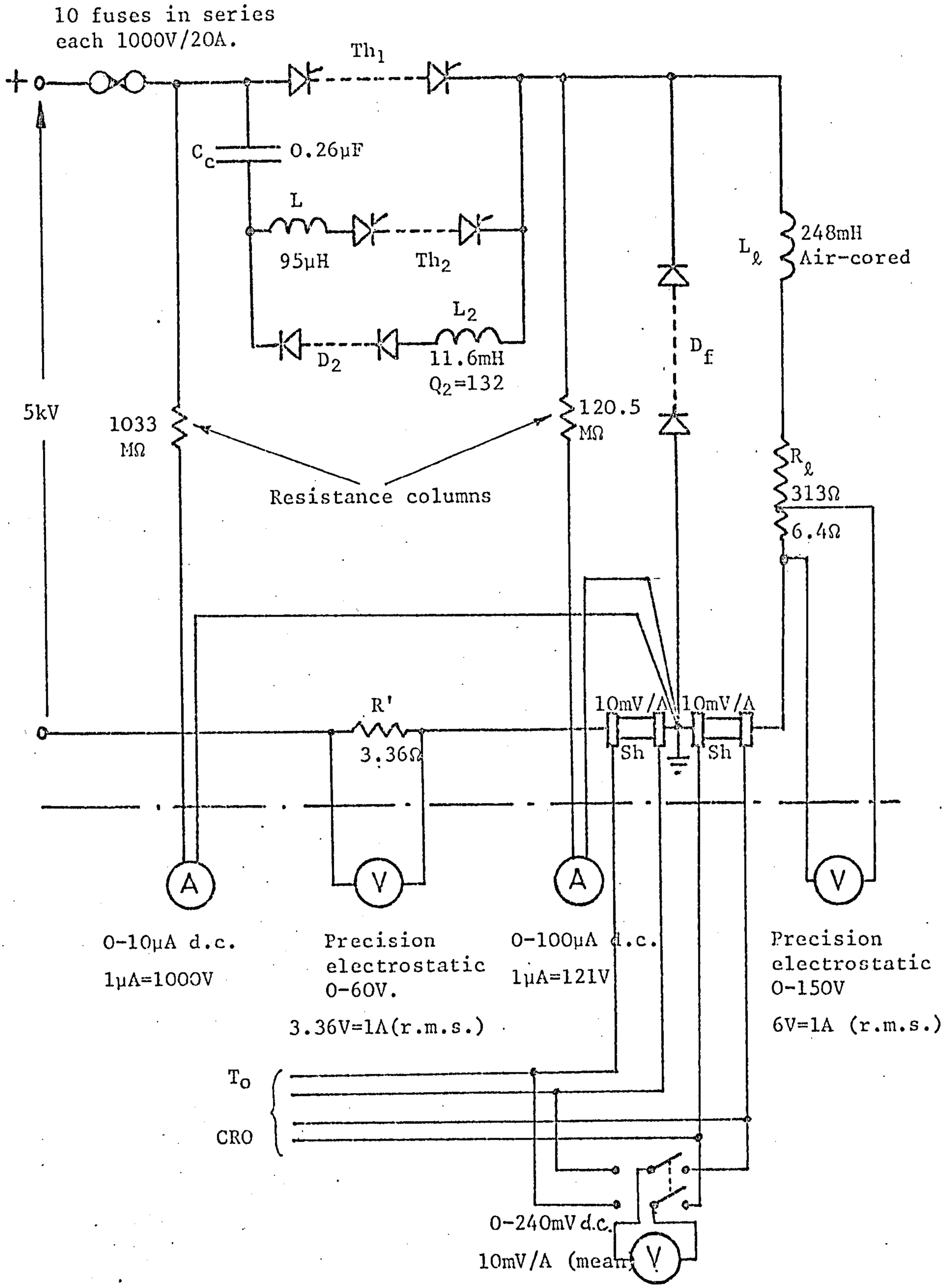

Figure 7.10: Variable frequency chopper instrumentation and component values.

(Further details - section I.3, Tables I.2, 7.1)

cases, influence meter scale factors. The resistance columns used for the input and output voltage measurement have been calibrated together against a digital voltmeter, and all the ammeters against a previously calibrated hot-wire meter connected in the earthy supply line. The mean currents are indicated from the voltage drops across the coaxial shunts Sh.

The need to position the meters outside the high voltage area which accommodates the power circuitry has necessitated the use of long screened coaxial, and twisted pair, connecting leads. Care has been necessary in order to avoid earth loops.

The operating conditions make the use of a dynamometer wattmeter inappropriate for power measurement. A substandard air-cored wattmeter of this type, used in conjunction with a current shunt having a time constant matched to the current coil of the meter, has been utilised elsewhere to measure chopper powers at a much lower voltage[46]. An air-cored wattmeter situated on the earthy side of the chopper did not prove successful here.

If the d.c. input voltage V_d is constant, the input power is given simply by the product of this voltage and the mean input current, irrespective of its waveshape. Since the supply filter (Figure I.9) is designed to limit the peak-peak voltage ripple to within 4% of V_d, this method of calculating the input power is used throughout. If the load current is smooth, the output power is similarly given by the product of the current and the mean value of the pulsed output voltage. Calculation of d.c. efficiency (equation 7.6) is based on this. However, the levels of load current ripple present, particularly at the lower operating

frequencies, make the method inappropriate for the measurement of total load power. A basic I^2R technique has therefore been adopted. The r.m.s. current is measured by an electrostatic voltmeter connected across a known section of the substantially non-inductive load resistor R_ℓ, whose d.c. resistance is accurately known. Air cored inductors are necessary for L_ℓ, to avoid iron losses.

The power loss in the supply line resistor R' is obtained from its r.m.s. current measured in a similar way.

7.8.2 Measured results

The ratio of the measured chopper mean output voltage to the d.c. input voltage for various values of mark/period ratio k and frequency are plotted in Figure 7.11. They are compared with the ideal values established from equation (7.1). Table 7.2 compares the measured and calculated mean d.c. output voltage and voltage regulation for the two extreme operating frequencies, with both voltage sharing networks.

The variations of chopper efficiency with frequency and with mark/period ratio k are shown in Figures 7.12 and 7.13 respectively. The three separate plots of efficiency are derived from equations (7.6), (7.7) and (7.8).

Figure 7.14 shows the measured values of peak-peak load current ripple for various values of frequency and k. For comparison, the characteristics derived from equation (V.11) are given also. The restricting effect of the minimum allowable mark on the working range of k, and therefore on the output voltage, as frequency is

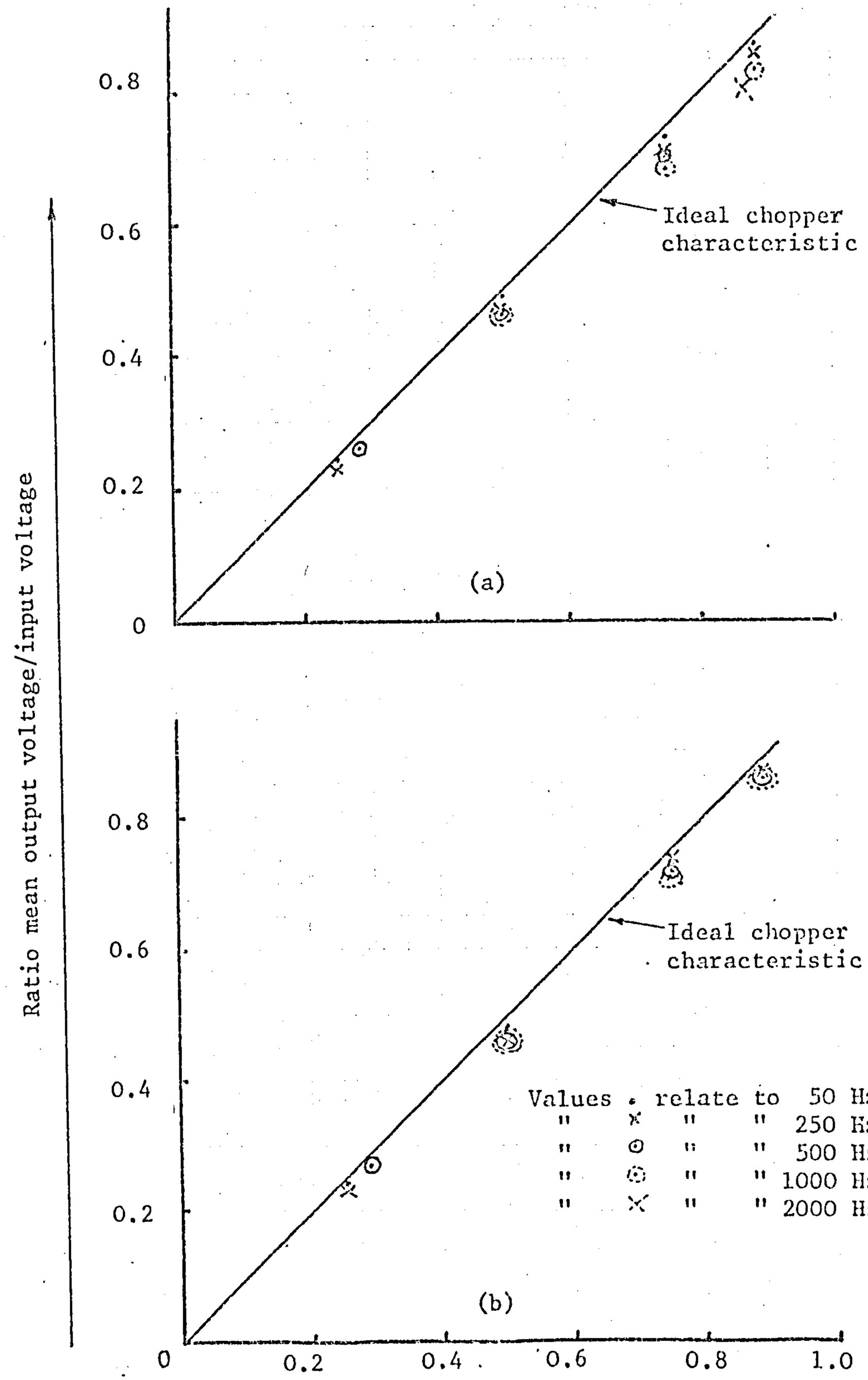

Figure 7.11: Variation of measured chopper mean output voltage with mark/period ratio.

(a) R-C plus SR sharing networks
(b) Regulating diode sharing networks

} (Table 7.1)

Voltage sharing network	Operating frequency	Calculated V_R (V) [equation (7.3) or (7.4)]	Calculated mean output voltage V_ℓ (V) equation(7.2)	Calculated voltage regulation (%) equation(7.5)	Measured mean output voltage V_ℓ (V)	Measured voltage regulation (%)
R-C's with S.R. Table 7.1 arrangement (a)	2000	4480	4080	3.8	3950	6.2
	50	2480	4290	1.0	4230	1.9
Regulating diodes. Table 7.1 arrangement (b)	2000	4840	4260	2.1	4260	2.1
	50	4840	4300	1.0	4230	2.5

Table 7.2: Sample chopper output voltage results (k = 0.887 constant)

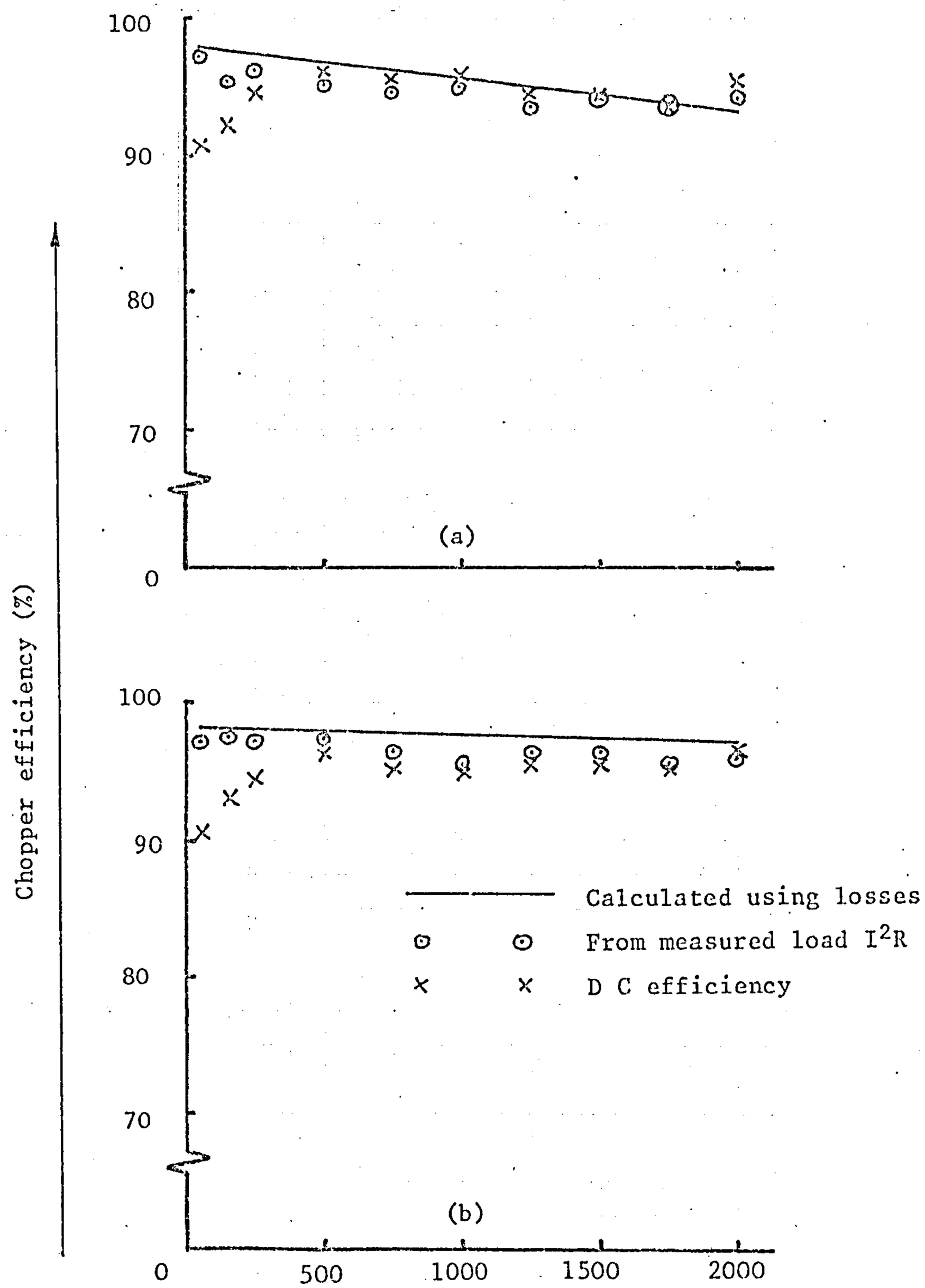

Figure 7.12: Variation of chopper efficiency with frequency at constant mark/period ratio (= 0.887)

(a) R-C plus SR sharing network
(b) Regulating diode sharing network

} (Table 7.1)

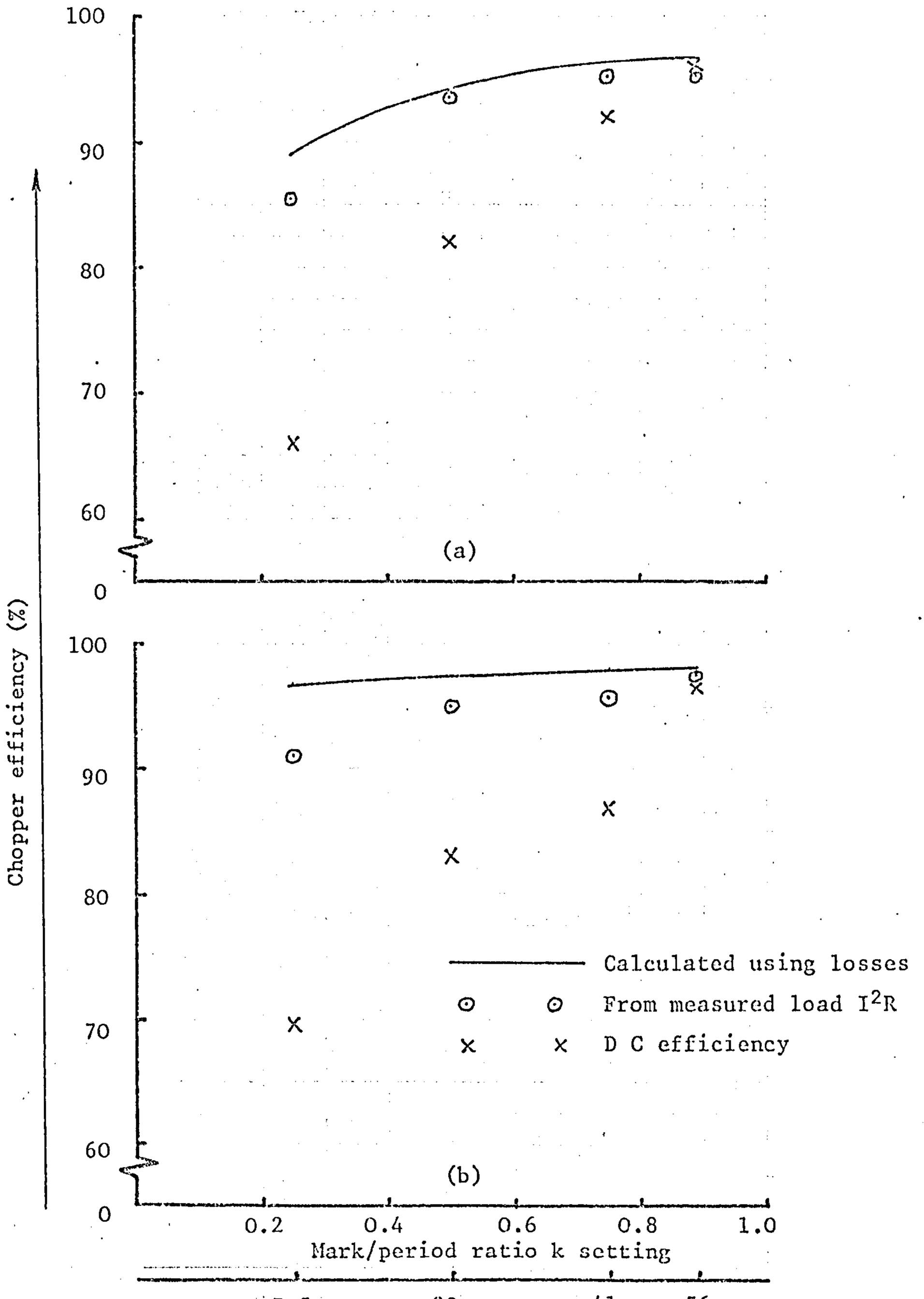

Figure 7.13: Variation of chopper efficiency with mark/period ratio at constant frequency (500 Hz)

(a) R-C plus SR sharing networks
(b) Regulating diode sharing networks

} (Table 7.1)

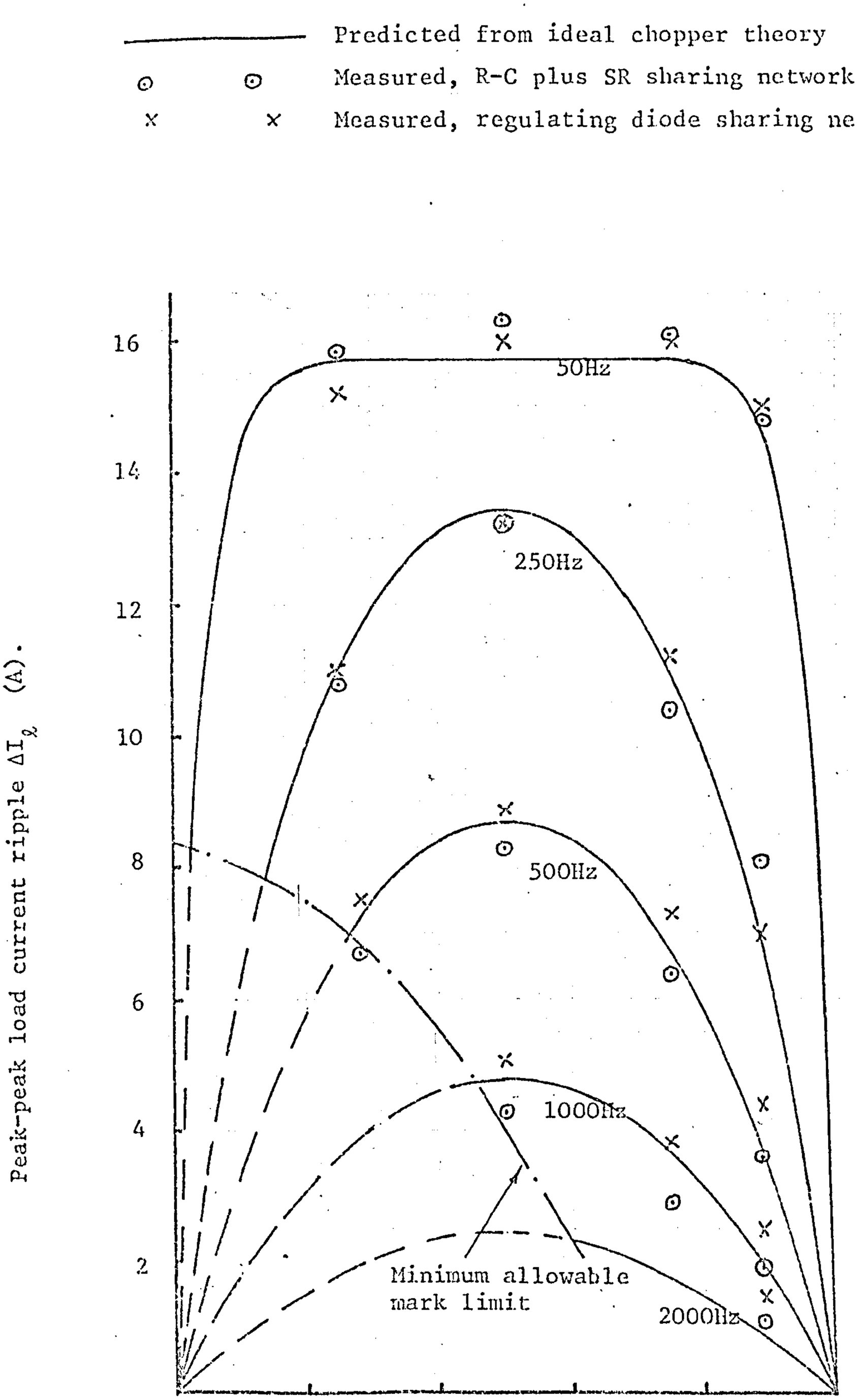

Figure 7.14: Variation of peak-peak load current ripple with mark/period ratio at different chopping frequencies.

increased is well demonstrated. The minimum mark characteristic has been drawn with an assumed minimum t_{m1} of 200μs and the appropriate value of t_{m2} calculated from equation (II.11).

7.9 DISCUSSION

7.9.1 Chopper output voltage

The measured mean d.c. output voltage falls, as expected, below the ideal value (Figure 7.11), the fall tending to be greater at high frequencies, though this is not consistently demonstrated owing to experimental inaccuracy. Close correlation between the measured and calculated values of voltage regulation in Table 7.2 cannot be expected since, by definition, regulation is the small difference between two large quantities. More meaningful is the acceptable agreement between the mean output voltage values. The calculated figures for the thyristor Th_1 peak reverse voltage V_R demonstrate the greater discharge of the commutating capacitor through the R-C networks than through the regulating diodes. This is particularly apparent at the lower frequency owing to the presence of the resistors R_s. However, the more moderate fall of V_R below V_d at high frequencies more affects the mean output voltage because t_{m2} is a larger proportion of the output voltage mark m (section 7.2).

7.9.2 Chopper efficiency

The values of efficiency calculated by the three different methods (section 7.6.2) correspond well at the higher chopping

frequencies (Figure 7.12), and mark/period ratios (Figure 7.13), where the load current ripple is low. The values obtained by using the measured r.m.s. load current are generally lower than those given by the predicted losses; some loss is inevitably unaccounted for, and there is an apparent deviation of the effective load resistance from the measured d.c. value, this being more pronounced at the higher levels of load current ripple. D.C. efficiency values are the lowest, since load ripple power is ignored in its calculation. This is naturally more evident at low frequencies and low values of k.

The efficiency falls slightly with increasing chopping frequency, more so with the R-C sharing network than with the regulating diode network. This can be anticipated from the results of the loss analysis (Figure 7.7). The relatively constant voltage sharing network losses, at a set operating frequency, are largely instrumental in reducing efficiency as k is lowered and the output power correspondingly reduced. Approximate output power values are provided in Figure 7.13 to give added dimension to the results.

7.9.3 Load current ripple

The measured peak-peak load current values compare adequately with the idealised characteristics (Figure 7.14), a peak-peak ripple of 15.7A indicating that the load current flow is discontinuous. The characteristics well illustrate the advantages of high frequency working for ripple limitation.

7.9.4 Summarising comments

No results have been quoted for thyristor and diode voltage sharing since this is, in all cases, satisfactory. Readily available components have been used. Although the thyristors are selected for fast turn-off, the diodes are standard types and proved, under preliminary test, to exhibit a wide spread of reverse recovery characteristics, some having very high values of Q_r (Table I.2). It must be stated that chopper operation would not have been possible with the basic R-C network (Figure 3.1). The inclusion of the series saturating reactor, to control the thyristor and diode reverse recovery effects, provides the base for practical high voltage d.c. chopping. Further, it allows the extension of operating frequencies into the low kilohertz range without invoking high device switching or voltage sharing network losses. Only when used in series with a freewheeling diode string does it introduce serious disadvantages; these depend greatly on the applied voltage waveform and the sharing components across the diodes.

Performance of the test chopper, in terms of output voltage and efficiency, is shown to be extremely good with both voltage sharing networks. Undoubtedly the modest current level contributes to this, in conjunction with the low sharing network losses. Extrapolating the calculated losses for increasing operating voltages yields the following results, assuming an unchanged current level. For 10kV, with the string derating factor f_s doubled, the calculated efficiency at 2000Hz would fall from 93% to 89% with the R-C networks; that with the regulating diode networks would remain virtually constant

at 97%. Extrapolating further to 20kV, with double the number of devices in series, the relevant efficiencies become 80% and 97%. The regulating diode components therefore provide most scope for high frequency working at very high voltage levels.

CHAPTER 8

CONCLUSIONS AND POSSIBLE FUTURE APPLICATIONS

8.1 CONCLUSIONS

8.1.1 Discussion

It has been demonstrated that forced commutation of series connected thyristors can be satisfactorily achieved by the use of suitable voltage sharing networks. These have been developed for the purpose. The networks remove the constraints on main circuit operation which are present with the usual resistive-capacitive networks. Their better control of thyristor reverse recovery effects and low loss are of particular importance in this respect. They provide reliable thyristor turn-off and, suitably chosen, allow operation at very high frequencies.

In general, the new voltage sharing networks provide more uniform voltage distribution than does the basic resistive-capacitive configuration. Consequently, fewer thyristors are required in series for a given operating voltage. It has been established that, with only voltage regulating diodes used as the shunt components, turn-off can be perfectly satisfactory despite the very poor voltage sharing. The networks are also suitable for naturally commutated thyristor strings, within the limitations imposed by the variable commutating voltage produced by firing angle control. They can readily be adapted for use with series connected diodes.

The series saturating reactor with shunt R-C components forms the

most simple arrangement, although the reactor becomes a large component at high voltage and current levels. The series saturating reactor can also be usefully employed with parallel voltage regulating diodes. Networks utilising regulating diodes have found little favour in the past. This unpopularity may be due to uncertainty regarding their reliability, the unavailability of high voltage types, and the cost in comparison with R-C components, which are required in addition if high dV/dt conditions are encountered. There is no doubt that, although reliable under healthy conditions, regulating diodes are more prone to damage than R-C components on circuit malfunction. Their relative costs are comparable at 5kV, amounting to about £1.40 per thyristor for the experimental chopper (Chapter 7). However, the cost of the regulating diode network increases approximately in proportion to the operating voltage whereas the rise is less pronounced with R-C components. Regulating diodes are the more appropriate for any future high voltage, high frequency applications, where the increased capital expenditure will be offset by the greater operating efficiency.

The shunt transformer networks are not particularly attractive in view of their increased complexity and generally inferior voltage sharing performance compared with the series saturating reactor plus shunt resistors and capacitors. The components are relatively inexpensive, amounting to £0.60 per thyristor for those used here (Chapter 5), but the higher additional cost of transformer manufacture is not included in this figure since the units were purpose-built in the department. The overall cost in addition to that of the R-C components therefore becomes significant. Nevertheless, these networks have the technical advantage of providing a reverse voltage across each

thyristor. They can therefore play a useful part in situations where turn-off is difficult.

The establishment of safe and efficient forced commutation opens the way to a new range of high voltage applications for thyristors. The potential importance of this depends on the satisfactory solution of the remaining associated problems and on the demand, in relation to other technical and economic factors, for the applications which then become feasible. The possible applications may be divided into two broad categories: those related to d.c.-a.c. conversion (inverters), and those to direct d.c.-d.c. conversion (choppers). These are reviewed, together with the outstanding technical problems, in subsequent sections.

8.1.2 Summary of the work covered

(a) The measurement of thyristor turn-off time, and thyristor and diode removed reverse recovery charge, leading to an assessment of the degree of influence which circuit factors have on these properties.

(b) The establishment of appropriate methods for measuring thyristor and diode minority carrier lifetime, which is necessary for the design of the series saturating reactor.

(c) Statement of the problems of operating thyristors or diodes in series, and of the defects of the basic resistive-capacitive voltage sharing network with forced commutation.

(d) The provision of voltage sharing networks, with a design procedure for each, which give improved performance at thyristor turn-off or diode reverse recovery. These networks have three main forms:

(i) A series saturating reactor used with parallel resistive-capacitive components.

(ii) Parallel transformers used with parallel resistive-capacitive components.

(iii) Parallel voltage regulating diodes used with or without other R-C and magnetic components.

(e) Overall assessment of the performance obtainable from networks (i) and (iii) used, in turn, on all the series thyristors and diodes in a high voltage, variable frequency, d.c. chopper.

8.2. POSSIBLE FUTURE APPLICATIONS

8.2.1 Forced commutation in the conventional h.v.d.c. converter

A number of methods have been proposed for forcing the commutation of mercury arc valves in the naturally commutated h.v.d.c., three-phase bridge converter[53]. These are aimed at overcoming the inherent delay in commutation (commutation time or overlap), and at removing the need to make allowance for the valve deionisation time (the equivalent of thyristor turn-off time), which is particularly important with the converter in the inverted mode. The converter can then effectively operate at a reduced or zero firing angle. This lessens its very considerable reactive power demand on the a.c. system and therefore reduces the capacitive compensation required[2,3,53].

Forced commutation has, however, proved unattractive both technically and economically with mercury arc valves. The capability of the thyristor for withstanding the increased electrical stress imposed

during commutation removes the technical constraint, but it remains to be seen whether forced commutation will become economically viable. At the present time this seems doubtful.

8.2.2 High voltage d.c. supply to a dead a.c. load

If there is no synchronous system on the receiving a.c. side of the inverter to establish the commutating voltage for the thyristors, forced commutation must be employed. Force-commutated inverters of the required form are used at low voltages, particularly for high or variable frequency a.c. supplies.

The relevance of force-commutated inverters to h.v.d.c. transmission lies in two possible applications:

(a) Where power is to be transmitted, probably by submarine cable, to a remote situation without its own synchronous a.c. system.

(b) In reinforcement of a.c. distribution systems by h.v.d.c. link[54].

The technically simpler alternative to forced commutation for (a) is to incorporate a rotating synchronous compensator to provide the converter commutating voltage and supply the reactive power. Forced commutation might be more attractive for small schemes. The need for forced commutation with (b) arises because reinforcement will be most effective if the d.c. links are capable of operating without a synchronous a.c. system at the receiving end[55]. Even at low voltages, force-commutated inverters are complex and expensive, and filtering of the output is essential if sinusoidal a.c. is required. As a consequence, their use has expanded only slowly. The cost of development for high voltages would be very heavy and the present trend of thought

is to avoid their use by always ensuring the receiving a.c. system is paralleled with a synchronous source.

8.2.3 D.C. choppers for traction

An efficient, reliable and smoothly controlled, variable voltage supply system for d.c. traction motor speed control has always been a great need. The d.c. chopper offers a performance which greatly surpasses that of the traditional series resistance control, though its reliability in prolonged service is not yet proved.

In addition to its use as a traction motor controller, the d.c. chopper can replace the usual motor-generator set for stepping down supply line voltage to about 100V for auxiliary supplies. The lack of electrical isolation is here a disadvantage and an alternative system using a force-commutated inverter and transformer to supply a.c. auxiliaries is more attractive.

The prospect of high voltage d.c. traction with a 20-25kV d.c. overhead supply appears to be remote in this country, where we are now committed to 50Hz a.c. traction except for Southern Region of British Rail. In this case high voltage d.c. would be inappropriate owing to the high traffic density and third rail system used. There may perhaps be developments in h.v.d.c. traction in countries which, as yet, have no established traction system.

8.2.4 High voltage d.c. transformation using choppers

High voltage d.c. transmission has so far been limited basically to the interconnection of separate a.c. systems at two points. The

reasons for this are as follows:

(a) The lack of a circuit breaker capable of interrupting d.c. at high voltages precludes any d.c. tee-off which requires independent switching. All on-load switching operations must be performed on the a.c. side of the converters or by valve grid control.

(b) There is no d.c. equivalent of the a.c. power transformer; distribution by direct current has therefore not been possible.

It is unlikely that the present balance between a.c. and d.c. working will be greatly changed for some years to come. However, the advantages of h.v.d.c. transmission[53] make it attractive when considering future supply system expansion[54], and it is worthwhile to consider the possible future role of the d.c. chopper in h.v.d.c. transmission systems. In principle, it can provide a solution to both limitations (a) and (b) above, and also serve as a controller of power flow.

Working on the assumption that a high voltage d.c. chopper should fulfil a similar purpose to the a.c. transformer, together with its additional switching and control functions, the following factors are important when considering the possible alternative forms of chopper which can be used:

(i) The ability to handle any likely type of load: resistive, inductive, with or without back e.m.f.

(ii) The ability to accept load immediately it is applied without the need to switch on.

(iii) The ability to automatically handle power flow in either direction.

(iv) Smoothing of current on the high voltage and low voltage sides.

(v) The ability to withstand all fault conditions and interrupt fault

current if used as a circuit breaker.

(vi) High efficiency.

(vii) Excellent reliability.

(viii) The ability to control output voltage.

Factor (ii) necessitates the commutation circuit being independent of the load, which eliminates a number of chopper configurations including the circuit used in Chapter 7. Point (iii) is also restrictive since it implies that the chopper must accept reverse power flow without any change of connection. A circuit which fulfils these particular requirements has been used at low voltages[56,57]. A mechanical switch would be needed in series to give complete electrical isolation.

8.3 OUTSTANDING FUNDAMENTAL PROBLEMS

8.3.1 Overcurrent protection at high voltages

Thyristor and diode overcurrent protection must be considered from two points of view, namely, overload and short circuit. The technique now being used with h.v.d.c. thyristor 'valves' is to connect sufficient series thyristor strings in parallel to allow for the worst surge conditions, and then rely on the constant current compounding[53] of the rectifying converter to control overload and slower rising fault currents. This compounding automatically reduces the output voltage sufficiently to maintain the current very nearly constant, even down to zero voltage. On severe short circuit, fast gate signal blocking and a.c. circuit breaker tripping are used.[1]

Constant current compounding can be similarly used on a chopper by suitable control of mark/period ratio. So also can gate signal suppression to give more rapid fault clearance, though reliance must be placed on the output filter inductance to sufficiently limit the rate of current rise. Satisfactory commutation is essential, as is adequate thyristor surge current rating, since thyristor forward blocking capability is first lost on excessive temperature rise. The rapid detection and isolation of the equipment from the d.c. supply is necessary on a commutation failure or a severe short circuit. The provision of such overcurrent protection poses a severe problem and two perhaps complementary forms are suggested below.

Fast acting H.R.C. fuses have been developed for semiconductor protection at a.c. voltages up to about 5kV. Fusing is usually more difficult in d.c. circuits where loads are frequently very inductive, and fuses must be operated at d.c. voltages well below their r.m.s. a.c. circuit rating under these circumstances[58]. Given the demand, it is to be expected that semiconductor fuse voltage ratings will increase to much higher levels. Progress is being made, particularly by Continental manufacturers in this direction. The H.R.C. fuse may therefore provide the ultimate overcurrent protection, but a shut-down of the equipment is necessary for replacement.

For automatic fault clearance and re-start, another protection system is required. Since use of a mechanical circuit breaker is not possible, the solution to this problem may lie in the use of an electrical interrupter with a mechanical isolating switch intended only for no-load operation. The 'electronic crowbar' technique could be

used to induce rising fault current from the thyristors to a fast-switching thyratron connected across the d.c. input lines. The thyratron has a much higher surge rating than the equivalent thyristors. A promising device for use in this way is the thyratron d.c. circuit breaker [59]. This utilises a deuterium-filled thyratron, triggered into conduction conventionally at its grid but turned off by the application of an axial pulsed magnetic field produced by an external coil wound concentrically with the thyratron case. Both turn-on and turn-off times are typically a few tens of microseconds. Experimental units have been tested up to 12kV, but much higher operating voltages are envisaged with peak currents in excess of 10kA.

8.3.2 Harmonics and their effects

The fast switching produced by forced commutation invariably gives waveforms which are grossly non-sinusoidal if alternating, and high in ripple content if direct. The harmonic currents and voltages create disturbances both in the power system and in neighbouring communication circuits.

The advent of h.v.d.c. transmission has led to considerable attention being given to the effects of harmonic currents fed back into the a.c. supply by the converter, and the effects of the ripple harmonics in the d.c. lines[53,60]. Telephone interference has posed problems. For traction application especially, interference could render track and other signalling circuits inoperable.

The viability of schemes utilising force-commutated thyristors could ultimately depend on the effectiveness of the filtering of the

stepped waveforms generated, and the additional costs incurred in making provision for this.

8.4 FUTURE WORK

It will be many years before some of these examples of forced commutation of thyristors find industrial application, since they represent a great advance in high voltage d.c. practice. There is considerable scope for further work in this field, and to further the ideas propounded, research is required into the following topics:

(a) The overcurrent protection of semiconductor rectifiers operating at high voltages.

(b) An investigation into suitable chopper circuits for the transformation of d.c. at high voltages in accordance with the requirements stated in section 8.2.4.

(c) The investigation of current and voltage harmonics and radio-frequency interference generated by high voltage choppers, together with the methods by which their deleterious effects can be diminished. These methods will fall into two areas:

(i) The precautions which can be taken in chopper design to reduce the rates of change of voltage and current which generate the interference.

(ii) The degree of filtering and screening required for interference suppression.

REFERENCES

1. Boksjo I.: 'A Thyristor Converter for H.V.D.C. in Regular Operation', Direct Current, Vol 2, No 2, May/June 1971, pp 58-62.

2. Hall J.K.: 'Methods of Achieving Commutation in Inverters by the Use of Capacitors', M.Sc.(Eng.) Thesis, University of London, 1964.

3. Hingorani N.G. and Hall J.K.: 'Use of Capacitors for Reduction of Commutation Angle in Static High-Power Converters', Proc.IEE, Vol 112, No 12, December 1965, pp 2333-2341.

4. Kitaoka T. and Ohno E.: 'Thyristor D.C. Choppers and High Voltage Inverters for D.C. Traction, IEE Conf. Publ. No 53, Part 1, May 1969, pp 263-270.

5. Bailey A.R. and Varley J.R.: 'The Use of High Frequency Choppers for Traction Purposes', IEE Conf.Publ. No 53, Part 1, May 1969, pp 271-276.

6. Band C.E. and Stephens J.H.: 'Development of and Operational Experience with a High Powered D.C. Chopper for 1500V D.C. Railway Equipment', IEE Conf.Publ. No 53, Part 1, May 1969, pp 277-288.

7. Jauquet C., Gouthière J. and Hologne H.: 'D.C. Choppers for Railway Applications', IEE Conf.Publ. No 53, Part 1, May 1969, pp 289-296.

8. Hey J.C.: 'Series Operation of Silicon Controlled Rectifiers' Application Note 200.4D, General Electric Co., Auburn, N.Y.

9. Hall J.K.: 'Forced Commutation of Thyristors Connected in Series-Strings', IEE Conf.Publ. No 53, Part 1, May 1969, pp 365-372.

10. Gentry et al.: 'Semiconductor Controlled Rectifiers', (Prentice-Hall, 1964).

11. Somos I.: 'Switching Characteristics of Silicon Power Controlled Rectifiers, II - Turn-off Action and dV/dt Self-switching', IEEE Trans.Comm. Electronics, Vol 83, No 75, November 1964, pp 861-871.

12. Dyer R.F. and Houghton G.K.: 'Turn-off Time Characterisation of Silicon Controlled Rectifiers', Direct Current, Vol 7, No 6, June 1962, pp 158-165.

13. Lebedev A.A. and Uvarov A.I.: 'The Charge Dissipation Time constant in a P-N-P-N Structure During Switch-off Under the Influence of a Reverse Anode Voltage', Radio Engng. Electronic Phys. (USA), Vol 12, No 4, April 1967, pp 634-639.

14. Kuz'min V.A.: 'The Turn-off Time of P-N-P-N Devices', Radio Engng. Electronic Phys. (USA), Vol 8, No 8, August 1964, pp 1161-1165.

15. 'Thyristor Design Trade-offs in Turn-off Specifications', Application Data Sheet No 54-580, May 1969, Westinghouse Electric Corp., Youngwood, Pa.

16. Dyer R.F.: 'Concurrent Characteristation of SCR Switching Parameters for Inverter Applications', SCP and Solid State Tech., Vol 8, No 4, April 1965, pp 15-20.

17. Irminger G.: 'Thyristor Circuitry', Brown Boveri Rev., Vol 53, No 10, October 1966, pp 657-671.

18. Von Zastrow E.E. and Galloway J.H.: "Commutation Behavior of Diffused High Current Rectifier Diodes', Application Note 200.42, General Electric Co., Auburn, N.Y.

19. Galloway J.H.: 'Application of Fast Recovery Rectifiers', Application Note 200.38, General Electric Co., Auburn, N.Y.

20. Amano H. and Koshiba O.: 'Transient Voltage Across Series-Connected Silicon Rectifier Cells Immediately After Commutation', Elect.Eng.Japan (USA), Vol 84, No 10, October 1964, pp 13-21.

21. Hall J.K.: 'Improvement of Turn-off Performance of Series-Connected Thyristors by Magnetic Components', IEEE Trans.Mag., Vol MAG-7, No 2, June 1971, pp 279-304.

22. Kuno H.J.: 'Analysis and Characterisation of P-N Junction Diode Switching', IEEE Trans. Electron Dev., Vol ED-11, No 1, January 1964, pp 8-14.

23. Kao Y.C. and Davis J.R.: 'Correlations Between Reverse Recovery Time and Lifetime of P-N Junction Driven by a Current Ramp', IEEE Trans. Electron Dev., Vol ED-17, No 9, September 1970, pp 652-657.

24. Hoffmann A. and Schuster K.: 'An Experimental Determination of the Carrier Lifetime in p-i-n Diodes From the Stored Carrier Charge', Solid State Electronics, Vol 7, No 10, October 1964, pp 717-724.

25. Pierce J.F.: 'Semiconductor Junction Devices' (Charles E. Merrill Books, Inc., Columbus, Ohio, 1967).

26. Weaver J.J.L., Eccles A.M. and Kelham W.O.: 'Development of a Thyristor Valve for H.V.D.C. Transmission', IEE Conf.Publ. No 53, Part 1, May 1969, pp 339-346.

27. Danders M, Etter P. and HoffmannM.: 'Results of Testing Thyristor Valves for H.V.D.C. Transmission in the Load-Testing Station for H.V. Converters in Mannheim-Rheiman', IEE Conf.Publ. No 53, Part 1, May 1969, pp 386-397.

28. Ohno E., Mitzuoka N. and Kimura Y.: 'Thyristor Strings for High Voltage Applications', IEE Conf.Publ. No. 53, Part 1, May 1969, pp 406-412.

29. Horigome T., Kurokawa K, Kishi K. and Ozo K.: 'A 100kV Thyristor Converter for High Voltage D.C. Transmission', IEEE Trans. Electron Dev., Vol ED-17, No 9, September 1970, pp 809-815.

30. Von Zastrow E.E.: 'The Series Connection of Rectifier Diodes', Application Note 200.39, General Electric Co., Auburn, N.Y.

31. Mapham N.: 'Overcoming Turn-on Effects in Silicon Controlled Rectifiers', Electronics, Vol 35, No 33, 17 Aug.1962, pp 50-51.

32. Weaver J.J.L.: 'H.V.D.C. Thyristor Converters', Conf. on H.V.D.C. Transmission, Bournemouth Coll. of Tech., May 1969.

33. Anwander E. and Etter P.: 'Thyristor Valve for 100kV.D.C. Bridge Voltage', Brown Boveri Rev., Vol 56, No 2, February 1969, pp 79-88.

34. Bedford B.D. and Hoft R.G.: 'Principles of Inverter Circuits', (Wiley and Co., New York, 1964).

35. HCR Alloy, Telcon Metals Limited, publ. No TP25-666.

36. Driver D.R.: 'Pulse-transformers, Part 1: Use of Nickel-iron Alloys', Design Electronics, Vol 7, No 9, pp 47-53.

37. Paice D.A. and Wood P.: 'Nonlinear Reactors as Protective Elements for Thyristor Circuits', IEEE Trans. Mag., Vol MAG-3, September 1967, pp 228-232.

38. Cherry E.C.: 'The Duality between Interlinked Electric and Magnetic Circuits and the Formation of Transformer Equivalent Circuits', Proc.Phys.Soc., Section B, Vol 62, 1949, pp 101-111.

39. Manteuffel E.W. and Phillips T.A.: 'The Shunt Loaded Magnetic Amplifier - II', AIEE Trans. (Comm. Electron), Vol 81, 1962, pp 447-457.

40. Zener Diode Handbook, International Rectifier Corp., 1960.

41. Acosta A.N.: 'Zener Diode - A Protective Device Against Voltage Transients', IEEE Trans. Ind. Gen. Appl., Vol. IGA-5, No 4, July/August 1969, pp 481-488.

42. Dakin C.J. and Cooke C.E.G.: 'Circuits for Digital Equipment', (Iliffe, 1967).

43. Gutzwiller F.W. and Sylvan T.D.: 'Power Semiconductor Ratings Under Transient and Intermittent Loads',

Application Note No 200.9, General Electric Co., Auburn, N.Y.

44. SCR Manual, General Electric Co., Auburn, N.Y.

45. Borst D.W., Diebold E.J. and Parrish F.W.: "Voltage Control by Means of Power Thyristors", IEEE Trans. Ind. Gen. Appl., Vol IGA-2, No 2, March/April, 1966.

46. Varley J.R.: 'Thyristor Control of D.C. Traction Motors', M.Sc. Thesis, University of Bradford, 1970.

47. Knapp P.: 'Solid-State Regulating Units for Motoring and Braking D.C. Traction Vehicles', Brown Bov. Rev., Vol 57, June/July 1970, pp 252-270.

48. Golden F.B.: 'Measure SCR Switching Losses the Easy Way', Appl.Inf. Sheet No 671.24, General Electric Co., New York, March 1970.

49. Mapham N.: 'The Rating of SCR's When Switching Into High Currents', Application Note No. 200.28, General Electric Co., New York, May 1963.

50. Dyer R.E.: 'The Rating and Application of SCR's Designed for Switching at High Frequencies', Reprint No. 660.13, General Electric Co., New York, August 1966.

51. Holloway B.W.L.: 'High Speed Switching Characteristics of Thyristors', Westinghouse Brake English Electric Semiconductors Ltd., report, 1970.

52. 'Provisional Frequency Ratings for High Frequency Power Thyristor D.1161.T17-20', Westinghouse Brake English Electric Semiconductors Ltd., data sheet, 1970.

53. Adamson C. and Hingorani N.G.: 'High Voltage Direct Current Power Transmission' (Garraway, 1960).

54. Brewer G.L. and Kidd D.A.: 'A Technical and Economic Appraisal of Thyristor Equipment for H.V.D.C. for Reinforcing A.C. Distribution Systems', IEE Conf. Publ. No. 53, Part 1, May 1969, pp 354-364.

55. Brewer G.L. and Frazer K.G.: 'D.C. Transmission in A.C. Distribution Systems', IEE Conf.Publ. No 22, Part 1, September 1966, pp 87-89.

56. Hall J.K.: 'The Problems of H.V.D.C. Transformation Using Choppers', Sixth Univ. Power Eng. Conf. held at U.M.I.S.T., January 1971, Paper 2.11.

57. Smith B.H.: 'A Simple Bilateral Variable Ratio D.C. Pulse Converter', IEEE Trans.Ind.Electron. Control Instr., Vol IECI-15, No 1, November 1968, pp 1-5.

58. Jacobs P.C.: 'Application of Fuses with Power Semiconductors in Direct Current Circuits', IEEE Conf. Record, 5th Ann. Meeting of Ind.Gen.Appl.Gp., October 1970, pp 487-491.

59. Baker B.O.: 'A High Speed Thyratron D.C., Circuit Breaker', IEE Conf.Publ. No. 70, September 1970, pp 113-117.

60. Robinson G.H.: 'Experience with Harmonics: New Zealand H.V.D.C. Transmission Scheme', IEE Conf. Publ. No 22, Part 1, September 1966, pp 442-444.

61. Mumetal Ring Cores, Telcon Metals Limited, publ. No. TP11-864.

APPENDIX I

EXPERIMENTAL APPARATUS

I.1 CIRCUITS FOR PRELIMINARY MEASUREMENTS ON THYRISTORS AND DIODES

(a) Thyristor turn-off time measuring circuit (Figure I.1).

Features additional to those mentioned in section 2.5.1 are:

(1) The thyristors (Th_s, Th_r and Th_f) are timed to conduct during their supply voltage negative half-cycle, energy then being drawn from the reservoir capacitors.

(2) The circuit gives the following maximum values:

forward current = 30A,

reverse voltage = 200V,

forward blocking voltage = 300V.

(3) Turn-off time measurements are made on a 545B Tektronics oscilloscope with a type CA plug-in unit. The current probe is a Hewlett-Packard type 1110A with a type 1111A amplifier and the 10x voltage probe is Tektronics type P6006.

(b) Timing circuit (Figure I.2) for the measuring circuit thyristors (Figure I.1).

(1) Thyristor A is gated during the supply voltage negative half-cycle and its conduction maintained by the 100μF capacitor discharging through the adjacent 100Ω resistor. When thyristor A turns on, a pulse is generated to trigger

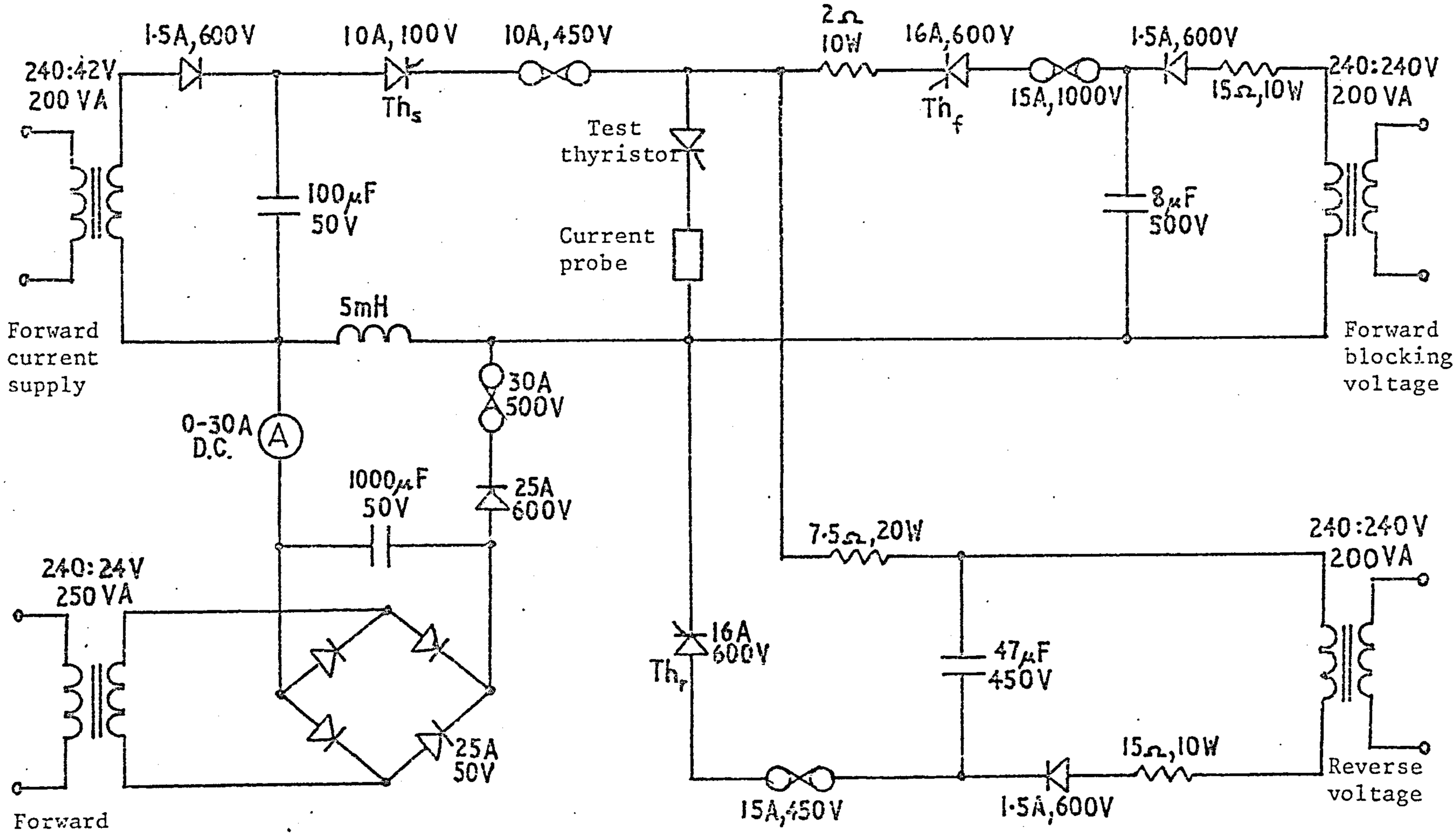

Figure I.1: Thyristor turn-off time measuring circuit.

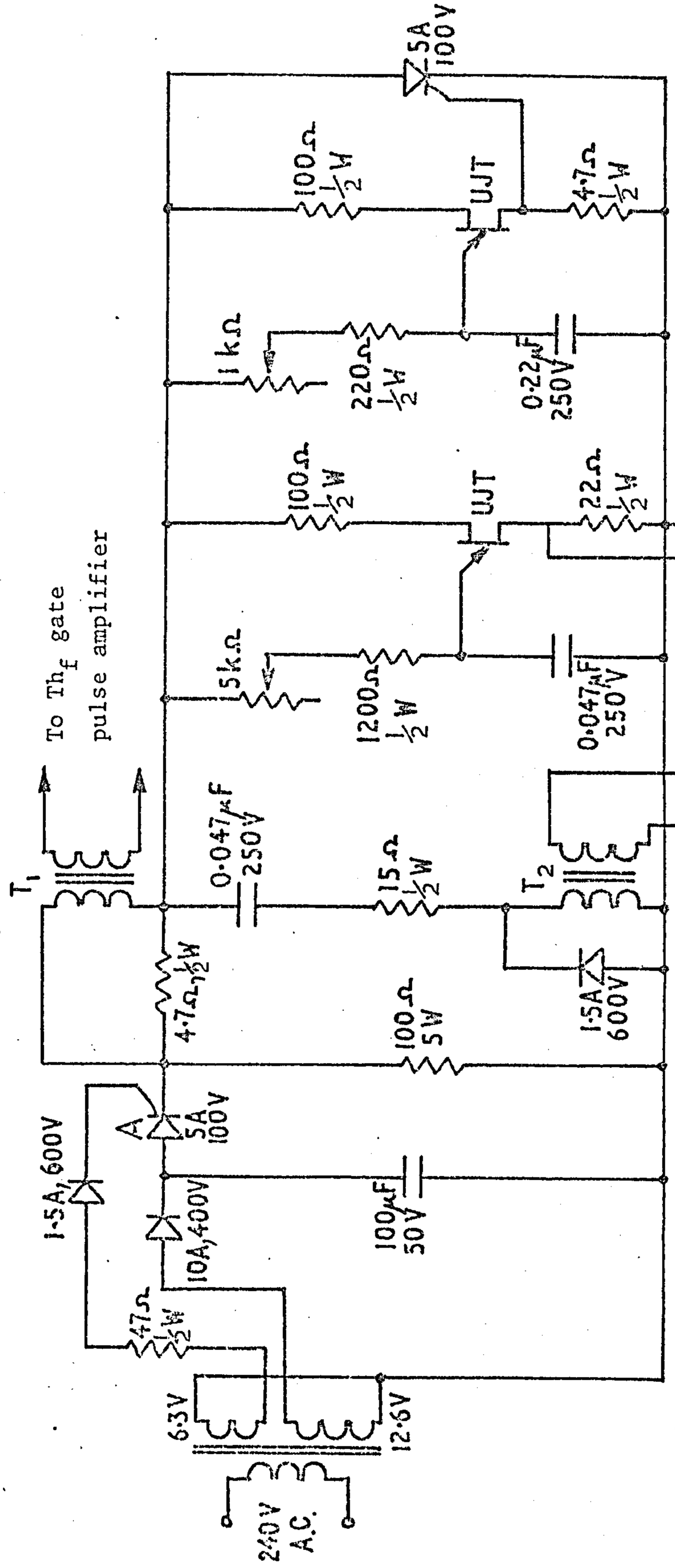

UJT - Unijunction transistor
GE type 2N1671A.

T_1 - transformer, STC core type CR071-16, 32:16 turns
T_2 - " " " , 16:8 turns

Figure I.2: Timing circuit for thyristor triggering in the turn-off time measuring circuit (Figure I.1)

the test thyristor and Th_s.

(2) Unijunction transistor circuits provide pulses with a controlled delay for the test thyristor turn-off (by Th_r) and forward blocking voltage re-application (by Th_f).

(3) Controlled timing provides variable test thyristor conduction from 50-250μs, and turn-off time range of 0-200μs for a 50μs forward current pulse.

(c) Triggered blocking oscillator pulse amplifier (Figure I.3).

(1) The circuit gives output pulses of 20μs width and up to 1A amplitude, depending on thyristor gate impedance; the risetime is 0.2μs.

(d) Manually operated reverse recovery charge measuring circuit (Figure I.4).

(1) Short leads are used for connections inside the dotted area to promote high rates of fall of forward current and to minimise the reverse hole-storage voltage spike.

(2) The operating sequence for switching is as follows:

(i) S_3 is switched to position 1 to charge the 40μF turn-off capacitor.

(ii) S_1 is closed then S_2 rapidly closed and opened to trigger the test thyristor.

(iii) S_3 is switched to position 2 to turn off the test thyristor.

Operations (ii) and (iii) are performed in rapid succession to limit the thyristor temperature rise to a minimum.

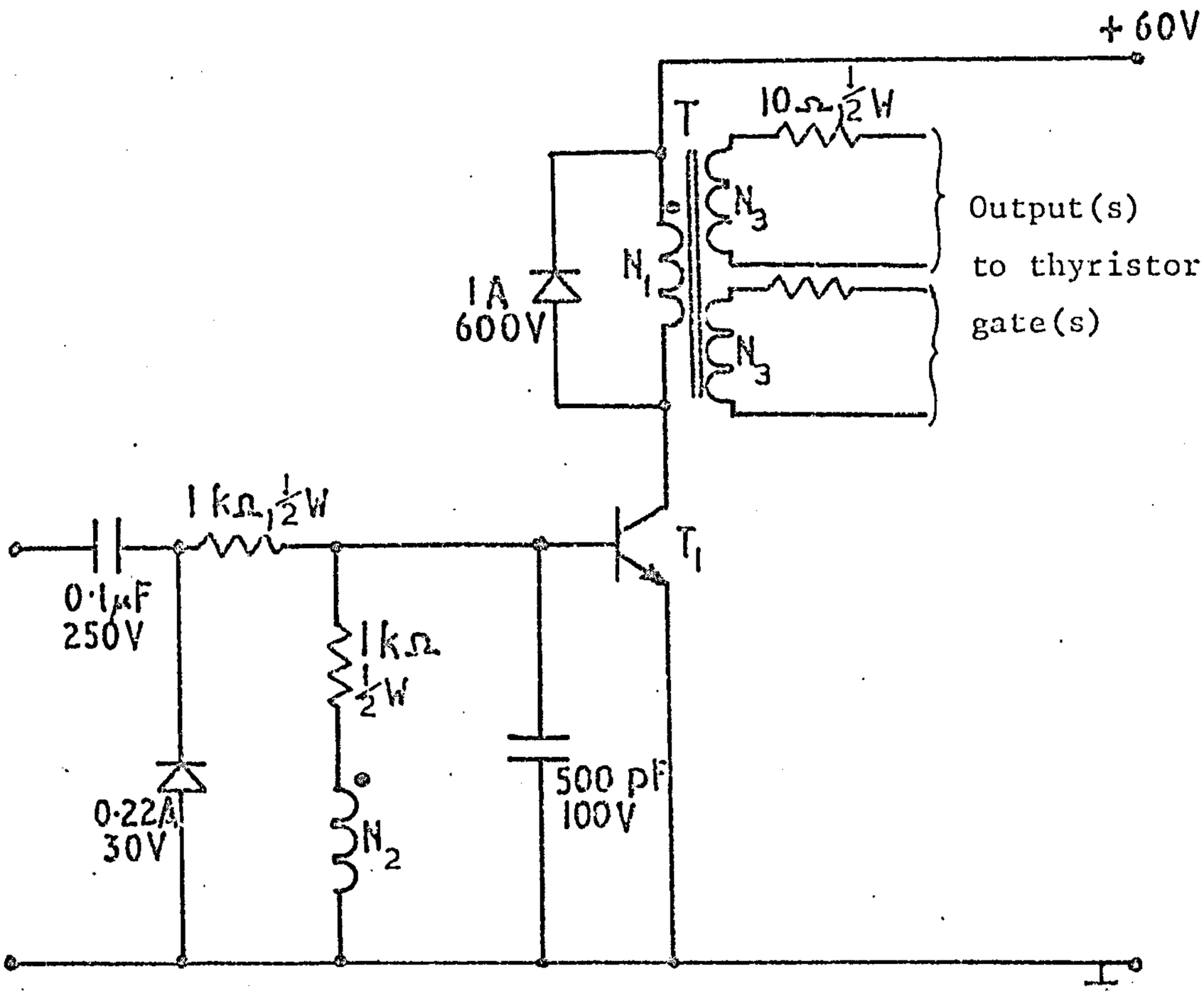

T_1 - Transistor, Ferranti type 2N3262

T - Transformer, Mullard ferrite E-core type FX1239

Windings: Primary, N_1 = 48 turns

Feedback, N_2 = 24 turns

Output(s) to thyristor(s) N_3 = 12 turns

Figure I.3: Triggered blocking oscillator pulse amplifier for thyristor gate supply.

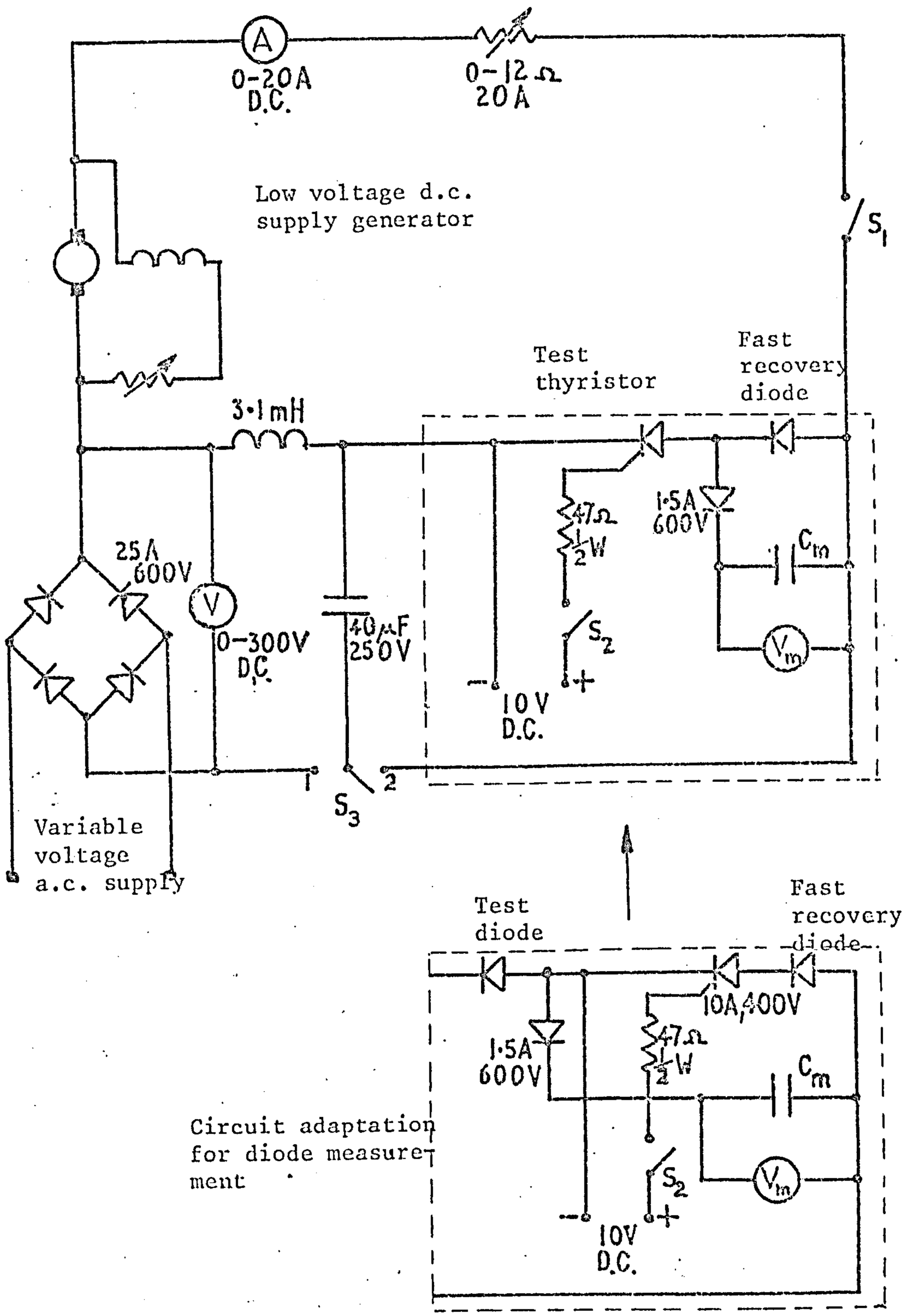

Circuit adaptation for diode measurement

Cm = 0.01 - 5.0μF, 1% tolerance

Vm - Precision electrostatic voltmeter 0-60V.

Figure I.4: Manually operated reverse recovery charge measuring circuit.

(3) Capacitor C_m must be discharged after each measurement.

(4) The fast recovery diode removed charge values must be known from previous measurements.

(5) The charge removed from the test thyristor or diode is the sum of that from the fast recovery diode and that stored in C_m (= C_mx indicated voltage on V_m)

I.2 CIRCUITS FOR TESTING THE VOLTAGE SHARING NETWORKS AT 5kV

(a) Power circuit of the 5kV, constant frequency chopper (Figure I.5).

(1) The 8.8mH inductance represents that of the supply.

(2) Test string Th_1 thyristor details are given in Table I.1.

(3) The 66μH inductor limits Th_2 di/dt at turn-on and also Th_1 rate of fall of forward current to 45A/μs.

(4) Overcurrent protection is provided by two 1000V fuses in series, because suitable fuses at higher voltage ratings are not available. These adequately protect the supply diode string and there is insufficient energy stored in the commutating capacitor C_c to damage the Th_1, Th_2 or D_2 devices.

(b) 50Hz chopper timing control arrangement (Figure I.6).

(1) The timing control circuit is basically the same as that of Figure I.2 with the first UJT pulse generator (giving the output shown to Th_r) absent and with minor component modifications on the second UJT circuit to provide the required timings.

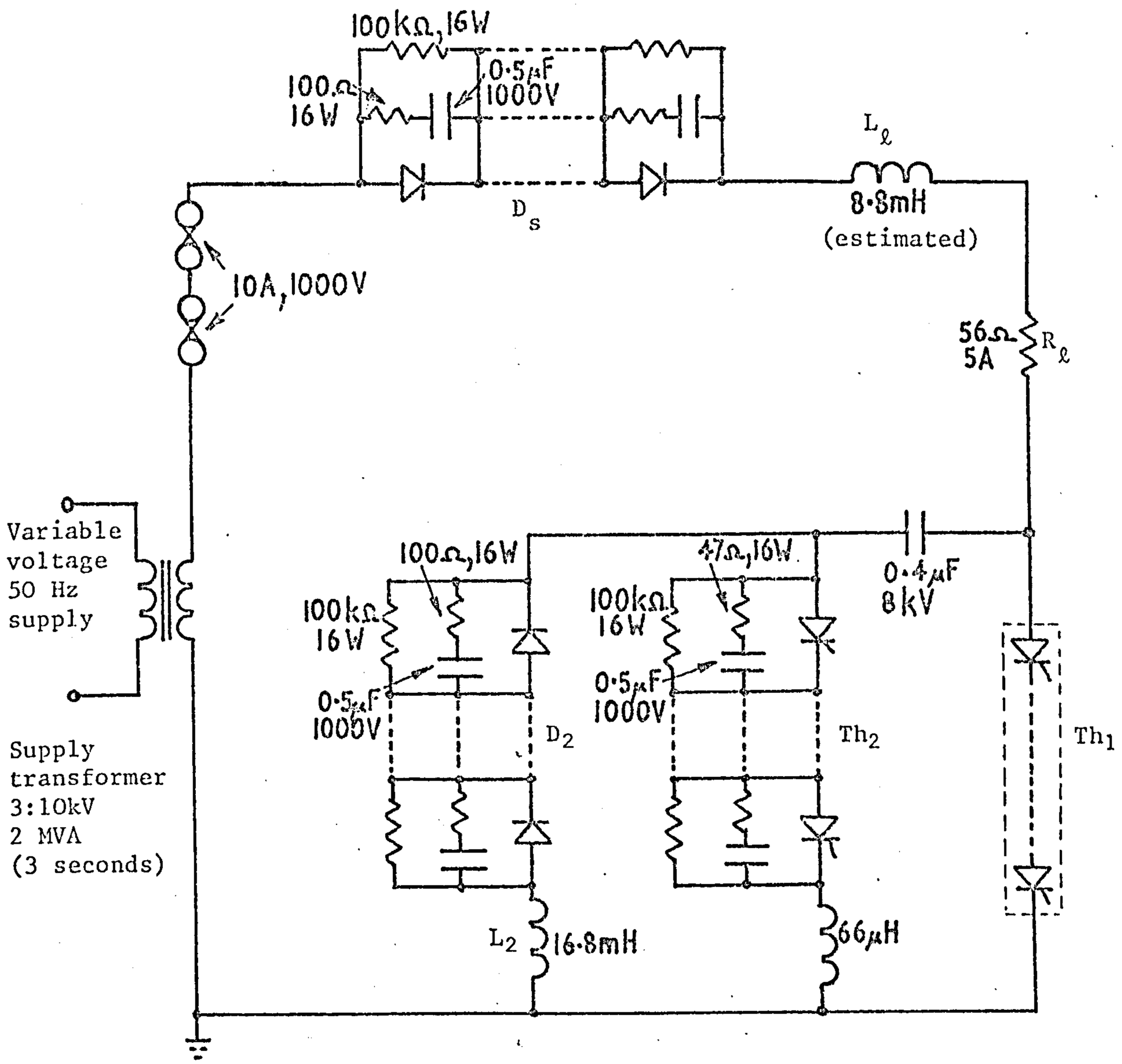

Power semiconductor components:

Supply diode string D_s - 15 diodes, IR type 12F120, (12A, 1200V, 150 A^2s)

Capacitor recharge
diode string D_2 - 10 diodes as above.

Turn-off thyristor string
Th_2 - 9 thyristors, Westinghouse type 24T8,
(12A, 800V, 160 A^2s)

Test thyristor string
Th_1 - 20 thyristors, GE type C36D (2N1849),
(16A, 400V, 40 A^2s)

Figure I.5: Power circuit for the 5kV, 50 Hz, chopper.
(Refers also to Figure 3.3)

Order in String	Thy-ristor number	Turn-off time(μs)	Reverse Recovery charge Q_r(μC)	$\Delta Q_r = Q_{rn} - Q_r$	τ_p (μs)
High voltage end	1	28	4	6.7 = Q_{r1}	20.2	0.44
	2	9	11	22.3	4.6	-
	3	12	9	20.8	6.1	-
	4	19	10	20.7	6.2	-
	5	27	8	20.5	6.4	-
	6	13	8	19.3	7.6	-
	7	22	8	19.1	7.8	-
	8	7	6	18.9	8.0	-
Forward conduction	9	2	7	16.9	10.0	-
	10	1	6	15.9	11.0	-
	11	18	7	14.9	12.0	-
	12	14	6	13.5	13.4	-
	13	25	9	13.3	13.6	-
	14	15	6	10.0	16.9	-
	15	10	6	9.9	17.0	-
	16	16	6	12.5	14.4	-
	17	24	5	9.9	17.0	-
	18	20	4	9.1	17.8	-
	19	4	8	8.4	18.5	-
Earthy end	20	8	13	26.9 = Q_{rn}	0	3.66

Measurements made with: forward current = 25A, $\left|\frac{di}{dt}\right|_{off}$ = 40A/μs, reverse voltage = 100V, forward blocking voltage = 100V, dV/dt = 100V/μs, stud temperature = ambient 20°C. Values of τ_p are measured by the method of section 2.7

Table I.1: Previously measured turn-off parameters of the thyristors in the test string Th_1 in the 5kV, 50Hz chopper (Figure 3.3).

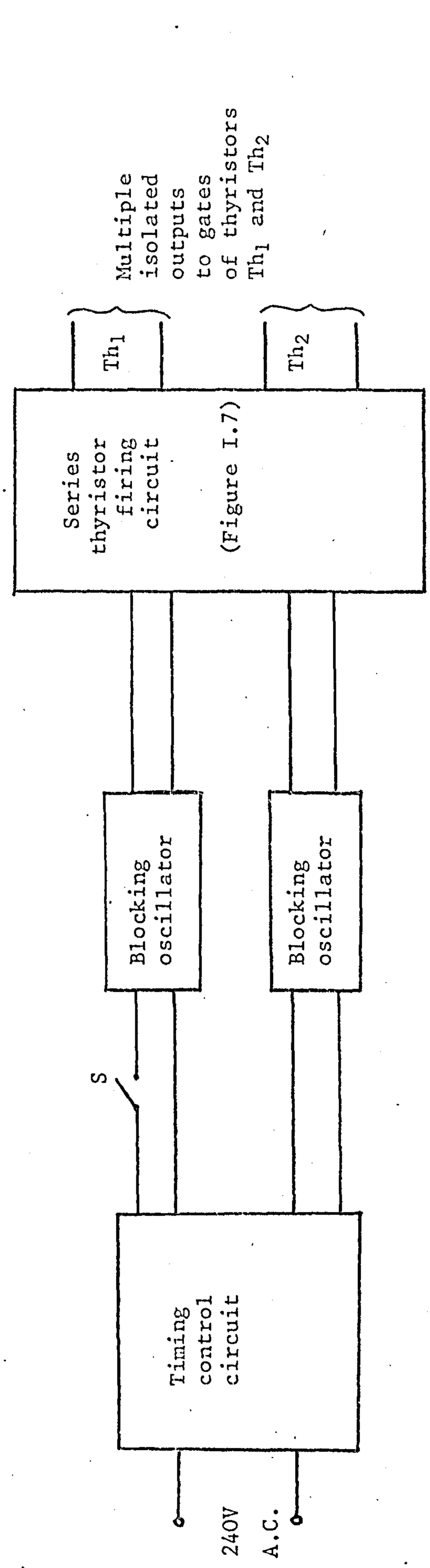

Figure I.6: Block diagram of the thyristor gate pulse supply arrangement for the 5kV, 50 Hz chopper.

(2) The blocking oscillator pulse amplifiers are identical to those of Figure I.3.

(3) The 240V input is suitably related in phase to the chopper supply voltage to give thyristor Th_1 triggering just prior to the supply voltage peak.

(4) The time delay between the output pulses for firing Th_1 and Th_2 is variable between 250μs and 1.2ms; normally 550μs is used.

(5) The chopper is started by first applying voltage with the controller switch S open to pre-charge the commutating capacitor C_c through Th_2. Chopping commences when S is closed.

(c) Series thyristor firing circuit (Figure I.7).

(1) The insulated cable forms a single turn primary for multiple pulse transformers T, one for each thyristor. The cable passes through the toroidal core of each transformer, the 20-turn secondary winding of which supplies the thyristor gate. Zener diodes restrict the gate voltage to a safe value.

(2) When thyristor Th_{t_1} (or Th_{t_2}) is gated, the associated 2μF capacitor charges with an oscillatory half cycle through the 6.6μH cable inductance. The cable current, of approximately 75A peak, induces virtually simultaneous gate pulses for the series thyristors. Thyristor Th_{t_1} (or Th_{t_2}), being reverse biased, then turns off and the 2μF capacitor discharges through the 100Ω resistor ready for the next cycle.

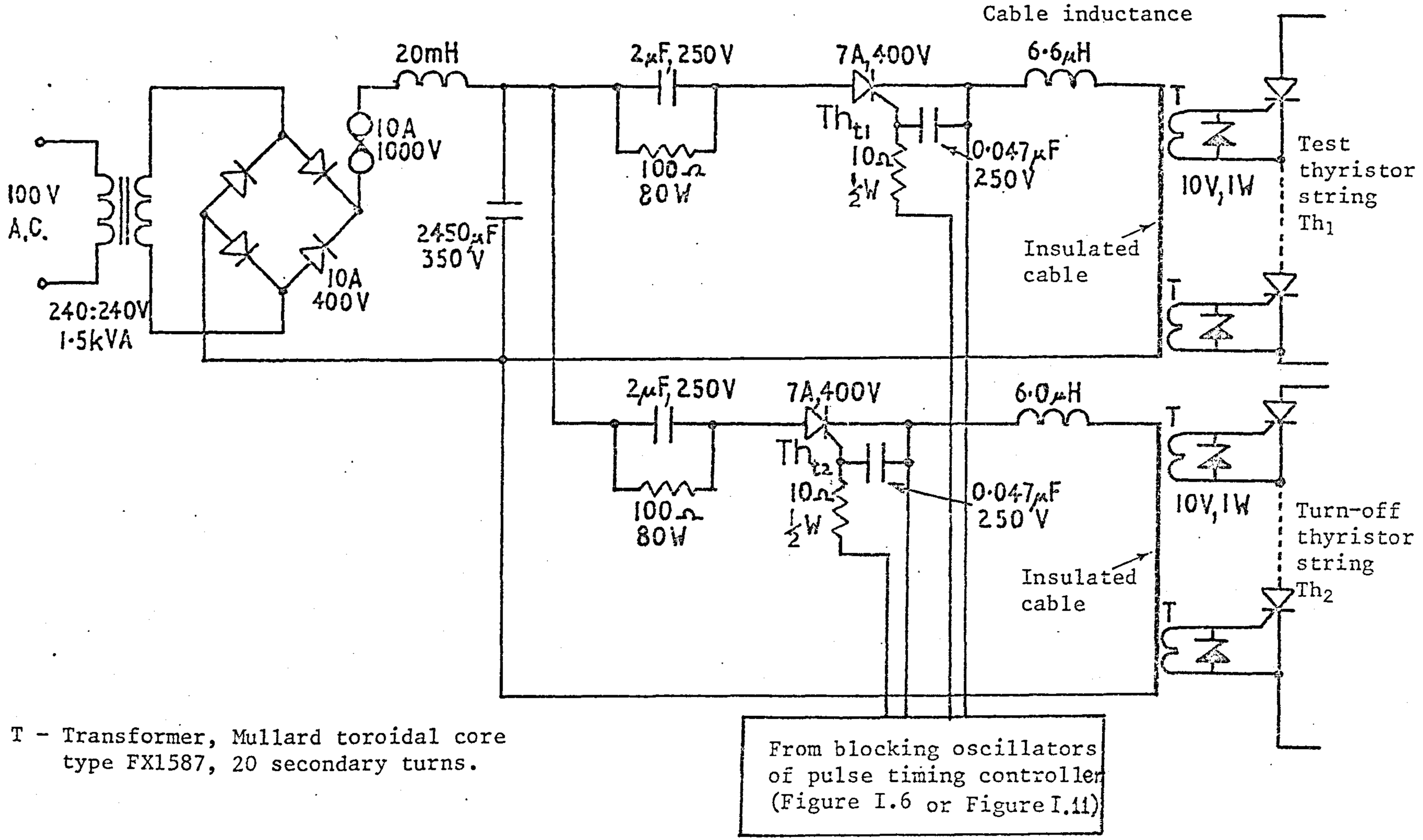

T – Transformer, Mullard toroidal core type FX1587, 20 secondary turns.

Figure I.7: Series thyristor firing circuit for the 5kV, 50Hz chopper and the 5kV, variable frequency d.c. chopper.

(3) The series thyristor gate current amplitudes vary with gate impedance; they are typically 2A peak, 10μs pulses with a .risetime of 1μs.

(4) The thyristor timing control circuit is situated remotely from the main equipment in the high voltage area, necessitating the use of two long gate supply leads of twin-core screened cable for Th_{t_1} and Th_{t_2}. Additionally, pick-up suppression capacitors are used across gate to cathode.

I.3 CIRCUITS FOR OVERALL COMPARISON OF THE VOLTAGE SHARING NETWORKS

(a) Power circuit and instrumentation for the 5kV, 50-2000Hz, d.c. chopper (Figure 7.10).

(1) The instruments shown below the chain dotted line are external to the high voltage area.

(2) The 95μll inductance in series with thyristor string Th_2 is included to limit di/dt to 40A/μs.

(3) The details of the devices in the thyristor and diode strings are given in Table I.2.

(4) Figure I.8 shows two views of the assembled equipment.

(b) Power supply circuits for the 5kV, 50-2000Hz, d.c. chopper (Figure I.9)

(1) The variable voltage alternator is rated for short-circuit testing at 3MVA for 3 seconds. It is driven by a 55h.p. induction motor with a flywheel and this limits continuous loading to approximately 40kW. Up to 60kW can be safely taken for 2-3

String devices	Manufacturer and type	Ratings	Range of measured T_{off} (μs)	Range of measured Q_r (μC)
Th_1 thyristors (15)	Westinghouse 34TB9 GHKO	35A, 900V $T_{off} \leq 20\mu s$ $dV/dt = 100V/\mu s$ $I^2t = 1470A_s^2s$	5.5 - 8.0	40 - 48
Th_2 thyristors (15)	ditto	ditto	ditto	32 - 40
D_2 diodes (15)	TAG MP 100	40A, 1000V	-	23 - 41
D_f diodes (29)	IR 25G100	25A, 1000V $I^2t - 3200A_s^2s$	-	54 - 105

Measurements made with: forward current = 20A, $\left|\frac{di}{dt}\right|_{off} = 40A/\mu s$, reverse voltage = 200V, temperature (stud) = 20°C.

For thyristor turn-off time: reverse voltage = 100V, forward blocking voltage = 100V.

Table I.2: Power semiconductor details for the 5kV, 50-2000Hz d.c. chopper, (Figures 7.1 and 7.10)

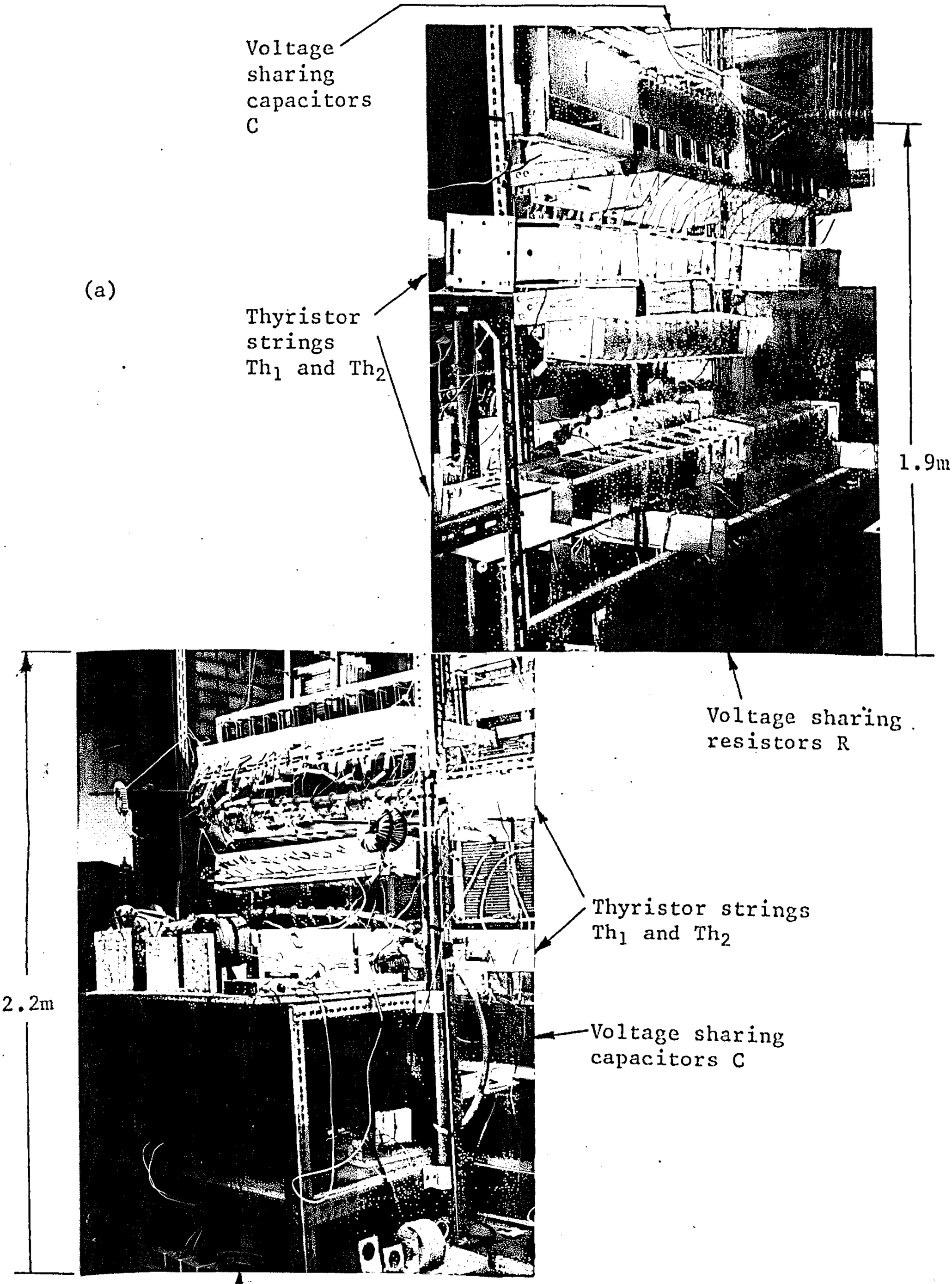

Figure I.8: Two views of the assembled 5kV, 50-2000 Hz, d.c. chopper.

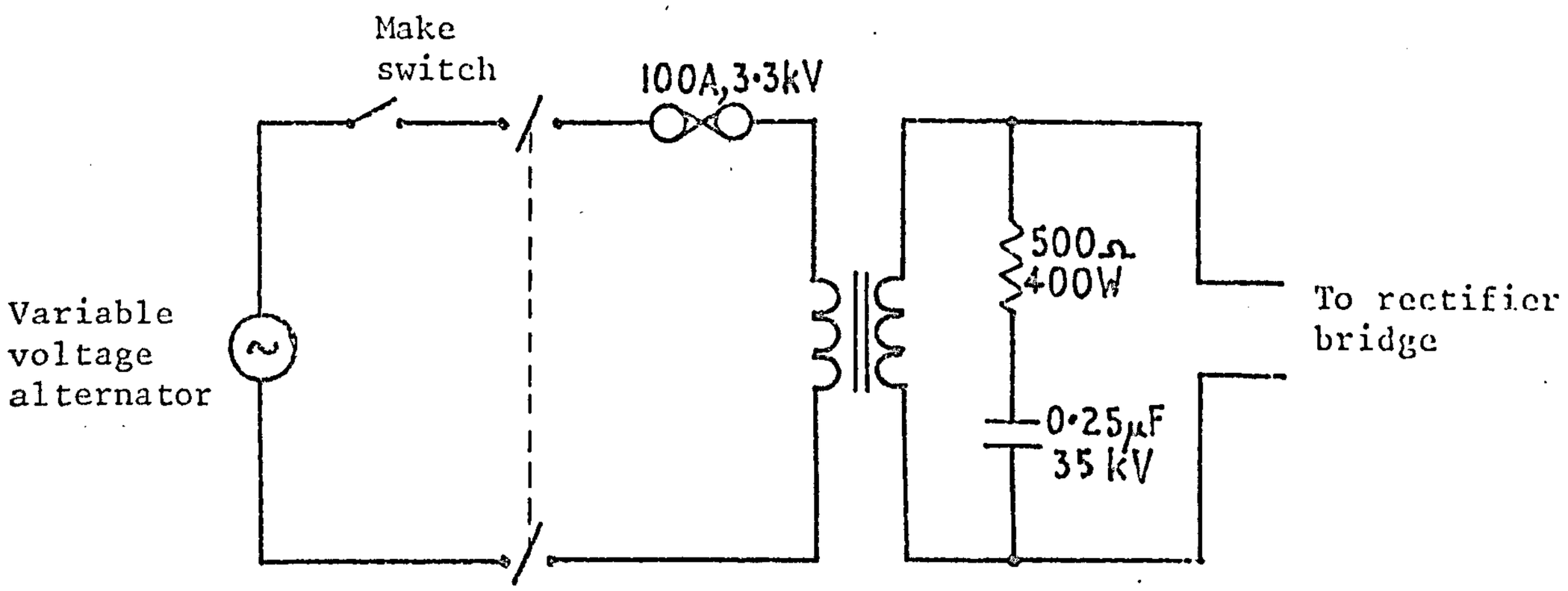

Diode strings - 25 diodes, IR type 25G100 (25A, 1000V, 3200 A^2s)

Figure I.9: Power supply arrangement for the 5kV, variable frequency, d.c. chopper.

(a) A.C. Supply

(b) Rectifier and filter.

minutes for chopper testing.

(2) The 0.25μF capacitor and 500 ohm resistor are connected across the transformer output for switching surge suppression.

(3) All fuses and all R-C voltage sharing components in the rectifier bridge have the ratings quoted.

(4) The 120kΩ resistor across the 167μF filter capacitor serves as a discharge resistor.

(5) Figure I.10 shows the assembled rectifier and filter.

(c) Controller for the 5kV, 50-2000Hz, d.c. chopper (Figure I.11).

(1) Switch S is included to allow chopper starting, as with the constant frequency chopper controller (Figure I.6).

(2) Each triggered blocking oscillator pulse amplifier is identical to that of Figure I.3 apart from modification of the transformer turns to $N_1 = 24$, $N_2 = 12$, $N_3 = 12$, to allow use of a 30V supply for reduction of transistor dissipation in view of the 2000Hz maximum frequency.

(3) Screened output leads are used to the series thyristor firing circuit (Figure I.7).

(4) The controller gives separate pulse outputs for Th_1 and Th_2 firing, of variable separation 24-424μs at 2200Hz.

(d) Variable frequency triangular waveform generator (Figure I.12).

(1) The triangular output voltage waveform is produced by the integrator OA. The 1MΩ potentiometer controls the rate of charging of the 0.011μF capacitor and therefore the output

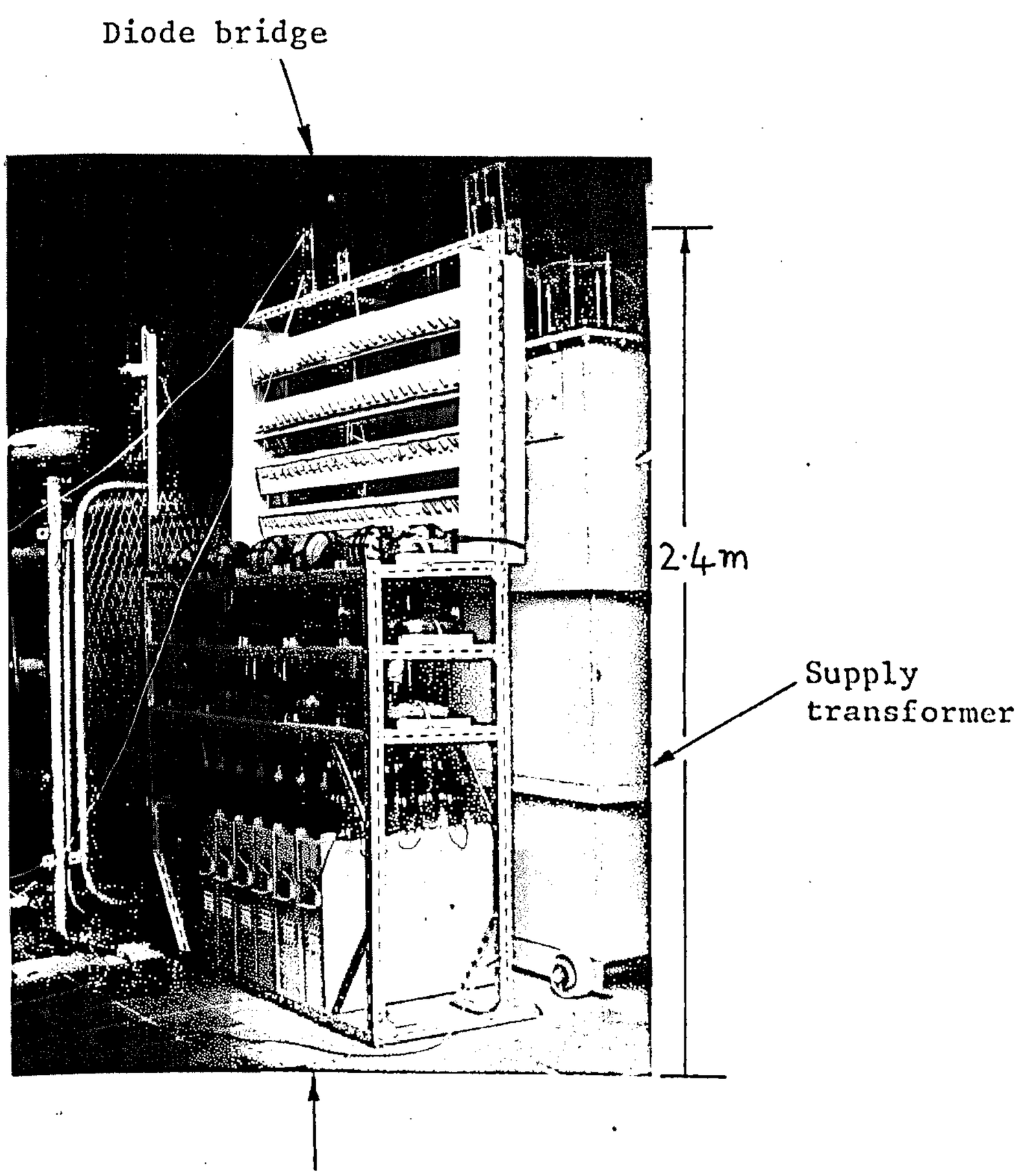

Figure I.10: Assembled 5kV d.c. supply rectifier and filter.

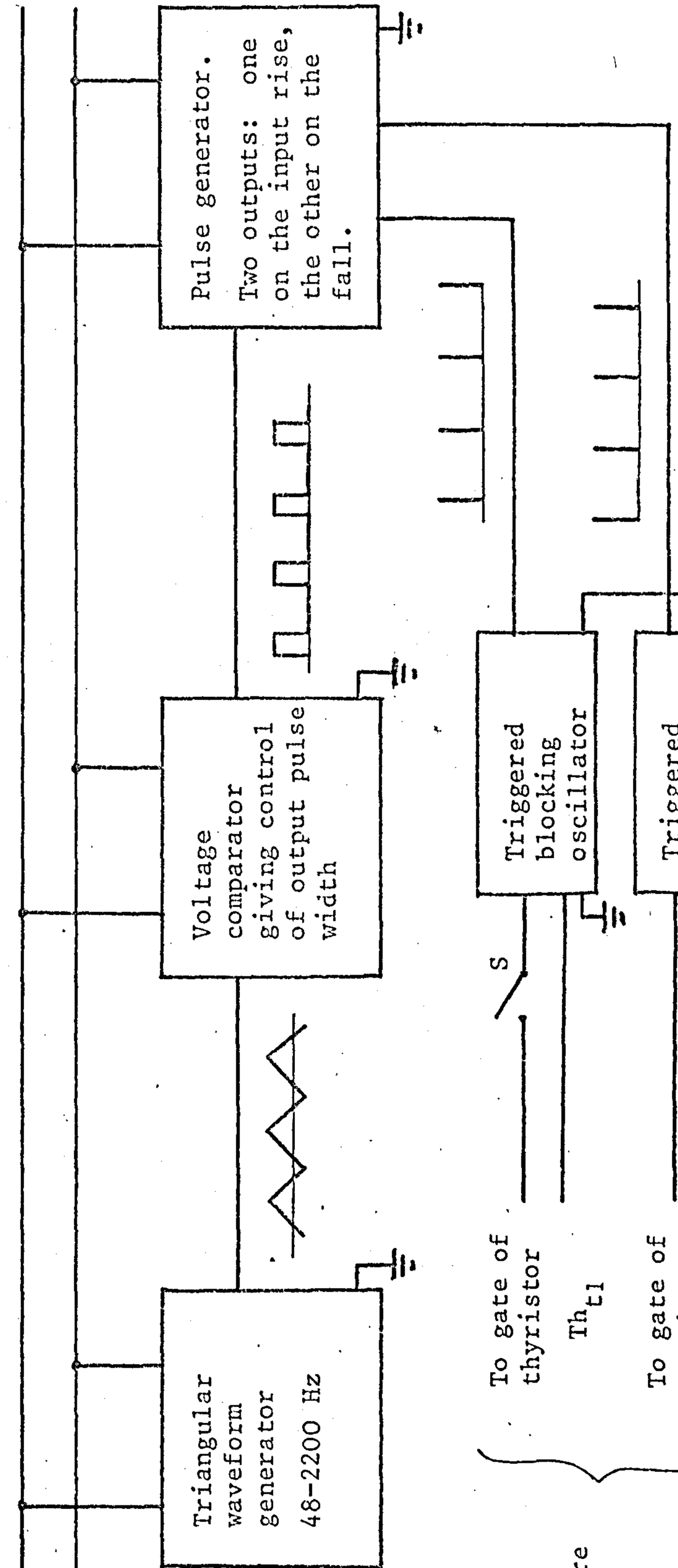

Figure I.7

Figure I.11: Block diagram of the controller for the 5kV, variable frequency, d.c. chopper.

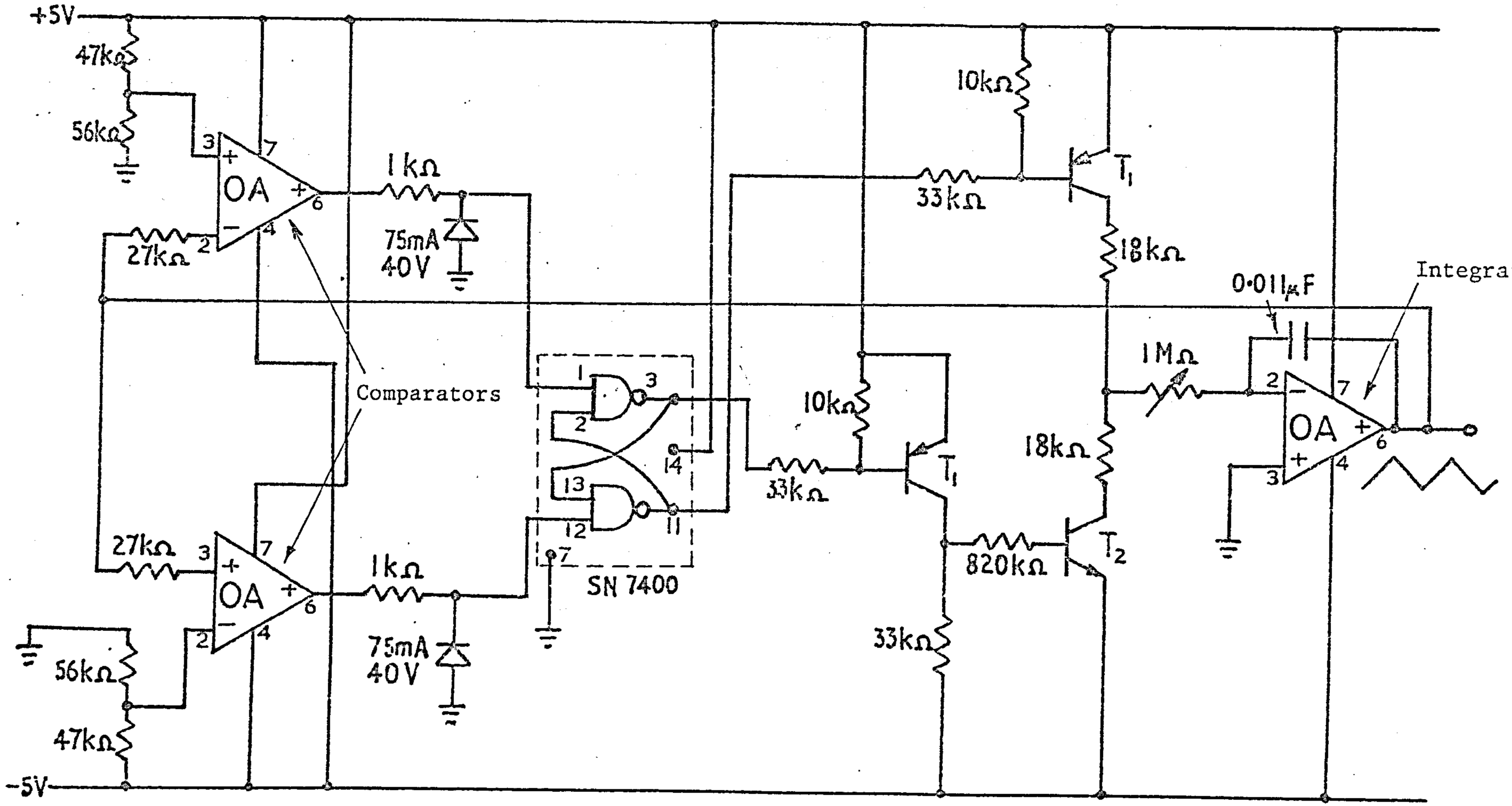

OA - Operational amplifier, Texas type SN741P. T_1 - Transistor, Ferranti type ZTX502

T_2 - " " " ZTX302

Figure I.12: Circuit of the variable frequency triangular waveform generator.

frequency.

(2) The ramp rising or falling output voltage is fed back to comparators OA each of which gives, in turn, a signal to the SN7400 NAND gates when the output reaches a set ±2.85V.

(3) A signal from either comparator reverses the state of the cross-coupled NAND gates which operate as a bistable. This switches off one ZTX502 transistor and switches on the other, thus reversing the polarity of the integrator input voltage, reversing the output voltage slope and establishing the peak value.

(e) Voltage comparator circuit (Figure I.13).

(1) The triangular input voltage is compared with a set voltage controlled by the 10kΩ potentiometer, giving a positive output voltage so long as the input is more negative than the set value.

(f) Pulse generator (Figure I.14).

(1) The first double NAND gate serves as a buffer and inverter.

(2) Each SN7400 quadruple NAND unit operates as follows. The initially uncharged 0.047μF capacitor charges through the 470Ω resistor when '1' input is applied to terminal 1; terminal 8 is maintained at '1' by the '0' on terminal 10, giving '0' at output terminal 11. When terminal 1 reverts to the '0' state, terminal 10 reverts to '1' and terminal 8 output switches to '0', giving an output pulse '1' at terminal

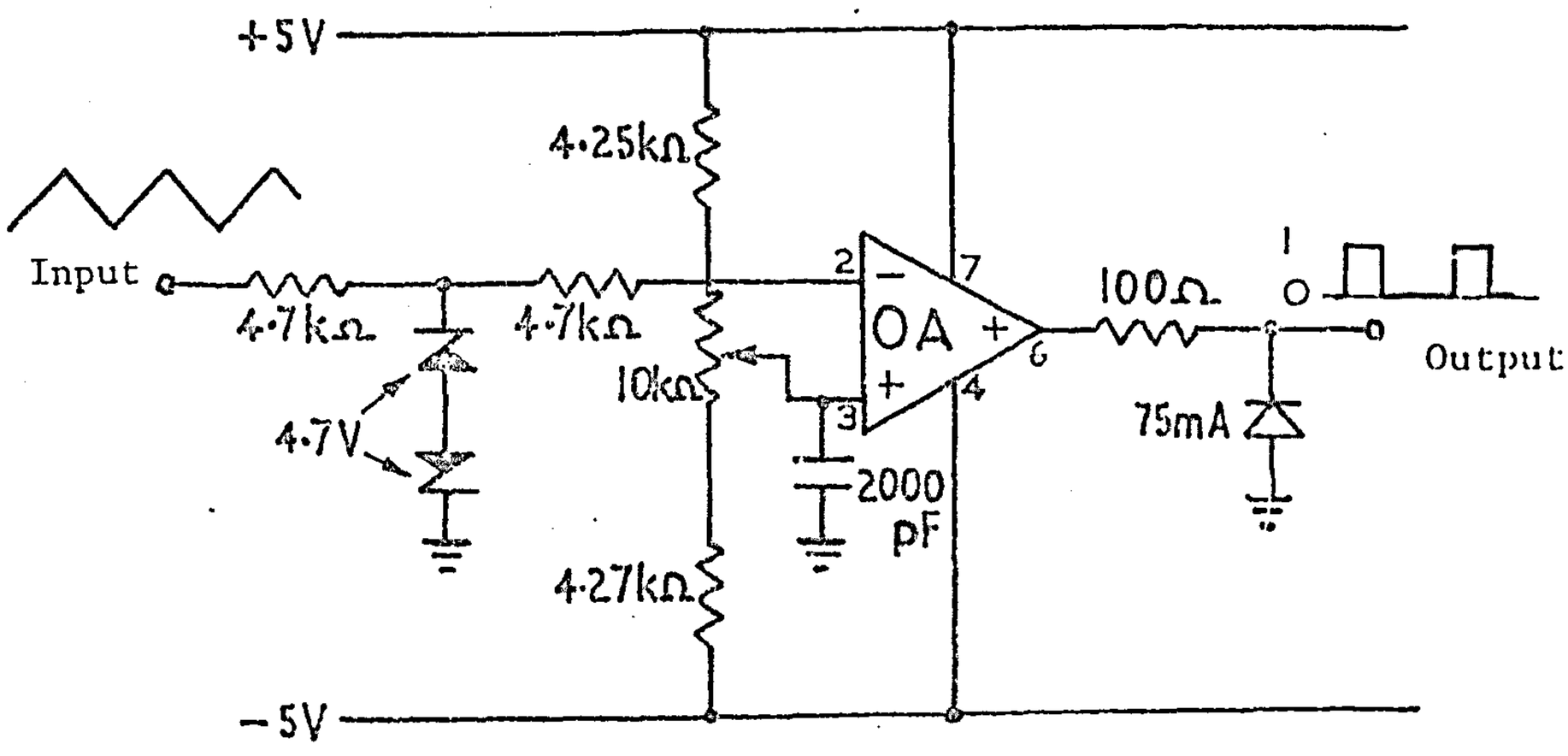

OA - Operational amplifier, Texas type SN741P

Figure I.13: Voltage comparator circuit

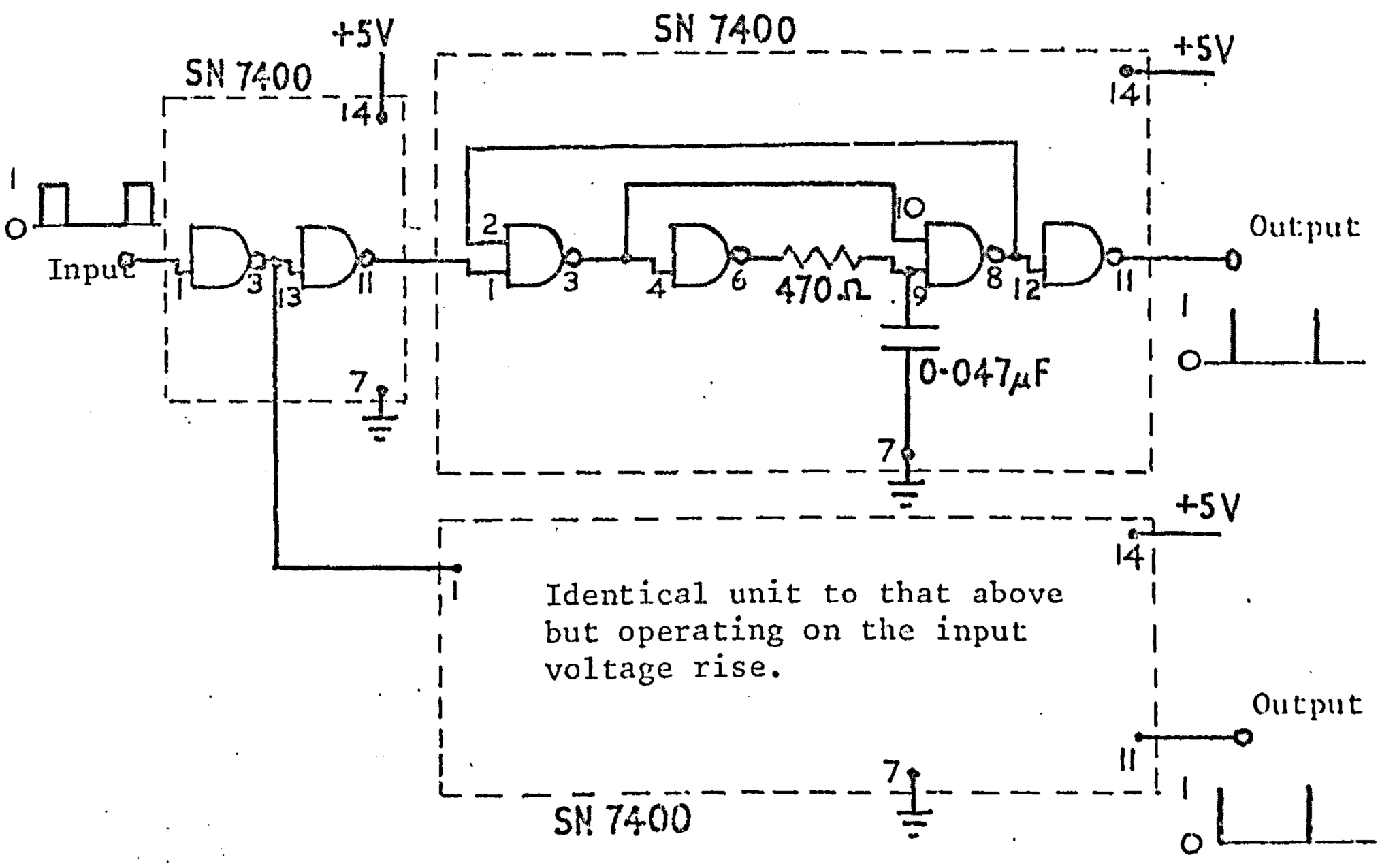

Figure I.14: Pulse generator circuit.

11 until the discharging 0.047μF capacitor potential (terminal 9) has fallen to '0' state. The feedback from 12 to 2 provides a constant output pulse width irrespective of any input judder.

(3) For the complete pulse generator, the upper quadruple unit gives a pulse on the fall of the input, and the lower unit on the input rise.

APPENDIX II

ANALYSIS OF THE CHOPPER CIRCUITS

II.1 INTRODUCTION

The idealised current and voltage waveforms for the two variations of the chopper circuit are given in Figures II.1 and II.2, and correspond with the appropriate oscillograms of Figures 3.4 and 7.3 respectively. The chopper circuits are repeated for convenience in their simplest form in Figure II.3. The two modes of operation, with and without voltage boost, will be analysed separately and any effects of subsidiary components, such as voltage sharing networks, will only be considered where they appreciably affect chopper performance.

II.2 CHOPPER OPERATING WITH VOLTAGE BOOST

II.2.1 Analysis

It is assumed that the supply voltage is constant at V_d, this being equal to the peak of the a.c. supply voltage (Figure 3.3).

(a) Th_2 is first gated to charge C_c.

Neglecting any oscillatory overshoot, C_c charges to a voltage V_d.

(b) Th_1 gated.

Two current components flow through Th_1:

(i) A current, supplied by the source, which rises exponentially

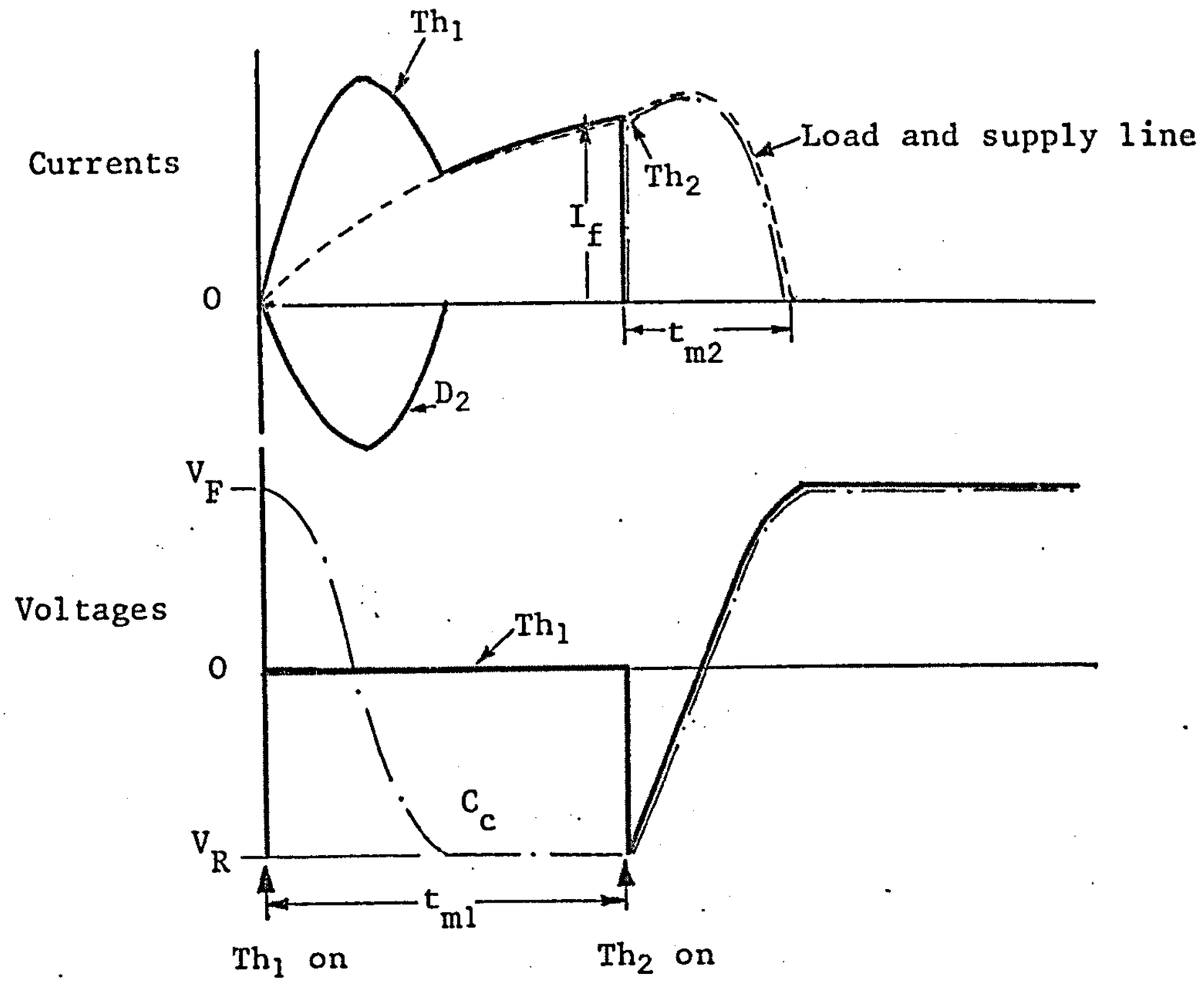

Figure II.1: Idealised current and voltage waveforms for the chopper operating with voltage boost.

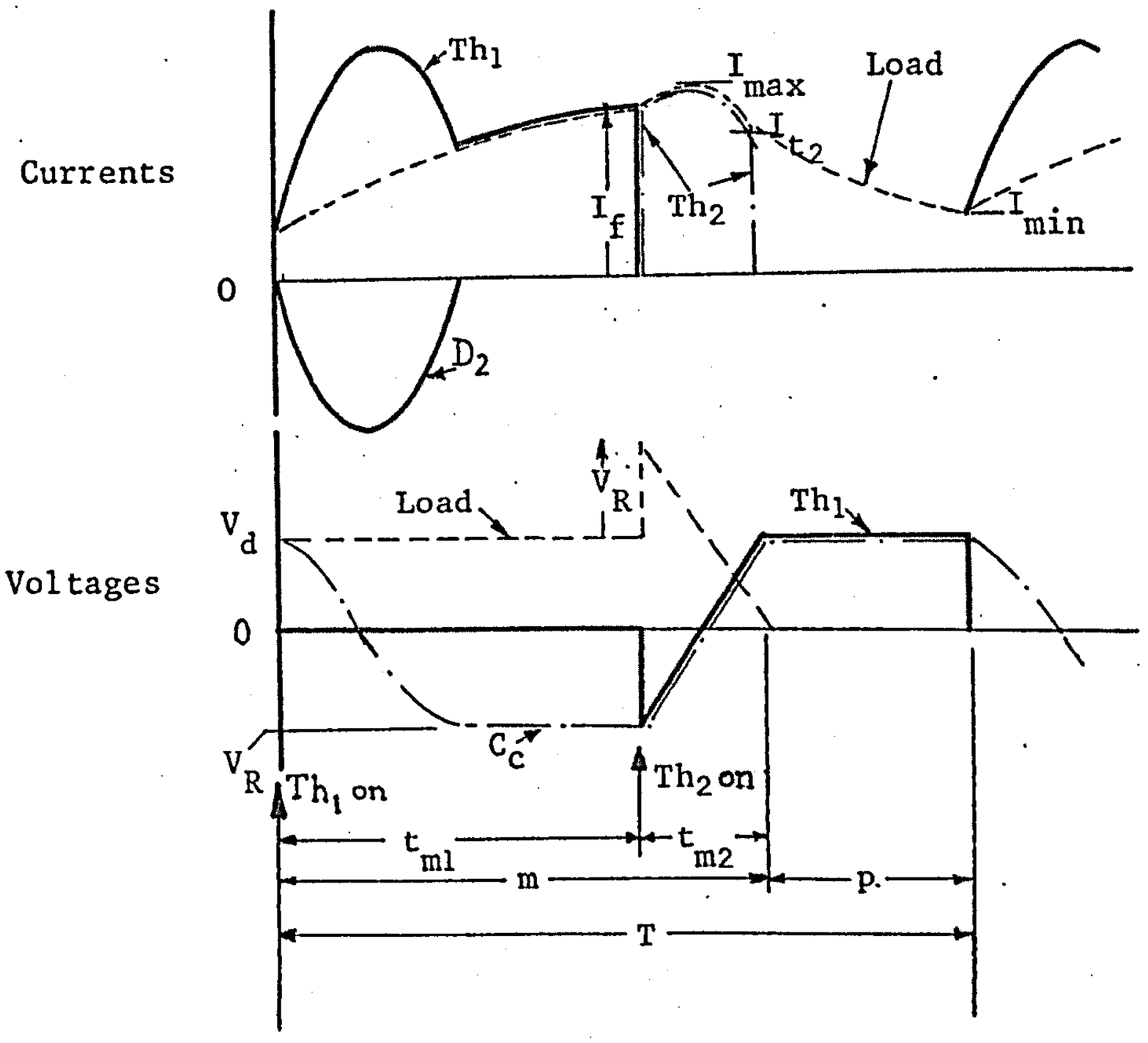

Figure II.2: Idealised current and voltage waveforms for the chopper operating without voltage boost.

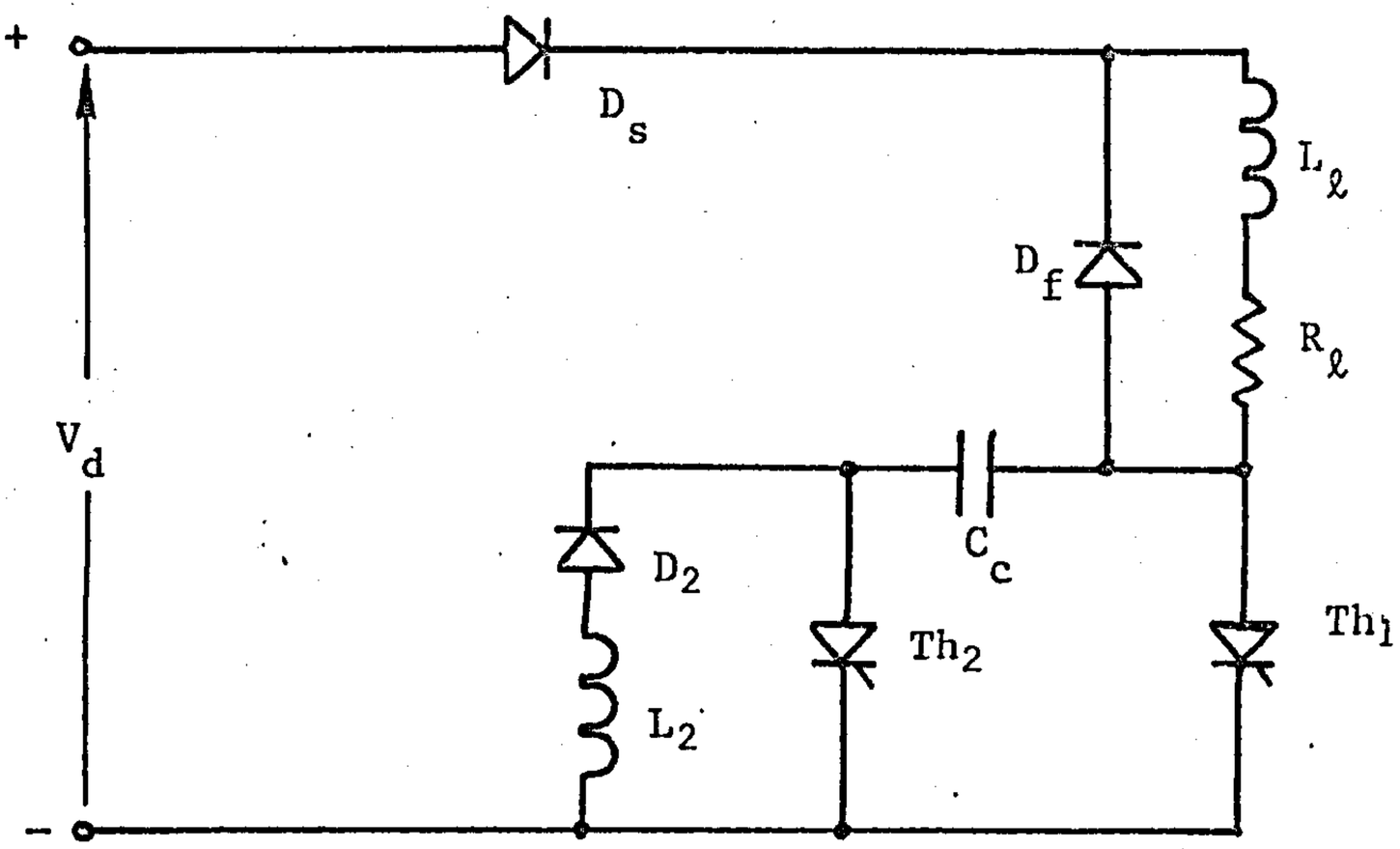

Figure II.3: Chopper circuit.
(a) With voltage boost, D_s connected, D_f absent
(b) Without " " , D_f " , D_s "

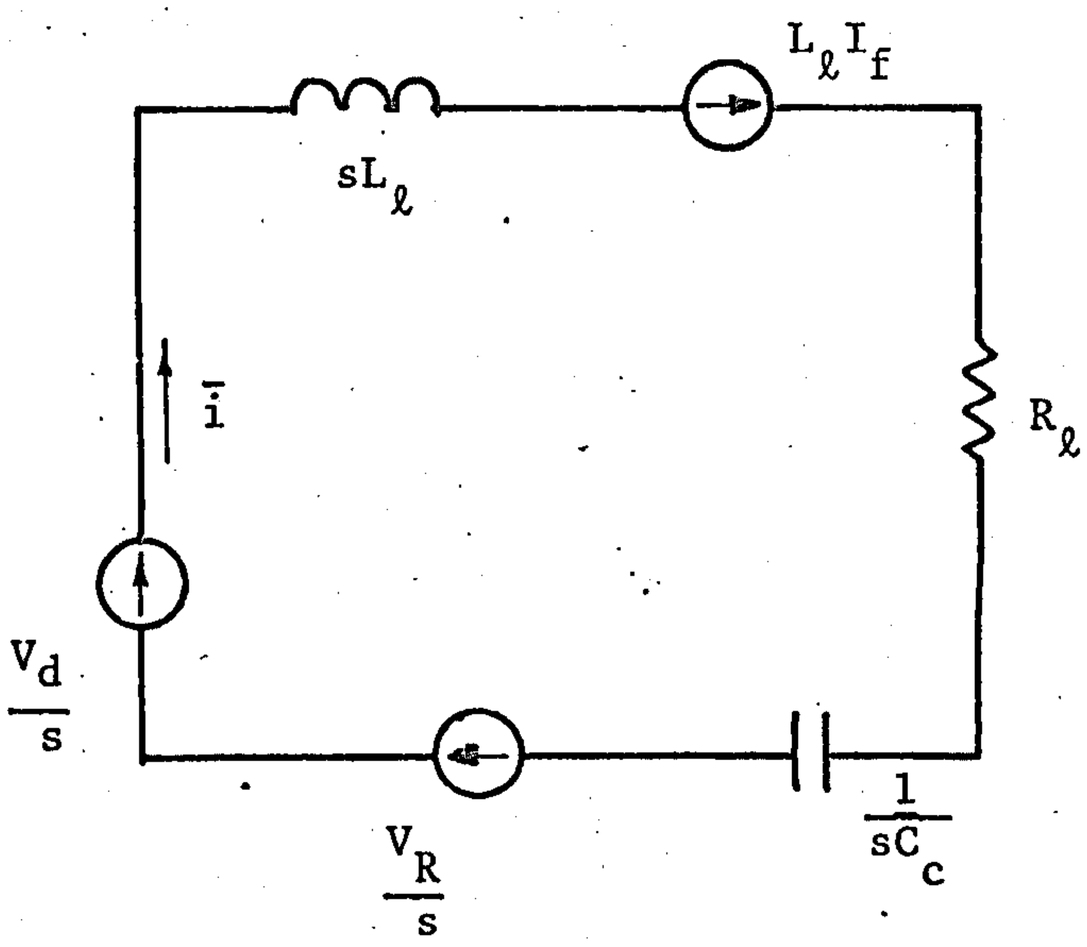

Figure II.4: Laplace operational circuit for thyristor Th_1 commutation.

from zero and is therefore given by

$$i = \frac{V_d}{R}\left(1 - e^{-R_\ell t/L_\ell}\right) \qquad \text{(II.1)}$$

If t_{m_1} is the duration of Th_1 conduction, when $t = t_{m_1}$, $i = I_f$ the chopped current value.

(ii) The commutating capacitor C_c charge reversal oscillation with current flow through L_2, D_2 and Th_1. This is a series oscillatory circuit with an initial voltage V_F across C_c. (For the first cycle, before voltage boost is effective, $V_F = V_d$). If R_2 is the effective resistance of inductor L_2, neglecting any other small resistance, the instantaneous oscillation current is given by

$$i = \frac{V_F}{\omega L_2} e^{-bt} \sin \omega t,$$

where $b = \frac{R_2}{2L_2} = \frac{\omega}{2Q_2}$

and $\omega^2 = \frac{1}{L_2 C_c} - b^2 = \frac{1}{L_2 C_c}\left(1 + \frac{1}{4Q_2^2}\right)$.

Q_2 is the coil Q-factor, $\omega L_2/R_2$.

The peak oscillatory current is given when $\omega t = \pi/2$.

Hence, peak oscillation current = $\frac{V_F}{\omega L_2} e^{-\pi/4Q_2}$.

C_c must charge the thyristor and diode shunt voltage sharing capacitors at appropriate points in the cycle (section 3.6.3). The first such instance applies when Th_1 turns on and the capacitors across Th_2 are charged. Then, more accurately,

$$\text{peak oscillation current} = \frac{V_F}{\omega L_2} e^{-\pi/4Q_2} \left(\frac{C_c}{C_c + C_{t_2}/n_{t_2}} \right). \quad \text{(II.2)}$$

The final capacitor voltage V_R available to commutate Th_1 is given by $\frac{1}{C}\int i\,dt$ for the oscillation current, with $\omega t = \pi$. Equation (7.3) makes full allowance for all the possible voltage drops with a free-wheeling diode D_f present. Adapting this equation to the boosted voltage situation and allowing for the presence of capacitors C gives

$$V_R = V_F\, e^{-\pi/2Q_2} \left(\frac{C_c}{C_c + C_{t_2}/n_{t_2}} \right) \left(\frac{C_c}{C_c + C_{d_2}/n_{d_2}} \right) \left(\frac{C_c}{C_c + C_{t_1}/n_{t_1}} \right) \quad \text{(II.3)}$$

(c) Th_2 gated to turn off Th_1.

From the Laplace operational circuit for Th_1 commutation (Figure II.4), the current $\bar{i}$ is given by

$$\bar{i} = \frac{(V_d + V_R)/L_\ell + sI_f}{s^2 + \frac{R_\ell}{L_\ell} s + \frac{1}{L_\ell C_c}} .$$

Letting $b_1 = \frac{R_\ell}{2L_\ell}$ and $\omega_1^2 = \frac{1}{L_\ell C_c} - b_1^2$, then

$$\bar{i} = \frac{V_d + V_R}{L_\ell} \left(\frac{1}{(s + b_1)^2 + \omega_1^2} \right) + I_f \frac{s}{(s + b_1)^2 + \omega_1^2} .$$

Manipulating this and taking the inverse transform gives the result

$$i = I_f e^{-b_1 t} \sqrt{1 + \left(\frac{V_d + V_R}{\omega_1 I_f L_\ell} - \frac{b_1}{\omega_1}\right)^2} \cdot \sin(\omega_1 t + \theta), \qquad \text{(II.4)}$$

where

$$\theta = \tan^{-1} \frac{1}{\left(\frac{V_d + V_R}{\omega_1 I_f L_\ell} - \frac{b_1}{\omega_1}\right)} .$$

The forward voltage across C_c and across Th_1 is given by

$$v_{cc} = \frac{1}{C_c} \int i \, dt$$

$$= \frac{I_f}{C_c} \sqrt{1 + \left(\frac{V_d + V_R}{\omega_1 I_f L_\ell} - \frac{b_1}{\omega_1}\right)^2} \int e^{-b_1 t} \sin(\omega_1 t + \theta)$$

$$= -\frac{I_f}{C_c} \sqrt{1 + \left(\frac{V_d + V_R}{\omega_1 I_f L_\ell} - \frac{b_1}{\omega_1}\right)^2} \frac{e^{-b_1 t}}{\sqrt{\omega_1^2 + b_1^2}} \cos(\omega_1 t + \theta - \gamma) + A,$$

where A is the constant of integration and $\gamma = \tan^{-1} \frac{b_1}{\omega_1}$.

When $t = 0$, $v_{cc} = - V_R$, giving A.

The complete expression for v_{cc} then becomes

$$v_{cc} = - V_R + I_f \sqrt{\frac{L_\ell}{C_c} \left\{1 + \left(\frac{V_d + V_R}{\omega_1 I_f L_\ell} - \frac{b_1}{\omega_1}\right)^2\right\}} \left[\cos(\theta - \alpha) - e^{-b_1 t} \cos(\omega_1 t + \theta - \gamma)\right] \qquad \text{(II.5)}$$

Line diode D_S blocks reverse current flow so that, from equation (II.4), charging of C_c ceases when $\omega_1 t + \theta = \pi$.

The final forward voltage V_F across Th_1 is then given by

$$V_F = -V_R + I_f \sqrt{\frac{L_\ell}{C_c}\left\{1 + \left(\frac{V_d + V_R}{\omega_1 I_f L_\ell} - \frac{b_1}{\omega_1}\right)^2\right\}} \times$$

$$\left[\cos(\theta - \gamma) - e^{-(b_1/\omega_1)(\pi-\theta)} \cdot \cos(\pi - \gamma)\right] . \qquad \text{(II.6)}$$

Also of particular importance is the Th_1 reverse bias time which is given by putting $v_{cc} = 0$ in equation (II.5) and solving for t. Since L_ℓ maintains the load current fairly constant at value I_f during this interval, and therefore the dV/dt of the capacitor voltage rise is similarly constant, this reverse bias time is approximately given (from i = CdV/dt) by

$$t_{rev} = \frac{C_c V_R}{I_f} \qquad \text{(II.7)}$$

Equation (II.6) shows that forward voltage V_F increases as current I_f increases and therefore as load resistance R_ℓ is reduced.

II.2.2 Experimental verification

Listing the relevant data from Figure I.5, and using values measured from the oscillogram of Figure 3.4:

$C_c = 0.4\mu F$, $L_2 = 16.8mH$, $Q_2 = 6.3$, $L_\ell = 8.8mH$, $R_\ell = 56\Omega$.

The thyristor and diode voltage sharing capacitors are:

For Th_1, $n_{t_1} = 20$, $C_{t_1} = 0.1\mu F$.

For Th_2, $n_{t_2} = 9$, $C_{t_2} = 0.5\mu F$.

For D_2, $n_{d_2} = 10$, $C_{d_2} = 0.5\mu F$.

$V_d = 1485V$, $t_{m_1} = 560\mu s$.

Table II.1 gives the measured and calculated results.

II.3 CHOPPER OPERATING WITHOUT VOLTAGE BOOST

II.3.1 Analysis

If the load current flow is discontinuous, the analysis is initially identical to that in the previous section except that V_d should be substituted for V_F, since D_f now limits capacitor C_c voltage to this value. This happens when v_{cc} of equation (II.5) reaches the value V_d, at which time D_f takes over load current conduction from Th_2. The current then decays exponentially to zero with time constant L_ℓ/R_ℓ. The interval t_{m_2} for which Th_2 conducts can therefore be obtained from

$$V_d = -V_R + I_f\sqrt{\frac{L_\ell}{C_c}\left\{1 + \left(\frac{V_d+V_R}{\omega_1 I_f L_\ell} - \frac{b_1}{\omega_1}\right)^2\right\}}\left[\cos(\theta - \alpha) - e^{-b_1 t_{m_2}}\cos(\omega_1 t_{m_2} + \theta - \gamma)\right] \qquad (II.8)$$

The value of the current (I_{t_2}) transferred from Th_2 to D_f is given by putting $t = t_{m_2}$ in equation (II.4). Peak load (and thyristor Th_2) current (I_{max}) is given, by equation (II.4), when $t = (\frac{\pi}{2} - \theta)/\omega_1$.

If the chopping mark-period ratio and frequency are such that the load conduction is continuous, the minimum value (I_{min}) to which the current decays during the off period p before Th_1 is next gated is given by

Quantity	Measured value	Calculated value	Remarks on calculated value
I_f	26A	25.7A	From equation (II.1) with $t = t_{m_1}$
Oscill. peak current	–	20A	From equation (II.2)
Exponential current rise	–	14.9A	From equation (II.1) with $t = \frac{\pi}{2\omega}$
Th_1 peak current	36A	34.9A	Sum of two previous results
V_R	3000V	3000V	From equation (II.3)
V_F	5000V	4870V	From equation (II.6)
t_{rev}	40µs	39.7µs	From equation (II.5) with $v_{cc} = 0$
t_{rev}	40µs	46.7µs	From equation (II.7)

Table II.1: Comparison of measured and calculated chopper operation with voltage boost.

$$I_{min} = I_{t_2} e^{-R_\ell p/L_\ell} \quad . \tag{II.9}$$

Th_1 then takes over this current so that equation (II.1) must be replaced by

$$I_f = \frac{V_d}{R}\left(1 - e^{-R_\ell t_{m_1}/L_\ell}\right) + I_{min}\, e^{-R_\ell t_{m_1}/L_\ell} \tag{II.10}$$

This equation is a suitably adapted statement of equation (V.4) derived in Appendix V.

Equations (II.6) and (II.7) are applicable for the calculation of Th_1 reverse bias time. By similarly assuming load current constant at I_f during t_{m_2}, an approximate expression for t_{m_2} is obtained, that is,

$$t_{m_2} = \frac{(V_d + V_R)C}{I_f} \tag{II.11}$$

II.3.2 Experimental verification

The required circuit component values are given in Figure 7.10 and the voltage sharing capacitor values in Table 7.1. Using the operating conditions relating to the oscillograms of Figure 7.3, the settings are

$f = 2015Hz$, $T = 496\mu s$, $t_{m_1} = 220\mu s$, $m = 410\mu s$, $p = 90\mu s$, $k = 0.827$, $V_d = 4900V$.

Table II.2 gives the measured and calculated results.

Quantity	Measured value	Calculated value	Remarks on calculated value
I_f	13.0A	12.9A	Equation (II.10)
I_{min}	12.0A	11.8A	Equation (II.4) with $t = t_{m_2}$ and and equation (II.9)
I_{max}	14.0A	13.8A	Equation (II.4) with $t = (\frac{\pi}{2} - \theta)/\omega_1$
V_R	4400V	4600V	Equation (II.3) with adjustment for sharing capacitors across D_f
Mean V_ℓ	3950V	3900V	From output voltage waveform area
Mean I_ℓ	12.4A	12.4A	Mean V_ℓ/R_ℓ
Mean I_ℓ	12.4A	12.8A	$(I_{max} + I_{min})/2$
t_{m_2}	190µs	181µs	Equation (II.8)
t_{m_2}	190µs	192µs	Equation (II.11)
t_{rev}	90µs	93µs	Equation (II.5) with $v_{cc} = 0$
t_{rev}	90µs	93µs	Equation (II.7)

Table II.2: Comparison of measured and calculated chopper operation without voltage boost.

APPENDIX III

DESIGN EXAMPLES FOR THE VOLTAGE SHARING NETWORKS

III.1 SERIES SATURATING REACTOR WITH SHUNT R-C COMPONENTS (Figure 3.6(a))

The saturating reactor must hold off reverse voltage from the thyristors for a period of 3 to 4 × τ_p for the slowest turn-off thyristor. The data relating to this example is given in Figures 4.3 and 4.4, and in Table 4.1, row (a). Hence SR must withstand reverse voltage for 4 × 3.66 = 15μs.

Using the peak reverse line voltage V_{RO} = 2700, and gradient α = 60V/μs for the idealised waveforms of Figure 4.2(b),

$$\text{required volt-second rating} = \frac{15}{2}\left[2700 + (2700 - 60 \times 15)\right] \times 10^{-6}$$

$$= 33.7 \times 10^{-3} \text{ Vs.}$$

Choosing a Telcon Metals HCR core of 0.0005" tape, size 9b, the relevant data is:[35]

flux density change required to saturate core (Figure 4.3) = 2.5 tesla,

net iron cross section A = 0.91×10^{-4} m^2 .

Therefore,

$$\text{required number of turns } N = \frac{33.7 \times 10^{-3}}{0.91 \times 2.5 \times 10^{-4}}$$

$$= 130 \text{ say.}$$

The anticipated voltage sharing performance must now be checked as in section 4.5. The figures quoted there relate to this example,

and a maximum thyristor voltage difference of 16V results.

Reverse voltage V_R when SR saturates = $2700 - 60 \times 15$

= 1800V.

Average thyristor voltage $\frac{V_R}{n} = \frac{1800}{20}$

= 90V.

$\therefore$ Extreme thyristor reverse voltages = $90 \pm 8V$

= 82V and 98V.

The maximum forward line voltage V_F is 5100V.

Therefore, using equation (3.9),

maximum thyristor forward voltage = $\frac{1}{20}(1800 + 5100) - 82$

= 263V.

III.2 SHUNT TRANSFORMER(S) AND R-C COMPONENTS

III.2.1 Multi-winding transformer with secondary capacitor and diode control

The circuit and component details are given in Figure 5.1(a) and Table 5.1, row (a) respectively. The oscillogram of Figure 5.3(b) gives

supply voltage reverse volt-second integral = $\frac{1}{2} \times 3000 \times \frac{50}{10^6}$

= 75×10^{-3} Vs.

For transformer core Mullard Ferroxcube toroid FX1076, saturation and retentivity flux densities are

$B_s = 0.38T$ and $B_r = 0.15T$; area $= 2.38 \times 10^{-4} m^2$.

$$\therefore \text{Total required pri. turns, } n N_1 = \frac{75 \times 10^{-3}}{2.38 \times 10^{-4}(0.38 - 0.15)}$$

$$= 1375.$$

Allow 1600 turns so that for 20 thyristors, 20 primary sections are required with 80 turns each. Volts/turn < 2.

$$\text{Peak applied voltage/pri. section} = \frac{3000}{20}$$

$$= 150V.$$

Neglecting linear fall of reverse voltage and damping,

$$\text{peak voltage across } C_2 = 2 \times 150 \times \left(\frac{N_2}{N_1}\right).$$

Assume therefore $N_1/N_2 = 1$, with 80 secondary turns, giving a peak voltage across C_2 and D_2 of less than 300V.

From equation (5.4), the minimum possible value of C_2, using the appropriate thyristor Q_r values (Table I.1), is

$$C_2 = 20\left(\frac{20 - 1}{2}\right)\left(\frac{26.9 - 6.7}{3000}\right)$$

$$= 1.3\mu F.$$

Adopt 2μF for C_2. Prediction of total transformer leakage inductance L_{t_2} is difficult. The measured value of 11.8μH gives, using equation (5.1),

$$T_{C_2} = \pi\sqrt{\frac{11.8 \times 2}{10^{12}}}$$

$$= 15.3\mu s.$$

The reverse recovery time of the slowest thyristor is 4μs, so this value of T_{C_2} is satisfactory.

Allowing for the linearly falling negative voltage by using equations IV.1 and IV.2 of Appendix IV gives a capacitor current I_{2pk} of 56.1A, which compares well with Figure 5.3(g).

For 50Hz operating frequency, C_2 must be virtually discharged in < 20ms. R = 2kΩ is suitable, with power rating ($\frac{1}{2} C_2V^2f = \frac{1}{2} \times \frac{2}{10^6} \times 300^2 \times 50$), giving 4.5W, say 5W.

Diode, Texas type 1S425 (10A, 600V, 50A repetitive peak current) is satisfactory for D_2,

The current rating of diodes D must be based on the charge flow through that across the fastest recovery thyristor which carries charge $\Delta Q_{r_{max}}$, plus additional charge reflected from the secondary during the current oscillation, at each commutation. The voltage rating of D should at least equal that of the thyristor in parallel.

III.2.2 Multiple transformers with secondary capacitor and diode control

The network and component details are given in Figure 5.1(b) and Table 5.1, row (d). The procedure is identical to that with the multi-winding transformer except in the choice of cores and volt-second withstand.

Required volt-second per transformer $= \frac{75}{20} \times 10^{-3}$

$= 3.75 \times 10^{-3}$ Vs.

For Mullard core FX 1239, E - core ferrite, $B_S = 0.38T$, $B_r = 0.15T$, area = 0.771×10^{-4} m^2,

required primary turns per transformer $= \dfrac{3.75 \times 10^{-3}}{(0.38 - 0.15) \times 0.771 \times 10^{-4}}$

$= 210.$

Assumed secondary turns $= 210.$

Measured leakage inductance per transformer (average) $= 350\mu H.$

Leakage inductance of 20 in parallel (referred to the secondary side) $= 17.5\mu H.$

Again, using 2μF for C_2 gives calculated T_{C_2} = 18.6μs (17μs measured), I_{2pk} = 50.7A (48.0A measured).

III.3 SHUNT VOLTAGE REGULATING DIODES (Figure 3.6(d))

III.3.1 Steady-state forward voltage sharing duty

Consider the voltage sharing components quoted in row (b) of Table 6.1, where $V_{zr} = V_{zf}$ = 300V (total), and to which the oscillograms of Figure 6.3 relate.

Manufacturer's quoted thyristor half-cycle leakage current $= 4.0mA.$

Peak leakage current $= \dfrac{\pi}{2} \times 4.0$

$= 6.3mA.$

Estimated thyristor leakage resistance R_{th} $= \dfrac{\text{voltage rating}}{6.3 \times 10^{-3}}$

$= \dfrac{400}{6.3}\ k\Omega$

$= 63.5k\Omega.$

Regulating diodes considered for Z_f (and Z_r) are two in series, Texas types 1S3200A (200V ± 5%, 1W, R_z = 1400Ω at 2mA) and 1S3100A (100V ± 5%, 1W, R_z = 600Ω at 2mA).

Using equation (6.5), for the 200V regulating diode,

$$\text{power dissipation} = \left(\frac{5000 - 200}{19 \times 63.5 \times 10^3}\right)^2 1400 + \left(\frac{5000 - 200}{19 \times 63.5 \times 10^3}\right) 200$$

$$= 0.80\text{W}.$$

At 50Hz, (waveform Figure 3.4(b)), this is effective for (20,1000 - 550 - 133)μs forward blocking time of total period 20,000μs.

$$\text{mean dissipation} = 0.80 \times \frac{19320}{20000}$$

$$= 0.77\text{W}.$$

III.3.2 Transient forward voltage sharing duty

A parallel plate approximation to the physical arrangement yields C_g = 1.87pF (Figure 6.1) at the high voltage end of the string. C_g is assumed to be constant at this value. The number of regulating diodes Z_f which operate is 5000/300 = 16 (= n in equation 6.6). For Z_f (V_{zf} = 300V, f = 50Hz),

$$\text{mean power dissipation} = 1.15 \times 300^2 \times \frac{1.87}{10^{12}} \times 16 \times \frac{15}{2} \times 50$$

$$= 1.16\text{mW}.$$

For the 200V regulating diode, (Figure III.1(b)), the mean power dissipation is $\frac{2}{3} \times 1.16 = 0.78$mW.

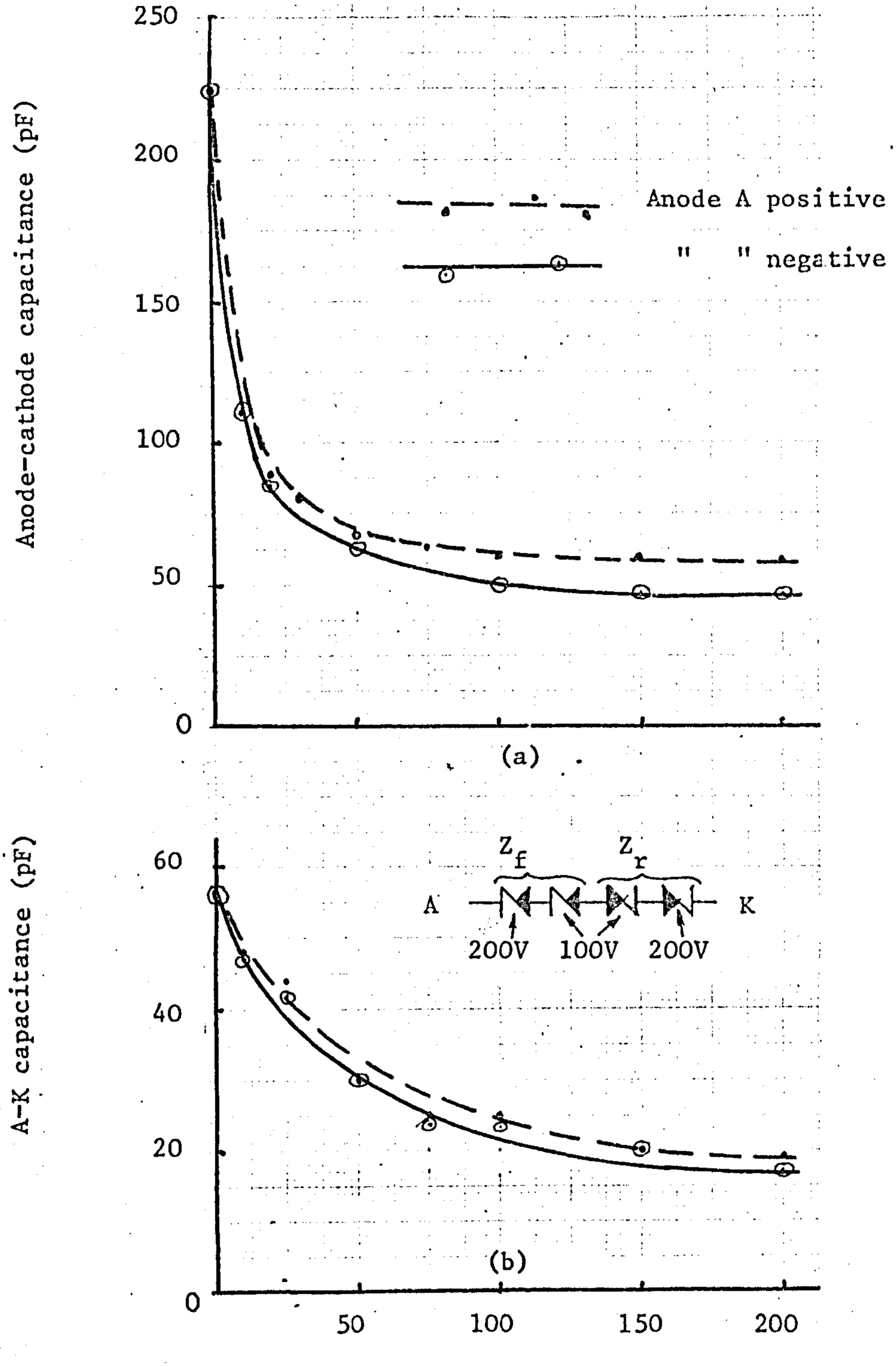

Figure III.1: Measured device capacitance variation with applied voltage

(a) Thyristor, GE type C36D, No. 8 in Table I.1

(b) Series back-to-back regulating diodes (section III.3.1)

Using the measured device capacitances (Figure III.1), the capacitance C_d of the thyristor and regulating diodes in parallel at a high blocking voltage is 60pF (= 17pF + 43pF). Hence C_g/C_d = 1.87/60 = 0.03. For this ratio, Figure 6.2 gives, for n = 16,

$$\frac{\text{maximum thyristor dV/dt}}{\text{total applied dV/dt}} = 0.165 \qquad (= C_x/C_d).$$

Hence, capacitance $C_x = 0.165 \times 60 = 10\text{pF}$

The capacitance from point Y to earth (Figure 6.4(b)) differs little from C_x. Therefore the regulating diode current I_{zf}, with a total applied dV/dt = 60V/μs, is

$$I_{zf} = C_x \frac{dV}{dt} = \frac{10}{10^{12}} \times 60 \times 10^6 = 600\mu\text{A}.$$

The dynamic resistance can be neglected at this low current, therefore using equation (6.7),

$$\text{peak power dissipation} = \frac{200 \times 600}{10^6} = 0.12\text{W}.$$

Using dV/dt figures across this thyristor and across the complete string gives a duration of 73μs for this pulse width.

III.3.3 Forward voltage sharing duty at thyristor turn-on

For the 50Hz test chopper, (Figure I.5), V_F = 5000V, the effective L = L_2 (= 16.8mH). Typical quoted thyristor turn-on time for Th_1 is 2.5μs. Assume one slow turn-on thyristor has a delay Δt_{on} of 1.5μs.

Equation (6.8) gives

$$I_{zfpk} = \frac{(5000 - 1.15 \times 300) \times 1.5 \times 10^{-6}}{16.8 \times 10^{-3}}$$

$$= 0.42A.$$

For the nominal 200V regulating diode,

$$\text{peak pulse power} = 1.15 \times 200 \times 0.42$$

$$= 96W.$$

Applying equation (6.10) for f = 50Hz,

$$\text{mean power dissipation} = 0.58 \times 200 \times 0.42 \times \frac{1.5}{10^6} \times 50,$$

$$= 3.6mW.$$

III.3.4 Reverse voltage sharing duty at thyristor turn-off

Applying the method of section 6.5.5 for a nominal reverse voltage V_R = 3000V, the anticipated number of reverse regulating diodes to operate x = 3000/300 = 10 (10 measured). From Table I.1 ΔQ_{rx-1} = (14.8 - 7.3) = 7.5μC.

Applying equation (6.11) for f = 50Hz, L = 66μH, I_{rpx} = 20A,

$$\text{total mean turn-off dissipation in } Z_r = \left(1.15 \times 200 \times \frac{7.5}{10^6} + \frac{1}{2} \times \frac{66}{10^6} \times \frac{20^2}{10}\right)50$$

$$= 152mW.$$

Equation (6.12) gives, allowing 4μs for reverse recovery time difference Δt_{rx-1} and a sinusoidal pulse,

$$\text{peak pulse power} = \frac{\pi}{2 \times 4} \times 10^6 \left(1.15 \times 200 \times \frac{7.5}{10^6} + \frac{1}{2} \times \frac{66}{10^6} \times \frac{20^2}{10}\right)$$

$$= 1200W.$$

III.3.5 Total regulating diode dissipation and temperature rise

(a) Forward voltage regulating diode Z_f.

For 50Hz operation, the total mean dissipation is the sum of that calculated in sections III.3.1, III.3.2, and III.3.3.

$$\text{Total mean dissipation} = 0.77 + 0.00078 + 0.0036$$
$$= 0.774\text{W}.$$

On this basis, the 1W diode chosen is satisfactory.

Figure III.2 shows the duty cycle and from this, the equivalent single rectangular pulse width t_p can be calculated.

$$96t_p = 0.12 \times 73 + 0.8 \times 19{,}317 + 96 \times 0.75$$
$$t_p = 162\mu\text{s}.$$

Since $t_p \ll T$, using equation (6.4) with $T = 20{,}000\mu\text{s}$, and (from the manufacturer's data) $\theta = 125\ ^\circ\text{C/W}$, $\theta_{(t_p)} = 0.5^\circ\text{C/W}$, gives

$$\theta_1 = 125 \times \frac{162}{20000} + 0.5$$
$$= 1.51\ ^\circ\text{C/W}.$$

Equation (6.2) gives

$$T_J - T_A = 96 \times 1.51$$
$$= 145^\circ\text{C}.$$

This exceeds the allowable 125°C rise. Owing to the almost continuous 0.8W duty, this equivalent pulse approach gives a very high result. Since the 96W pulse is very short, it can

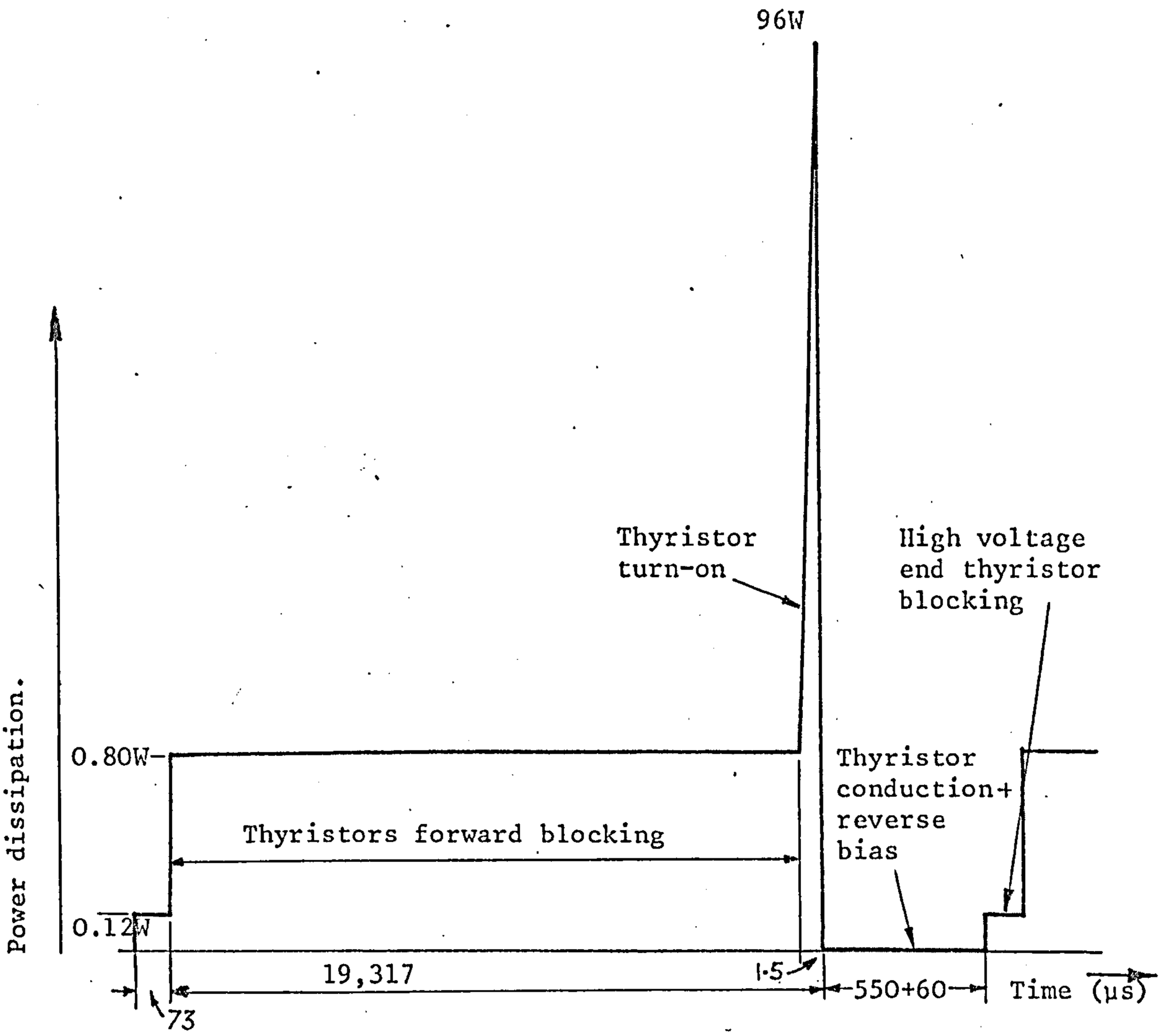

Figure III.2: Duty cycle of the 200V forward voltage regulating diode Z_f across a thyristor in string Th_1 under worst conditions.

(Section III.3.5).

be assumed that the temperature drops to equilibrium between these pulses. Superposition then gives

$$T_J - T_A = 0.8 \times \theta + 96 \times \theta_{(tp)},$$

where the actual pulse width t_p is 1.5μs.

Now for 100μs pulse width, quoted $\theta_{(t_p)} = 0.278^{\circ}C/W.$

Using the approach described in section 6.5.1,

$$\theta_{(t_p)} = 0.278\sqrt{\frac{1.5}{100}}$$

$$= 0.034^{\circ}C/W.$$

Then,

$$T_J - T_A = 0.8 \times 125 + 96 \times 0.034$$

$$= 103^{\circ}C.$$

This is satisfactory.

(b) Reverse voltage regulating diode, Z_r.

Section III.3.4 gives the mean dissipation as 0.152W with a sinusoidal pulse power peak of 1200W. The equivalent rectangular pulse duration is $2 \times 4/\pi = 2.54\mu s$.

$$\theta_{(t_p)} = 0.278\sqrt{\frac{2.54}{100}}$$

$$= 0.044^{\circ}C/W.$$

Equation (6.4) gives

$$\theta_1 = 125 \times \frac{2.54}{20,000} + 0.044$$

$$= 0.06^{\circ}C/W.$$

Equation (6.2) gives

$$T_J - T_A = 1200 \times 0.06$$
$$= 72^{\circ}C.$$

This is satisfactory.

APPENDIX IV

ANALYSIS OF THE SHUNT TRANSFORMER VOLTAGE SHARING NETWORK

IV.1 WITH THE CONSTANT REVERSE VOLTAGE WAVEFORM (Figure 3.2(a))

Considering the simplified equivalent circuit of Figure 5.2, and neglecting thyristor reverse recovery effects, the Laplace operational equation, with C_2 initially uncharged, is

$$\frac{V_R\ N_2}{n\ N_1 s} = \bar{i}\left(L_{t_2}s + R_{t_2} + \frac{1}{C_2 s}\right),$$

giving

$$\bar{i} = \frac{V_R\ N_2}{n\ N_1 L_{t_2}}\left(\frac{1}{s^2 + \frac{R_{t_2}}{L_{t_2}}s + \frac{1}{L_{t_2}C_2}}\right).$$

The inverse transform gives

$$i = \frac{V_R\ N_2}{n\ N_1} \cdot \frac{1}{\omega L_{t_2}} e^{-at} \sin \omega t,$$

where $a = \frac{R_{t_2}}{2L_{t_2}}$ and $\omega^2 = \frac{1}{L_{t_2}C_2} - a^2$.

If R_T is neglected, the peak of the current half cycle is

$$I_{2pk} = \frac{V_R\ N_2}{n\ N_1}\sqrt{\frac{C_2}{L_{t_2}}},$$

and the duration of the current half-cycle is given when $\omega t = \pi$.

$$\therefore\ T_{C_2} = \sqrt{L_{t_2}C_2}.$$

IV.2 WITH THE LINEARLY CHANGING VOLTAGE WAVEFORM (Figure 3.2(b))

This analysis refers to the practical chopper waveform used (Figure 5.3(b)). Let the instantaneous reverse voltage, referred to the secondary side, be given by

$$v = \frac{N_2}{n\ N_1}(V_R - \alpha t)$$

Then in Laplace form,

$$\bar{i}\left(L_{t_2}s + R_{t_2} + \frac{1}{C_2 s}\right) = \frac{N_2}{n\ N_1}\left(\frac{V_R}{s} - \frac{\alpha}{s^2}\right),$$

$$\bar{i} = \frac{N_2}{n\ N_1}\left[\frac{V_R}{\omega L_{t_2}} \cdot \frac{\omega}{(s+a)^2+\omega^2} - \alpha C_2\left(\frac{1}{s} - \frac{s+2a}{(s+a)^2+\omega^2}\right)\right].$$

The inverse transform gives

$$i = \frac{N_2}{n\ N_1}\left(\frac{V_R}{\omega L_{t_2}} e^{-at}\sin \omega t - \alpha C_2 + \frac{\alpha}{\omega}\sqrt{\frac{C_2}{L_{t_2}}}\, e^{-at}\sin(\omega t+\theta)\right)$$

where $\theta = \tan^{-1}\omega/a$.

Simplifying this by assuming $R_T = 0$ gives

$$i = \frac{N_2}{n\ N_1}\left(V_R\sqrt{\frac{C_2}{L_{t_2}}}\sin \omega t - \alpha C_2(1 - \cos \omega t)\right) \qquad \text{(IV.1)}$$

Now maximum current occurs when $di/dt = 0$, that is when

$$V_R\sqrt{\frac{C_2}{L_{t_2}}}\cos \omega t = \alpha C_2 \sin \omega t,$$

$$\omega t = \tan^{-1}\left(\frac{V_R}{\alpha\sqrt{L_{t_2} C_2}}\right) \qquad \text{(IV.2)}$$

APPENDIX V

BASIC D.C. CHOPPER THEORY

V.1 MEAN D.C. OUTPUT VOLTAGE

The simple idealised step-down chopper is shown with the appropriate waveforms in Figure V.1. Switch S operates rapidly to successively connect and disconnect the d.c. supply with the load. The switch is closed for a mark period m, when supply voltage V_d is applied to the load and current is supplied from the d.c. source; it is open for a space period p, when the load inductance L_ℓ circulates the decaying load current through the freewheeling diode D_f. The waveforms of Figure V.1(b) and (c) apply for the case of continuous load current conduction (i.e. $I_{min} > 0$). The mean d.c. output voltage is given by

$$V_\ell = V_d\left(\frac{m}{m + p}\right)$$

$$= V_d\left(\frac{r}{r + 1}\right), \qquad (V.1)$$

where r is the mark/space ratio, m/p.

It is frequently convenient to express the mean d.c. output voltage in the alternative form

$$V_\ell = \frac{m}{T} \cdot V_d \, , (= k \, V_d)$$

$$V_\ell = m.f \, V_d \, , \qquad (V.2)$$

where $T = (m + p) = 1/f$. Hence, if the mark duration is maintained

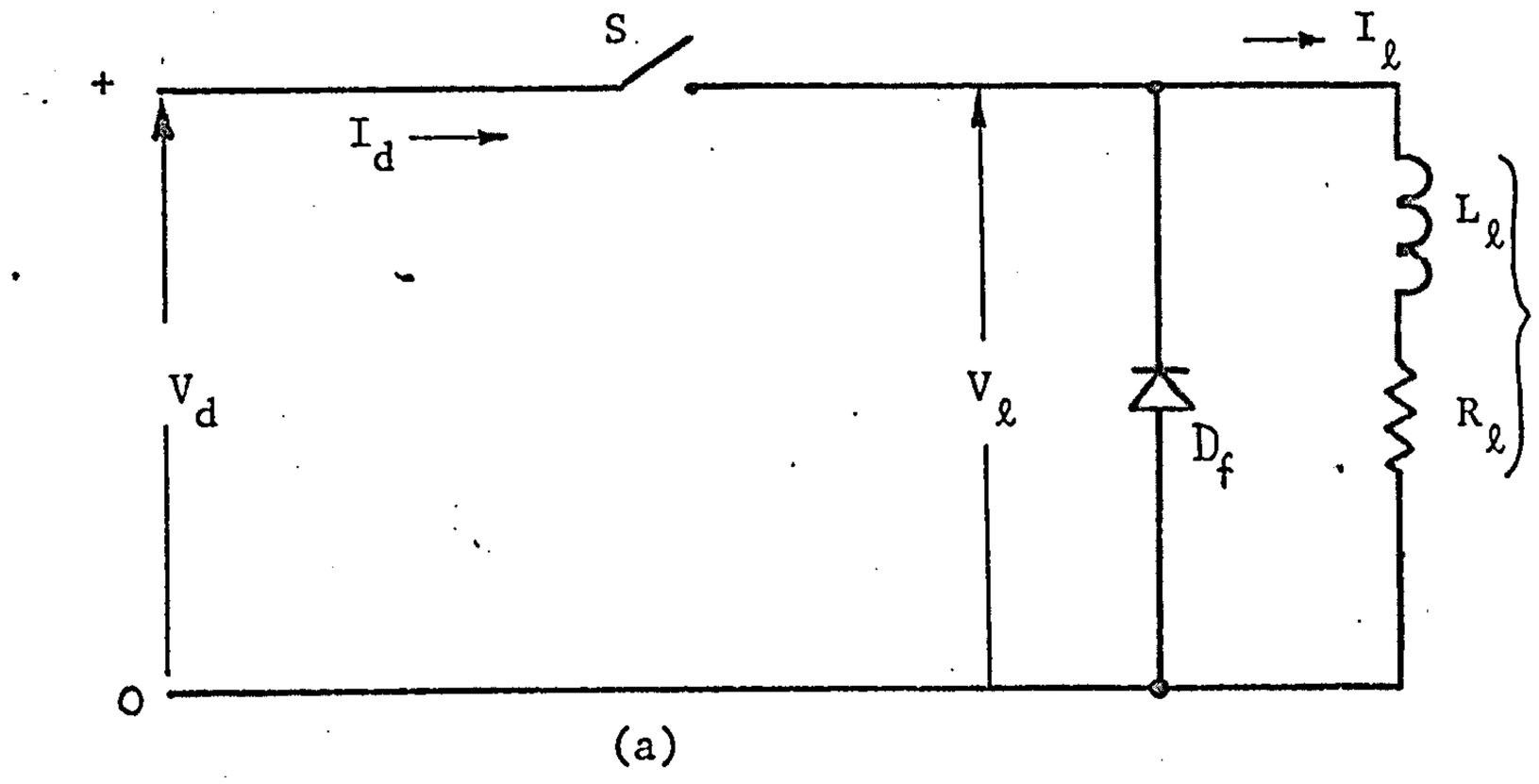

(a)

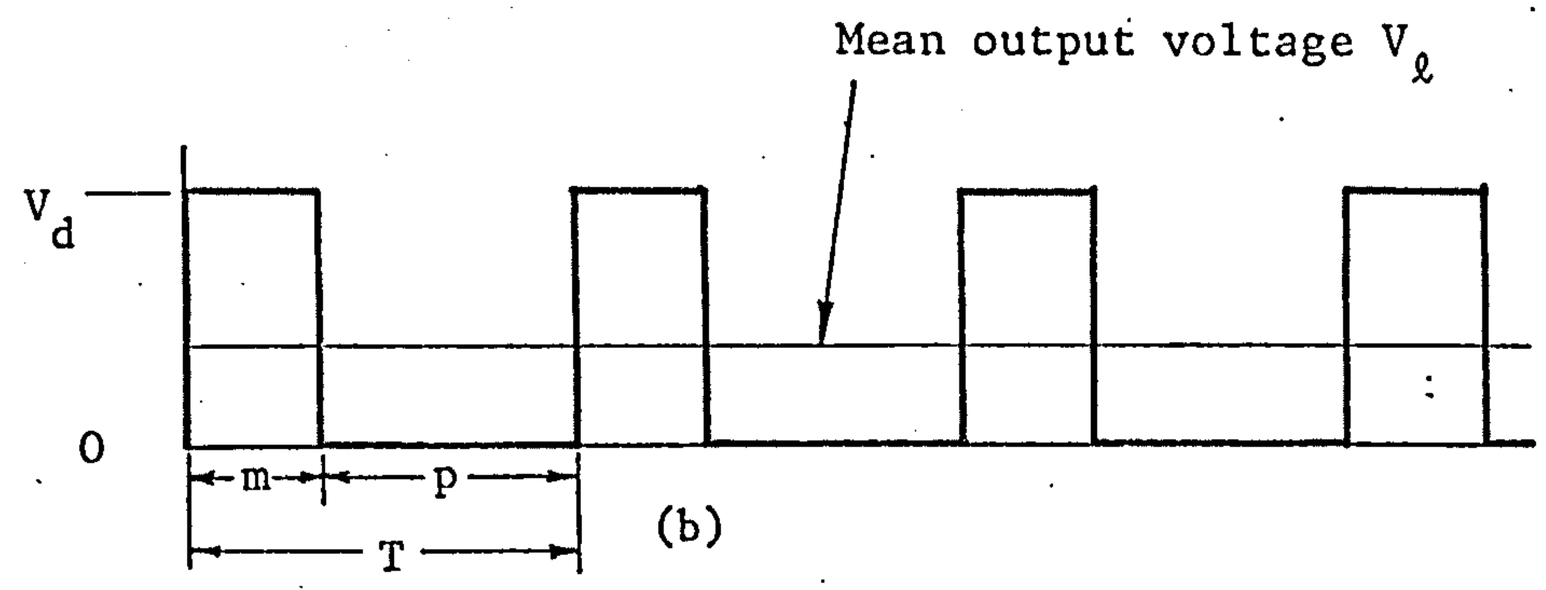

(b)

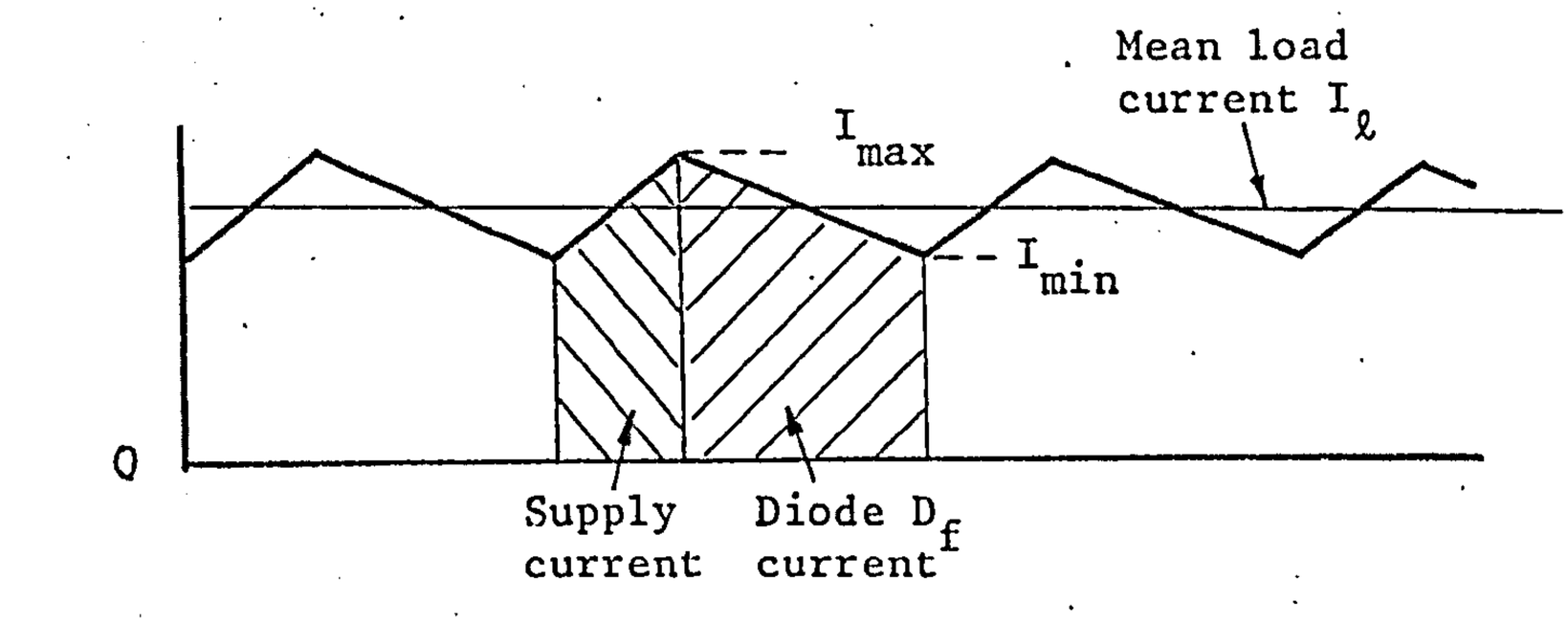

(c)

Figure V.1: Basic chopper operation.

(a) Basic circuit.

(b) Output voltage waveform.

(c) Load current waveform.

constant and the space varied by change of frequency, the mean output voltage increases proportionally with frequency. The converse method of control, produced by keeping the space constant and controlling the frequency to vary the mark, provides a linearly falling output voltage with frequency increase. This characteristic is given by substituting the equivalent (1/f - p) for mark m in equation (V.2), then

$$V_\ell = V_d(1 - pf) \qquad (V.3)$$

Practical chopper circuits usually have definite minimum allowable mark and space durations (section 7.1). These provide the chopper operating limits, as can be seen from Figure V.2 which shows the characteristics of equations (V.2) and (V.3) drawn with assumed fixed minimum allowable mark at low output voltage and fixed allowable space at high output voltages. Neglecting other considerations, the intersection of these characteristics gives the maximum possible operating frequency at a single, specific value of output voltage. Any operating point, say P, must lie within the envelope shown, and it is evident that as chopping frequency is increased, the available range of output voltage becomes more restricted. Instead of using the mean output voltage as base, the per unit output voltage (mark/period ratio, k) may be used.

By equating the mean d.c. chopper input power with that supplied to the load for the idealised conditions of zero internal chopper loss and perfectly smooth supply voltage V_d and load current I_ℓ, it can be shown that the current is stepped up in the same ratio as the voltage is stepped down[34]. This is made possible by the action of freewheeling diode D_f, and results in the d.c. chopper exhibiting

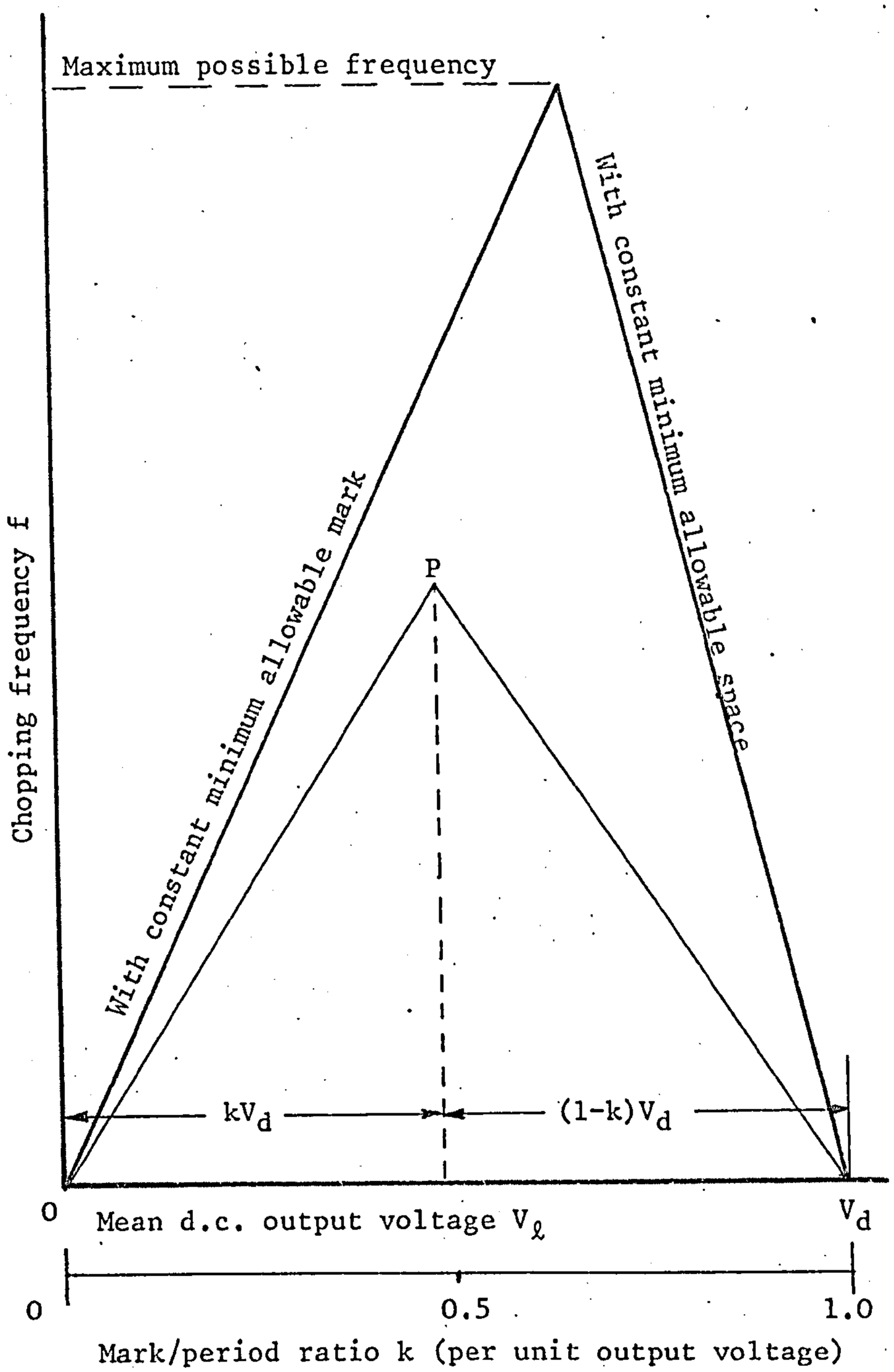

Figure V.2: Variation of the basic chopper mean d.c. output voltage with frequency; mark or space duration maintained constant.

the same basic input-output characteristics as the a.c. transformer.

V.2 LOAD CURRENT RIPPLE

V.2.1 Maximum and minimum current ripple values

Currents I_{max} and I_{min} (Figure V.1(c)) are determined as follows. With the switch S in Figure V.1(a) closed, the load current rises. Then

$$L_\ell \frac{di}{dt} + i R_\ell = V_d .$$

In Laplace operational form, this becomes

$$L_\ell s\bar{i} - L_\ell I_{min} + \bar{i}R_\ell = V_d/s$$

$$\bar{i} = \frac{V_d}{sL_\ell}\left(\frac{1}{s + R_\ell/L_\ell}\right) + \frac{I_{min}}{s + R_\ell/L_\ell}$$

$$= \frac{V_d}{R_\ell}\left(\frac{1}{s} - \frac{1}{s + R_\ell/L_\ell}\right) + \frac{I_{min}}{s + R_\ell/L_\ell} .$$

The inverse transform gives

$$i = \frac{V_d}{R_\ell}\left(1 - e^{-R_\ell t/L_\ell}\right) + I_{min}e^{-R_\ell t/L_\ell} .$$

When $t = m$, $i = I_{max}$, and letting the ratio $L_\ell/R_\ell = T_\ell$,

$$I_{max} = \frac{V_d}{R_\ell}\left(1 - e^{-m/T_\ell}\right) + I_{min}e^{-m/T_\ell} . \qquad (V.4)$$

With switch S open, the falling load current flowing through diode D_f is given by

$$L_\ell \frac{di}{dt} + i R_\ell = 0.$$

In Laplace operational form

$$L_\ell s\bar{i} - L_\ell I_{max} + \bar{i}R_\ell = 0,$$

$$\bar{i} = \frac{I_{max}}{s + R_\ell/L_\ell} .$$

The inverse transform gives

$$i = I_{max} e^{-t/T_\ell} .$$

When $t = p$, $i = I_{min}$. Therefore

$$I_{min} = I_{max} e^{-p/T_\ell} . \qquad (V.5)$$

Equating I_{max} as given by equation (V.5) with that from equation (V.4),

$$I_{min} e^{p/T_\ell} = I_{min} e^{-m/T_\ell} + \frac{V_d}{R_\ell}\left(1 - e^{-m/T_\ell}\right),$$

which gives

$$I_{min} = \frac{V_d(e^{m/T_\ell} - 1)}{R_\ell(e^{T/T_\ell} - 1)} . \qquad (V.6)$$

Substituting this expression for I_{min} back in equation (V.5) gives

$$I_{max} = \frac{V_d(e^{T/T_\ell} - e^{p/T_\ell})}{R_\ell(e^{T/T_\ell} - 1)} . \qquad (V.7)$$

V.2.2 Mean load current

The energy supplied to inductor L as current rises is returned during the current fall, giving zero net energy input to L during a complete ripple. It follows that the net volt-second integral and the mean voltage across L are zero. The mean load current I_ℓ is therefore given by

$$I_\ell = V_\ell / R_\ell$$

$$I_\ell = V_d mf / R_\ell \qquad (V.8)$$

It is complicated to define the mean current level in terms of I_{max} and I_{min} for the exponential current changes analysed in the previous section. Only when k = 0.5 will the mean current be the arithmetic average of I_{max} and I_{min}. However, if the approximation of linear current changes is made, which is not unreasonable for load time constants T_ℓ which are long relative to the mark and space, then the mean current will be the average of I_{max} and I_{min}, that is

$$I_\ell = \frac{1}{2}\left(I_{max} + I_{min}\right). \qquad (V.9)$$

V.2.3 Maximum peak-peak ripple current

The peak-peak ripple current ΔI_ℓ (= $I_{max} - I_{min}$) is, using equations (V.6) and (V.7), given by

$$\Delta I_\ell = \frac{V_d}{R_\ell}\left(\frac{e^{T/T_\ell} - e^{(T-m)/T_\ell} - e^{m/T_\ell} + 1}{e^{T/T_\ell} - 1}\right) \qquad (V.10)$$

where (T - m) = p. Let the operating frequency and therefore T be constant, with m the independent variable. Peak-peak ripple is a maximum or minimum when $d(\Delta I_\ell)/dm = 0$. From this, maximum peak-peak ripple occurs when (T - m) = m, that is, at unity mark/space ratio, k = 0.5. Substituting this condition back into equation (V.10) gives the maximum peak-peak ripple current.

V.3 VARIABLE OPERATING FREQUENCY CHARACTERISTICS

V.3.1 Control to give minimum load current ripple

Variable frequency operation can usefully be used to limit load current ripple throughout the required range of mark/period ratio k demanded by the output voltage variation.

For a given value of k, and load time constant T_ℓ, minimum ripple occurs when the frequency is at its highest possible value. For this condition, operation must be always at the constant allowable minimum mark or space, as appropriate for the required output voltage (Figure V.2). Owing to the losses at commutation, the imposition of a lower maximum frequency than that shown may be necessary in practice.

V.3.2 Control to give constant load current ripple

The required variation of frequency with ratio k to produce constant peak-peak ripple current ΔI_ℓ can be obtained using equation (V.10). This can be re-stated in terms of frequency f and ratio k as

$$\Delta I_\ell = \frac{V_d}{R}\left(\frac{e^{1/T_\ell f} - e^{(1-k)T_\ell f} - e^{k/T_\ell f} + 1}{e^{1/T_\ell f} - 1}\right) \qquad (V.11)$$

If, for a fixed chosen frequency f, the variation of peak-peak ripple ΔI_ℓ is plotted against k, the resulting characteristic has a shape resembling a parabola with, as has been shown, maximum ripple at k =0.5 (Figure 7.14). A similar form of characteristic results if the required variation of frequency with k is plotted to maintain constant peak-peak ripple ΔI_ℓ, maximum frequency being necessary when k = 0.5.

APPENDIX VI

ESTIMATION OF THE VARIABLE FREQUENCY CHOPPER LOSSES

VI.1 MAIN CHOPPER COMPONENT LOSSES

VI.1.1 Thyristor and diode forward conduction losses

Constant forward voltage drops of 1.5V per thyristor and 1.0V per diode are assumed. Times t_{m_1}, t_{m_2}, m, p, and T are in micro-seconds.

(a) Thyristor string Th_1, (Figure VI.1(a))

The mean forward current is given by

$$\frac{10^6}{T}\left[\int_0^{173/10^6} 24\,\sin(18.2\times10^3 t)\,dt + \int_0^{t_{m_1}} \left\{\frac{V_d}{R_\ell}\left(1 - e^{-R_\ell t/L_\ell}\right) + I_{min}e^{-R_\ell t/L_\ell}\right\}dt\right].$$

Substituting the circuit values given in Figure 7.10 and Table 7.1,

$$\text{mean } Th_1 \text{ current} = \frac{1}{T}\left[2645 + 15.6t_{m_1} - 792(15.6-I_{min})\left(1-e^{-t_{m1}/792}\right)\right]$$

Then, Th_1 conduction loss = mean Th_1 current $\times$ $1.5n_{t_1}$

= mean Th_1 current $\times$ 22.5.

For f = 1000Hz, T = 1000μs, t_n = 690μs, I_{min} = 12.5A; loss = 277W.

(b) Thyristor string Th_2 (Figure VI.1(b))

Assuming constant Th_2 current at value I_f,

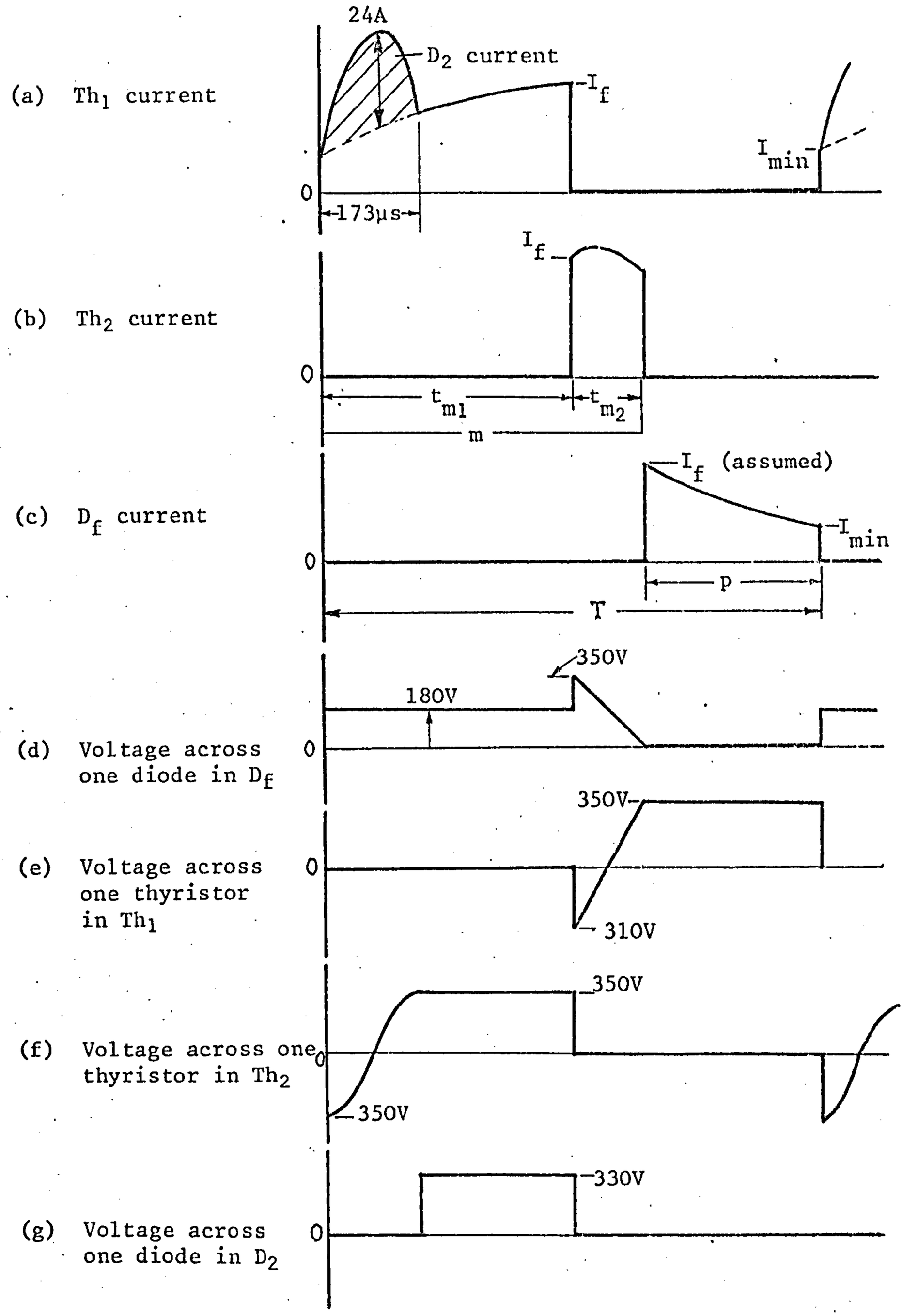

Figure VI.1: Idealised individual thyristor and diode waveforms with representative values, for the 5kV variable frequency chopper.

$$\text{Th}_2 \text{ conduction loss} = 1.5n_{t_2} I_f \frac{t_{m_2}}{T}$$

$$= 22.5 \frac{I_f \, t_{m2}}{T} .$$

For f = 1000Hz, T = 1000μs, t_{m_2} = 175μs, I_f = 14.0A; loss = 55W.

(c) Diode D_2 (Figure VI.1(a))

The shaded area of Figure VI.1(a) gives

$$D_2 \text{ conduction loss} = \frac{1.0n_{d_2}10^6}{T} \int_0^{173/10^6} 24 \sin(18.2\times10^3 t)dt$$

$$= \frac{39700}{T} .$$

For f = 1000Hz, T = 1000μs, loss = 40W.

(d) Diode D_f (Figure VI.1(c))

For the exponential current decay from value I_f,

$$D_f \text{ conduction loss} = \frac{1.0}{T} n_{df} 10^6 \int_0^{p/10^6} I_f e^{-R_\ell t/L_\ell} dt$$

$$= \frac{23000}{T} I_f \left[1 - e^{-p/792}\right] .$$

For f = 1000Hz, T = 1000μs, I_f = 14.0A, p = 113μs; loss = 43W.

VI.1.2 Thyristor and diode switching losses

Where saturating reactors are used in series with the thyristors and diodes, the switching losses are assumed to be negligible. For the only case where this is not so, namely, for diodes D_f with the regulating diode voltage sharing network, the reverse recovery loss is estimated from the measured heat sink temperature rise by the

procedure given in reference 44. The method is as follows.

Rate of heat flow from sink = $h\ A\ \eta(T - T_A)$ watts

and $h = h_r + h_c$

where h = heat transfer coefficient. ($W/in^2\ ^oC$)

A = surface area = 2 × 5in. × 5in. = $50in^2$

η = heat sink effectiveness factor

T = heat sink maximum temperature = 80^oC

T_A = ambient temperature = 22^oC

h_r = radiation coefficient ($W/in^2\ ^oC$)

h_e = convection coefficient ($W/in^2\ ^oC$)

Square plates of side 5in. and separated by 2.2in. have h_r = 0.0022 $W/in^2\ ^oC$ for an emissivity of 0.9. For unpolished aluminium, emissivity = 0.1, hence h_r = 0.0022 × 0.1/0.9 = 0.000245 $W/in^2\ ^oC$. The appropriate nomogram gives h_c = 0.0041 for a measured temperature difference of 58^oC at 1000Hz, giving a total h = 0.00435 $W/in^2\ ^oC$. The effectiveness factor η, allowing for less than the total plate area reaching the maximum temperature measured adjacent to the diode stud, is 0.81.

Hence the total heat transfer is calculated to be 10.2W per plate at 1000Hz. The diode conduction loss at this frequency (section VI.1.1) is 43/29 = 1.48W, giving a reverse recovery loss of 8.7W per diode. With 600V regulating diodes across the power diodes and 5kV applied, the number of diodes blocking this voltage is 8. Hence, the total switching loss is (8.7 × 8) = 70W. This loss is proportional to frequency provided the reverse recovery conditions are unaltered. In this case the D_f forward current interrupted I_{min} = 12.5A and,

assuming the loss is proportional to reverse recovery charge removed, which is in turn proportional to I_{min}, the loss can be estimated from

$$D_f \text{ reverse recovery loss} = 70 \times \frac{f}{1000} \times \frac{I_{min}}{12.5} \quad W.$$

VI.1.3 Resistance losses

(a) Inductor L_2.

From Figure VI.1(a), the peak current through L_2 is 24A.

Therefore

$$\text{resistance loss} = \left(\frac{24}{\sqrt{2}}\right)^2 \frac{173}{T} \times R_2$$

$$= \frac{80,200}{T} \quad W.$$

For f = 1000Hz, T = 1000μs; loss = 80W.

(b) Resistor R'.

Using measured values of r.m.s. line current,

$$\text{resistance loss in } R' = (\text{r.m.s. } I_d)^2 R'$$

$$= 3.36(\text{r.m.s. } I_d)^2.$$

For f = 1000Hz, r.m.s. I_d = 13.0A; loss = 568W.

VI.2 R-C VOLTAGE SHARING NETWORK LOSS

VI.2.1 Loss in resistors R_S

This loss is calculated using the rms value of the voltage waveform across the resistor. For each string,

$$R_S \text{ power loss} = \frac{n \times (\text{rms. voltage})^2}{R_S} .$$

(a) R_S across thyristors Th_1, (Figure 6.1(e)).

$$\text{Total } R_S \text{ power loss} = \frac{15}{T\times10^4}\left[\int_o^{t_{m2}} \left(-310 + \frac{660}{t_{m_2}} t\right)^2 dt + 350^2 p\right]$$

$$= \frac{15}{T}\left[3.68 t_{m_2} + 12.3p\right] .$$

For f = 1000Hz, T = 1000μs, t_{m_2} = 200μs, p = 120μs; loss = 33W.

(b) R_S across thyristors Th_2, (Figure VI.1(f))

$$\text{Total } R_S \text{ power loss} = \frac{15}{T\times10^4}\left[\frac{350^2}{2}.173 + (t_{m_1}-173)350^2\right]$$

$$= \frac{183}{T}\left[t_{m_1} - 87\right].$$

For f = 1000Hz, T = 1000μs, t_m = 690μs; loss = 110W.

(c) R_S across diodes D_2, (Figure VI.1(g))

$$\text{Total } R_S \text{ power loss} = \frac{15 \times 330^2}{34\times10^3\ T}\left(t_{m_1} - 173\right)$$

$$= \frac{48}{T}\left(t_{m_1} - 173\right) .$$

For f = 1000Hz, T = 1000μs, t_m = 690μs; loss = 25W.

(d) R_S across diodes D_f (Figure VI.1(d))

$$\text{Total } R_S \text{ power loss} = \frac{29}{34\times10^3 T}\left[180^2 t_{m_1} + \int_o^{t_{m_2}} \left\{350 - \left(\frac{350}{t_{m_2}}\right) t\right\}^2 dt\right]$$

$$= \frac{29}{34\times10^3}\frac{1}{T}\left[180^2 t_{m_1} + \frac{350^2}{3} t_{m_2}\right].$$

For f = 1000Hz, T = 1000μs, t_m = 690μs, t_m = 200μs; loss = 26W.

VI.2.2 Loss in resistors R

The loss for each string is given by substituting the appropriate values in the expression

$$\text{R power loss} = n\,C(V_r + V_f)f.$$

(a) For Th_1, (Figure IV.1(e)), $$\text{R power loss} = 15 \times \frac{0.085}{10^6}(350^2 + 310^2)f$$
$$= 0.276f.$$

(b) For Th_2, (Figure IV.1(f)), $$\text{R power loss} = 15 \times \frac{0.085}{10^6}(2 \times 350^2)f$$
$$= 0.313f.$$

(c) For D_2, (Figure IV.1(g)), $$\text{R power loss} = 15 \times \frac{0.05}{10^6}(330^2)f$$
$$= 0.0816f.$$

(d) For D_f, (Figure IV.1(d)), $$\text{R power loss} = 29 \times \frac{0.1}{10^6}(350^2)f$$
$$= 0.355f.$$

For f = 1000Hz, these losses, in order, are 276, 313, 82 and 355W.

VI.2.3 Saturating reactor core loss

The core loss for the two HCR-cored inductors in series with Th_f and D_2 and for the two Mumetal cores in series with D_f is given in the manufacturer's data[35,61]. Loss in the ferrite core is assumed negligible.

VI.3 REGULATING DIODE VOLTAGE SHARING NETWORK LOSS

Many assumptions are necessary in predicting these losses owing to the number of unknowns, and these are mainly based on experience.

Their ultimate justification is provided by the adequacy of three, 1W, 200V regulating diodes in series for fulfilling the duty without serious heating. There is only one exception which is noted.

VI.3.1 Steady state loss in the forward regulating diodes Z_f

The manufacturer's quoted maximum thyristor leakage current is 15mA at 900V. First, letting the voltage across just one thyristor be clipped to 600V, for the other thyristors,

$$\text{leakage current} = \frac{(5000 - 600)}{14} \times \frac{15}{900} \text{ mA}$$

$$= 5.25\text{mA}.$$

If now eight ($\approx$ 5000/600) thyristors have their Z_f diodes operating and carrying the above current, then

$$\text{total regulating diode dissipation} = 8 \times \frac{5.25}{10^3} \times 600 \times \text{duty cycle}$$

$$= 26 \times \frac{\text{forward blocking period}}{T}$$

This is only very approximate.

(a) Z_f across thyristors Th_1 (Figure VI.1(e))

The forward blocking period is $(\frac{1}{2}t_{m_2} + p)$ approximately.

For f = 1000Hz, T = 1000μs, t_{m_2} = 175μs, p = 113μs; loss = 5W.

(b) Z_f across thyristors Th_2 (Figure VI.1(f))

The forward blocking period is $(t_{m_1} - 173/2)$μs.

For f = 1000Hz, T = 1000μs, t_{m_1} = 710μs; loss = 16W.

VI.3.2 Steady state loss in the reverse regulating diodes Z_r

The waveforms of reverse voltage across Th_1 and Th_2 demonstrate that it is not worthwhile estimating the very small resulting regulating diode power dissipation.

(a) Z_r across diodes D_2 (Figure VI.1(g))

The reverse blocking period is $(t_{m_1} - 173)\mu s$. The method for forward thyristor blocking is then used.

For $f = 1000Hz$, $T = 1000\mu s$, $t_{m_1} = 710\mu s$; loss = 14W.

(b) Z_r across diodes D_f (Figure VI.1(d))

The reverse blocking period is t_{m_1} for 8 diodes, and t_{m_2} for a number which reduces from 17 ($\simeq$ 10000/600) to zero during t_{m_2}, giving an average of 8 then. Hence the effective blocking period is $(t_{m_1} + t_{m_2})$ for 8 diodes.

For $f = 1000Hz$, $T = 1000\mu s$, $t_{m_1} = 710\mu s$, $t_{m_2} = 175\mu s$; loss = 23W.

VI.3.3 Loss in regulating diodes Z_f at thyristor turn-on

The saturating reactor in series with the thyristors controls this loss. After thyristor reverse recovery has left SR flux at or near the $-\Phi_r$ value, the leakage currents during reverse and forward blocking have little effect. A linear mathematical approximation to the resetting magnetisation characteristic, and an assumed maximum turn-on time difference of say 2μs for the last 8 ($\simeq$ 5000/600) thyristors to turn-on, gives the charge flow through the regulating diodes.

(a) Z_f across thyristors Th_1

The assumed linear ΔB-H characteristic of the 65 turn, HCR core, size 11b, gives $i = 0.376t$, and the charge flow

$$q = 0.188t^2 \ \mu C$$

where t is in μs, and represents the time measured from the instant when only 8 thyristors remain blocking. Then for the slowest turn-on thyristor (t = 2), q is 0.75μC. The resulting power dissipation in its shunt regulating diode Z_f (600V total) is, using equation 6.1,

$$\text{dissipation at turn-on} = 1.15 \times 600 \times \frac{0.75}{10^6} \times f$$

$$= \frac{0.52}{10^3} f.$$

For the eight last blocking thyristors, this value can be averaged giving

$$\text{total } Z_f \text{ dissipation at turn-on} = \frac{8}{2} \times \frac{0.52}{10^3} f$$

$$= \frac{2.08}{10^3} \times 10^{-3} f$$

For f = 1000Hz; loss = 2W.

(b) Z_f across thyristors Th_2

The FX1076 ferrite core with 50 turns saturates in 1.14μs so that the saturated portion of its B-H characteristic must also be represented linearly for an assumed turn-on time difference of 2μs. The current-time characteristic is approximately

$$i = \int_{t=0}^{t=1.14} 0.285t + \int_{t=1.14}^{t=2} (4.33t - 4.6)$$

$$\therefore \quad q = \int_0^{1.14} 0.285t \, dt + \int_{1.14}^{2} (4.33t - 4.6)dt$$

$$= 2.09\mu C.$$

Again for the 8 last blocking thyristors,

$$\text{total } Z_f \text{ dissipation at turn-on} = 1.15 \times \frac{2.09}{2\times10^6} \times 600 \times 8 \quad f$$

$$= 5.8 \times 10^{-3} \quad f.$$

For f = 1000Hz; loss = 6W.

VI.3.4 Loss in regulating diodes Z_r at thyristor and diode reverse recovery

For Th_1, Th_2 and D_2 there will be no appreciable loss caused by voltage spikes generated by the reverse recovery current, since this is controlled by the series SR. The approach of Chapter 4 and illustrated in Figure 4.4 is used here, although mathematical approximation is adopted for simplicity.

(a) Z_r across thyristors Th_1

Owing to device selection, the first 8 thyristors to block reverse voltage have a minority carrier lifetime differing little from an average measured value of 1.25μs. For a forward chopped current I_f of 13.3A, the internal charge natural decay is given by

$$q = 1.25 \times 13.3e^{-t/1.25}.$$

The linear magnetisation curve approximation (i = 0.376t) yields

$$q = 0.188t^2.$$

Equating these expressions gives a solution of t = 3μs at which time the

reverse current is 1.12A. For an assumed reverse recovery time spread of 0.5μs above and below the average, the charge flow through Z_r across the fastest recovery thyristor is 1.12μC, and for the 8th fastest it is zero, giving an average of 0.66μC.

$$\text{Total } Z_r \text{ dissipation during reverse recovery} = 8 \times 600 \times \frac{0.66}{10^6} \times f$$

$$= \frac{2.7}{10^3} f.$$

For f = 1000Hz; loss = 3W.

(b) Z_r across thyristors Th_2.

Since these thyristors turn off under the influence of minimal reverse voltage, any effects due to reverse recovery charge flow can be safely neglected.

(c) Z_r across diodes D_2.

Here the spread of minority carrier lifetimes (3μs to 4.5μs measured) is such as to make separate consideration of the extreme values desirable. The diode current is assumed to be sinusoidal with 24A peak, and it is further assumed that the reverse recovery charge flow is equivalent to the chopping of 5A forward current. Hence the extreme exponential charge decay characteristics of the blocking diodes are

$$q = 5 \times 3e^{-t/3}$$

$$q = 5 \times 4.5\, e^{-t/4.5}$$

For the 100 turn, HCR size 11b core, i = 0.161t, giving

$$q = 0.081t^2.$$

The appropriate two solutions at which q = 0 are t = 5.5 and 7.0μs. The respective removed charge values are 2.4 and 3.9μC giving a difference value of 1.5μC.

Averaging this value for 8 blocking diodes gives,

$$\text{total } Z_r \text{ dissipation during reverse recovery} = 8 \times 600 \times \frac{1.5}{2\times10^6} f$$

$$= \frac{3.6}{10^3} f.$$

For f = 1000Hz; loss = 4.0W

(d) Z_r across diodes D_f.

Diode reverse recovery current flows when the forward current I_{min} reverts to Th_1 and the 0-5kV output voltage jump is impressed across D_f. For the 8 fastest recovery diodes whose Z_r's then operate, the extreme values of Q_r previously measured at 20A, 200V, 45A/μs rate of current fall, are 54μC and 75μC, giving ΔQ_r = 21μC. Assuming that ΔQ_r is proportional to the forward current interrupted (I_{min}),

$$\text{individual (200V) regulating diode maximum dissipation} = 1.15 \times 200 \times \frac{I_{min}}{20} \times \frac{21}{10^6} f$$

$$= \frac{0.241}{10^3} I_{min} f.$$

With the most arduous conditions of I_{min} = 12.8A, f = 2000Hz,

required reg. diode power rating > 6.2W.

N.B. 10W devices are used across fastest recovery diodes.

$$\text{Total } Z_r \text{ dissipation} = \left(\frac{1}{2} \times \frac{0.241}{10^3} \times 3 \times 8\right) I_{min} f$$

$$= \frac{2.9}{10^3} I_{min} f.$$

For f = 1000Hz, I_{min} = 12.5; loss = 37W.

The regulating diode power dissipation produced by its suppressing any hole storage voltage spike is neglected.

LIST OF PRINCIPAL SYMBOLS

C	Parallel voltage sharing capacitor (or capacitance)
C_c	Commutating capacitor (or capacitance)
C_2	Voltage controlling capacitor (or capacitance) for shunt transformers
f	Operating frequency
f_s	Thyristor string voltage derating factor
f_{fm}	String experimental forward voltage factor
f_{rm}	String experimental reverse voltage factor
I_f	Thyristor or diode forward current turned off
$\left\|\frac{di}{dt}\right\|_{off}$	Rate of fall of forward current at turn off
I_h	Thyristor holding current
I_{rp}	Peak reverse current during reverse recovery
i_m	Instantaneous saturating reactor magnetising current
I_{2pk}	Peak value of shunt transformer secondary current half-cycle
I_d	D.C. chopper input current (mean)
I_ℓ	D.C. chopper load current (mean)
k	D.C. chopper mark/period ratio
L	Inductor (or inductance) in series with the thyristor(s)
L_{t_2}	Shunt transformer total leakage inductance referred to the secondary side
L_ℓ	Load inductance
m	Mark of chopper output voltage
N	Number of saturating reactor turns
n	Number of thyristors or diodes in series
N_1	Shunt transformer primary turns per section
N_2	Shunt transformer secondary turns
P	Power pulse peak value
p	Space in chopper output voltage
Q_f	Internal excess charge corresponding to I_f
Q_h	Internal excess charge corresponding to I_h
Q_r	Thyristor or diode removed reverse recovery charge
ΔQ_r	Difference of removed reverse recovery charge between two devices

R	Resistor (or resistance) in series with C
R_s	Parallel voltage sharing resistor (or resistance)
R_{th}	Thyristor leakage resistance
R_{t_2}	Shunt transformer total winding resistance referred to the secondary side
R_z	Regulating diode dynamic resistance
R_ℓ	Load resistance
T	Period of the operating cycle (= 1/f)
T_{off}	Thyristor turn-off time
t_{rr}	Thyristor or diode reverse recovery time
T_A	Ambient temperature
T_J	Device junction temperature
T_s	Device stud temperature
Δt_{on}	Difference between thyristors' turn-on times
t_{rs}	Time for saturating reactor to magnetise from $+\Phi_s$ to $-\Phi_s$
t_{fs}	Time for saturating reactor to magnetise from $-\Phi_s$ to $+\Phi_s$
T_{c_2}	Duration of shunt transformer secondary current half-cycle
t_{m_1}	Duration of thyristors Th_1 conduction in the mark m
t_{m_2}	Duration of thyristors Th_2 conduction in the mark m
T_ℓ	Load time constant, L_ℓ/R_ℓ
V_{FBO}	Thyristor forward blocking voltage
V_F	Peak forward voltage applied to the thyristor string
V_R	Steady peak reverse voltage applied to the thyristor string
V_{RO}	Voltage applied from C_c to provide thyristor turn-off (if $>V_R$)
V_f	Individual thyristor forward voltage after turn-off
V_r	Individual thyristor steady peak reverse voltage at turn-off
V_{zf}	Nominal voltage of the regulating diode(s) Z_f controlling the forward voltage across each thyristor
V_{zr}	Nominal voltage of the regulating diode(s) Z_r controlling the reverse voltage across each thyristor or diode
V_d	D.C. chopper input voltage
V_ℓ	D.C. chopper output voltage (mean) across the load
α	Slope of the linearly rising line voltage waveform
θ	Steady-state thermal resistance
θ_1	Transient thermal impedance
τ_p	Minority-carrier lifetime in the device *n*-base layer
Φ_s	Core saturation flux
Φ_r	Core retentivity flux